Gemcitabine Resistance Elicits a Calcium Dependent Epigenetic Reprogramming in Pancreatic Cancer

Dissertation

for the award of the degree

“Doctor of Philosophy (Ph.D.)”

Division of Mathematics and Natural Sciences
of the Georg-August-Universität Göttingen

within the doctoral program IMPRS in Molecular Biology

of the Georg-August University School of Science (GAUSS)

submitted by

Ana Patricia Kutschat

from São Paulo, Brazil

Göttingen, 2021

Thesis Supervisor

Prof. Steven Johnsen

Gene Regulatory Mechanisms and Molecular Epigenetics Lab, Mayo Clinic

Thesis Committee

Prof. Matthias Dobbelstein

Institute of Molecular Oncology, University Medical Center Göttingen

Prof. Johannes Söding

Quantitative and Computational Biology Group, Max Planck Institute for Biophysical Chemistry

Members of the Examination Board

Referee: Prof. Steven Johnsen

Gene Regulatory Mechanisms and Molecular Epigenetics Lab, Mayo Clinic

2nd Referee: Prof. Matthias Dobbelstein

Institute of Molecular Oncology, University Medical Center Göttingen

Further members of the Examination Board

Prof. Johannes Söding

Quantitative and Computational Biology Group, Max Planck Institute for Biophysical Chemistry

Prof. Volker Ellenrieder

Department of Gastroenterology, Gastrointestinal Oncology and Endocrinology, University Medical Center Göttingen

Dr. Nico Posnien

Department of Developmental Biology, Georg August University of Göttingen

Dr. Ufuk Günesdogan

Department of Developmental Biology, Georg August University of Göttingen

Date of oral examination: 26th of February of 2021

Table of Contents

Affidavit

Herewith I declare, that I prepared the PhD Thesis "Gemcitabine Resistance Elicits a Calcium Dependent Epigenetic Reprogramming in Pancreatic Cancer" on my own and with no other sources and aids than quoted.

Göttingen, 11th of January of 2021 _____

Ana Patricia Kutschat

Abstract

Pancreatic cancer is a dismal malignancy with a 5-year survival rate of 7-9%, one of the worst among all cancer types. Patients with pancreatic ductal adenocarcinoma (PDAC) usually present an advanced stage of the disease upon diagnosis and often develop chemotherapy resistance. As the disease progresses, patients are commonly administered a gemcitabine-based therapy, which is known for its clinical benefits, but also low response and concomitant high resistance rates. For this reason, the mechanism driving gemcitabine resistance has been extensively studied in pancreatic cancer. In fact, several gemcitabine metabolizing enzymes have been identified as prognostic, correlating with gemcitabine response rates in patient biopsies. Still, the molecular consequences of gemcitabine resistance in tumors remain elusive. Chemotherapeutic agents are known to not only act on their targets, but to also elicit stress and therefore trigger stress-induced apoptosis. Thus, it is plausible that chemotherapy resistance is not only mediated by a bypass of the pathway directly targeted by the chemotherapeutic agent, but also by an altered response to stress cues.

In this study we investigated the molecular consequences of gemcitabine resistance in PDAC tumors. For this, a gemcitabine resistant cell line was established by treating treatment-naïve PDAC cells with increasing concentrations of gemcitabine. By studying the genomic, epigenomic and transcriptomic changes associated with acquired gemcitabine resistance, we identified a main driver of gemcitabine resistance and unraveled a novel mechanism employed by these tumors to overcome stress and activate alternative pathways. Copy number variation analyses revealed an amplification of a segment of chromosome 11, which included genes previously associated with gemcitabine resistance, such as Ribonucleotide Reductase Catalytic Subunit M1 (*RRM1*) as well as other genes, like Stromal Interaction Molecule 1 (*STIM1*). RRM1 is a known target of gemcitabine and proliferation studies confirmed that its amplification and upregulation drove gemcitabine resistance in our system.

In order to elucidate further molecular mechanisms affected by acquired gemcitabine resistance, an epigenetic profiling of the cells was traced. This led to the identification of a dampened ER stress response in gemcitabine resistant compared to parental cells. Gemcitabine resistant cells failed to activate stress

responsive transcription factors, such as Activating Transcription Factor 4 (ATF4), while also displaying a drop in active transcription histone marks around ATF4 binding sites and target genes. Interestingly, the stress response is tightly coupled to calcium signaling and an important ER calcium sensor, STIM1, was identified to be co-amplified with *RRM1* in gemcitabine resistant cells. In fact, the co-amplification of the neighboring genes, *RRM1* and *STIM1*, was shown to have a high co-occurrence rate in different treatment naïve cancer cell lines as well as several primary tumors, suggesting it may also spontaneously occur in tumors.

STIM1 is an ER calcium sensor, which upon ER calcium depletion interacts with the calcium channel ORAI calcium release-activated calcium modulator 1 (ORAI1). This stimulates the influx of calcium from the extracellular matrix into the cytosol, a process referred to as Store Operated Calcium Entry (SOCE). Interestingly, calcium measurements revealed that *STIM1*-amplifying cells displayed an increased SOCE, which in turn led to a dampened ER stress response. Moreover, this increase in SOCE elicited an aberrant activation of the Nuclear Factor of Activated T cells (NFAT) family of transcription factors. Finally, analysis of primary tumors as well as treatment-naïve and gemcitabine treated Patient-Derived Xenografts (PDXs) corroborated our findings *in vivo*.

Taken together, our study characterizes molecular mechanisms driving gemcitabine resistance in PDAC and unravels the role of calcium signaling in these tumors. While the amplification of *RRM1* drove gemcitabine resistance, the upregulation of *STIM1* elicited a heightened SOCE leading to ER stress resistance and aberrant NFAT activation. Thus, STIM1 was identified as a rheostat balancing between ER stress-responsive and NFAT-driven epigenetic programs upon stress. Finally, we propose STIM1 as a novel therapeutic target for the treatment of gemcitabine resistant as well as STIM1-overexpressing tumors.

1. Introduction

1.1. PDAC incidence and prognosis

Among all cancer types, pancreatic ductal adenocarcinoma (PDAC) patients face one of the worst prognoses with a 7-9% 5-year survival rate, mainly due to late diagnosis and chemotherapy resistance (American Cancer Society, 2020). While 53% of the patients are diagnosed with a metastatic tumor, those patients who can undergo a tumor resection usually face a relapse in 1-2 years (American Cancer Society, 2020; Oettle et al., 2013). Thus, the understanding of PDAC and the study of alternative diagnostic and treatment options is of ultimate importance.

1.1.1. Development of PDAC

Several external risk factors, which include smoking, type 2 diabetes, obesity and a history of chronic pancreatitis, are associated with PDAC development (American Cancer Society, 2020; Kirkegård et al., 2018; Malka et al., 2002). After Vogelstein's model for the development of colorectal cancer (Faeron and Vogelstein, 1990), Hruban et. al proposed a model for PDAC development. In this model, the pancreas first presents ductal lesions, pancreatic intraepithelial neoplasms (PanINs), which evolve from a low-grade lesion, with minimal atypia to high-grade lesions with severe cytological and architectural atypia. These lesions are initially non-invasive, but later develop into adenocarcinoma as they accumulate mutations over time (Fig. 1) (Distler et al., 2014; Hruban et al., 2000). Low grade PanINs are characterized by *K-RAS* mutations, which lead to a constitutively active signaling cascade and only progress to invasive pancreatic cancers when followed by silencing of tumor suppressors (Buscail et al., 2020; Di Magliano and Logsdon, 2013). After *K-RAS* mutation, 90% of the lesions present a loss of heterozygosity or silencing of the tumor suppressor, *CDKN2A* (Rozenblum et al., 1997). It was suggested that the *K-RAS* mutation alone leads to senescence, but upon silencing of *CDKN2A*, a key regulator of the G1/S-phase transition in cell cycle, the cells are able to overcome this and undergo cell cycle. This allows for a fast cell proliferation and further promotes tumor formation (Tu et al., 2018).

Later in PDAC development, the tumor suppressor genes *TP53* and *SMAD4* are lost (Rozenblum et al., 1997). These high-grade PanIN lesions present an accumulation

of mutations, shortening of telomeres and increased reactive oxygen species (ROS) levels, which would normally trigger a p53 dependent DNA-damage response, cell cycle arrest and apoptosis. Thus, the loss of *TP53* allows cells to proliferate even under aberrant events (Hezel et al., 2006). While the ablation of *TP53* is essential for cell cycle progression, the consequences of *SMAD4* loss are still under investigation. Some studies propose that in the presence of a mutated *K-RAS*, loss of *SMAD4* leads to accelerated fibrosis, loss of acinar cells and neoplastic changes (Bardeesy et al., 2006; Kojima et al., 2007). Taken together, the loss of tumor suppressor genes together with mutations in oncogenes allow PanIN lesions to develop into carcinomas.

Furthermore, it has been shown that misregulation of several other transcriptional regulators drive the development of lesions and initiation of carcinomas. One such example is KLF4, which together with K-RAS stimulates the formation of PanINs promoting their reprogramming and plasticity (Wei et al., 2016). GLI1 is also required for K-RAS driven PanINs and accelerates tumor formation by activating NF-κB signaling (Nolan-Stevaux et al., 2009; Rajurkar et al., 2012). PRRX1B has been shown to be upregulated in PanINs being associated with increased proliferation and a first de-differentiation step from epithelial cells to more invasive carcinoma cells. While PRRX1B was not found to promote metastasis and a more aggressive oncogenic phenotype, the other isoform, PRRX1A, has been shown to promote EMT in PDAC and was found to be upregulated in metastatic cancer cells (Reichert et al., 2013; Takano et al., 2016). In conclusion, genetic aberrations accompanied by transcriptional misregulation drive PDAC initiation and development, while also giving rise to different pancreatic cancer subtypes, as discussed below.

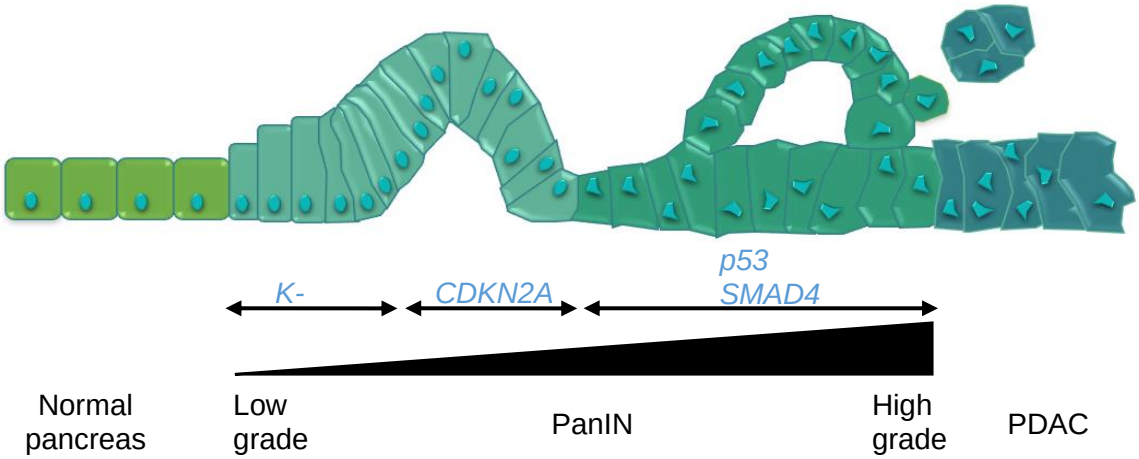

Fig. 1 PDAC development model. The scheme shows the progression of a normal pancreas into a low grade PanIN to a high grade one and finally to PDAC. The mutation of *K-RAS* and silencing of *CDKN2A*, *p53* and *SMAD4* are essential for the development of the lesions into PDAC. The scheme was based on the publication from Hruban et al.

1.1.2. PDAC heterogeneity and subtypes

Transcriptomic analysis of PDAC revealed the tumors' high heterogeneity and context dependency. In an attempt to first classify adenocarcinomas for a better targeted therapy, Collisson et al. microdissected and profiled 27 resected PDAC tumors. The authors identified 62 genes, which were intrinsically variably expressed and conferred different properties to these tumors. This gave rise to three molecular subtypes termed: classical, quasimesenchymal (QM) and exocrine-like. While the classical subtype was characterized for being more dependent on the transcription factor GATA6 and having higher expression of epithelial and cell adhesion genes, the QM subtype enriched for mesenchymal genes. The exocrine-like subtype comprised digestive enzyme genes and could not be verified in further cell culture and mice studies, raising the possibility that it originates from contaminating tissues, from the stroma or normal pancreatic cells (Collisson et al., 2011).

A further study by Moffitt et al. not only subtyped PDAC tumors, but also characterized the tumor stroma and metastases. PDAC was classified into classical and basal-like, where the classical signature greatly overlapped with the classical signature defined by Collisson et al. The basal-like subtype showed a more aggressive phenotype and was found to be enriched in metastases. The stroma was classified into activated and normal stroma, characterized by a more inflammatory environment and better prognosis, respectively. Interestingly, the basal-like, normal

and activated stroma signatures included genes comprised in QM signature defined by Collisson et al. (Moffitt et al., 2015).

A third classification based on gene expression and tumor histology identified the following subtypes: squamous, pancreatic progenitor, immunogenic and aberrantly differentiated endocrine exocrine (ADEX). The squamous subtype showed the worst prognosis and was characterized by the upregulation of the transcription factor ΔNp63, while early development transcription factors were enriched in the pancreatic progenitor subtype. The ADEX subtype comprised genes involved in exocrine and endocrine differentiation and the immunogenic subtype upregulated genes involved in immune suppression. When compared to the Collisson et al. classification, the squamous signature correlated with the QM subtype, while the classical signature comprised the ADEX and pancreatic progenitor subtypes. The immunogenic signature did not correlate with any previously reported subtype (Bailey et al., 2016).

In an attempt to validate the several subtype classifications, Raphael et al. molecularly characterized and classified 146 resected tumors as low or high purity samples. Low purity tumors comprised the exocrine-like, QM, ADEX and immunogenic subtypes, suggesting that these arise mainly due to impurities, such as high stroma content, present in the microdissection samples. High purity samples comprised the squamous/basal-like and the classical/pancreatic progenitor subtypes, further validating these classifications (The Cancer Genome Atlas Research Network et al., 2017).

Chan-Seng-Yue et al. further stratified the basal-like and classical signatures into 5 subtypes: basal-like A and B, classical A and B and hybrid. The signatures of basal-like A and B overlapped with the previously defined basal-like signature from Moffit et al. The same is true for the classical A and B signatures and the published classical subtype by Moffitt et al. The hybrid subtype comprised several distinct expression profiles and was most likely a mixture of basal-like and classical tumor cells. Generally, classical A and B signatures were found in early stage PDAC, and late stage PDAC was mainly composed of basal-like A tumors. Basal-like B and hybrid carcinomas were predominantly resectable, while basal-like A was not.

Interestingly, several independent studies have observed that even though intratumor heterogeneity may be high, such that one tumor may be comprised of several subtypes, metastatic tumors were mainly comprised of one specific subtype and that chemotherapy response was also highly subtype dependent. There is a consensus that most liver metastases are basal-like even if originating from a tumor, which is of a different subtype (Chan-Seng-Yue et al., 2020; Ligorio et al., 2019; Makohon-Moore et al., 2017; Moffitt et al., 2015). This suggests that metastatic cells face a higher selective pressure imposed by extrinsic factors than primary tumors. Very limited data is available on the subtype of metastases after chemotherapy. Chan-Seng-Yun were the first to report the switch of a basal-like B metastasis to the classical A subtype after adjuvant treatment (Chan-Seng-Yue et al., 2020). Regarding chemotherapy response, Collisson et al. reported that QM cell lines were more sensitive to gemcitabine, while erlotinib was more effective in classical carcinomas *in vitro* (Collisson et al., 2011). Moffitt et al. further showed that patients with basal-like tumors presented a better response to adjuvant therapy, while Chan-Seng-Yun found that basal-like A tumors were more chemoresistant and basal-like B, classical A and B and hybrid carcinomas more sensitive to chemotherapy (Chan-Seng-Yue et al., 2020; Moffitt et al., 2015). In accordance with that, Aung et al. reported that patients with classical PDAC responded better to FOLFIRINOX (Aung et al., 2018) and Kloesch et al. showed that a loss of the classical driver GATA6 confers tumor resistance to 5-FU and gemcitabine (Kloesch et al., 2020). Taken together, PDAC tumors are composed of several subtypes, which can be selected for during disease progression as well as by chemotherapy treatment. Still, currently, the same chemotherapeutic agent is applied to all subtypes, regardless of their specific vulnerabilities.

1.1.3. Standard PDAC treatment

PDAC treatment includes tumor resection, radiation and chemotherapy. While 40% of the patients present a locally advanced tumor without metastases, less than 20% classify for tumor resection and 30-40% of the patients display metastatic tumors (American Cancer Society, 2020; Ryan and Mamon, 2020a). Patients qualifying for resection present relatively small tumors, without metastases and distant major peripancreatic vessels (Ryan, 2020a; Ryan and Mamon, 2020a, 2020b). In case the

tumor is local, but does not entirely fulfill all of these requirements or is too big, it is classified as borderline resectable. Recently, more and more patients with locally advanced and borderline resectable tumors are administered neodjuvant therapy with or without chemoradiotherapy prior to surgical reevaluation (Ryan and Mamon, 2020b).

Neodjuvant treatment consists of combination treatments including gemcitabine with nab-paclitaxel and FOLFIRINOX (5-FU, leucovin, irinotecan and oxaliplatin). The treatment lasts for six months and can be followed by an additional round of radiochemotherapy. Afterwards, the patient's health condition and tumor are re-evaluated and tumors may be resected. After surgery, patients receive another six months of adjuvant therapy. In this case, patients displaying good health conditions are administered FOLFIRINOX, while secondary treatment options include gemcitabine with capecitabine, gemcitabine alone or S-1 (tegafur, gimeracil and oteracil) alone. Following, patients who previously received gemcitabine-based therapies are recommended to undergo an additional six months of chemoradiotherapy. This is not recommended in the case of adjuvant FOLFIRINOX treatment, as it is unknown, whether the patients can handle chemoradiotherapy following FOLFIRINOX treatment (Ryan and Mamon, 2020b). If, after neoadjuvant treatment, locally advanced and borderline resectable tumors do not qualify for surgical removal, patients may continue chemotherapy, receive alternative chemotherapeutic agents or enter clinical trials (Ryan and Mamon, 2020a).

For patients facing a relapse and/or a metastatic tumor and an Eastern Cooperative Oncology Group (ECOG) Performance Status (PS) of 0-1, first-line therapy options include FOLFIRINOX, FOLFOX (5-FU, leucovin and oxaliplatin) or gemcitabine in combination with nab-paclitaxel (Conroy et al., 2011). In fact, FOLFIRINOX and FOLFOX are preferred over gemcitabine and nab-paclitaxel as gemcitabine is metabolized in the liver and thus presents higher hepatic toxicity. Still, patients presenting an ECOG PS of 2 qualify for second-line therapy options such as S-1 alone, gemcitabine alone, gemcitabine with S-1 or gemcitabine with capecitabine. Even though the response rate to gemcitabine treatment is low and the hepatic toxicity high, gemcitabine-based therapies are preferred in this case, due to the clinical benefit to patients (Rothenberg et al., 1996). Furthermore, although combination treatments of gemcitabine with capecitabine and gemcitabine with S-1

have shown worse side effects and no changes in overall survival, the response rate was significantly increased when compared to gemcitabine treatment alone (Cunningham et al., 2009; Herrmann et al., 2007; Nakai et al., 2012; Ueno et al., 2013). S-1 treatment alone is currently emerging as an alternative to gemcitabine-based therapies. It is particularly attractive due to lower hematologic toxicity, better objective response rate and similar overall survival when compared to gemcitabine (Ueno et al., 2013). Still, availability to S-1 is limited to Japan and Europe, as it remains unavailable in the US (Ryan, 2020a). Thus, as PDAC progresses, patients are likely administered gemcitabine-based therapies, which present low response and overall survival rates, but offer clinical benefits to patients.

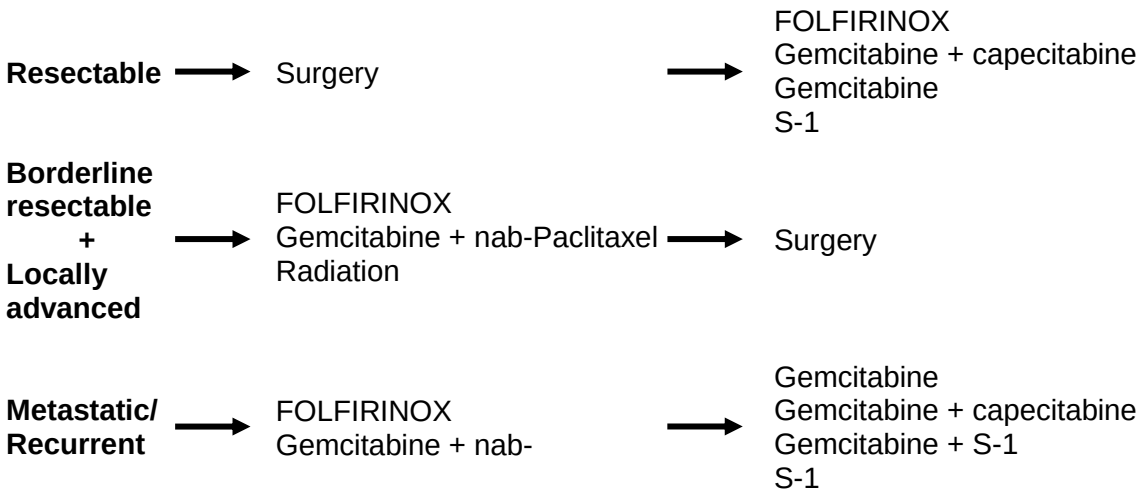

Fig. 2 PDAC treatment options. Scheme depicting standard PDAC treatments. Tumors qualifying for resection are removed and adjuvant therapy is employed. For locally advanced and borderline resectable tumors, patients undergo neoadjuvant and adjuvant therapy prior and after resection, respectively. Metastatic and recurrent tumors are treated with a wide range of chemotherapeutic agents.

1.1.4. Gemcitabine metabolism and mechanism of action

As described previously, most PDAC patients receive a gemcitabine-based therapy during cancer treatment. Gemcitabine is a deoxycytidine analog (2',2'-difluorodeoxycytidine, dFdC), which is transported into the cell and metabolized analogously to deoxycytidine. Its metabolic intermediates affect DNA replication by stalling DNA Polymerase and interfere with *de novo* deoxynucleotide synthesis (Fig. 3) (De Sousa Cavalcante and Monteiro, 2014; Wong et al., 2009).

First gemcitabine is actively transported into the cell, as it is highly hydrophilic and, for this reason, cannot diffuse through the plasma membrane. Two different types

of transporters, the concentrative and equilibrative nucleoside transporters (NT) import gemcitabine. While the concentrative NT (CNT) depends on transporting the nucleoside against the concentration gradient at the exchange of sodium ions, the equilibrative NT (ENT) is bidirectional and transports nucleosides following the intra- and extracellular nucleoside concentrations (Mackey et al., 1998a). Most of gemcitabine is taken up by the human equilibrative nucleoside transporter 1 (hENT1) and to a lesser extent by the human equilibrative nucleoside transporter 2 (hENT2) and the human concentrative nucleoside transporters 1 and 3 (hCNT1 and hCNT3) (García-Manteiga et al., 2003; Mackey et al., 1998b, 1999; Ritzel et al., 2001).

Once inside the cell, gemcitabine is mono- (dFdCMP), di- (dFdCDP) and triphosphorylated (dFdCTP) by deoxycytidine kinase (dCK), pyrimidine nucleoside monophosphate kinase (CMPK) and possibly by nucleoside diphosphate kinase (NDPK), respectively. The monophosphorylation of gemcitabine by dCK being the rate-limiting step in gemcitabine anabolism (Bouffard et al., 1993; Hatzis et al., 1998; Heinemann et al., 1988; Van Rompay et al., 1999; Wong et al., 2009). This opens a window of opportunity for the cell to mitigate the effects of gemcitabine, by employing cytosolic 5'-nucleotidase 1A (NT5C1A) to dephosphorylate monophosphorylated gemcitabine. As the dephosphorylation is much faster than the monophosphorylation step by dCK, the amount of metabolized and cytotoxic gemcitabine products is reduced (Hunsucker et al., 2001, 2005). Furthermore, gemcitabine can be deaminated by cytidine deaminase (CDA) into 2',2'-difluorodeoxyuridine (dFdU) becoming inactivated in the cell (Heinemann et al., 1992; Xu and Plunkett, 1992).

Regarding targets, gemcitabine affects nucleotide metabolism as well as DNA replication. Monophosphorylated gemcitabine can be deaminated by deoxycytidylate deaminase (DCTD) being converted into 2',2'-difluorodeoxyuridine monophosphate (dFdUMP). This compound inhibits thymidylate synthase (TS) affecting deoxynucleotide triphosphate (dNTP) pools (Bergman et al., 2000; Heinemann et al., 1992; Xu and Plunkett, 1992). Diphosphorylated gemcitabine further affects deoxynucleotide metabolism by inhibiting ribonucleotide reductase (RNR) and preventing the enzyme from reducing ribonucleotide diphosphates (NDP) to deoxyribonucleotide diphosphates (dNDP). Ribonucleotide reductase is a

key enzyme in dNTP synthesis and is composed by two homodimeric subunits. The dimer formed by ribonucleotide reductase catalytic subunit M1 (RRM1) contains the catalytic subunits and binds a second smaller dimer formed by either ribonucleotide reductase regulatory subunits M2 (RRM2) or ribonucleotide reductase regulatory TP53 inducible subunit M2B (RRM2B) subunits. RRM2 and RRM2B contain an iron-sulfur cluster, which stores the reducing equivalents used during catalysis by RRM1. They are also highly allosterically regulated by ATP and all dNTPs (Reichard, 1997; Stubbe, 2003; Uhlin and Eklund, 1994). The inhibition of RNR by diphosphorylated gemcitabine has severe consequences for the cell, as dNTP pools are drastically reduced, while, in a compensatory mechanism, available deoxynucleosides and gemcitabine are increasingly triphosphorylated (Heinemann et al., 1990). This then intensifies the cytotoxic effects of gemcitabine in the cell increasing the pools of triphosphorylated gemcitabine and thus its chances of being incorporated into DNA. Upon incorporation of triphosphorylated gemcitabine into DNA, DNA Polymerase is able to incorporate one additional dNTP before stalling. DNA repair mechanisms are unable to remove triphosphorylated gemcitabine at the internal as well as at the 3' end position, triggering cell cycle arrest and finally apoptosis (Huang et al., 1991). This way, gemcitabine not only impairs DNA replication, but also inhibits key processes in nucleotide metabolism.

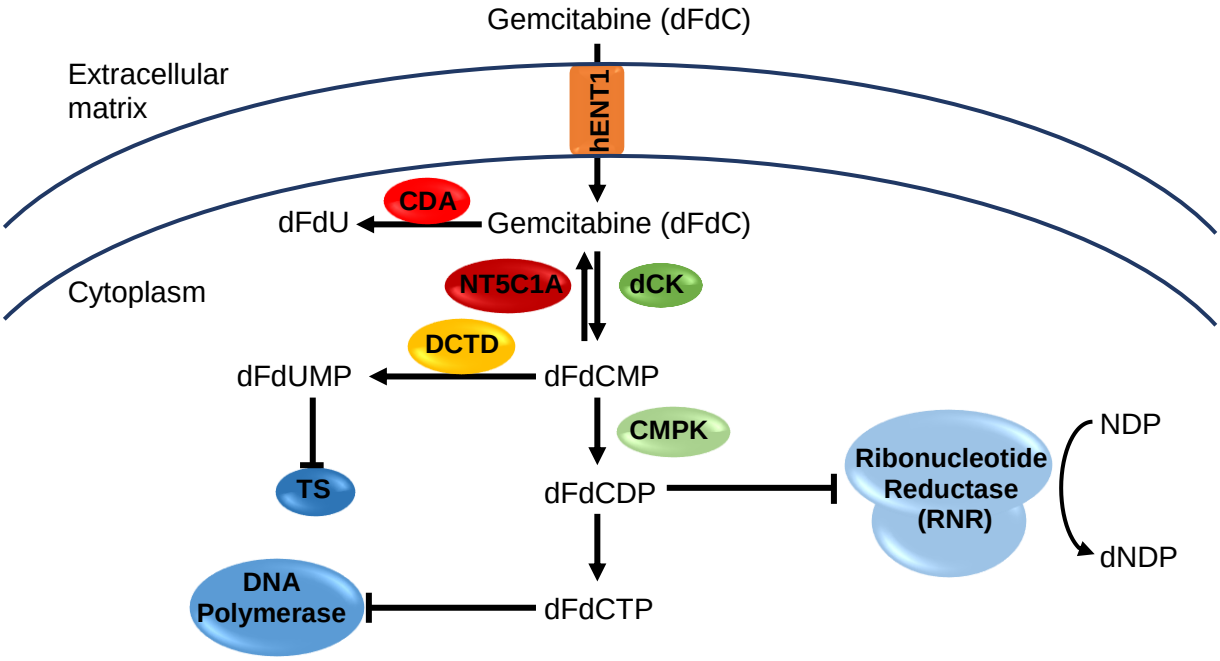

Fig. 3 Gemcitabine metabolism and targets. Gemcitabine is mainly imported by hENT1, but also by hENT2, hCNT1 and hCNT3. It is later monophosphorylated (dFdCMP) by dCK, diphosphorylated (dFdCDP) by CMPK and finally triphosphorylated (dFdCTP) possibly by nucleoside diphosphate kinase. Gemcitabine is deaminated by CDA being inactivated in the cell in the form of dFdU. dFdCMP is also deaminated by CDTD and its product inhibits thymidylate synthase (TS). dFdCDP inhibits ribonucleotide reductase, significantly lowering the dNTP pool in the cell. dFdCTP stalls DNA Polymerase shortly after being incorporated into the daughter strand. The figure was based on the publication by de Sousa Cavalcante et al.

1.1.5. Gemcitabine resistance in PDAC

Even though chemotherapy, specially gemcitabine, is widely administered to PDAC patients, a very small fraction of these patients responds to treatment. When first undergoing clinical trials, gemcitabine was extremely attractive compared to 5-FU as 24% of gemcitabine-treated PDAC patients profited from clinical benefits compared to 5% of 5-FU-treated patients. The median survival rate for gemcitabine-treated patients also slightly increased to 5.65 months compared to 4.41 months for 5-FU-treated patients (Burris et al., 1997). Unfortunately, response rates to gemcitabine were low, with 89% of the patients not responding to gemcitabine treatment and facing chemotherapy resistance (Casper et al., 1994). Gemcitabine resistance is suggested to arise due to extrinsic and intrinsic factors, these being the tumor stroma and the rewiring of gemcitabine metabolism in cancer cells, respectively (Amrutkar and Gladhaug, 2017; De Sousa Cavalcante and Monteiro, 2014).

Regarding extrinsic factors, the exact role of the tumor stroma in chemotherapy resistance is still under investigation. The stroma of pancreatic cancer is known to account for up to 90% of the tumor volume and is suggested to hamper drug delivery and/or scavenge chemotherapy. It is composed of an extracellular matrix rich in hyaluronic acid, fibronectin, secreted protein acidic and rich in cysteine (SPARC) and collagens, cancer-associated fibroblasts (CAFs), inflammatory cells and blood vessels. Key signaling pathways, such as TGFβ and Hedgehog, foster tumor as well as stromal growth and tumor differentiation (Ligorio et al., 2019; Neesse et al., 2011).

In fact, combinatory targeting of the Hedgehog pathway with gemcitabine administration has shown very promising results. In a mouse model, Olive et al.

showed that by inhibiting the Hedgehog pathway and co-treating with gemcitabine, the stroma was reduced, while the tumor showed a higher vascularization. This allowed for a better drug delivery and chemotherapy response. Unfortunately, the stroma quickly became resistant to Hedgehog inhibition, growing back and impeding gemcitabine delivery after 2 weeks of co-treatment (Olive et al., 2009). Reduced fibrosis upon Vitamin-D receptor activation and depletion of hyaluronic acid and collagen have also led to increased drug delivery and response in mouse models (Chauhan et al., 2013; Jacobetz et al., 2013; Provenzano et al., 2012; Sherman et al., 2014). Still, in a different study, SPARC levels did not correlate with overall survival and response to gemcitabine or gemcitabine and nab-Paclitaxel treatment in patients (Hidalgo et al., 2015). Furthermore, the stroma volume was only indicative of chemotherapy response rates in patients after accounting for the expression of gemcitabine transporters, such as hENT1, in tumors (Koay et al., 2014a, 2014b). Thus, whether the tumor stroma provides an effective physical barrier to gemcitabine is still under debate. Still, another role has been accredited to the stroma, this being that of scavenging gemcitabine. Higher levels of active, triphosphorylated gemcitabine (dFdCTP) were found in CAFs compared to tumor cells, while the opposite was true for levels of inactive, deaminated gemcitabine (dFdU). Stromal cells also expressed lower levels of gemcitabine inactivating enzymes, suggesting that they, rather than tumor cells, are more affected by gemcitabine treatment (Hessmann et al., 2018).

Even though the role of the stroma in chemotherapy resistance is still under debate, it is clear that the expression levels of gemcitabine targets and metabolic enzymes are key in gemcitabine resistance. Levels of the nucleotide transporter proteins, hENT1 and hCNT1, in naïve as well as gemcitabine treated patients and cell lines correlated with gemcitabine response (Bhutia et al., 2011; Farrell et al., 2009; Mori et al., 2007; Spratlin et al., 2004). High dCK levels have also been associated with better overall survival and gemcitabine responsiveness in patients (Kroep et al., 2002; Maréchal et al., 2010; Sebastiani et al., 2006). This indicates that the rate-limiting steps of gemcitabine uptake and metabolism are key for patients' response to gemcitabine-based therapy. Taken together, dCK and hENT1 have been suggested as prognostic markers (Maréchal et al., 2012).

Gemcitabine inactivating enzymes, such as CDA and NT5C1A, have also been shown to play an important role in gemcitabine resistance. In neuroblastoma, CDA levels have been shown to negatively correlate with gemcitabine response, while in ovarian cancer, this observation did not hold (Ferrandina et al., 2010; Ogawa et al., 2005). Furthermore, CDA levels varied greatly in human tumor xenografts of pancreatic, lung, colorectal, ovarian and head and neck tumors upon gemcitabine treatment (Kroep et al., 2002). More recently, a study has shown that tumor associated macrophages induce the upregulation of *CDA* in PDAC cells, conferring gemcitabine resistance to the tumor (Weizman et al., 2014). NT5C1A is also robustly expressed by PDAC patients and its overexpression in PDAC mouse models as well as HEK293T cells resulted in increased gemcitabine resistance (Hunsucker et al., 2001; Patzak et al., 2019).

Ribonucleotide reductase levels have also been associated with gemcitabine resistance, although its prognostic value is still under debate. In gemcitabine resistant cell lines, an overexpression of *RRM1* has been reported to drive gemcitabine resistance (Nakahira et al., 2007; Nakano et al., 2007; Wang et al., 2015; Zhou et al., 2019). *In vivo* studies confirmed this finding, identifying *RRM1* as the most highly overexpressed gene in gemcitabine resistant tumors, being upregulated by 25-fold (Bergman et al., 2005). Still, the prognostic value of RRM1 remains under debate, as one study reported a negative correlation between RRM1 levels and gemcitabine responsiveness in patients, another study described a positive correlation and a third patient study did not corroborate any of these findings (Akita et al., 2009; Aoyama et al., 2017; Maréchal et al., 2012). Taken together, gemcitabine resistance in PDAC is primarily driven by the up- and downregulation of target and metabolic genes, while also being modulated by the stroma's scavenging ability and physical barrier.

1.2. The Integrated Stress Response (ISR)

Many chemotherapeutic drugs are known to not only act on their specific targets, but to also trigger a more general cellular stress response. Furthermore, due to the hypoxic and nutrient deprived environment of tumors, cancer cells experience chronic stress (Avril et al., 2017). The integrated stress response (ISR) is activated in response to stress cues such as amino acid deprivation, viral infection, heme

deprivation and the accumulation of unfolded proteins in the endoplasmic reticulum (ER) signaling ER stress. It converges at the halt of global cap-dependent translation, achieved by the phosphorylation of the eukaryotic translation initiation factor 2 alpha subunit (eIF2α). This leads to the cap-independent translation of the activating transcription factor 4 (ATF4), which can then fine-tune the stress response, triggering the transcription of pro-survival genes and, if the cell fails to respond, of apoptotic genes (Fig. 4) (Pakos-Zebrucka et al., 2016).

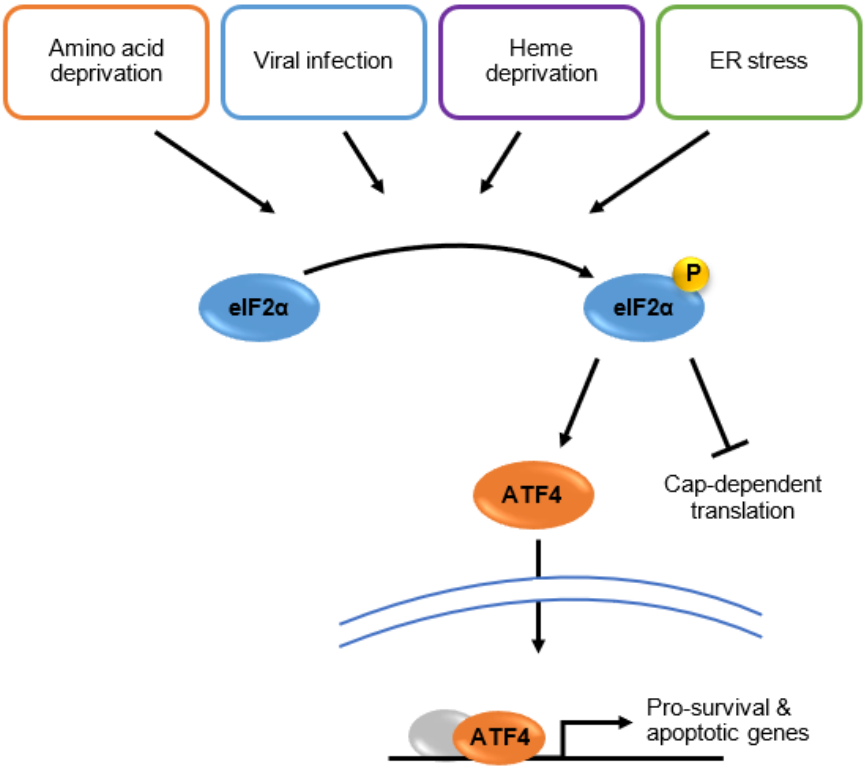

Fig. 4 An overview of the integrated stress response. Different sources of stress activate their respective stress kinase, which phosphorylates eIF2α, shutting down cap-dependent translation and activating ATF4. ATF4 promotes the transcription of stress responsive pro-survival and apoptotic genes. Figure based on Pakos-Zebrucka et al.

1.2.1. ISR in pancreatic diseases

The ISR is of great importance in the pancreas, playing a role in insulin-secreting pancreatic β cells, acute and chronic pancreatitis and possibly in pancreatic cancer. It is the main trigger of type I diabetes, where the pancreas produces little or no pro-insulin. Because glucose levels are constantly fluctuating in pancreatic β cells, pro-insulin production in the ER is accordingly highly variable. This can cause an acute accumulation of unfolded pro-insulin in the ER, triggering ER stress. Furthermore,

mutations in the insulin coding region can prevent proper protein folding in the ER, also leading to the accumulation of unfolded pro-insulin and ER stress. For these reasons, it is crucial that pancreatic β cells express robust amounts of ISR sensors and mediators to properly cope with such stresses; activating the pro-survival branch of the ISR and, only if needed, undergoing apoptosis. Several studies have shown that mutations in ISR components can lead to a failure in the stress response, increased apoptosis of pancreatic β cells and, consequently, to type I diabetes (Harding et al., 2001; Ladiges et al., 2005; Wang et al., 1999).

A very similar phenomenon is found in pancreatic acinar cells that produce and secrete digestive enzymes, such as trypsinogen and chymotrypsinogen, and, when malfunctioning, can trigger acute and chronic pancreatitis. In pancreatitis, acinar cells fail to properly fold, post-translationally modify, package and/or secrete digestive enzymes. This leads to an early intrapancreatic activation of these enzymes and consequently to the digestion of the pancreas followed by inflammation (Gukovskaya et al., 2019; Habtezion, 2015; Pandol et al., 2007). Several studies have shown that in the early stages of pancreatitis development, mice presented an increase in the stress response, more specifically in ER stress response (Kubisch et al., 2006; Logsdon and Ji, 2013; Lugea et al., 2012; Sah et al., 2014; Waldron et al., 2018) . Thus, again, the correct folding of digestive enzymes is crucial for proper functioning of acinar cells and a robust and functional ER stress response is critical to resolve this. Mutations in trypsinogen and trypsinogen inhibitor proteins have been shown to lead to an accumulation of unfolded proteins in the ER, triggering ER stress and predisposing people to pancreatitis (Hegyi and Sahin-Tóth, 2019; Teich et al., 2006).

The role of the ISR in pancreatic cancer is not as well characterized as in pancreatitis and diabetes, but the ISR is commonly hijacked in several cancer types and there are some suggestions that ER stress may contribute to gemcitabine resistance. In general, the tumor microenvironment is highly deprived of nutrients and oxygen, thus it is common that cancer cells activate the ISR. In fact, during nutrient starvation, tumors activate the ISR and are able to, this way, maintain amino acid homeostasis. Furthermore, nutrient starvation promotes a metabolic plasticity triggered by the ISR, which is crucial for cancer cells to quickly adapt to changing environments (Sun et al., 2015; Ye et al., 2010). Hypoxia is also common in tumors,

triggering ER stress and inhibiting cap-dependent translation with the aim of reducing energy consuming processes (Blais et al., 2004; Koritzinsky et al., 2006). Interestingly, it was shown that some solid tumors even rely on hypoxia and ER stress to activate *LAMP3*, a gene tightly associated with metastasis (Mujcic et al., 2013). Thus, even though some cancer cells undergo apoptosis due to ISR activation, tumors usually adapt and use the pro-survival branch of the ISR to thrive in stressful environments. Furthermore, although these studies were conducted mainly in solid tumors other than pancreatic cancer, it is very plausible that the ISR has similar effects in PDAC, as the latter also presents high levels of hypoxia and nutrient deprivation.

Regarding ISR in pancreatic cancer specifically, very recently a study described that ER stress activation results in quiescent and immune evading pancreatic cancer cells. Furthermore, these cells were shown to constitute the bulk of macrometastases found in the liver, linking ER stress to metastasis (Pommier et al., 2018). ER stress has also been implicated in gemcitabine resistance, in two opposite ways. In one study, gemcitabine resistant tumors were sensitized by ER stress inducers, such as Orlistat and Thapsigargin, while in another study ER stress promoted gemcitabine resistance in PDAC (Palam et al., 2015; Tadros et al., 2017). In conclusion, many processes in pancreatic cancer and in the pancreas in general are highly dependent on the ISR and more specifically on ER stress and on the fine-tuning between its pro-survival and pro-apoptotic branches.

1.2.2. The ISR balance – pro-survival or apoptotic?

As seen in the previous section, the ISR helps many systems cope with stresses and survive them. Still, when failing to resolve the stress, the ISR may lead to apoptosis and cell death. The exact mechanisms behind this switch between pro-survival and apoptotic pathways remains under investigation. It is believed that the ISR signal duration and the levels of phosphorylated eIF2α (peIF2α) and translated ATF4 highly influence the cell's decision to survive the stress or not (Fig. 5).

The pro-survival branch is mainly characterized by an initial alleviation of translation, a highly energy consuming process, and by the upregulation of autophagy and anti-apoptotic genes. By phosphorylating eIF2α and, consequently, shutting down cap-

dependent translation, viral mRNA and globin translation is reduced, thus instantly counteracting viral infections and adjusting globin to heme levels, while preventing the accumulation of globin aggregates (Balachandran et al., 2000; Han et al., 2001). Less translation also leads to a diminished consumption of amino acids helping the cells cope with nutrient deprivation (Vazquez de Aldana et al., 1994). The ER is also less overwhelmed with proteins to be folded, thereby, alleviating ER stress (Guan et al., 2017; Ron, 2002). This immediate response is followed by the translation and activation of ATF4. Several studies have shown that upon different kinds of stresses, ATF4 can upregulate the expression of several autophagy genes, such as *MAP1LC3*, *ATG5* and *SQSTM1* (B'Chir et al., 2013; Rouschop et al., 2010). Autophagy is, thus, initially activated in the cells, as it helps catabolize proteins, replenishing the pool of amino acids, while also lowering the amount of unfolded and viral proteins, therefore further alleviating stress (Kroemer et al., 2010; Ye et al., 2010). Interestingly, a study has shown that the early activation of autophagy does not necessarily mean that all cells undergo autophagy to survive stress. In fact, what Suraweera et al. noticed is that upon proteasome inhibition, a depleted amino acid, such as cysteine, triggers the ISR and consequently autophagy. But, once this critical amino acid is replenished by the cell, peIF2α is dephosphorylated and autophagy is suppressed (Suraweera et al., 2012). Another mechanism employed by the cell to overcome stress is the upregulation of anti-apoptotic genes, such as *MCL-1* and *cIAP1* and *cIAP2* by ATF4 (Hamanaka et al., 2009; Hu et al., 2012, 2004).

It is important to note that the termination of the ISR is crucial for cell survival, as the synthesis of essential proteins has to resume. This is achieved by the dephosphorylation of peIF2α by the phosphatase GADD34, an ATF4 target, thereby restoring cap-dependent translation (Ma and Hendershot, 2003; Novoa et al., 2001). Thus, a timely termination of the ISR can also influence the cell's ability to survive or not in response to stress (Tabas and Ron, 2011). In fact, upon prolonged stress, ATF4 upregulates DNA damage inducible transcript 3 (*DDIT3*), which encodes for the transcription factor CHOP. In response to ER stress, ATF4 and CHOP have been shown to promote the transcription of several pro-apoptotic genes, such as the BCL2 family members, *PUMA* and *BIM* (Galehdar et al., 2010; Puthalakath et al., 2007). Furthermore, CHOP upregulates the oxidase *ERO1α* turning the oxidizing

environment in the ER into a hyperoxidizing environment. This has severe consequences as reactive oxygen species accumulate in the ER and proteins cannot be properly folded, aggravating ER stress and promoting apoptosis (Marciniak et al., 2004). Another important target gene of ATF4 and CHOP is tribbles pseudokinase 3 (*TRIB3*), which was shown to repress tumorigenesis and promote apoptosis by inhibiting AKT activation (Ohoka et al., 2005; Salazar et al., 2015). TRIB3 was also shown to negatively regulate ATF4, dampening the stress response and its own expression (Jousse et al., 2007; Liew et al., 2010). Furthermore, Liew et al. showed that pancreatic β cells that have the *TRIB3* Q43R polymorphism have a greater stabilization of TRIB3 and thus are much more prone to stress-induced apoptosis. As a consequence, these cells fail to cope with the normal ER stress associated with pro-insulin production undergoing cell death at a higher frequency, failing to secrete insulin and leading to type I diabetes (Liew et al., 2010). In conclusion, peIF2α and ATF4 are key mediators of the stress response, instantly relieving the cells from the energy consuming process of translation, while activating autophagy, anti-apoptotic and pro-apoptotic genes. The activation intensity and duration of peIF2α and ATF4 are key determinants of the cellular ability to thrive under stress or to undergo programmed cell death.

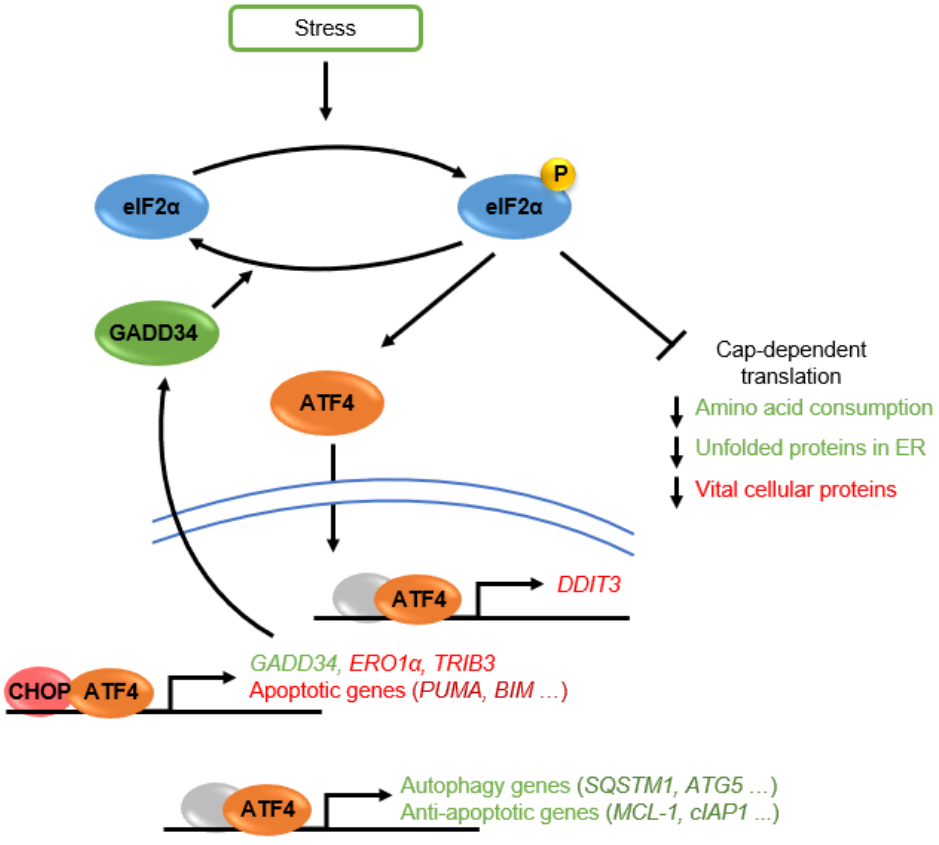

Fig. 5 Activation of pro-survival and apoptotic pathways by the ISR. The phosphorylation of eIF2α by stress kinases inhibits cap-dependent translation, which relieves the cell from consuming amino acids and from accumulating unfolded proteins in the ER. Still, if translation is not resumed, vital proteins become scarce potentiating stress and triggering apoptosis. The activation of ATF4 leads to the upregulation of autophagy, anti-apoptotic and apoptotic genes. GADD34 provides a feedback mechanism by dephosphorylating peIF2α, while CHOP dimerizes with ATF4 to regulate apoptotic genes. In green and red are pro-survival and apoptotic target genes and processes, respectively.

1.2.3. ER stress

ER stress response, as shown in the previous sections, is essential for the proper functioning of the pancreas, while its role in pancreatic cancer and chemotherapy response is still being studied. The accumulation of unfolded proteins signals ER stress, triggering the unfolded protein response (UPR). In this process, different ER protein chaperones act as sensors, which, upon disturbances, activate ER stress mediators. These relay the signal activating several transcription factors and responsive genes, while also stimulating the ISR by phosphorylating eIF2α (Urra et al., 2016; Walter and Ron, 2011). As the ER is a central organelle for several cellular processes, the UPR is tightly coupled to and can be further activated by changes in the oxidizing environment and perturbations in calcium levels in the ER as well as by variations in ATP and glucose levels in the cell (Rutkowski and Hegde, 2010).

1.2.3.1. ER stress mediators

ER stress mediators are the bridge between ER homeostasis and the stress response, phosphorylating eIF2α and activating b-ZIP transcription factors: activating transcription factor 6 (ATF6), X-box binding protein 1 (XBP1) and ATF4. The ER stress mediators are comprised of three transmembrane ER proteins: ATF6, inositol requiring enzyme 1 (IRE1), and PKR-like ER kinase (PERK). While ATF6 activates UPR-responsive genes including mainly protein chaperone genes, IRE1 leads to the upregulation of protein chaperone, lipid synthesis and ER-associated protein degradation (ERAD) genes (Hetz, 2012; Hillary and Fitzgerald, 2018; Vekich et al., 2012). PERK leads to the activation of the transcription factor nuclear factor erythroid 2-related factor 2 (NRF2) and of the ISR by phosphorylating eIF2α and triggering ATF4 accumulation. Consequently PERK stimulates the transcription of *CHOP*, *GADD34*, pro-survival, apoptotic and antioxidant genes (Fig. 6) (Maas and Diehl, 2015; Pakos-Zebrucka et al., 2016).

ATF6 is an ER-transmembrane protein, which upon ER stress, is vesicle transported by COPII to the Golgi apparatus. There, site-1 protease (S1P) cleaves off the luminal domain of ATF6 and site-2 protease (S2P) removes the transmembrane anchor of ATF6. The N-terminus of ATF6 is then released in the cytosol translocating into the nucleus and activating several ER protein chaperone genes, such as heat shock protein family A (Hsp70) member 5 (GRP78) and protein disulfide isomerase family A member 6 (PDIA6) (Haze et al., 1999; Schindler and Schekman, 2009; Vekich et al., 2012; Ye et al., 2000). Furthermore, ATF6 can upregulate *XBP1*, the substrate of another ER stress mediator, IRE1 (Yoshida et al., 2001). Thus, ATF6 not only senses ER stress, but also activates responsive genes to cope with stress and potentiates ER stress response by upregulating ER stress mediator targets.

IRE1 is a kinase, but also has RNase activity, splicing the XBP1 mRNA. Upon ER stress, IRE1 autophosphorylates *in trans*, oligomerizing and stabilizing its RNase active site. Oligomerized IRE1 binds TRAF2, fostering the mitogen-activated protein kinase (MAPK) signaling pathway. This leads to the activation of JNK, which, in turn, stimulates the pro-apoptotic protein BIM and inhibits the anti-apoptotic protein BCL2, promoting apoptosis (Urano et al., 2000; Xu et al., 2005). Still, IRE1 also fosters pro-survival pathways, by promoting the accumulation of XBP1. IRE1 splices out an intron of the XBP1 mRNA by using its RNase activity to cut the XBP1 transcript at two different positions. This leads to the shifting of the open reading frame, such that the mRNA can be properly translated (Ali et al., 2011; Shamu and Walter, 1996; Yoshida et al., 2001). XBP1 then translocates into the nucleus activating mainly pro-survival genes, such as protein chaperones, ERAD subunits and lipid synthesis protein coding genes. Thus, XBP1 promotes the proper folding of newly synthesized proteins and the degradation of unfolded proteins, while also stimulating the production of phospholipids for ER membrane expansion (Hetz, 2012; Lee et al., 2003). The negative regulation of XBP1 involves the destabilization of IRE1 oligomers due to an accumulation of phosphates and charge repulsion or by the action of receptor of activated C kinase 1 (RACK1) and protein phosphatase 2A (PP2A), which dephosphorylate IRE1 oligomers. As a consequence, less XBP1 mRNA is spliced and translated, dampening the stress response (Qiu et al., 2010; Walter and Ron, 2011).

The third ER stress mediator is PERK, which senses unfolded proteins in the ER and undergoes oligomerization and autophosphorylation. PERK does not only phosphorylate itself, but also has NRF2 and eIF2α as substrates (Carrara et al., 2015; Cullinan et al., 2003; Harding et al., 2009; Mukaigasa et al., 2018; Wang et al., 2018). NRF2 is a transcription factor, which upon phosphorylation by PERK, translocates into the nucleus and activates metabolic enzymes and antioxidant protein coding genes (Cullinan et al., 2003; Hayes and Dinkova-Kostova, 2014; Mukaigasa et al., 2018). Thus, upon ER stress, PERK and consequently NRF2 activation lead to an antioxidant response, protecting the cell and the ER from reactive oxygen species.

PERK also phosphorylates eIF2α leading to an inhibition of global cap-dependent translation and a cap-independent translation of ATF4, triggering the transcription of the aforementioned pro-survival and apoptotic genes. Furthermore, ATF4 together with CHOP promote the transcription of *GADD34*, a phosphatase whose main substrate is peIF2α and which negatively regulates PERK-dependent ER stress response (Harding et al., 2009; Marciniak et al., 2004). Interestingly, ATF4 was also shown to upregulate endoplasmic reticulum to nucleus signaling 1 (*ERN1*), the gene coding for IRE1, thus fostering the splicing of XBP1 and positively regulating the stress response (Tsuru et al., 2016). XBP1, in turn, was proven to upregulate DnaJ homolog subfamily C member 3 (DBAJC3), which binds to the kinase domain of PERK inhibiting it and lowering pNRF2 and peIF2α levels (Lee et al., 2003; Yan et al., 2002). Thus, PERK directly links ER stress to the ISR and is tightly regulated by its downstream targets as well as the targets of other ER stress mediators.

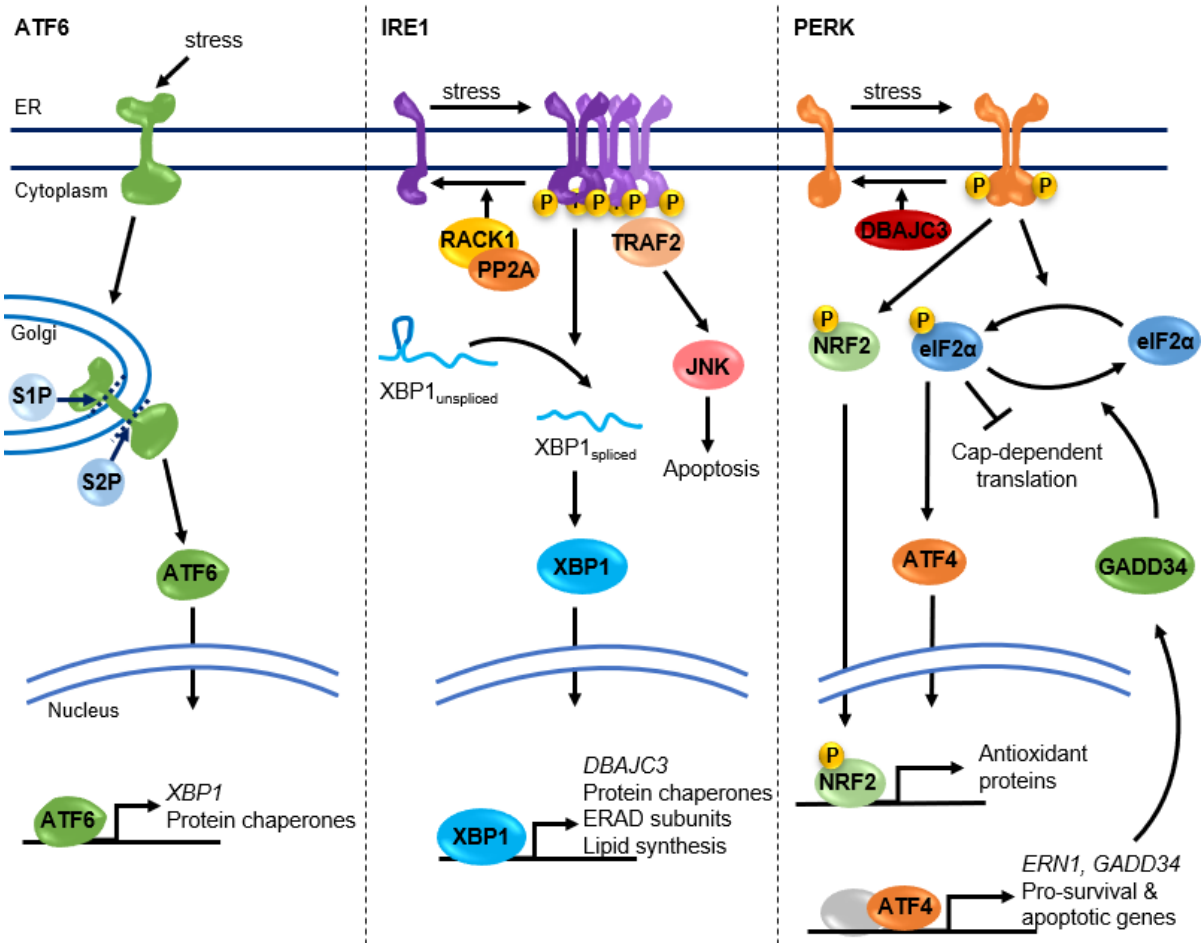

Fig. 6 The ER stress mediators ATF6, IRE1 and PERK trigger the ER stress response. Upon ER stress, ATF6 is transported to the Golgi apparatus, where it is cut by S1P and S2P and released in the cytoplasm. Active ATF6 then translocates into the nucleus upregulating protein chaperone genes and *XBP1.* Following ER stress, IRE1 autophosphorylates, activating JNK and promoting apoptosis. It also splices the mRNA of XBP1, which then translocates into the nucleus activating protein chaperones, ERAD subunit and lipid synthesis protein coding genes. It also upregulates *DBAJC3*. IRE1 is negatively regulated by the destabilization of its oligomers through charge repulsion or by the phosphatase complex RACK-1-PP2A. PERK is the third ER stress mediator, which dimerizes and autophosphorylates upon stress. PERK phosphorylates NRF2, which becomes active upregulating antioxidant genes. The ISR is also triggered by PERK, which phosphorylates eIF2α leading to a global shut down of translation and ATF4 activation. As ATF4 translocates into the nucleus, *GADD34*, *ERN1*, pro-survival and apoptotic genes are upregulated. The figure was based and modified from Walter et al. and Carreras-Sureda et al.

1.2.3.2. ER stress sensors

ER stress is a result from protein chaperones in the ER responding to the accumulation of unfolded proteins triggered by environmental changes. These changes encompass disturbances in the oxidizing environment and calcium levels in the ER as well as overall cellular ATP levels and culminate in the accumulation of unfolded proteins. Proteins being folded in the ER contain several disulfide bonds,

requiring an oxidizing environment. Thus, failure to recycle protein disulfide isomerases upon oxidative stress, leads to an accumulation of misfolded proteins, which lack disulfide bonds. Furthermore, protein chaperones need ATP to bind and release proteins, coupling protein folding to overall energy levels in the cell. Calcium is a second messenger, which is stored in the ER and released upon distinct signals, including ER stress. It is buffered and used as a co-factor by protein chaperones, linking the UPR to several cellular processes such as apoptosis, oxidative phosphorylation and transcriptional activation (Fig. 7) (Carreras-Sureda et al., 2018; Ma and Hendershot, 2004; Zhang et al., 2019b).

The general protein chaperone, GRP78, is the main sensor of unfolded proteins and direct regulator of ER stress mediators. Under unstressed conditions, GRP78 inhibits the ER stress mediators by directly interacting with their luminal domains, which in turn hinder the ATPase activity of GRP78. Upon stress, GRP78 binds unfolded proteins and hydrolyzes ATP to ADP trapping the unfolded protein and dissociating from ER stress mediators triggering ER stress. Only after successfully folding of the protein and exchanging ADP for ATP is GRP78 able to inhibit ER stress mediators again (Bertolotti et al., 2000; Kopp et al., 2019). Thus, GRP78 is the major sensor of accumulated unfolded proteins in the ER and of cellular ATP levels, while being the main activator of the stress response.

Further protein chaperones, such as protein disulfide isomerases, which catalyze the formation of disulfide bonds and are thus direct readouts of the ER redox state, have also been shown to regulate specific ER stress mediators. Upon oligomerization of IRE1 under stress, two intermolecular disulfide bonds form, stabilizing the complex (Liu et al., 2003). The protein disulfide isomerase, PDIA6, can in turn break these disulfide bonds, destabilizing the complex and dampening the ER stress response (Eletto et al., 2014). ATF6 also presents inter- and intramolecular disulfide bonds, which can be resolved by the protein disulfide isomerase PDIA5 upon stress. This facilitates the trafficking of ATF6 to the Golgi apparatus, but is not sufficient to promote ATF6 activation (Higa et al., 2014; Nadanaka et al., 2007). Taken together, protein disulfide isomerases regulate ER stress mediators, while providing a direct link between the redox state in the ER and the UPR.

Calcium has also been tightly associated with protein chaperones, modulating the ER stress response by affecting chaperoning activity, while also providing a link between ER protein chaperones and other processes in the cell (Carreras-Sureda et al., 2018; Gutiérrez and Simmen, 2018). ER protein chaperones buffer almost all calcium in the ER, while also using it as a co-factor. One such example is GRP78, which alone buffers about 25% of ER calcium (Lièvremont et al., 1997). Furthermore, the glycoprotein chaperones, calnexin (CNX) and calreticulin (CRT), also bind calcium and, in fact, the structure of the C-terminal domain of CRT is highly dependent on how many calcium ions it binds and overall calcium levels in the ER (Giraldo et al., 2010). Calcium buffering in the ER and in the cell is essential, as it controls the amount of calcium which can be released upon a stimulus, fine tuning the cellular response to stimuli (Smith and Eisner, 2019). Furthermore, the chaperoning activity of GRP78, CNX and CRT depends on calcium and is reduced upon low calcium levels in the ER. Thus, calcium levels directly influence protein chaperoning, the UPR and ER stress activation (Ivessa et al., 1995; Prins and Michalak, 2011; Vassilakos et al., 1998).

Recent studies have shown that ER protein chaperones can also directly regulate ER calcium levels by controlling ER calcium influx and efflux. The protein disulfide isomerase PDIA19 has been shown to activate the sarco/endoplasmic reticulum ATPase (SERCA) pump under stress, promoting an influx of calcium in the ER (Ushioda et al., 2016). GRP78 has also been implicated in promoting the efflux of calcium from the ER by inhibiting endoplasmic reticulum protein 44 (ERp44) under normal, but not stressed conditions. ERp44, in turn, inhibits calcium efflux through the inositol 1,4,5-triphosphate receptor (IP_3R). Thus, under normal conditions GRP78 prevents ERp44 from inhibiting IP_3R leading to calcium efflux. Upon stress, ERp44 can successfully obstruct IP_3R, hindering further calcium release from the ER (Higo et al., 2010). Thus, several protein chaperones try to restore calcium levels in the ER in order to facilitate protein folding. Furthermore, by regulating ATP dependent calcium pumps and calcium efflux, protein chaperones affect oxidative phosphorylation and calcium dependent apoptosis in the mitochondria (Carreras-Sureda et al., 2018; Gutiérrez and Simmen, 2018). This way, calcium allows protein chaperones to not only fine tune their activity and trigger the ISR, but also to modulate the mitochondrial response to ER stress.

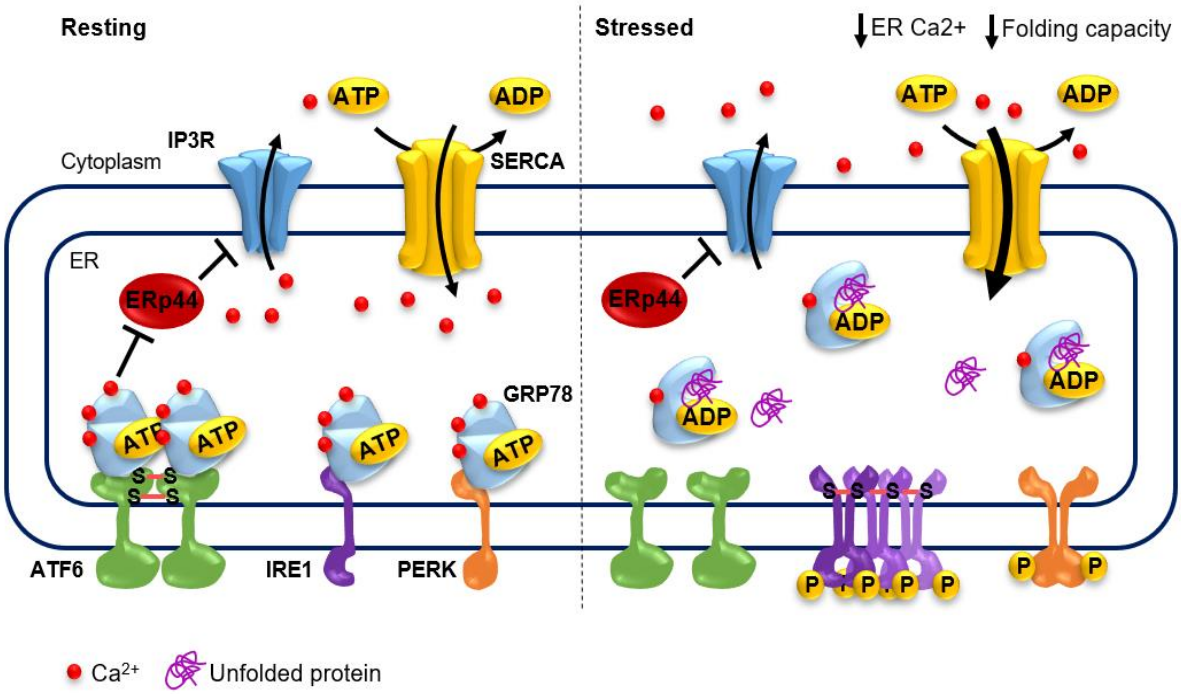

Fig. 7 ER stress is triggered by the dissociation of protein chaperones from ER stress mediators upon accumulation of unfolded proteins. During resting conditions, GRP78 inhibits the activation of ER stress mediators, which in turn hinder the ATPase activity of GRP78. Furthermore, GRP78 buffers 25% of ER calcium and regulates Calcium efflux by inhibiting ERp44. ATF6 is further stabilized by disulfide bonds sensing the redox state in the ER. Upon stress, GRP78 dissociates from ER stress mediators as it hydrolyzes ATP and starts folding proteins. Calcium levels highly modulate the protein folding activity of GRP78 and other protein chaperones. Thus, in an attempt to restore calcium levels and increase its folding activity, GRP78 no longer inhibits ERp44 allowing it to obstruct IP_3R and hinder calcium efflux. At the same time calcium influx is stimulated by further activation of SERCA. Furthermore, IRE1 oligomers are stabilized by disulfide bonds, which are only resolved once the oxidizing environment in the ER is restored. Thus, once protein disulfide isomerases are functioning normally again, IRE1 oligomers are reduced and destabilized, dampening the ER stress response. The figure was based on and adapted from Carreras-Sureda et al. and Gutiérrez et al.

1.3 Calcium signaling

As seen in the previous section, calcium is one of the major players during ER stress, modulating protein chaperone activity, while also integrating the ER stress response with other cellular processes. Calcium homeostasis is achieved by several channels, exchangers and pumps in the ER, mitochondrial and cytoplasmic membrane. Ion gradients and ATP are consumed in order to maintain low cytosolic and high ER calcium levels. Upon stimuli, calcium is released from storage organelles, such as the ER, activating transcription factors in the cytoplasm, while also affecting mitochondrial activity.

1.2.4. Calcium homeostasis

Under resting conditions, the cytoplasmic free calcium concentration is 100nM, being 10,000 times lower than the extracellular calcium concentration (1mM) (Monteith et al., 2017). The free calcium levels in the ER are, in turn, higher and range between 100-800µM, while total ER calcium concentrations range between 1-3mM (Carreras-Sureda et al., 2018). Calcium pumps and calcium ion exchangers create these gradients, allowing calcium to flow through channels flooding the cytoplasm upon stimuli (Fig. 8A, B).

In the cytoplasmic membrane, plasma membrane Ca^{2+}-transporting ATPase (PMCA) pumps calcium from the cytoplasm into the extracellular matrix at the cost of ATP hydrolysis (Strehler and Zacharias, 2001). The plasmalemmal sodium Na+/Ca2+ exchangers (NCXs) also export calcium from the cytoplasm by allowing sodium ions go down the concentration gradient (Blaustein et al., 2008). Calcium influx is facilitated by calcium channels, which open in response to different stimuli. Voltage-gated calcium channels respond to electric stimuli, promoting an influx of calcium mainly in neurons, endocrine, smooth muscle and cardiac cells (Catterall, 2011). The transient receptor potential (TRP) family of calcium channels are responsible for responding to other environmental stimuli such as light, temperature, chemicals and mechanical stress. Only two TRP channels are known to be constitutively active, that being TRPV5 and TRPV6, which are expressed in the kidney and gastrointestinal tract and are responsible for absorbing calcium (den Dekker et al., 2003). It has been shown that stimuli can also promote the opening of both voltage-gated and TRP channels at the same time. One such example is that of insulin secretion by pancreatic β cells, which relies on voltage gated as well as TRP proteins. The hormone glucagon-like peptide 1 (GLP-1), promotes the opening of voltage-gated channels, TRPM4 and TRPM5 leading to a depolarization of the cytoplasmic membrane and thus stimulating the secretion of insulin in pancreatic β cells (Shigeto et al., 2015; Uchida et al., 2011).

Another calcium channel family in the cytoplasmic membrane is the calcium release-activated calcium channel (ORAI) family, which comprises ORAI calcium release-activated calcium modulators 1, 2 and 3 (ORAI1, ORAI2 and ORAI3), ORAI1 being the best characterized one. ORAI is activated upon ER calcium store depletion

promoting the increase of cytoplasmic calcium levels in a process called store operated calcium entry (SOCE) (Prakriya and Lewis, 2015a). Thus, ORAI has a unique function, by which it can promote calcium influx in a depolarized cell as well as in response to internal signals and changes in cellular microdomains (Berridge et al., 2000; Parekh, 2011). Stromal interaction molecules (STIMs) are ER transmembrane proteins, which sense the drop in ER calcium levels, undergoing conformational changes, oligomerizing and activating ORAI at ER-cytoplasmic membrane junctions (Jing et al., 2015; Prakriya and Lewis, 2015a). ORAI channel activity is further modulated by the number of STIM it interacts with, being highest in a ratio of 2-8 STIM per ORAI. Thus, the stoichiometric ratio of STIM to ORAI determines the rate of calcium influx and the total calcium levels imported by the cell (Hoover and Lewis, 2011; Li et al., 2011). The STIM protein family is comprised by stromal interaction molecule 1 (STIM1) and stromal interaction molecule 2 (STIM2). STIM1 has a high affinity for calcium ions, thus, sensing big changes in ER calcium levels due to stimuli and rapidly activating SOCE (Luik et al., 2008). STIM2, on the other hand, has a lower affinity for calcium, being more susceptible to small calcium changes and activating SOCE to control resting calcium levels (Brandman et al., 2007). SOCE is further regulated by phosphorylation and redox modulation of STIM, pH and temperature (Bogeski et al., 2010; Lopez et al., 2012; Prakriya and Lewis, 2015a; Saul et al., 2016). Furthermore, the ER transmembrane protein SOCE-associated regulatory factor (SARAF) senses ER calcium levels and upon replenishing of the stores, promotes the dissociation of STIM1 and STIM2 from ORAI (Jha et al., 2013; Palty et al., 2012). Calcium has also been proven to regulate SOCE, but the exact mechanism is still under investigation (Prakriya and Lewis, 2015a). Thus, ORAI and STIM bridge changes in ER calcium levels and calcium influx in the cytoplasm (Fig. 8B).

ER calcium levels are further monitored and maintained by the IP_3R, which releases ER calcium into the cytosol upon inositol 1,4,5-triphosphate (IP_3) binding. G-protein coupled receptors (GPCRs) and receptor tyrosine kinases (RTK) lead to the production of IP_3 , which activates IP_3R triggering ER calcium efflux upon several external signals (Berridge et al., 2000). In turn, ER calcium levels are restored by SERCA, which hydrolyze ATP in order to transport calcium ions against the concentration gradient back into the ER (Vandecaetsbeek et al., 2011). Still, even

in the absence of stimuli, calcium leaks from the ER counteracting SERCA by means which are still being elucidated (Lomax et al., 2002; Mogami et al., 1998). Recently, transmembrane and coiled-coil domains 1 (TMCO1) has been described to homotetramerize, forming a calcium channel and allowing ER leakage upon calcium overload in the ER by SERCA (Wang et al., 2016).

Calcium levels are further controlled in the mitochondria. Calcium is imported into the mitochondria by the mitochondrial calcium uniporter (MCU), at the cost of protons and the electrochemical gradient (Perocchi et al., 2010; De Stefani et al., 2016). Whereas sodium ions are exchanged during the efflux of calcium from the mitochondria by the Na^+/Ca^{2+} Li^+-permeable exchanger (NCLX), a protein highly homologous to NCX in the plasma membrane (Palty et al., 2010). Calcium regulation in the mitochondria is tightly coupled to ER calcium levels and changes in mitochondrial calcium levels can rewire metabolism or trigger apoptosis (Carreras-Sureda et al., 2018; Gutiérrez and Simmen, 2018). Taken together, calcium homeostasis is achieved by calcium pumps, channels and exchangers, which communicate across organelles ensuring appropriate calcium levels in all cellular compartments.

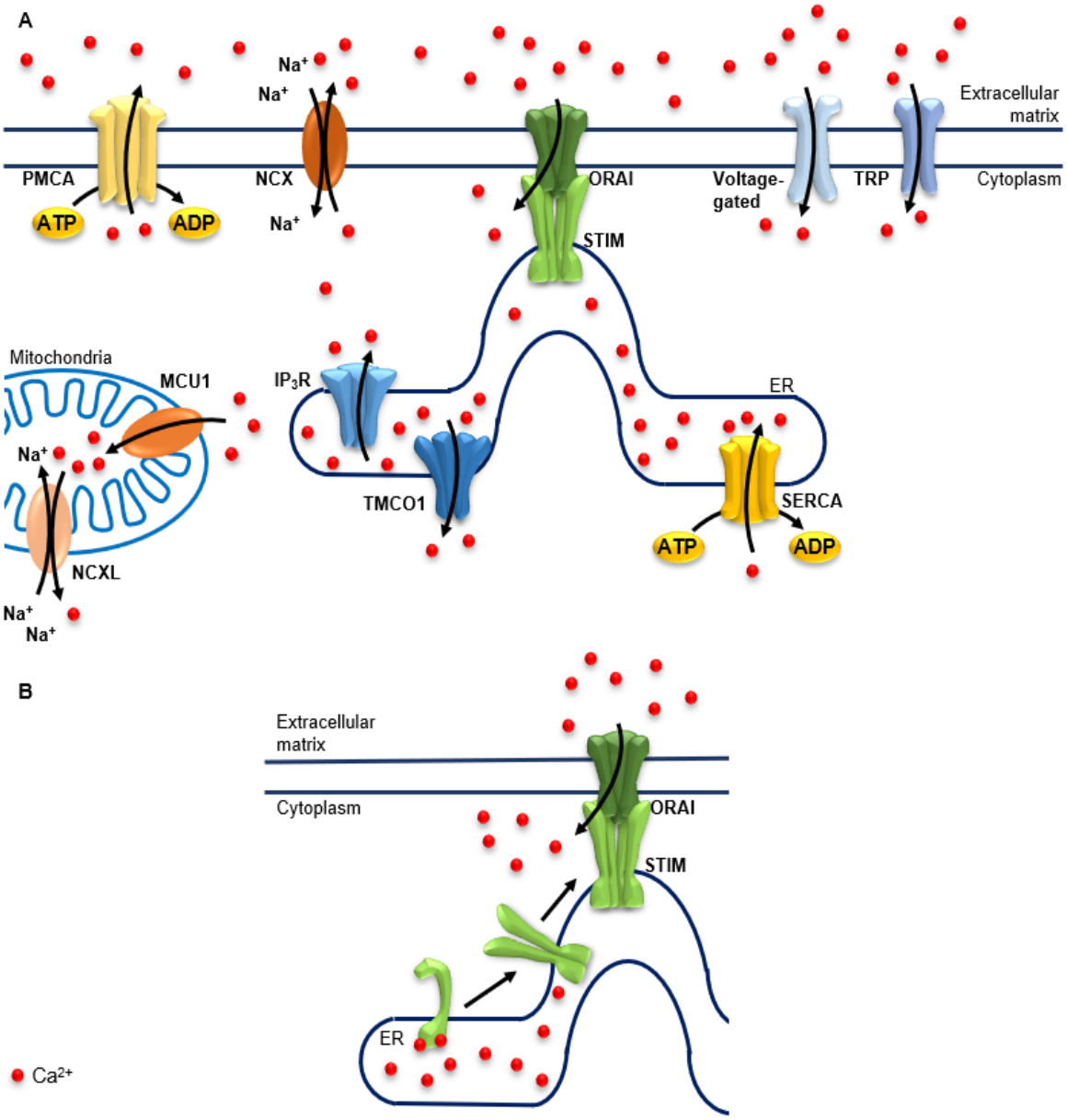

Fig. 8 Pumps, channels and exchangers ensure Calcium homeostasis in the cell. A. ATP- driven pumps, sodium exchangers and inducible channels are responsible for calcium homeostasis in the cell. B. Under resting conditions, STIM binds and buffers calcium and does not interact with ORAI. When ER calcium levels drop, STIM oligomerizes, activating ORAI and promoting an influx of calcium into the cytoplasm. In blue, yellow, orange and green are calcium channels, pumps, exchangers and SOCE members, respectively. Even though MCU is not an exchanger, its activity is directly influenced by the proton gradient in the mitochondria. The figures were based on Monteith et al. and Jing et al.

1.2.5. Calcium-dependent signaling

The importance of calcium in mediating cellular responses to environmental stimuli has been first reported in 1883, where electrolytes were described to be essential for muscle contraction (Ringer, 1883). Since then, great advances in calcium signaling have been made and its importance in the most distinct cellular processes recognized. The intensity of calcium uptake by the cell and its organelles together with the amount of calcium released by cellular stores determine the kinetics and intensity of the response to a stimulus. Furthermore, changes in calcium levels in different cellular compartments can have drastic consequences. Increases in mitochondrial calcium levels upon stimuli can lead to metabolic changes or apoptosis. Meanwhile, higher cytoplasmic calcium levels can trigger the activation of several calmodulin-dependent proteins culminating in the activation of a diverse range of transcription factors (Fig. 9) (Berridge et al., 2000, 2003; Carreras-Sureda et al., 2018; Giorgi et al., 2018).

In non-excitable cell systems, G-protein coupled receptors (GPCRs) and receptor tyrosine kinases (RTKs) relay external events to the cell often by activating calcium-dependent signaling cascades in the cell. Upon substrate binding, GPCRs and RTKs are activated, phosphorylating phospholipase C (PLC). Once activate, PLC hydrolyzes phosphatidylinositol 4,5-bisphosphate (PIP_2) into inositol 1,4,5-triphosphate (IP_3) and diacylglycerol (DAG) (Hanlon and Andrew, 2015; Lemmon and Schlessinger, 2010). IP_3 then interacts with the IP_3R in the ER, promoting the release of calcium from the ER into the cytoplasm. As cytoplasmic calcium increases, protein kinase C (PKC) binds calcium and DAG, thereby, being activated. PKC then phosphorylates several targets, such as components of the MAPK pathway, amplifying the stimulus sensed by GPCRs and RTKs (Lipp and Reither, 2011; VanRenterghem et al., 1994). This way, PKC activity and the overall signaling intensity are directly modulated by cytoplasmic calcium levels. Consequently, several calcium channels, pumps and exchangers modulate PKC activity. STIM1 and ORAI1 positively regulate PKC, by sensing the calcium depletion from the ER and promoting SOCE, leading to a further increase in cytosolic calcium levels. Still, PKC activity itself and SOCE are negatively regulated by PMCA, NCX and SERCA, which pump calcium out of the cytoplasm into the extracellular matrix and ER

restoring resting calcium levels (Lipp and Reither, 2011). Mitochondrial pumps and exchangers can also affect signal intensity and SOCE, as they can significantly buffer cytoplasmic calcium. Depending on MCU levels, more or less calcium is pumped from the cytoplasm into the mitochondria. This leads to a fast depletion of calcium from the cytoplasm and a slow replenishment of the ER with calcium, modulating PKC and SOCE, respectively (Giorgi et al., 2018). Thus, GPCRs and RTKs rely on an increase in cytosolic calcium levels to activate PKC and the MAPK pathway. Consequently, the kinetics of the response are highly regulated by calcium pumps, channels and exchangers in all cellular compartments, as these are closely interconnected.

In fact, there is a tight coupling between ER and mitochondrial calcium levels. Upon several stimuli, such as ER stress, calcium is released through the IP_3R channel and taken up by the mitochondrial MCU. A significant, but relatively low, increase in mitochondrial calcium boosts oxidative phosphorylation and thus ATP production. Still, an overflow of calcium in the mitochondria can trigger apoptosis (Giorgi et al., 2018; Monteith et al., 2017). Thus, by regulating IP_3R and SERCA, as discussed in the previous section, ER protein chaperones are not only regulating their chaperoning activity, but are also modulating the mitochondrial response to ER stress (Carreras-Sureda et al., 2018; Gutiérrez and Simmen, 2018). Taken together, calcium allows the ER to easily communicate with the mitochondria, influencing energy production and cell death initiation based on external and internal cues.

Moreover, increased cytoplasmic calcium levels due to stress or any other signal also lead to the activation of calmodulin-dependent proteins, such as kinases and phosphatases. These, in turn, promote the activation and/or de-repression of several other transcription factors (Dewenter et al., 2017; Feske, 2007). Calcium/calmodulin-dependent protein kinase II (CAMKII) is activated upon calmodulin binding and autophosphorylation, being able to then translocate to the nucleus and phosphorylate Calcium/calmodulin-dependent protein kinase IV (CAMKIV). CAMKII and CAMKIV further phosphorylate and activate several transcription factors in the cytoplasm and in the nucleus (Ma et al., 2014). Still in the cytoplasm, CAMKII releases NFκB from an inhibitory complex by activating inhibitor of nuclear factor kappa B kinase subunit beta (IKK2) (Gray et al., 2017; Kashiwase et al., 2005; Ling et al., 2013). Once in the nucleus, cAMP response element binding

protein (CREB) is activated upon Ser133 phosphorylation by CAMKIV, while CAMKII phosphorylates CREB at Ser133 or at Ser142 activating or inhibiting it, respectively (Cruzalegui and Means, 1993; Sun et al., 1994). Another common target of CAMKII and CAMKIV is the serum response factor (SRF), which is activated upon phosphorylation by both enzymes (Flück et al., 2000; Miranti et al., 1995). CAMKII, in turn, is also linked to stress, as it phosphorylates and activates the stress responsive transcription factor heat shock factor 1 (HSF1) at Ser230 (Holmberg et al., 2001; Peng et al., 2010). Protein C-ets-1 (ETS1) is also phosphorylated by CAMKII, but in this case leading to an inhibition of ETS-1 (Cowley and Graves, 2000; Pognonec et al., 1988). Interestingly, CAMKII and CAMKIV can also phosphorylate histone deacetylase 4 (HDAC4) promoting its nuclear export. HDAC4 is known to not only deacetylate histones, but also to repress SRF and myocyte enhancer factor 2 (MEF2). This way, CAMKII and CAMKIV indirectly further activate SRF, while also promoting MEF2 activity (Backs et al., 2006, 2011; Davis et al., 2003).

The phosphatase calcineurin (CaN) also becomes active upon calmodulin binding, dephosphorylating transcription factors, which are usually kept inactive by phosphorylation in the cytoplasm. The main substrate of CaN is the family of nuclear factor of activated T cells (NFATs), which is crucial for T cell activation, differentiation and development, while also promoting cancer development (Macian, 2005; Monteith et al., 2017). Upon dephosphorylation of NFATs by CaN, the nuclear import signal is unmasked, allowing NFATs to translocate into the nucleus and activate target genes (Macian, 2005). Additionally, CaN is suggested to activate MEF2, although the exact mechanism is still under investigation (Van Oort et al., 2006). Furthermore, CaN can be inhibited upon phosphorylation by CAMKII, decreasing NFAT translocation (Kreusser et al., 2014; MacDonnell et al., 2009).

Transcriptional changes are further fine-tuned by the activity of their activators, which is modulated by their affinity for calmodulin and calcium levels. CAMKII has a much lower affinity for calmodulin than CaN, thus CaN activation is more robust and faster compared to CAMKII activation (Dewenter et al., 2017). Thus, local calcium levels directly influence the amount of calcium-bound calmodulin and consequently the intensity of CaN and CAMKII activation. Local calcium levels have also been shown to play a role in the activation of individual members of the NFAT family.

Upon SOCE, a local increase in calcium levels is sufficient to activate nuclear factor of activated T cells 2 (NFATc2), while nuclear factor of activated T cells 3 (NFATc3) requires higher levels of nuclear calcium to be activated (Kar and Parekh, 2015). Taken together, disturbances in calcium levels upon stimuli can lead to the activation of several signaling cascades and calmodulin-dependent kinases, culminating in the activation, de-repression and inhibition of a diverse range of transcription factors. These effects on transcription factor activity are further directly modulated by calcium levels in different cellular compartments, the kinetics by which these levels change and the affinity of several proteins for calcium.

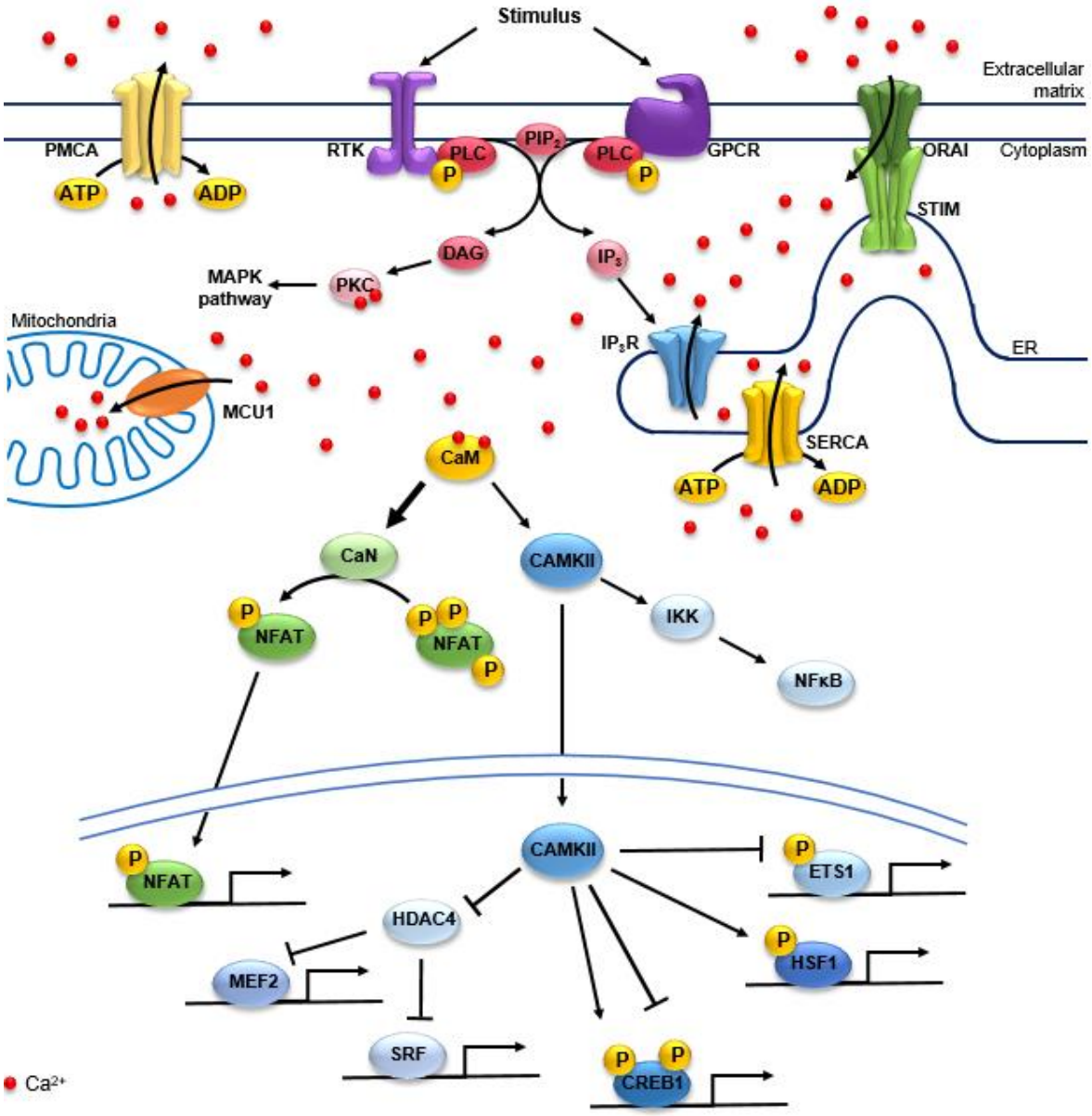

Fig. 9 Calcium signaling scheme. Upon a stimulus, GPCRs or RTKs are activated, phosphorylating PLC and promoting the breakdown of PIP_2 to DAG and IP_3. The latter promotes the opening of the channel IP_3R, raising cytosolic calcium levels. While calcium pumps and MCU1 try to restore cytosolic calcium levels, SOCE further promotes the influx of calcium into the cytoplasm. DAG and calcium activate PKC and consequently the MAPK pathway. Calmodulin (CaM) binds calcium, activating CaN and CAMKII. CaN dephoshorylates NFATs promoting its translocation into the nucleus and activity. In the cytosol, CAMKII activates NFκB by activating IKK. CAMKII further activates HSF1, while repressing ETS1. CREB1 can be phosphorylated by CAMKII at two sites, one repressive (Ser142) and one activating (Ser133). Upon the inhibition of HDAC4 by CAMKII, MEF2 and SRF are de-repressed and activated. In yellow are calcium pumps, in orange MCU1, in blue calcium channels and in green the components of SOCE, STIM and ORAI. Concerning signaling components, receptors are in purple and their downstream effectors in pink/red. Factors activated by CaN in green and factors activated and/or repressed by CAMKII in blue. The figure was based on and adapted from Dewenter et al. and Feske et al.

1.3. Epigenetics and transcriptional regulation

As shown in the last section, calcium can trigger the activation of several different families of transcription factors. This induces changes in the transcriptome and proteome of the cell, ultimately creating a response to the original stimulus. The changes in transcriptome are extremely fast, starting to be detected already minutes after the original signal. This is only possible, because epigenetic proteins allow for a very plastic and adaptive gene regulation by quickly de-repressing and repressing genes. Upon binding of a transcription factor to DNA, epigenetic readers, writers and erasers are recruited, leading to chromatin re-arrangements and ultimately to the activation or inhibition of transcription.

1.3.1. Transcription factors and gene regulation

Transcriptional regulation is crucial for a proper stimulus response and for the maintenance of the cell and its identity. Cancer cells very often hijack pathways or reprogram their identity by aberrantly activating transcription factors and thus changing their overall transcriptome. Examples of such activities are the activation of ATF4 and ISR in many cancers and of ΔNp63 and NFAT in pancreatic cancer. By dimerizing with various transcription factors, acting on promoter regions as well as distal regulatory elements and recruiting different epigenetic regulators, ATF4, ΔNp63 and NFAT activate pro-survival and apoptotic genes, drive the basal subtype of pancreatic cancer and regulate tumor growth in PDAC, respectively (Baumgart et al., 2013; Hamdan and Johnsen, 2018; Pakos-Zebrucka et al., 2016) (Fig. 10A, B).

Transcription factors (TFs) are proteins which regulate transcription upon DNA binding in a sequence-specific manner and recruiting co-factors for gene activation or repression (Reiter et al., 2017). DNA sequences recognized by TFs range between 6-12bp and are spread across the genome. Thus, there are millions of gene regulatory regions for TFs to bind and the likelihood of it binding one site over another is influenced by their interaction partners and the environment (Wunderlich and Mirny, 2009). TFs can bind DNA as homo- and heterodimers or as trimers having their binding affinity altered according to their binding partners (Jolma et al., 2013, 2015). As TFs bind in a complex, their sequence specificity may change due to stereochemical requirements (Slattery et al., 2011). Furthermore, TFs, as many other proteins, are more stable in a complex, thus, binding to DNA is stronger and lasts longer (Chen et al., 2014; Gebhardt et al., 2013). Taken together, cooperativity between TFs can highly affect their activity and targets (Fig. 10A).

A great example of this is ATF4 and its binding partners. As discussed previously, ATF4 is the major transcription factor activated by the ISR and can modulate the cellular response to stress regulating pro-survival and apoptotic genes. ATF4 heterodimerizes with a wide range of TFs, activating a different set of genes, depending on its binding partner. It is proposed that heterodimers of ATF4 and CHOP rather activate apoptotic genes, such as *PUMA* and *BIM*, while also regulating the negative feedback loop of the ISR by upregulating *GADD34* (Pakos-Zebrucka et al., 2016). Interestingly, ATF4 can also dimerize with the CAAT box/enhancer-binding proteins (C/EBPs), binding CCAAT-enhancer binding protein-activating transcription factor (C/EBP-ATF) response elements (CAREs). CAREs comprise half of the ATF binding sequence and half of the C/EBP binding sequence, thus being only recognized by ATF-C/EBP dimers. Genes regulated by ATF4-C/EBP dimers encompass amino acid deprivation responsive genes and other stress-dependent transcription factors, such as ATF3 and CHOP (Kilberg et al., 2009; Vallejo et al., 1993). Other dimerization partners of ATF4 include the activator protein 1 (AP1), FOS and JUN, even though their effects in activating pro-survival and apoptotic genes are not well defined (Chevray and Nathans, 1992; Hai and Curran, 1991).

The calcium-dependent family of TFs, NFAT, also heterodimerizes with different TFs, including ELK1 and STAT3 in pancreatic cancer (Baumgart et al., 2013; König

et al., 2010a). Interestingly, NFATc1 and NFATc2 can displace SMAD3 repressors complexes from *c-MYC* regulatory regions upon TGFβ signaling, while also binding to the *c-MYC* promoter as NFATc1/NFATc2-ELK1 dimers in response to serum in PDAC (König et al., 2010b; Singh et al., 2010). More generally, NFATc1/NFATc2-STAT3 dimers promote inflammation-driven pancreatic cancer development and proliferation (Baumgart et al., 2014, 2016). NFATc2-STAT3 dimers are further stabilized by glycogen synthase kinase 3β (GSK-3β), which is implicated in the inflammatory response of tumors (Baumgart et al., 2016). Taken together, upon dimerization with different factors, NFATs promote the development and growth of PDAC by activating growth promoting protein coding genes.

Furthermore, TFs can regulate gene expression by binding regulatory elements, which are proximal or distal to the target gene's transcriptional start site (TSS). Distal regulatory elements, enhancers, can be further classified into typical enhancers and super-enhancers (SE), the latter being characterized by a much higher density of TFs and co-factors than the former (Lovén et al., 2013). While typical enhancers modulate the expression of a wide range of genes, SEs are mainly associated with the regulation of lineage-specific programs (Whyte et al., 2013). Interestingly, NFATc1-STAT3 dimers have been shown to rather bind typical enhancer elements, while ΔNp63 has been associated with SE regions to regulate and drive the basal subtype in PDAC (Baumgart et al., 2014; Hamdan and Johnsen, 2018) (Fig. 10B).

The bridging between typical enhancers and SEs and promoters is mediated by co-factors. In fact, TFs regulate gene expression by binding to very specific regulatory elements and recruiting different co-factors to these regions. Co-factors modify chromatin by post-translationally modifying histone tails and DNA itself and, thus, creating new binding sites for further proteins (discussed in the next section). Ultimately, the co-factors recruit or block recruitment of RNA Polymerase to the promoter region, activating or repressing gene expression, respectively (Reiter et al., 2017). Taken together, TFs bind typical enhancers, SEs and promoter regions, recruiting co-factors and regulating target gene expression. The binding of TFs to a regulatory element is highly dependent on sequence specific binding and their dimerization partners. This way, TFs ensure a fast and specific response to stimuli, while also maintaining cellular identity.

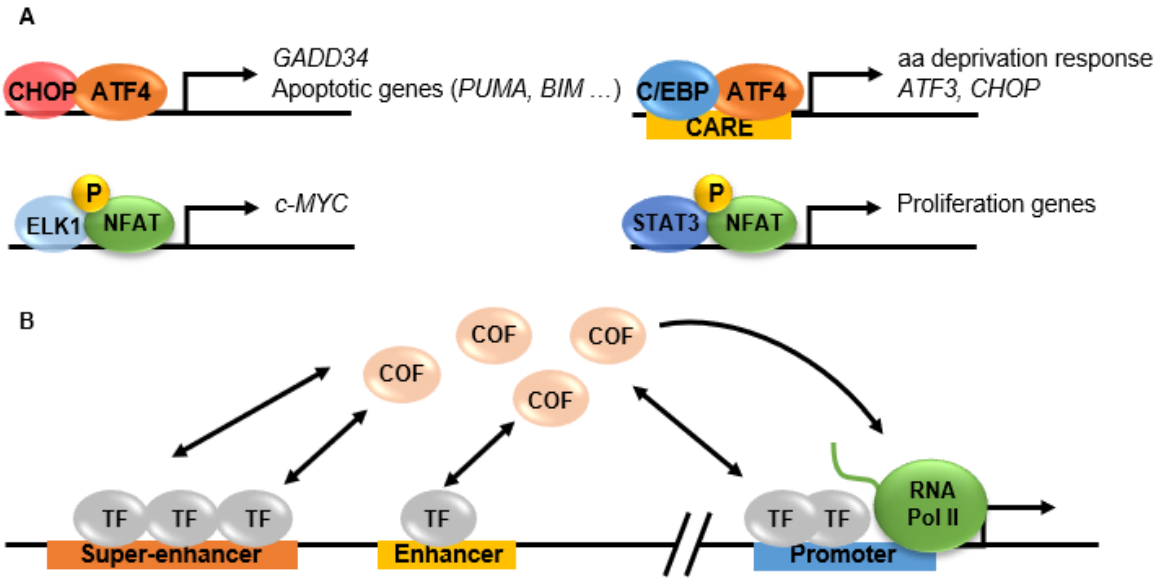

Fig. 10 Transcription factor cooperative binding and localization at TSS proximal and distal regulatory elements. A. Transcription factor binding to DNA depends on its recognition sequence and binding partner. As TFs heterodimerize, they activate a different set of genes. For example, while CHOP-ATF4 dimers activate mainly apoptotic genes, ATF4-C/EBP dimers promote the transcription of amino acid (aa) deprivation responsive genes. Furthermore, ATF4-C/EBP dimers bind CAREs rather than the normal ATF4 or C/EBP recognition sequences, thus activating a very specific set of genes. NFATc1 and NFATc2 dimerize with ELK1 or STAT3 upon different stimuli to promote cell proliferation in both cases. B. TFs bind promoter as well as typical enhancer and super-enhancer regions, interacting with several co-factors (COF) and promoting or also blocking transcription. The figure was based on and adapted from Reiter et al.

1.3.2. Active and repressive histone marks

As seen previously, TFs can regulate genes by recruiting co-factors that add, remove and recognize post-translational modifications on histone tails and ultimately promote or block RNA Polymerase recruitment to the promoter region. DNA is wrapped around nucleosomes, which are composed of histone octamers consisting of four homodimers of histones 2A, 2B, 3 and 4 (H2A, H2B, H3 and H4, respectively). Each histone has a tail, which can be, among others, acetylated, methylated and ubiquitinated by different epigenetic writers. The type and position of the histone modification is crucial as it can signal gene activation or silencing upon recognition by different epigenetic readers. Furthermore, epigenetic erasers can remove histone modifications further affecting transcription by preventing epigenetic readers to bind to these modifications and promote the activation or repression of genes (Allis and Jenuwein, 2016). Thus, epigenetic writers, erasers and readers

confer plasticity to gene regulation by quickly adding, removing and recognizing active and repressive histone modifications, respectively (Fig. 11).

Histone marks associated with transcriptional repression include trimethylated Lys9 and Lys27 on H3 (H3K9me3 and H3K27me3, respectively), together with monoubiquitinated Lys119 on H2A (H2AK119ub). Interestingly, regions marked by H3K27me3 in the genome are still accessible for TFs and RNA Polymerase to bind, even though RNA Polymerase cannot progress into the gene, whereas areas with H3K9me3 are so densely packed with nucleosomes that binding of any TF is impaired (Breiling et al., 2001; Dellino et al., 2004; Soufi et al., 2012). Furthermore, H2AK119ub has been proposed to block transcription initiation, most likely by preventing the deposition of active histone marks, while also affecting transcription elongation (Weake and Workman, 2008; Zhou et al., 2008).

The writers, polycomb repressor complex 1 and 2 (PRC1 and PRC2, respectively), catalyze the ubiquitination of H2AK119 and methylation of H3K27, respectively, while PRC1 can also function as a reader, recognizing H3K27me3 and then catalyzing the ubiquitination of H2AK119 (Laugesen et al., 2016; Weake and Workman, 2008). Interestingly, PRC2 has also been reported to recognize H3K27me3, further promoting the spread and maintenance of this histone mark (Hansen et al., 2008; Margueron et al., 2009). The mono-, di- and trimethylation of H3K9 is catalyzed by histone lysine methyltransferases (KMT) including suppressor of variegation 3-9 homolog 1 and 2 (SUV39H1 and SUV39H2, respectively) (Becker et al., 2016). The reader of methylated H3K9 is heterochromatin protein 1 (HP1), which upon recognizing H3K9me2 and H3K9me3, recruits SUV39H1 to these sites, further promoting the spread of H3K9me3 (Lachner et al., 2001; Schotta et al., 2002). Interestingly, NFATc2 has been shown to promote the silencing of the tumor suppressor *CDKN2B* by recruiting SUV39H1 and promoting a first local H3K9me3. The mark is then extended as HP1 recognizes H3K9me3 and further recruits H3K9-specific methyltransferases (Baumgart et al., 2012).

Thus, the removal of these modifications by histone deubiquitinases (DUBs) and lysine demethylases (KDMs) is essential to restore transcription. Interestingly, ATF4 has been shown to recruit lysine demethylase 4C (KDM4C) to ISR responsive genes, promoting the demethylation of H3K9me3 and consequently the de-

repression of pro-survival genes (Zhao et al., 2016). Furthermore, PRC2 has been proven to silence *NFATc1* in pancreatic acinar cells, but not pancreatic cancer. Upon the activation of K-RAS in pancreatic cancer, PRC2's activity has been shown to be reversed, de-repressing *NFATc1* (Chen et al., 2017).

Concerning active histone marks, the best characterized ones are acetylated Lys27 on H3 (H3K27ac), acetylated Lys5, Lys8, Lys12 and Lys16 on H4 (H4K5ac, H4K8ac, H4K12ac and H4K16ac, respectively), monomethylated Lys4 on H3 (H3K4me1), trimethylated Lys4 on H3 (H3K4me3) and monoubiquitinated Lys120 on H2B (H2BK120ub). All marks have been correlated with active transcription, but their location suggests that each mark affects a different step of transcription. H3K27ac, H4K5ac, H4K8ac, H4K12ac and H4K16ac are found in enhancer, as well as promoter, regions, while H3K4me1 mainly occupies enhancer regions and H3K4me3 is largely found at promoters (Li et al., 2019; Nagarajan et al., 2015; Taylor et al., 2013; Zhao and Garcia, 2015). H2BK120ub mainly occupies the gene body correlating with active transcriptional elongation (Weake and Workman, 2008).

E1A binding protein p300 and cAMP-response element-binding CREB-binding protein (p300/CBP) recognize transcription factors on chromatin, being recruited to such sites and acetylating neighboring nucleosomes on H3K27 (Chan and La Thangue, 2001). In fact, NFATs have been proven to recruit p300/CBP to the *c-MYC* promoter, leading to a hyperacetylation of the promoter region and, thus, further activating *c-MYC* (König et al., 2010b). p300/CBP together with lysine acetyltransferase (KAT) also acetylate H4 giving rise to H4K5ac, H4K8ac, H4K12ac and H4K16ac (Nicholson et al., 2015). Furthermore, H3K4me1 has been shown to be linked to H3K27ac. The mono-, di- and trimethylations of H3K4 are catalyzed by the mixed lineage leukemia complexes (MLLs) and by the SET domain containing 1A and 1B, histone lysine methyltransferases (SETD1A and SETD1B, respectively) (Nicholson et al., 2015). MLL3 and MLL4 have been suggested to be recruited to determined sites by recognizing H3K27ac and methylating neighboring H3K4 (Wang et al., 2017). Furthermore, H2BK120ub stimulates SETD1A and SETD1B activity, promoting the deposition of H3K4me3 (Holt et al., 2015). Consequently, the ubiquitination of H2BK120 by Ring finger protein 20 and 40 (RNF20 and RNF40, respectively) has been shown to be a pre-requisite for the trimethylation of H3K4 (Sun and Allis, 2002). Thus, a series of histone modifications decorate promoters

and enhancers laying the ground for readers to facilitate transcription. Bromo- and extraterminal domain proteins (BETs) are key in mediating this, as they recognize H4K5ac, H4K8ac, H4K12ac and H4K16ac, while BET bromodomain containing 4 (BRD4) recruits cyclin-dependent kinase 9 (CDK9) to these sites, fostering the release of promoter proximally paused RNA Polymerase II, and thereby promoting transcriptional elongation (Filippakopoulos et al., 2012; Moon et al., 2005). This way the removal of these modifications by DUBs, histone deacetylases (HDACs) and KDMs also affects transcription. In fact, during amino acid deprivation, ATF4 knock-out cells are only able to activate some ISR responsive genes upon HDAC inhibition. This suggests that the recruitment of histone acetyltransferases (HATs) by ATF4 is crucial for transcription and its removal can de-activate genes (Shan et al., 2012). In conclusion, epigenetic writers, readers and erasers mediate gene activation and repression by adding or removing and by recognizing active and repressive histone marks. This process is mediated by transcription factors, which recruit different epigenetic writers and erasers to regulatory elements of their target genes.

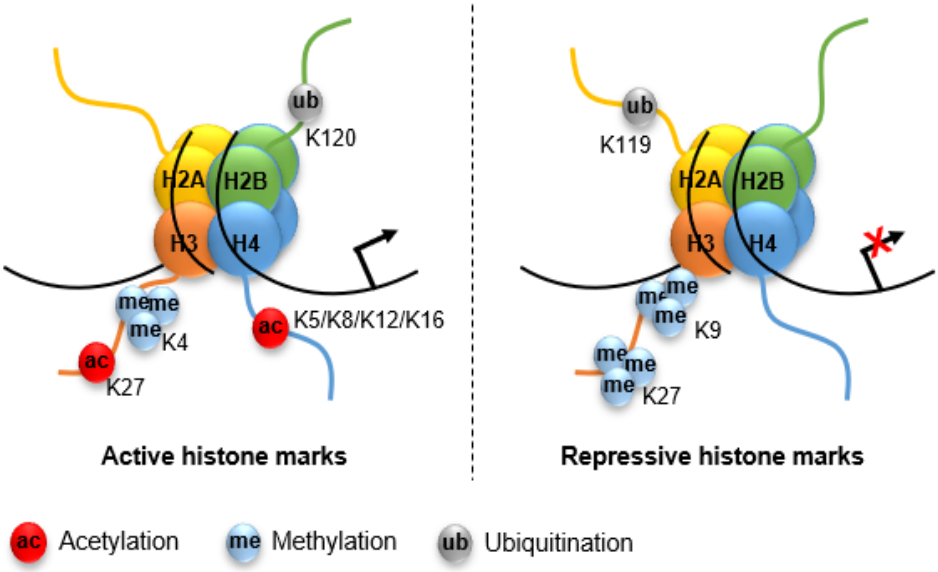

Fig. 11 Active and repressive histone marks. The scheme depicts the active histone marks (H3K27ac, H3K4me1, H3K4me3, H4K5ac, H4K8ac, H4K12ac, H4K16ac and H2B120ub) and the repressive histone marks (H3K27me3, H3K9me3 and H2AK119ub).

1.3.3. Chromatin and genome organization

The recruitment of co-factors by TFs and histone modifications leads to major chromatin rearrangements in the cell. Repression of transcription is often

accompanied by chromatin condensation, while transcriptional activity is associated with a more accessible chromatin. Condensed and silenced regions are typically located close to the nuclear lamina, whereas more accessible and active regions are brought together by a multitude of co-factors and are centrally located in the nucleus. Furthermore, bridging between enhancers and promoters takes place as chromatin regions are brought together and co-factors from both regions cooperate, potentiating gene regulation (Fig. 12) (Plank and Dean, 2014; Pombo and Dillon, 2015).

Two chromatin regions are brought together through looping, where CCCTC-binding factor (CTCF) and cohesin form a ring extruding a chromatin loop, consequently bringing two regions of chromatin in close proximity. This allows for distal regulatory elements, typical enhancers and SEs, to interact with promoter regions (Dixon et al., 2012; Lupiáñez et al., 2015). This interaction is supposed to be very dynamic and further facilitated by co-factors, such as the mediator and BRD4. The mediator is a complex known to bridge enhancers to promoters by interacting with TFs and other co-activators on enhancers and recruiting the pre-initiation complex of RNA Polymerase II to promoter regions. Transcription initiation is also triggered by the mediator, as it phosphorylates the C-terminal domain (CTD) of RNA Polymerase II on Ser5 (Soutourina, 2018). The mediator can also bind cohesin further promoting the contact between two chromatin regions through looping, bridging enhancers to promoters (Kagey et al., 2010). Furthermore, upon promoter-enhancer looping, the local concentration of co-activators, such as BRD4, the mediator complex, and RNA Polymerase II increases, favoring and augmenting transcription (Reiter et al., 2017; Sabari et al., 2018). Taken together, TFs are recruited to promoters, typical enhancers and SEs upon stimuli or for cellular homeostasis, leading to a change in histone modifications and consequently chromatin structure. Chromatin looping and TFs together with co-activators favor an interaction between promoters, typical enhancers and SEs, thus facilitating and triggering the transcription of target genes.

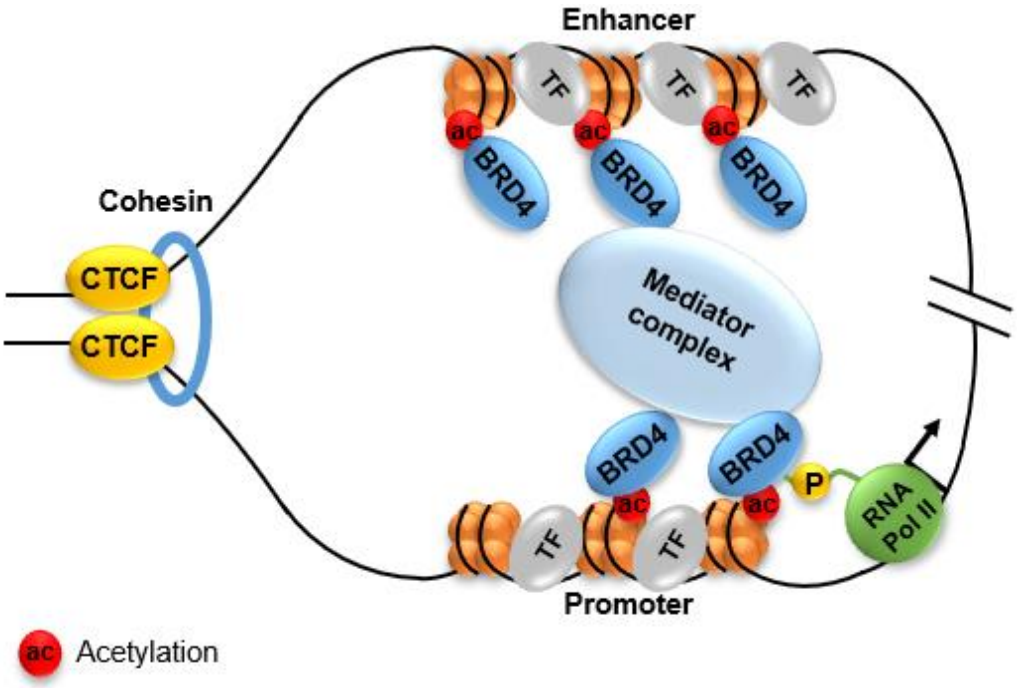

Fig. 12 Enhancers and promoters interact promoting transcription. Transcription factors bind promoters and enhancers, recruiting several histone modifiers. Epigenetic readers recognize histone marks and interact with co-activators. The mediator complex bridges enhancers to promoters and phosphorylates the CTD of RNA Polymerase II promoting transcription initiation. CTCF and cohesin bring distal chromatin regions in close proximity, further facilitating the interactions between factors on enhancers and promoters. The figure was based on and adapted from Soutourina et al. and Reiter et al.

1.4 Objectives of this study

PDAC patients face a 5-7% 5-year survival rate, mainly due to late diagnosis and chemotherapy resistance, where 77% of the patients do not respond to the commonly used therapy agent, gemcitabine (American Cancer Society, 2020; Burris et al., 1997). Thus, it is of utmost importance to understand the traits acquired upon and the mechanisms driving gemcitabine resistance in order to monitor resistance development and to give a more suitable treatment to patients, improving their response to chemotherapy and increasing their lifespan.

Many correlative studies have pointed at several gemcitabine metabolizing proteins as being indicative of the responsiveness of patients to gemcitabine (Farrell et al., 2009; Kroep et al., 2002; Maréchal et al., 2012; Spratlin et al., 2004). Furthermore, the prognostic value of the gemcitabine target, ribonucleotide reductase, in gemcitabine resistance has been of debate. While several cell line studies and one *in vivo* study have shown that resistant cells and tumors rely on an upregulation of

RRM1 to overcome gemcitabine toxicity, studies on patient biopsies have not been as straightforward (Nakahira et al., 2007; Nakano et al., 2007; Wang et al., 2015; Zhou et al., 2019). Three patient studies came to different conclusions as to whether RRM1 levels are of prognostic value for gemcitabine responsiveness in PDAC (Akita et al., 2009; Aoyama et al., 2017; Maréchal et al., 2012). A hurdle of these studies is that they have analyzed the expression levels of putative markers in naïve patient biopsies, as biopsies from treated patients are rare. Therefore, these studies did not consider that the expression of many of these markers may change during the establishment of resistance. Furthermore, even though the cell line and *in vivo* studies are more consistent, they mainly focused on transcriptomic changes, not tracing an entire profile of gemcitabine resistance.

Gemcitabine, as any chemotherapeutic drug, apart from inhibiting ribonucleotide reductase and DNA Polymerase, induces cellular stress, such that resistant cells, most likely, have to adapt to a highly stressful environment (Avril et al., 2017). The ISR is a major mechanism for the cell to cope with different kinds of stresses activating pro-survival and apoptotic genes (Pakos-Zebrucka et al., 2016). In fact, various cancers hijack the pro-survival branch of the ISR to cope with their stressful environment (Avril et al., 2017; Mujcic et al., 2013; Rouschop et al., 2010; Sun et al., 2015; Ye et al., 2010). Thus, it is plausible that gemcitabine resistant cells adapt and perceive stress differently, possibly heavily relying on the ISR to survive the stress induced by gemcitabine. This would further imply that resistant cells would be selected for not only overcoming gemcitabine's toxicity, but for also thriving under general stress.

The fact that cancer cells are highly susceptible to the accumulation of genetic mutations, amplifications and deletions would be a form to adapt to gemcitabine and stress. It is possible that upon the selective pressure of continuous gemcitabine treatments, tumors with certain genetic backgrounds thrive better and are selected for. Epigenetics also poses a highly plastic system, which can be modulated by tumors in response to gemcitabine and stress. In fact, the ISR relies on the epigenetic plasticity of the cell, being highly dependent on the activity of transcription factors, such as ATF4 (Pakos-Zebrucka et al., 2016; Wortel et al., 2017). Branches of the ISR are also tightly linked to calcium signaling in the cell, which can additionally activate several transcription factors, modulating transcription and gene

regulation (Carreras-Sureda et al., 2018; Dewenter et al., 2017; Gutiérrez and Simmen, 2018). Thus, in order to survive gemcitabine and general stress, resistant cells may adopt a different genetic and epigenetic landscape and respond differently to stress and other stimuli compared to naïve cells. In this case, not only would the activation of certain transcription factors be affected, but also the histone marks and target genes be different before and after the establishment of gemcitabine resistance.

Taken together, we hypothesize that gemcitabine resistance leads to genetic, epigenetic and transcriptomic changes, which allow gemcitabine resistant tumors to not only thrive under gemcitabine, but also under general stress stimuli. We, therefore, aim to compare treatment-naïve with gemcitabine resistant tumors on a transcriptional, epigenetic and genetic level. With these approaches, we plan to further characterize cellular traits acquired upon gemcitabine resistance. Finally, we intend to propose novel targets for precision oncology and alternative treatment options for patients facing gemcitabine resistance.

2. Publication

STIM1 Mediates Calcium-dependent Epigenetic Reprogramming in Pancreatic Cancer

Ana P. Kutschat[1], **Feda H. Hamdan**[2], Xin Wang[1], Alexander Q. Wixom[2], Zeynab Najafova[1], Christine S. Gibhardt[3], Waltraut Kopp[4], Jochen Gaedcke[1], Philipp Ströbel[5], Volker Ellenrieder[4], Ivan Bogeski[3], Elisabeth Hessmann[4], Steven A. Johnsen[2]

[1]Clinic for General, Visceral and Pediatric Surgery, University Medical Center Göttingen, Göttingen, Germany, [2]Gene Regulatory Mechanisms and Molecular Epigenetics Lab, Division of Gastroenterology and Hepatology, Mayo Clinic, Rochester, MN, [3]Molecular Physiology, Institute of Cardiovascular Physiology, University Medical Center Göttingen, Georg-August-University, Göttingen, Germany, [4]Department of Gastroenterology, Gastrointestinal Oncology and Endocrinology, University Medical Center Göttingen, Göttingen, Germany, [5]Department of Pathology, University Medical Center Göttingen, Göttingen, Germany

A.P.K. and F.H.H. contributed equally to this work.

Running title: Ca^{2+}-led epigenetic rewiring in pancreatic cancer

Keywords: RRM1, STIM1, SOCE, ER stress, NFAT

Financial support: This project was funded by grants from the *Deutsche Krebshilfe* (70112505; PIPAC consortium) to S.A.J., Z.N., J.G., V.E. and E.H., the *Deutsche Forschungsgemeinschaft* (SFB1190 and SFB1027) to I.B., the *National Cancer Institute* (CA 102701) to S.A.J. and the *National Institute of Diabetes and Digestive and Kidney Diseases* (T32 DK07198) to S.A.J.

Correspondence: Steven A. Johnsen, Gene Regulatory Mechanisms and Molecular Epigenetics Lab, Division of Gastroenterology and Hepatology, Mayo Clinic, 200 First Street SW, Rochester, MN 55905, USA, phone: +1-507-255-6138, fax: +1-507-255-6318 Johnsen.Steven@mayo.edu

Conflict of interest: The authors declare no potential conflicts of interest.

Acknowledgments: The authors thank M. Dobbelstein, J. Choo, F. Wegwitz, E. Prokakis and J. Henck for fruitful discussions. F. Wegwitz and E. Prokakis for assistance in microscopy.

Author Contributions: Conceptualization: A.P.K., F.H.H., X.W., C.S.G., I.B. and S.A.J. Investigation: A.P.K., F.H.H., X.W., A.Q.W., Z.N., C.S.G., W.K., E.H. and S.A.J. Formal analysis: A.P.K., F.H.H., X.W., Z.N., C.S.G., I.B., E.H., S.A.J. Methodology: J.G., P.S. Funding acquisition: Z.N., J.G., V.E., I.B., E.H. and S.A.J. Supervision: S.A.J. Writing – original draft: A.P.K. and S.A.J. Writing – review & editing: all authors.

This manuscript has been accepted by AACR's journal, *Cancer Research*, on the 6th of January 2021.

A.P.K. conducted the experiments shown in this thesis, with the exception to the ones listed as follows. F.H.H. developed the gemcitabine resistant cell line (GemR) and prepared the mRNA-seq and H3K27ac ChIP-seq libraries in untreated Par and GemR. X.W. prepared the mRNA-seq libraries in vehicle and thapsigargin treated Par, GemR and STIM1-depleted GemR. X.W. and A.P.K. prepared the ATF4 and H3K27ac ChIP-seq libraries in vehicle and thapsigargin treated Par, GemR and STIM1-depleted GemR together. A.Q.W. established the STIM1 overexpressing Par, BxPC-3 and CFPAC-1 cell lines. F.H.H generated the data shown in Fig. 20C-H and Fig. 29E-F. Z.N. generated the data shown in Fig. 25B. C.S.G measured the absorbance of cell titer blue shown in Fig. 13C, Fig. 18B, Fig. 21B and D, Fig. 22B and D and Fig. 23D. W.K, J.G., P.S. and E.H. generated the PDXs and W.K. performed the immunohistochemistry shown in Fig. 30B-C and in Fig. 31A-B.

2.1 Abstract

Pancreatic Ductal Adenocarcinoma (PDAC) displays a dismal prognosis due to late diagnosis and high chemoresistance incidence. For advanced disease stages or patients with comorbidities, treatment options are limited to gemcitabine alone or in combination with other drugs. While gemcitabine resistance has been widely attributed to the levels of one of its targets, RRM1, the molecular consequences of gemcitabine resistance in PDAC remain largely elusive. Here we sought to identify genomic, epigenomic, and transcriptomic events associated with gemcitabine resistance in PDAC and their potential clinical relevance. We found that gemcitabine-resistant cells displayed a co-amplification of the adjacent *RRM1* and *STIM1* genes. Interestingly, RRM1, but not STIM1, was required for gemcitabine resistance, while high STIM1 levels caused an increase in cytosolic calcium concentration. Higher STIM1-dependent calcium influx led to an impaired ER stress response and a heightened NFAT activity. Importantly, these findings were confirmed in patient and patient-derived xenograft samples. Taken together, our study uncovers previously unknown biologically relevant molecular properties of gemcitabine-resistant tumors, revealing an undescribed function of STIM1 as a rheostat directing the effects of calcium signaling and controlling epigenetic cell fate determination. It further reveals the potential benefit of targeting STIM1-controlled calcium signaling and its downstream effectors in PDAC.

2.2 Statement of significance

Gemcitabine-resistant and some naïve tumors co-amplify *RRM1* and *STIM1*, which elicit gemcitabine resistance and induce a calcium signaling shift, promoting ER stress resistance and activation of NFAT signaling.

2.3 Introduction

Pancreatic ductal adenocarcinoma (PDAC) patients display a dismal 7-9% 5-year survival rate due to late diagnosis and therapeutic resistance (American Cancer Society, 2020). The current first-line treatment includes FOLFIRINOX (5-fluorouracil-oxaliplatin-irinotecan) with the combination of gemcitabine and nab-paclitaxel as an alternative. Still, patients displaying a more advanced disease or comorbidities that preclude intensive therapy generally receive either gemcitabine alone or in combination with either capecitabine or S-1 (tegafur-gimeracil-oteracil) (Ryan, 2020b; Sohal et al., 2018). Thus, inevitably, with disease progression, gemcitabine-based treatment is administered to most patients. Unfortunately, the response to such therapy is low and variable, establishing gemcitabine resistance as a major hurdle in PDAC treatment (Cunningham et al., 2009; Hamada et al., 2017; Scheithauer et al., 2003). Therefore, it is of utmost importance to understand the effects of gemcitabine treatment on PDAC.

Many studies attribute gemcitabine resistance to the upregulation of one of its main targets, ribonucleotide reductase (Akita et al., 2009; Bergman et al., 2005; Nakahira et al., 2007; Nakano et al., 2007; Wang et al., 2015; Zhou et al., 2019), while also identifying differential expression of gemcitabine metabolizing enzymes as predictive of treatment response (Farrell et al., 2009; Maréchal et al., 2012). Still, the broader effects of gemcitabine on tumors remain elusive. Previous studies suggested that gemcitabine sensitivity highly depends on genetic changes in the tumor and the cellular response to chemotherapeutic-induced stress (Tiriac et al., 2018). In addition to or as a result from acting on its primary target, many chemotherapies induce apoptosis through cell stress. The integrated stress response pathway is activated upon ER stress, amino acid deprivation, heme deprivation or viral infection and elicits two responses. First, cells attempt to resolve the stress source by inducing pro-survival genes and, if failing to do so, activating apoptotic genes (Pakos-Zebrucka et al., 2016). Consequently, cells heavily rely on the transcription factor ATF4, which is translated and translocates to the nucleus upon stress mediating the activation of stress-induced genes (Harding et al., 2000; Lu et al., 2004). Furthermore, stress conditions, such as ER or oxidative stress, are tightly coupled to calcium signaling. This stress-calcium interplay controls the transcription of apoptotic, invasive, or proliferative genes and can thus dramatically

alter cellular phenotype (Monteith et al., 2017; Zhang et al., 2019a). The cellular stress response is highly variable and depends on the molecular and epigenetic context of the cell. Therefore, chemotherapy-resistant cells may present an altered dependency on the integrated stress response, rendering the targeting of the latter potentially useful in certain contexts. Thus, a better understanding of the molecular mechanisms affected by gemcitabine resistance and their response to cellular stress is of great importance.

Here we investigated gemcitabine resistance in PDAC by characterizing gemcitabine-resistant cells and validated our results in patient samples as well as in naïve and gemcitabine-treated patient-derived xenografts. We identified an amplification in chromosome 11 harboring genes involved in resistance and genes whose functions were elusive in this context. Among them is *STIM1*, whose overexpression provokes an aberrant calcium signaling program, eliciting ER stress-resistance, a rewiring of several transcription factors and widespread epigenetic reprogramming in resistant cells. Taken together, our data provide new insights into mechanisms accompanying gemcitabine-resistance in PDAC and reveal a novel alteration of calcium signaling which may influence tumor progression.

2.4 Results

2.4.1 Amplification in chromosome 11 confers gemcitabine resistance

To study chemoresistance in PDAC, a gemcitabine-resistant human cell line (GemR) was established by treating parental L3.6pl (Par) cells with increasing gemcitabine concentrations (Fig. 13A). Cells were considered resistant once the half maximal inhibitory concentration (IC_{50}) was 50-fold higher in GemR (IC_{50}:223.70 nM ± 26.45 nM) compared to Par (IC_{50}:3.70 nM ± 0.11 nM) (Fig. 13B-C).

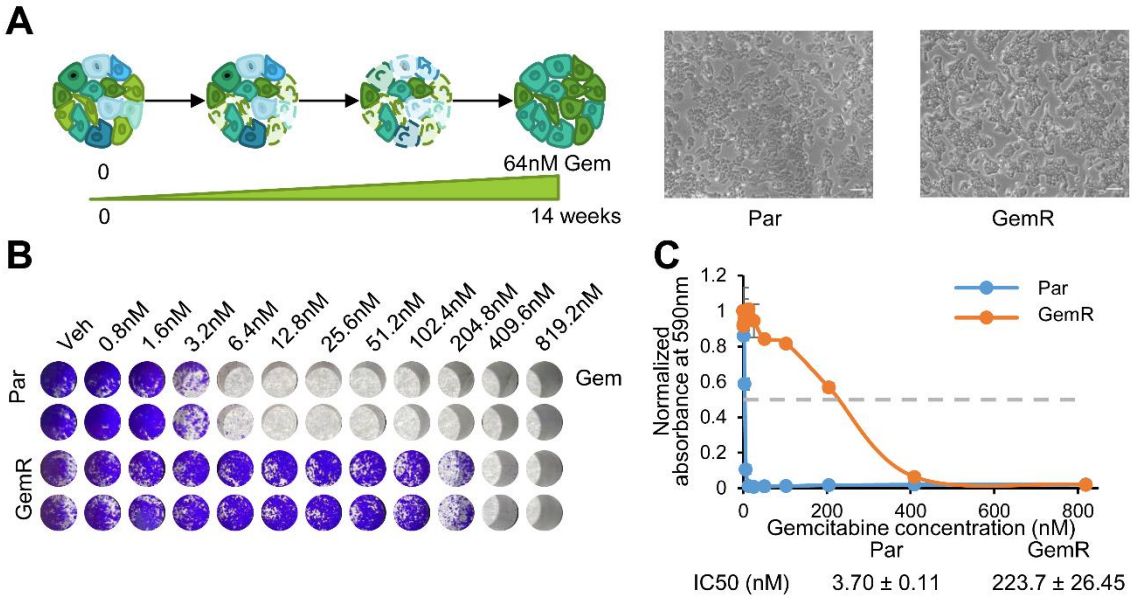

Fig. 13 Establishment of gemcitabine resistant L3.6pl (GemR). (A) Scheme depicting the establishment of GemR. Images of Par and GemR. Scale=1.36mm. (B) Crystal violet staining of a 7 days proliferation assay of Par and GemR treated with gemcitabine (Gem). (C) Proliferation assay of Par and GemR treated with gemcitabine for 7 days. The absorbance of cell titer blue was normalized to the respective vehicle absorbance. Mean ±SD, n=2. IC_{50} values ±SD, n=2.

Transcriptome-wide mRNA sequencing and low coverage whole genome sequencing was performed on GemR and Par to identify acquired traits upon resistance. Gene Set Enrichment Analysis (GSEA) showed an enrichment for the “Gemcitabine Resistance UP" signature in GemR. Surprisingly, 11 out of 16 of the significantly enriched genes identified were located on chromosome 11 (Fig. 14A and Table S1). Copy number variation analysis revealed that a region of chromosome 11 (chr11: 3,810,838-10,012,224), encompassing most of the genes contained within this signature, was amplified in GemR compared to Par. *RRM1* was identified as highly amplified and upregulated in GemR along with other genes

whose association with gemcitabine resistance are unknown (Fig. 14B-D and Table S2).

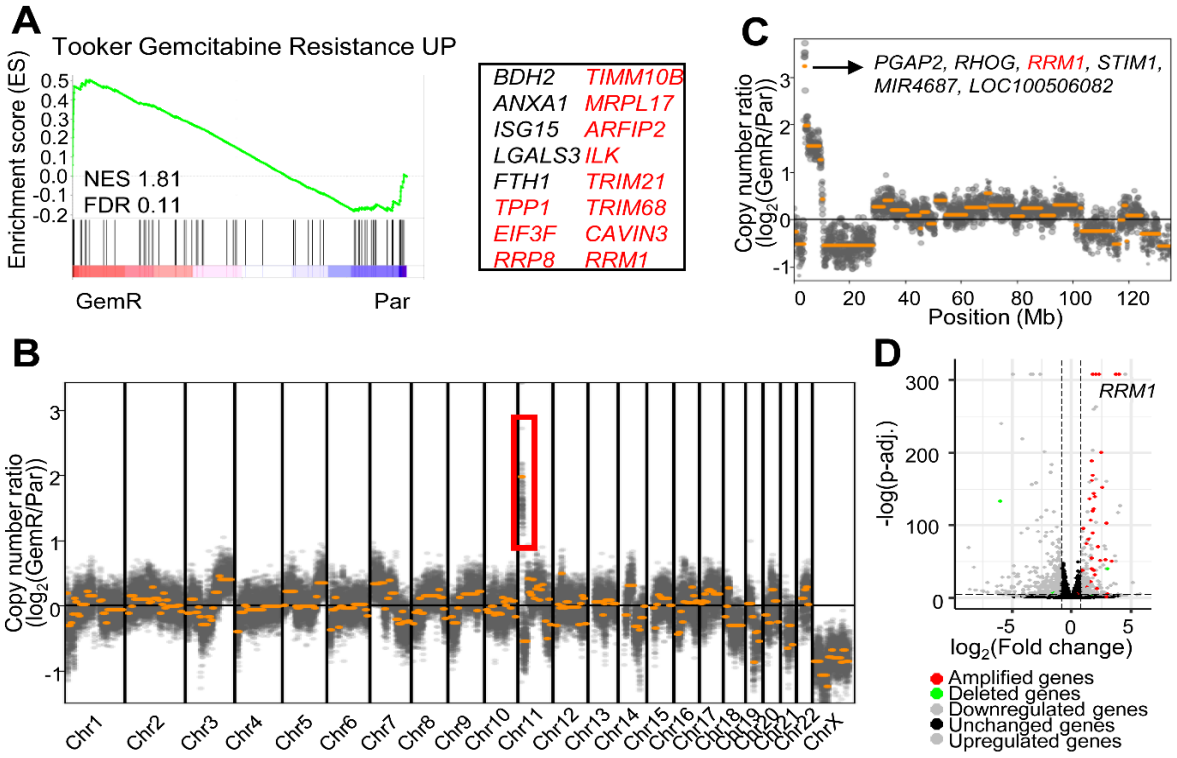

Fig. 14 GemR amplify a portion of chromosome 11. (A) GSEA showing an enrichment of the gemcitabine resistance signature in GemR. Significantly enriched genes are listed and classified into amplified genes on chr11 (in red). (B) Genome-wide copy number variation analysis of GemR compared to Par. Highlighted in a red box is the identified amplification in chr11. (C) Copy number variation analysis of GemR compared to Par in chr11 and highest amplified genes. (D) Volcano plot of differentially regulated, amplified and deleted genes in GemR compared to Par.

RRM1 is a ribonucleotide reductase subunit and one of the main targets of gemcitabine (De Sousa Cavalcante and Monteiro, 2014). Its upregulation has also been tightly associated with this chemotherapeutic agent, being reported to drive gemcitabine resistance *in vitro* and *in vivo* (Bergman et al., 2005; Nakahira et al., 2007; Nakano et al., 2007; Wang et al., 2015; Zhou et al., 2019). Consistently, we found that RRM1 levels correlate with gemcitabine resistance *in vitro* and that RRM1 depletion restores gemcitabine sensitivity in GemR (Fig. 15A-C). Interestingly, the amplified region not only includes *RRM1*, but extends for over 6 Mb. While the role of RRM1 in gemcitabine resistance has been established, the effects of the co-amplification of the various other genes remain elusive. It is therefore plausible that co-amplified genes confer additional advantageous molecular properties to tumor cells.

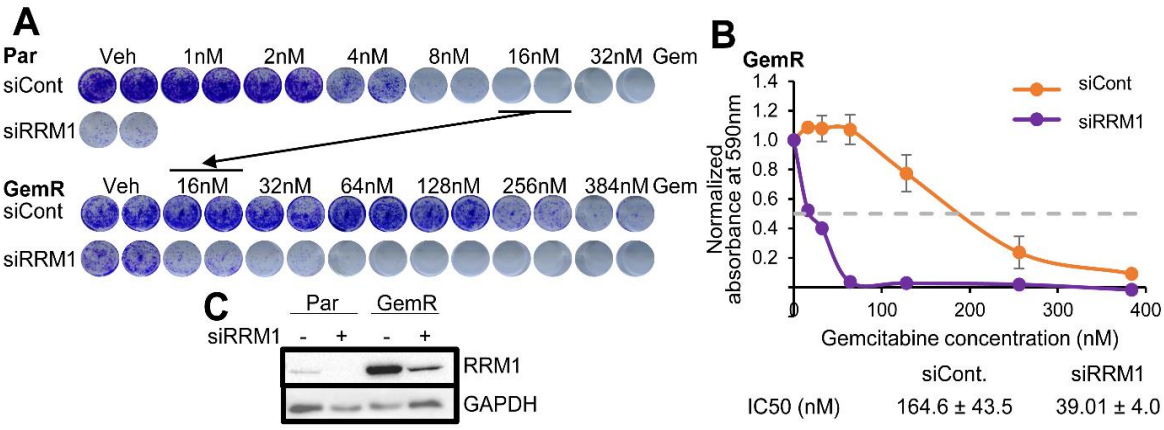

Fig. 15 *RRM1* amplification drives gemcitabine resistance. (A) Crystal violet staining of a 7 days proliferation assay upon RRM1 knockdown and treatment with gemcitabine (Gem) in Par and GemR. (B) GemR proliferation assay upon RRM1 knockdown and treatment with gemcitabine for 7 days. The absorbance of solubilized crystal violet was normalized to the respective vehicle absorbance. Mean ±SD, n=2. IC_{50} values ±SD, n=2. (C) Western blot validation of RRM1 knockdown in Par and GemR.

2.4.2 GemR display attenuated ATF4 activity and diminished ER-stress response

We hypothesized that additional genes co-amplified on chromosome 11 may influence the cellular phenotype. As the epigenetic landscape can shape the cellular response to external stimuli and provides an excellent readout for transcription factor and upstream signaling activity, we compared the epigenomic profiles of Par and GemR. For this, we performed chromatin immunoprecipitation followed by next-generation sequencing (ChIP-seq) for the active transcription mark H3K27ac. Despite the identified amplification, about an equal number of acetylated regions were lost and gained in GemR compared to Par (Fig. 16A). Bioinformatic characterization of these regions revealed that sequence motifs for AP1 transcription factors were enriched in both gained and lost regions. Motifs for the transcription factor ATF3 were also enriched in the gained regions, likely due to the sequence similarity to AP1 motifs. Interestingly, regions displaying decreased H3K27ac levels showed an enrichment for the motifs of the stress-responsive transcription factor ATF4 and its downstream target CHOP (Fig. 16B-C).

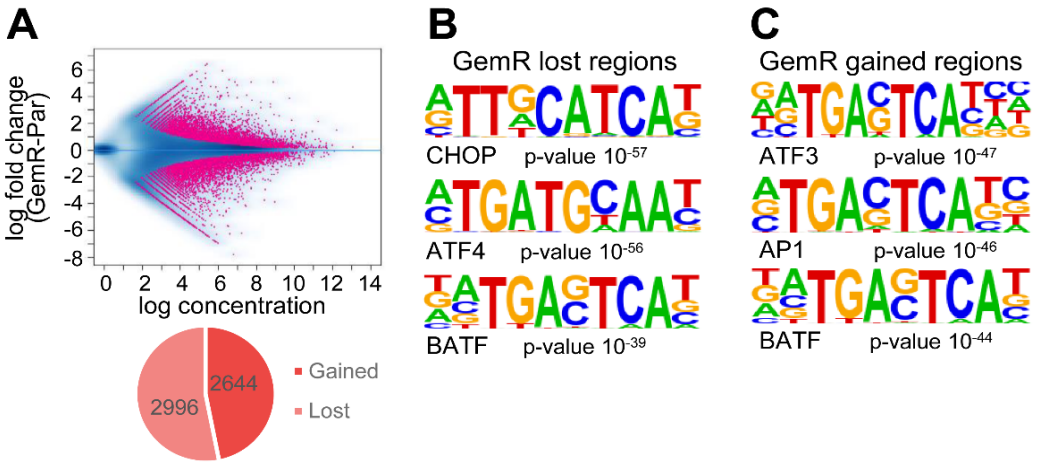

Fig. 16 Motifs of stress responsive transcription factors are enriched in H3K27ac lost regions in GemR. (A) MA plot and pie chart of differentially occupied H3K27ac regions in GemR and Par. (B) Top three hits of motif analysis in H3K27ac gained regions in GemR compared to Par. (C) Top most significantly enriched motifs in H3K27ac lost regions in GemR.

Given the reported importance of ATF4 in mediating stress response, we performed ChIP-seq for ATF4 in Par following induction of ER stress by thapsigargin. Interestingly, 24% of the lost H3K27ac regions in GemR overlapped with ATF4 peaks. Consistently, lower H3K27ac signal intensity was observed at those sites in GemR compared to Par (Fig. 17A). Accordingly, ATF4 target genes displayed decreased H3K27ac occupancy near their transcriptional start site (TSS) in GemR (Fig. 17B).

To investigate whether ATF4 activity and the stress response were affected in GemR compared to Par, we induced ER stress in Par and GemR. Strikingly, upon ER stress, ATF4 protein levels, which dramatically increased in Par, were not detectable in GemR (Fig. 17C). Consistently, GemR failed to activate ATF4 target genes, such as *TRIB3*, *ERN1* and *DDIT3* (encoding CHOP) (Fig. 17D). In conclusion, GemR are unable to activate ATF4 translation and induce downstream ER stress responsive genes.

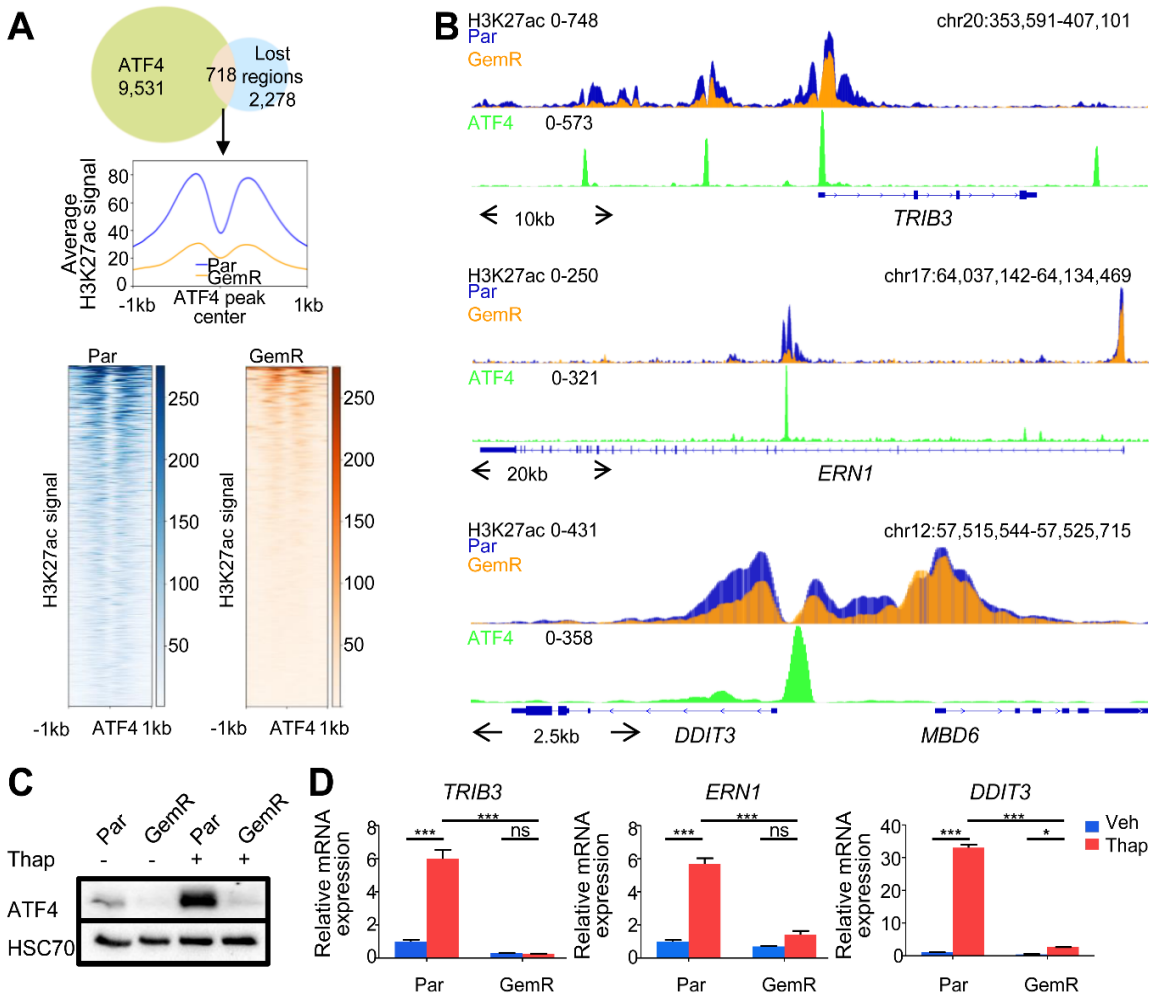

Fig. 17 ATF4 activity and ER stress response are dampened in GemR. (A) Venn diagram of ATF4 peaks in Par after thapsigargin (Thap) treatment and H3K27ac lost regions in GemR. Aggregate plot and heatmaps of H3K27ac on ATF4 summits of overlapping regions. (B) ATF4 and H3K27ac profiles around the TSS of stress responsive genes. (C) Western blot of ATF4 in Par and GemR treated with thapsigargin (Thap). (D) Expression of stress responsive genes upon thapsigargin (Thap) treatment in Par and GemR. Mean ±SD, n=3. *P≤0.05, **P≤0.01, ***P≤0.001, ns=not significant.

2.4.3 *STIM1* amplification elicits a higher store-operated calcium entry driving ER stress resistance

Long-term thapsigargin treatment inhibits cell proliferation via induction of the ER stress response pathway. Therefore, we examined whether GemR displayed differential responsiveness to thapsigargin compared to Par. Indeed, GemR were significantly more resistant to the anti-proliferative effects of thapsigargin (IC_{50}: >819.2 nM) compared to Par (IC_{50}: 5.09 nM ± 0.20 nM) (Fig. 18A-B). Consistently, analysis of DepMap data revealed that thapsigargin sensitivity highly correlated with gemcitabine sensitivity in pancreatic cancer cell lines (Fig. 18C). ER stress is

triggered by the accumulation of unfolded proteins or changes in redox, calcium, or nutrient levels in the ER (Carreras-Sureda et al., 2018; Pakos-Zebrucka et al., 2016). Furthermore, thapsigargin is a SERCA-pump inhibitor, which affects ER calcium storage. Therefore, we examined whether protein-coding genes involved in these processes were aberrantly regulated and amplified in GemR. Interestingly, *STIM1*, an ER calcium sensor coding gene, was among the most amplified and highly upregulated genes in GemR, being co-amplified with *RRM1* in a focal amplification within the larger amplified region on chr11. Previous studies have also reported the upregulation of *STIM1* and *RRM1* upon gemcitabine treatment and gemcitabine resistance in pancreatic cancer cells (Kondratska et al., 2014; Zhou et al., 2019). Notably, analysis of DepMap data revealed that *RRM1* and *STIM1* amplifications are highly correlated in cancer cell lines, including pancreatic cancer. Additionally, analysis of TCGA data revealed that 5% of pancreatic cancer patients display a gain of both genes irrespective of treatment modality (Fig. 18D). Consistently, we were able to identify several established cell lines that displayed an amplification and an increased expression of STIM1. For example, the pancreatic and colorectal cancer cell lines Panc1 and DLD1, respectively, highly co-expressed RRM1 and STIM1, while the osteosarcoma cell line SJSA only expressed high levels of STIM1 (Fig. 18E).

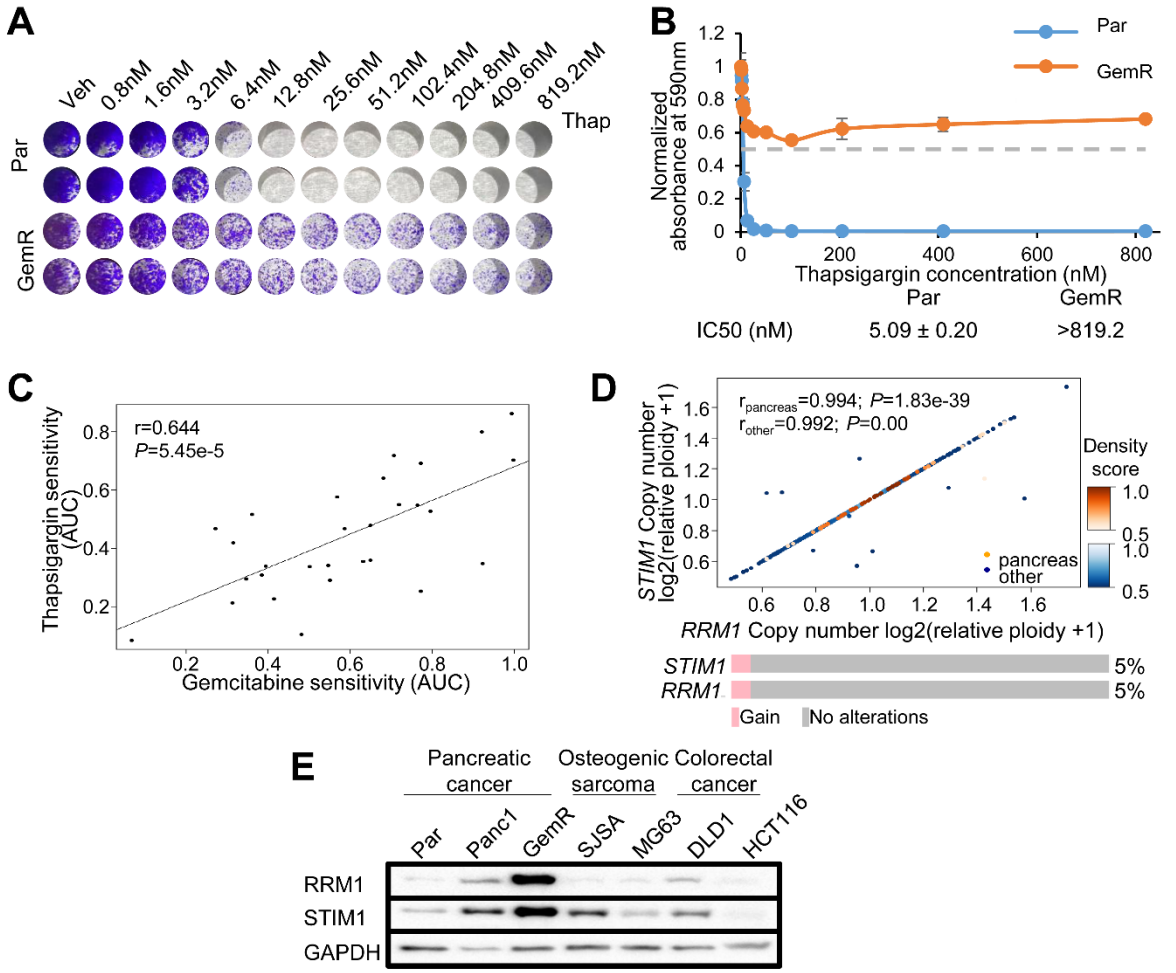

Fig. 18 Amplification of *STIM1* leads to increased SOCE. (A) Crystal violet staining of a 7 days proliferation assay of Par and GemR treated with thapsigargin (Thap). (B) Proliferation assay of Par and GemR treated with thapsigargin for 7 days. The absorbance of cell titer blue was normalized to the respective vehicle absorbance. Mean ±SD, n=2. IC_{50} values ±SD, n=2. (C) Scatter plot showing the Spearman correlation of gemcitabine and thapsigargin sensitivity in pancreatic cancer cell lines obtained from DepMap. r=0.644, P=5.45e-5. (D) Density scatter plot showing the Spearman correlation of the copy number of RRM1 and STIM1 in pancreatic and other cancer cell lines obtained from DepMap. $r_{pancreas}$=0.994, P=1.83e-39; r_{other}=0.992, P=0.00. Oncoprint and co-occurence probability of a gain of STIM1 and RRM1 in pancreatic cancer patients from TCGA PanCancer Atlas Studies data (cBioportal). (E) Western blot of STIM1 and RRM1 levels in pancreatic, colorectal and osteosarcoma cell lines.

STIM1 is an ER calcium sensor that interacts with and activates ORAI calcium channels in the plasma membrane following ER calcium store depletion. This leads to ORAI channel opening, allowing extracellular calcium to enter the cytosol in a process termed store-operated calcium entry (SOCE) (Prakriya and Lewis, 2015b; Soboloff et al., 2012). Fluorescence calcium measurements revealed comparable calcium levels at resting conditions and upon thapsigargin-induced ER calcium store depletion in Par and GemR. However, GemR displayed a highly increased SOCE compared to Par, which could be reversed by STIM1 depletion (Fig. 19A). While

recent studies have pointed at the effects of STIM1 on ER stress response (Conceicao et al., 2020; Gilon et al., 2018), no such correlation has been reported in cancer. Moreover, the possible effects elicited by increased SOCE on ER stress response remain elusive. Thus, we investigated whether higher STIM1 levels, and consequently increased SOCE, could lead to ER stress resistance in GemR. To address this, SOCE was prevented by either treating with the SOCE inhibitor, CM4620, or by chelating extracellular calcium from the media with EGTA before the induction of ER stress by thapsigargin. Notably, as assessed via ATF4 accumulation, treatment with either CM4620 or EGTA restored the stress response to thapsigargin in GemR to levels comparable to thapsigargin treatment alone in Par (Fig. 19B and D). This confirms that ER stress resistance in GemR is conferred by elevated SOCE elicited by STIM1. This conclusion was further supported by the ability of combined CM4620 or EGTA and thapsigargin treatment to rescue the expression of ER stress responsive genes in GemR (Fig. 19C and E).

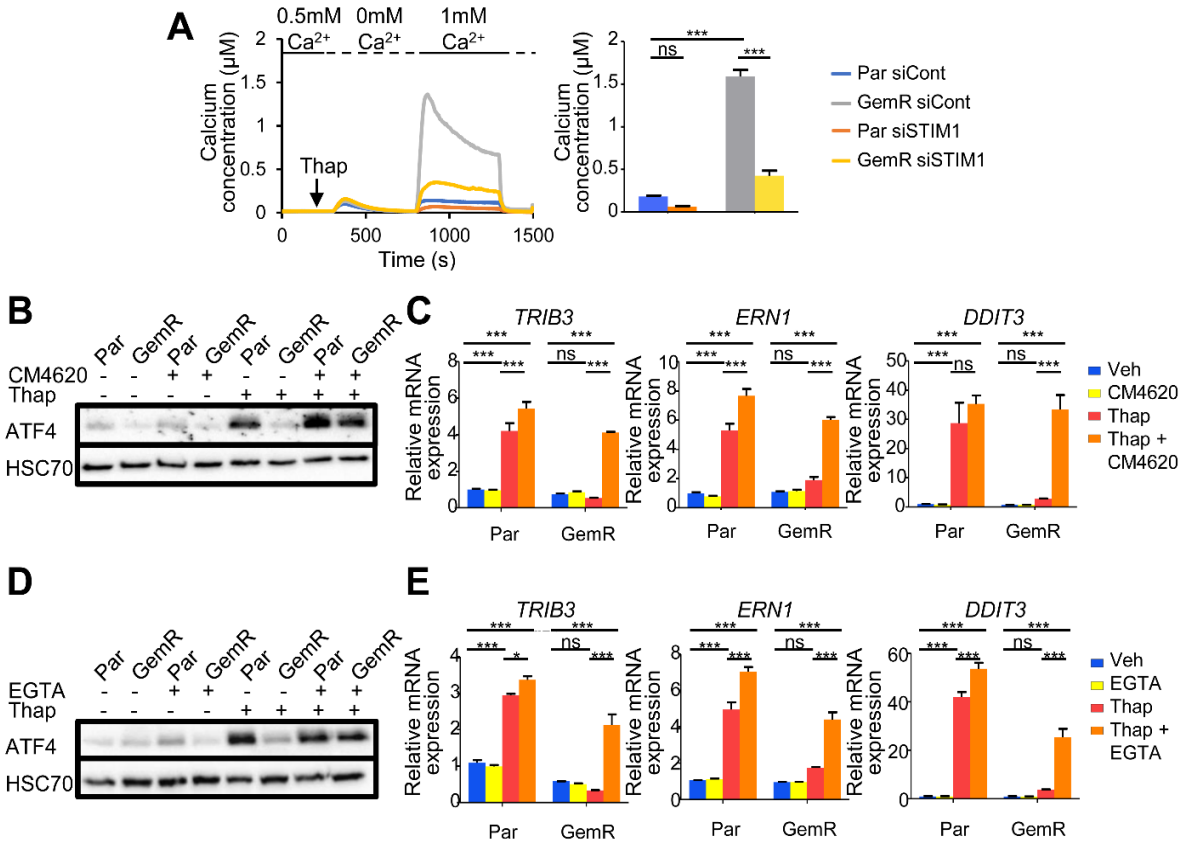

Fig. 19 Increased SOCE elicits ER stress resistance in GemR. (A) Fura-2 based cytosolic calcium imaging and quantification of $\Delta SOCE_{max}$. Mean ±SEM, n=334 (Par siCont), 143 (Par siSTIM1), 347 (GemR siCont), 243 (GemR siSTIM1). (B) Western blot showing ATF4 levels upon SOCE inhibition by CM4620 and thapsigargin (Thap) treatment in Par and GemR. (C) Expression of stress responsive genes upon SOCE inhibition by CM4620 and thapsigargin (Thap) treatment in Par and GemR. Mean ±SD, n=3. (D) Western blot depicting ATF4 levels upon EGTA and thapsigargin (Thap) treatments in Par and GemR. (E) Expression of stress responsive genes upon EGTA and thapsigargin (Thap) treatment in Par and GemR. Mean ±SD, n=3. *P≤0.05, **P≤0.01, ***P≤0.001, ns=not significant.

Moreover, overexpression of STIM1 in Par cells was sufficient to lower ATF4 levels and impair the induction of stress responsive genes upon thapsigargin treatment (Fig. 20A-B). Similarly, STIM1 overexpression in other pancreatic cancer cell lines, namely BxPC-3 and CFPAC-1, decreased ATF4 accumulation and dampened the induction of stress-responsive genes following thapsigargin treatment (Fig. 20C-H).

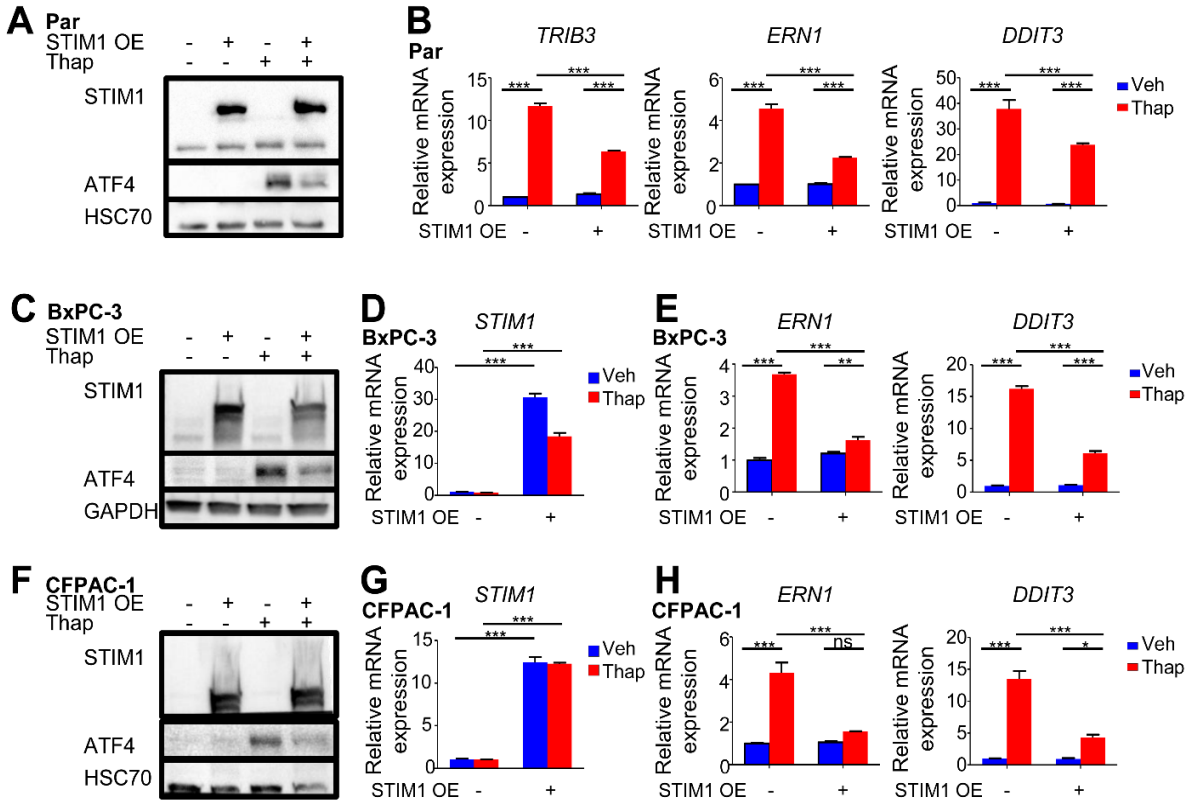

Fig. 20 STIM1 overexpression leads to a dampened ER stress response in PDAC. (A) Western blot of STIM1 and ATF4 levels upon STIM1 overexpression and thapsigargin (Thap) treatment in Par. (B) Expression of stress responsive genes upon STIM1 overexpression and thapsigargin (Thap) treatment in Par. Mean ±SD, n=3. (C) Western blot of STIM1 and ATF4 levels upon STIM1 overexpression and thapsigargin (Thap) treatment in BxPC-3. (D) Validation of STIM1 overexpression in BxPC-3. Mean ±SD, n=3. (E) Expression of stress responsive genes upon STIM1 overexpression and thapsigargin (Thap) treatment in BxPC-3. Mean ±SD, n=3. (F) Western blot of STIM1 and ATF4 levels upon STIM1 overexpression and thapsigargin (Thap) treatment in CFPAC-1. (G) Validation of STIM1 overexpression in CFPAC-1. Mean ±SD, n=3. (H) Expression of stress responsive genes upon STIM1 overexpression and thapsigargin (Thap) treatment in CFPAC-1. Mean ±SD, n=3. *P≤0.05, **P≤0.01, ***P≤0.001, ns=not significant.

Consistent with these effects, inhibition of SOCE with CM4620 (Fig. 21A-D) or STIM1 depletion (Fig. 21E-I) restored the anti-proliferative effects of thapsigargin in GemR.

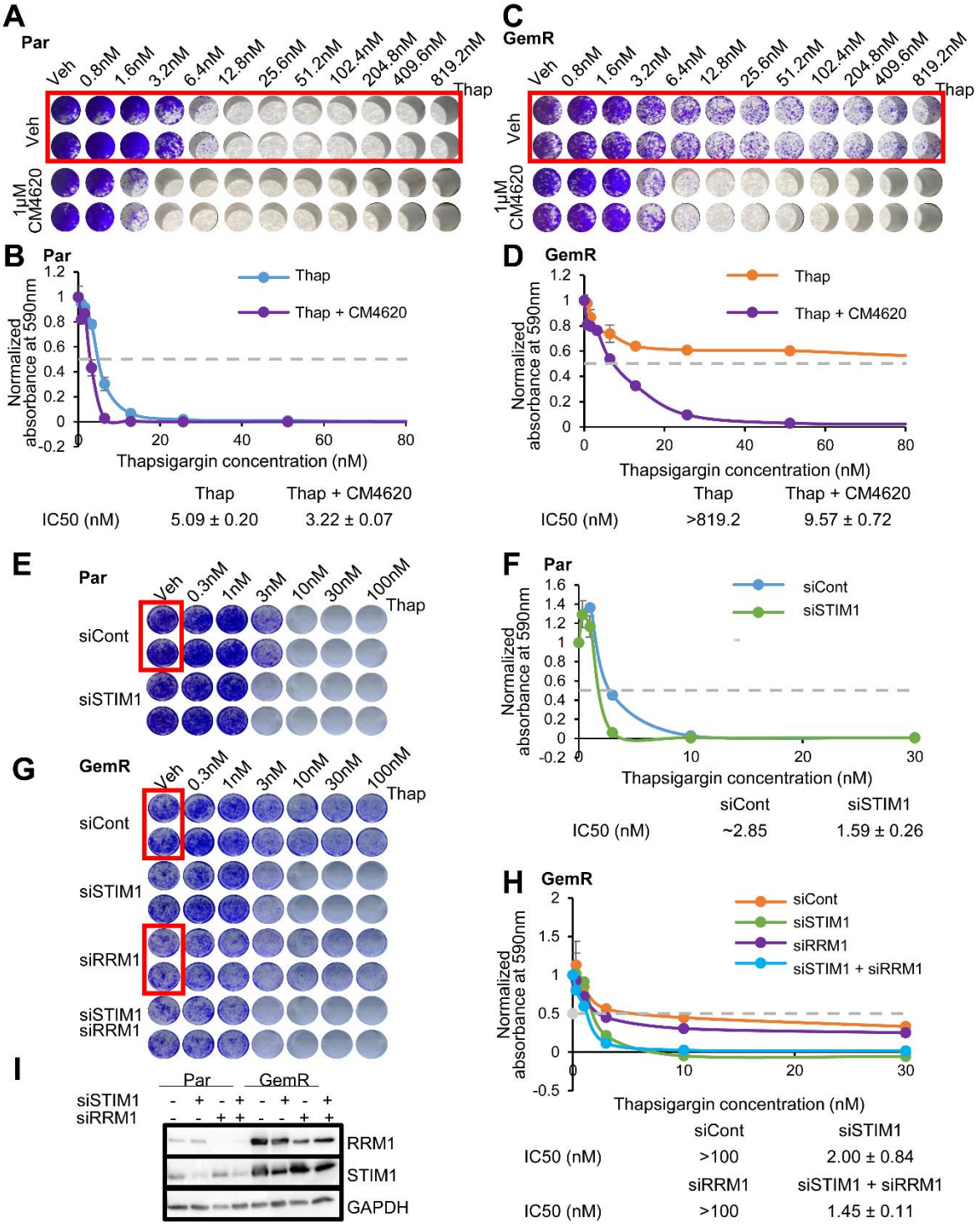

Fig. 21 SOCE impairment sensitizes GemR to ER stress. (A) Crystal violet staining of a 7 days proliferation assay in Par upon CM4620 and thapsigargin (Thap) treatments. In a red box are the thapsigargin (Thap) only treated Par, also shown in Fig. 6A. (B) Proliferation assay of Par treated with CM4620 and thapsigargin (Thap) for 7 days. The absorbance of cell titer blue was normalized to the respective vehicle absorbance. Mean ±SD, n=2. IC_{50} values ±SD, n=2. The profile of Par treated with thapsigargin (Thap) only was previously depicted in Fig. 6B. (C) Crystal violet staining of a 7 days proliferation assay in GemR upon SOCE inhibition by CM4620 and thapsigargin (Thap) treatment. In a red box are the thapsigargin (Thap) only treated GemR, also shown in Fig. 6A. (D) Proliferation assay of GemR treated with thapsigargin and the SOCE inhibitor CM4620 for 7 days. The absorbance of cell titer blue was normalized to the respective vehicle absorbance. Mean ±SD, n=2. IC_{50} values ±SD, n=2. The profile of GemR treated with thapsigargin (Thap) only was previously shown in Fig. 6B. (E) Crystal violet staining of a 7 days proliferation assay in Par upon STIM1 depletion and treatment with thapsigargin (Thap). Highlighted in a red box is the control, vehicle-treated Par, which was previously shown in Fig. 3A. (F) Proliferation assay of Par depleted from STIM1 and treated with thapsigargin (Thap) for 7 days. The absorbance of solubilized crystal violet was normalized to the respective vehicle absorbance. Mean ±SD, n=2. IC_{50} values ±SD, n=2. (G) Crystal violet staining of a 7 days proliferation assay in GemR upon STIM1 and/or RRM1 knockdown and treatment with thapsigargin (Thap). Highlighted in a red box are the control, vehicle-treated GemR and vehicle-treated RRM1-depleted GemR, which were previously shown in Fig. 3A. (H) Proliferation assay of GemR depleted from STIM1 and/or RRM1 and treated with thapsigargin (Thap) for 7 days. The absorbance of solubilized crystal violet was normalized to the respective vehicle absorbance. Mean ±SD, n=2. IC_{50} values ±SD, n=2. (I) Western blot validation of STIM1 and RRM1 knockdown in Par and GemR.

This was further validated in the colorectal cancer cell line DLD1, which expressed higher levels of both STIM1 and RRM1 and was more resistant to the anti-proliferative effects of thapsigargin compared to HCT116. Consistently, SOCE inhibition restored the sensitivity of DLD1 to thapsigargin to levels similar to HCT116 (Fig. 22A-D). Thus, higher levels of STIM1, and thereby SOCE, in GemR as well as other tumor cell lines provide a survival advantage under ER stress conditions.

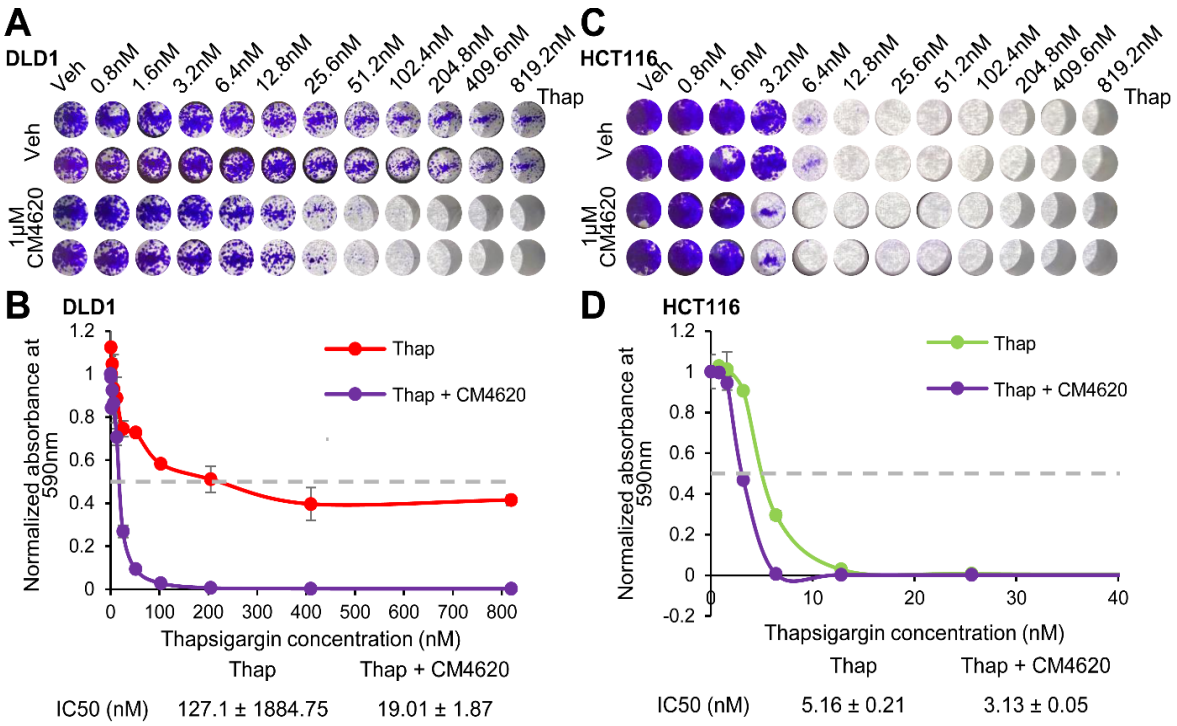

Fig. 22 STIM1 levels correlate with ER stress resistance in colorectal cancer. (A) Crystal violet staining of a 7 days proliferation assay in DLD1 upon SOCE inhibition by CM4620 and thapsigargin (Thap) treatment. (B) Proliferation assay of DLD1 treated with CM4620 and thapsigargin (Thap) for 7 days. The absorbance of cell titer blue was normalized to the respective vehicle absorbance. Mean ±SD, n=2. IC_{50} values ±SD, n=2. (C) Crystal violet staining of a 7 days proliferation assay in HCT116 upon SOCE inhibition by CM4620 and thapsigargin (Thap) treatment. (D) Proliferation assay of HCT116 treated with CM4620 and thapsigargin (Thap) for 7 days. The absorbance of cell titer blue was normalized to the respective vehicle absorbance. Mean ±SD, n=2. IC_{50} values ±SD, n=2.

Since *STIM1* and *RRM1* are commonly co-amplified and have important physiological functions, we tested whether they act synergistically. For this, we monitored cell proliferation upon STIM1 and/or RRM1 depletion and thapsigargin or gemcitabine treatment. RRM1 levels did not influence cell growth upon thapsigargin treatment and the depletion of both RRM1 and STIM1 was not synergistic (Fig. 21G-I). Similarly, while RRM1 depletion restored gemcitabine responsiveness, STIM1 knockdown did not appreciably influence GemR growth upon gemcitabine treatment nor did it synergize with RRM1 depletion (Fig. 13A, Fig. 21I and Fig. 23A-B). Furthermore, SOCE inhibition did not influence the effects of gemcitabine treatment on cell proliferation in either GemR or Par cells (Fig. 1A-B and Fig. 23C-D). Together, these findings confirm that while *STIM1* and *RRM1* are co-amplified in human tumors and cancer cell lines, they independently affect calcium-associated ER stress and gemcitabine responsiveness, respectively.

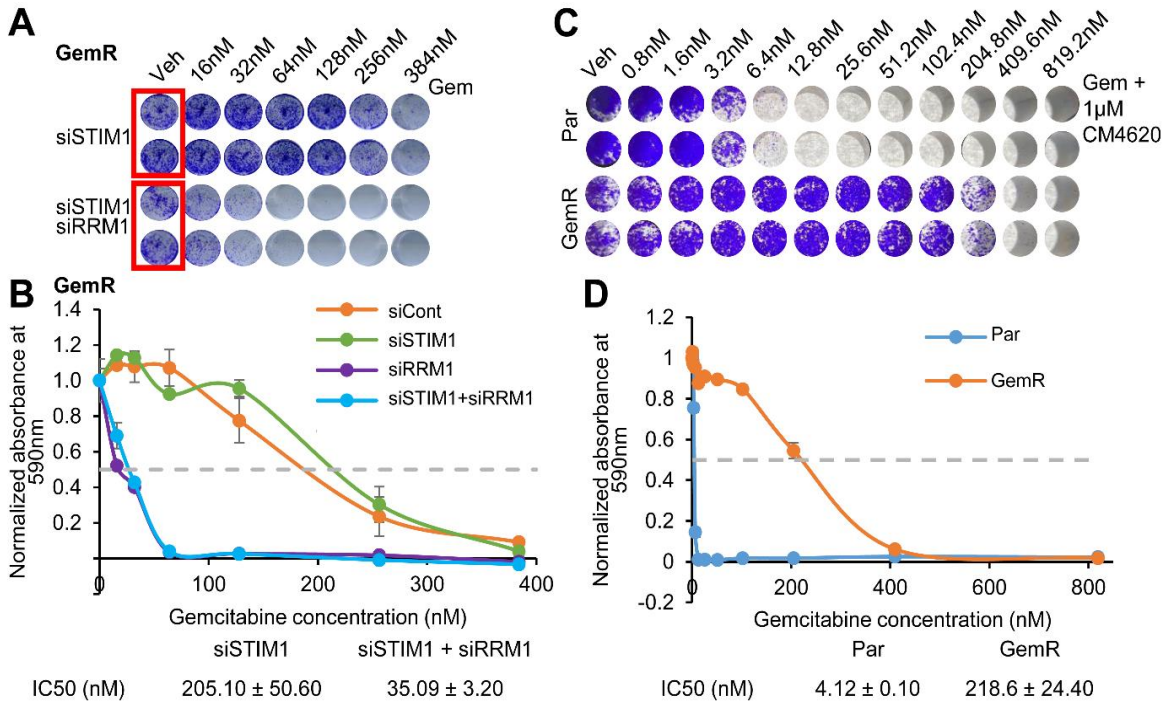

Fig. 23 *STIM1* amplification does not affect gemcitabine resistance in GemR. (A) Crystal violet staining of a 7 days proliferation assay of STIM1 and/or RRM1 depleted GemR treated with gemcitabine (Gem). In red boxes are the vehicle-treated and STIM1 or STIM1 and RRM1 depleted GemR, also shown in Fig. 9G. (B) Proliferation assay of GemR depleted from STIM1 and/or RRM1 and treated with gemcitabine (Gem) for 7 days. The absorbance of solubilized crystal violet was normalized to the respective vehicle absorbance. Mean ±SD, n=2. IC_{50} values ±SD, n=2. The profiles of GemR siCont and GemR siRRM1 were previously depicted in Fig. 1C. (C) Crystal violet staining of a 7 days proliferation assay in Par and GemR upon CM4620 and gemcitabine (Gem) treatments. The crystal violet staining of a 7 days proliferation of Par and GemR treated with gemcitabine (Gem) only can be found in Fig. 1B. (D) Proliferation assay of Par and GemR treated with CM4620 and gemcitabine (Gem) for 7 days. The absorbance of cell titer blue was normalized to the respective vehicle absorbance. Mean ±SD, n=2. IC_{50} values ±SD, n=2. The profiles of Par and GemR treated with gemcitabine (Gem) only can be found in Fig. 1C.

2.4.4 STIM1 depletion restores ER stress-induced transcriptomic and epigenomic changes

To further characterize the role of STIM1 in ER stress resistance, we performed mRNA sequencing in Par, GemR, and STIM1-depleted GemR treated with thapsigargin. Consistent with GemR being resistant to ER stress, gene set enrichment analysis (GSEA) displayed an enrichment of the “Unfolded Protein Response” in Par compared to GemR following treatment with thapsigargin (Fig. 24A and Table S3). Hierarchical clustering revealed two gene clusters whose expression was influenced by STIM1 (Fig. 24B). Genes within cluster 1 were upregulated in thapsigargin-treated Par, but failed to be activated in GemR. Importantly, their induction was rescued by STIM1 depletion in GemR, and were

thus referred to as “down (DN-)reversed” genes. Cluster 2 genes were not induced in Par, but upregulated in GemR in response to thapsigargin. Notably, STIM1 depletion in GemR reversed their induction by thapsigargin and were therefore referred to as “UP-reversed” genes (Table S4). Consistent with our observations, the DN-reversed cluster includes the ER-stress responsive genes *TRIB3*, *ERN1* and *DDIT3*, whose induction by thapsigargin was rescued upon STIM1 depletion in GemR (Fig. 24C). Moreover, STIM1-depletion restored ATF4 accumulation in response to thapsigargin treatment in GemR (Fig. 24D). To validate our findings in another pancreatic cancer cell line, we assessed the induction of DN-reversed genes in *STIM1*-amplified Panc1 cells. Here we observed low levels of induction of DN-reversed genes and ATF4 upon thapsigargin treatment, which were rescued by STIM1 depletion (Fig. 24E-F).

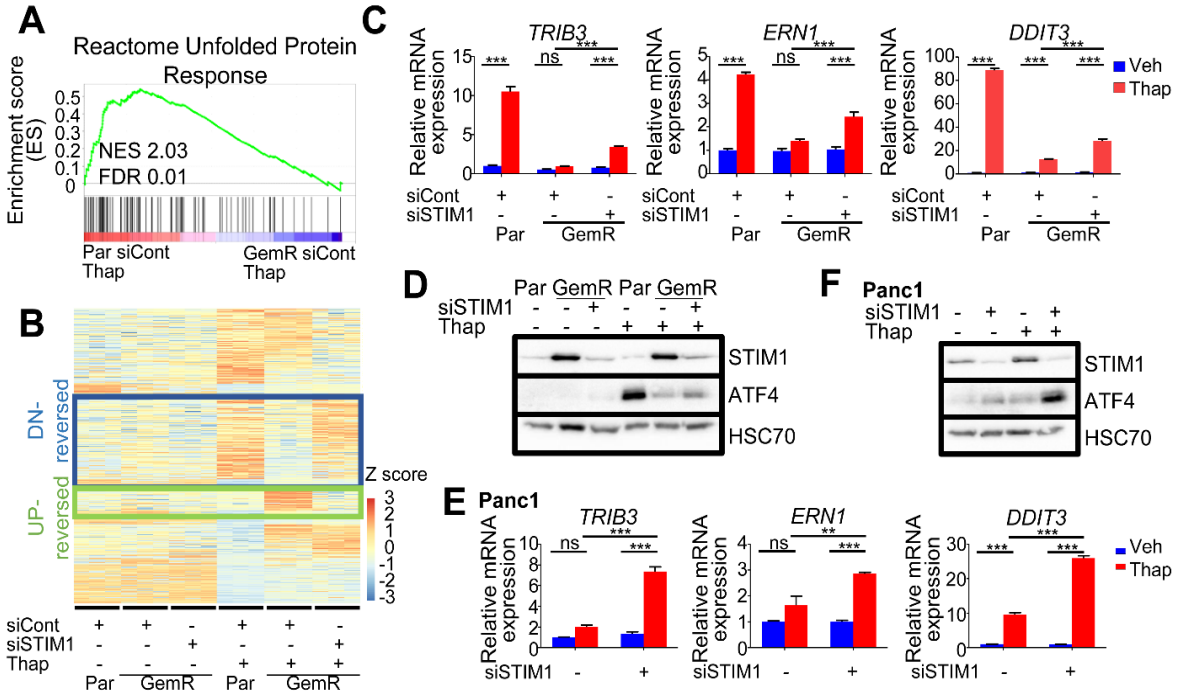

Fig. 24 STIM1 depletion sensitizes GemR to ER stress. (A) GSEA showing an enrichment for the unfolded protein response upon thapsigargin (Thap) treatment in Par. (B) Heatmap showing the Z-score of each gene ordered into 4 clusters identified by hierarchical clustering highlighting gene clusters: DN-reversed and UP-reversed. (C) Expression of DN-reversed genes upon thapsigargin (Thap) treatment in Par, GemR and STIM1-depleted GemR. Mean ±SD, n=3. (D) Western Blot of ATF4 and STIM1 levels upon a STIM1 knockdown and thapsigargin (Thap) treatment in Par and GemR. (E) Expression of DN-reversed genes upon thapsigargin (Thap) treatment in Panc1 and STIM1-depleted Panc1. Mean ±SD, n=3. (F) Western Blot of ATF4 and STIM1 levels upon a STIM1 knockdown and thapsigargin (Thap) treatment in Panc1. *P≤0.05, **P≤0.01, ***P≤0.001, ns=not significant.

We next sought to uncover the molecular and transcriptional mechanisms responsible for the differential gene regulation observed in GemR. Based on our initial epigenome mapping studies, we rationalized that ER stress-induced gene expression changes may be coupled to epigenetic reprogramming. Indeed, in accordance with the gene expression data, H3K27ac occupancy increased near the TSS of DN-reversed genes in Par, but not in GemR upon thapsigargin treatment. STIM1 depletion as well as SOCE inhibition by CM4620 in GemR partially rescued the H3K27ac gain on the TSS of these genes with thapsigargin (Fig. 25A-C).

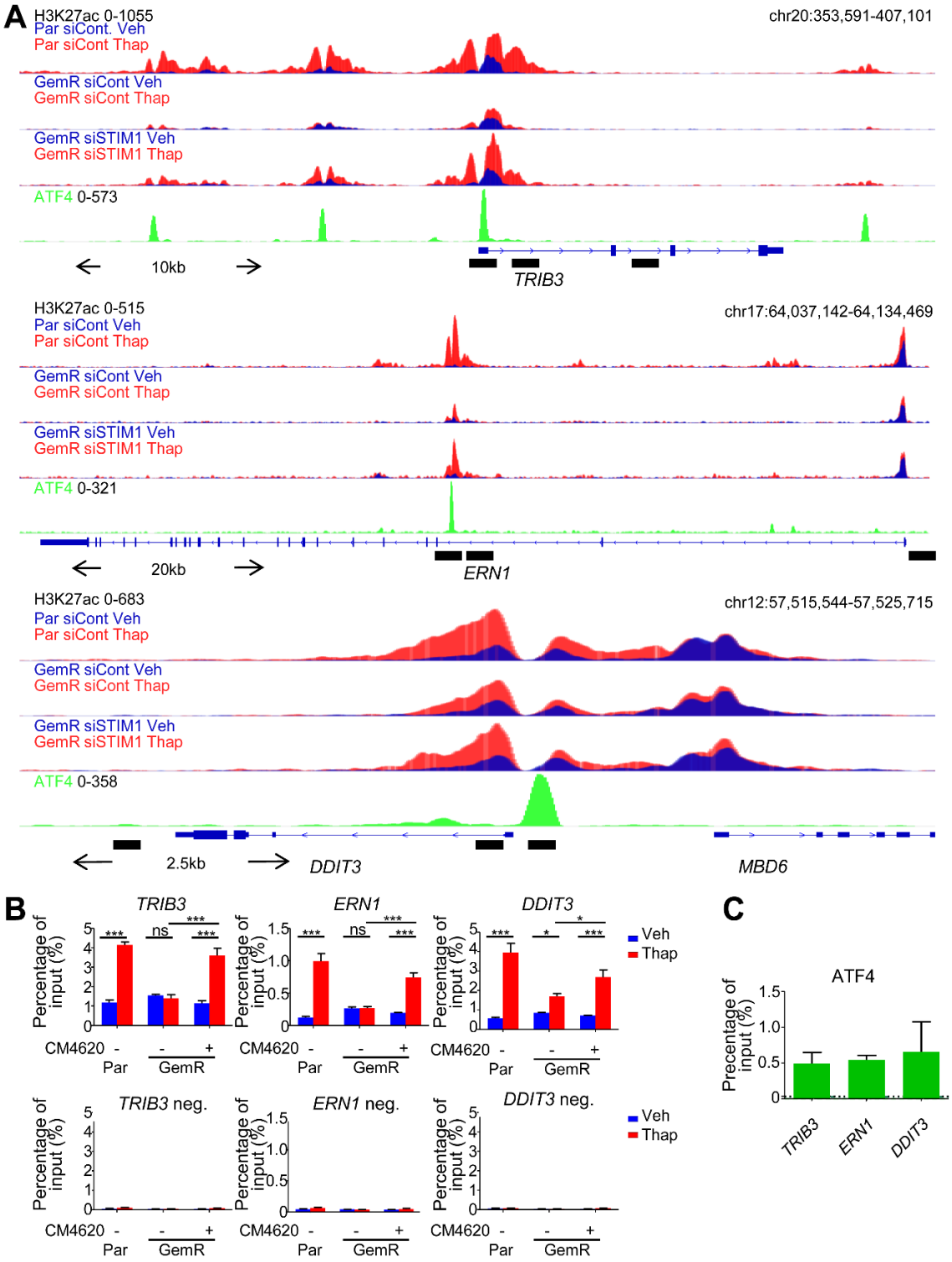

Fig. 25 SOCE impairment partially rescues H3K27ac profile around ER stress responsive genes in GemR. (A) ATF4 profile in Par treated with thapsigargin (Thap) and H3K27ac profile in Par and GemR upon thapsigargin (Thap) treatment and STIM1 depletion. Black boxes indicate the regions used for ChIP qPCR. (B) ChIP qPCR of positive and negative H3K27ac sites around the TSS of TRIB3, ERN1 and DDIT3 in Par and GemR upon SOCE inhibition by CM4620 and thapsigargin (Thap) treatment. Each condition is depicted as a percentage of its corresponding input. Mean ±SD, n=3. (C) ChIP qPCR of positive ATF4 sites around the TSS of TRIB3, ERN1 and DDIT3 in Par treated with thapsigargin (Thap). The average ATF4 signal on the negative sites around TRIB3, ERN1 and DDIT3 is shown as a light green, dark green and black dotted line, respectively. Each

condition is depicted as a percentage of its corresponding input. Mean ±SD, n=2. *P≤0.05, **P≤0.01, ***P≤0.001, ns=not significant.

Consistent with our earlier findings, STIM1-depletion in GemR restored an enrichment of ATF4 and CHOP motifs in H3K27ac gained regions upon thapsigargin treatment in a manner similar to what we observed following thapsigargin treatment in Par cells (Fig. 26A), where 53% of ATF4 peaks overlapped with H3K27ac gained regions in Par (thapsigargin vs vehicle). On these regions, a significant increase in H3K27ac was only observed in Par and STIM1-depleted GemR, but not in GemR upon thapsigargin treatment (Fig. 26B-D). This confirms that GemR cells fail to recruit epigenetic factors to DN-reversed genes in a STIM1-dependent manner, indicating that STIM1-dependent SOCE rewires the cellular epigenome and transcriptome, attenuating the activation of stress-specific genes.

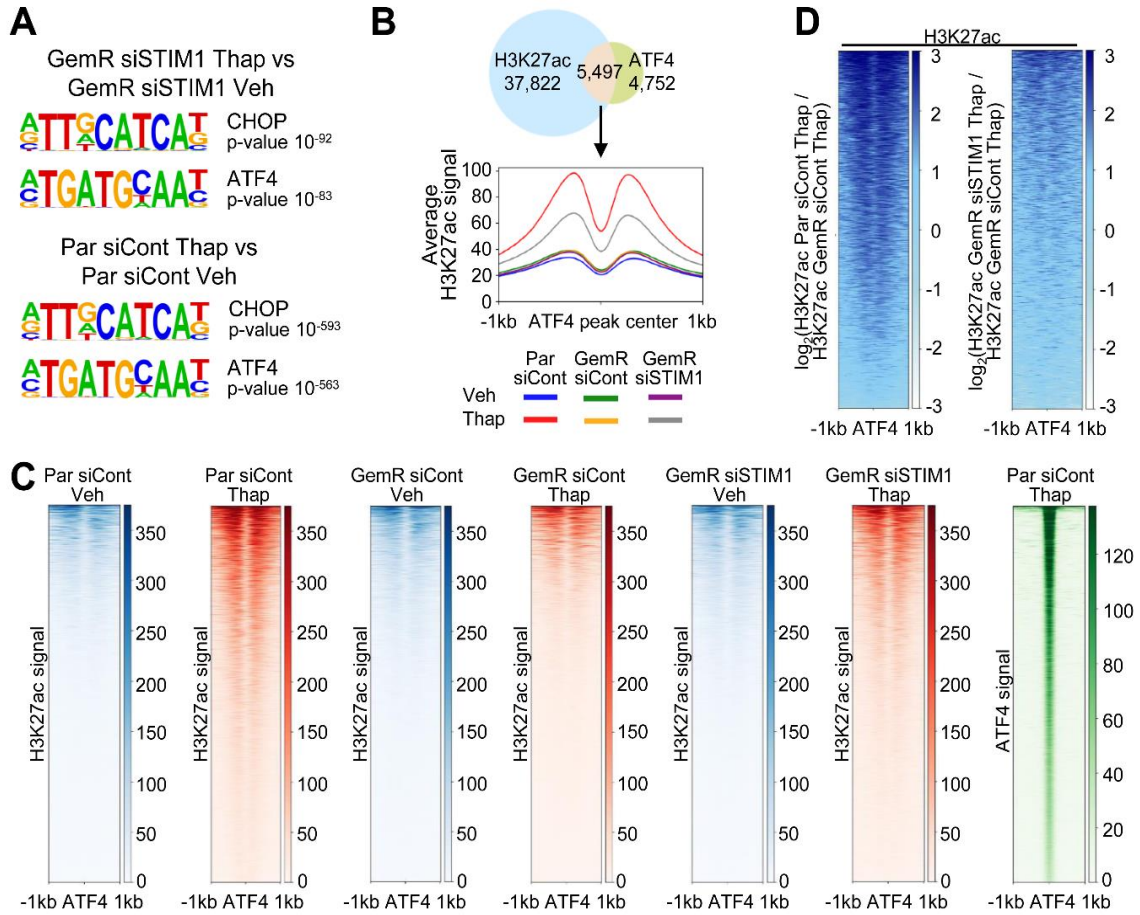

Fig. 26 STIM1 knockdown rescues H3K27ac profile around ATF4-occupied regions in GemR. (A) Top most significantly enriched motifs on gained H3K27ac regions in thapsigargin-treated (Thap) STIM1-depleted GemR compared to vehicle-treated STIM1-depleted GemR (top) and on gained H3K27ac regions in Par treated with thapsigargin (Thap) compared to vehicle-treated Par (bottom). (B) Venn diagram of ATF4 peaks in Par treated with thapsigargin (Thap) and gained H3K27ac regions in Par treated with thapsigargin (Thap) compared to vehicle-treated Par. Aggregate plot of H3K27ac on ATF4 summits of overlapping regions. (C) Heatmaps of H3K27ac and ATF4 on ATF4 summits of overlapping regions from Fig. 14B. (D) Bigwig compare of Par (left) and STIM1-depleted GemR (right) upon thapsigargin (Thap) treatment both compared to GemR treated with thapsigargin (Thap) on ATF4 summits of the overlapping regions identified in Fig. 14B.

2.4.5 NFAT is aberrantly activated in *STIM1*-amplified cells

After characterizing the effects of *STIM1* amplification on ER stress-induced gene expression, we examined genes that were specifically induced by thapsigargin in the presence of *STIM1* amplification (UP-reversed cluster), which included *KDM7A, KRT14* and *KLF4*. These genes were upregulated upon thapsigargin treatment in GemR, but less induced in Par and STIM1-depleted GemR (Fig. 27A). Similarly, SOCE inhibition diminished the induction of these genes by thapsigargin in GemR (Fig. 27B). These effects were not limited to GemR since *STIM1*-amplified Panc1 cells also displayed an upregulation of *KDM7A* and *KLF4* upon thapsigargin treatment in a STIM1-dependent manner (Fig. 27C). Moreover, H3K27ac signal intensity on the TSS of UP-reversed genes displayed a significant increase in GemR compared to Par and STIM1-depleted GemR upon thapsigargin treatment (Fig. 27D).

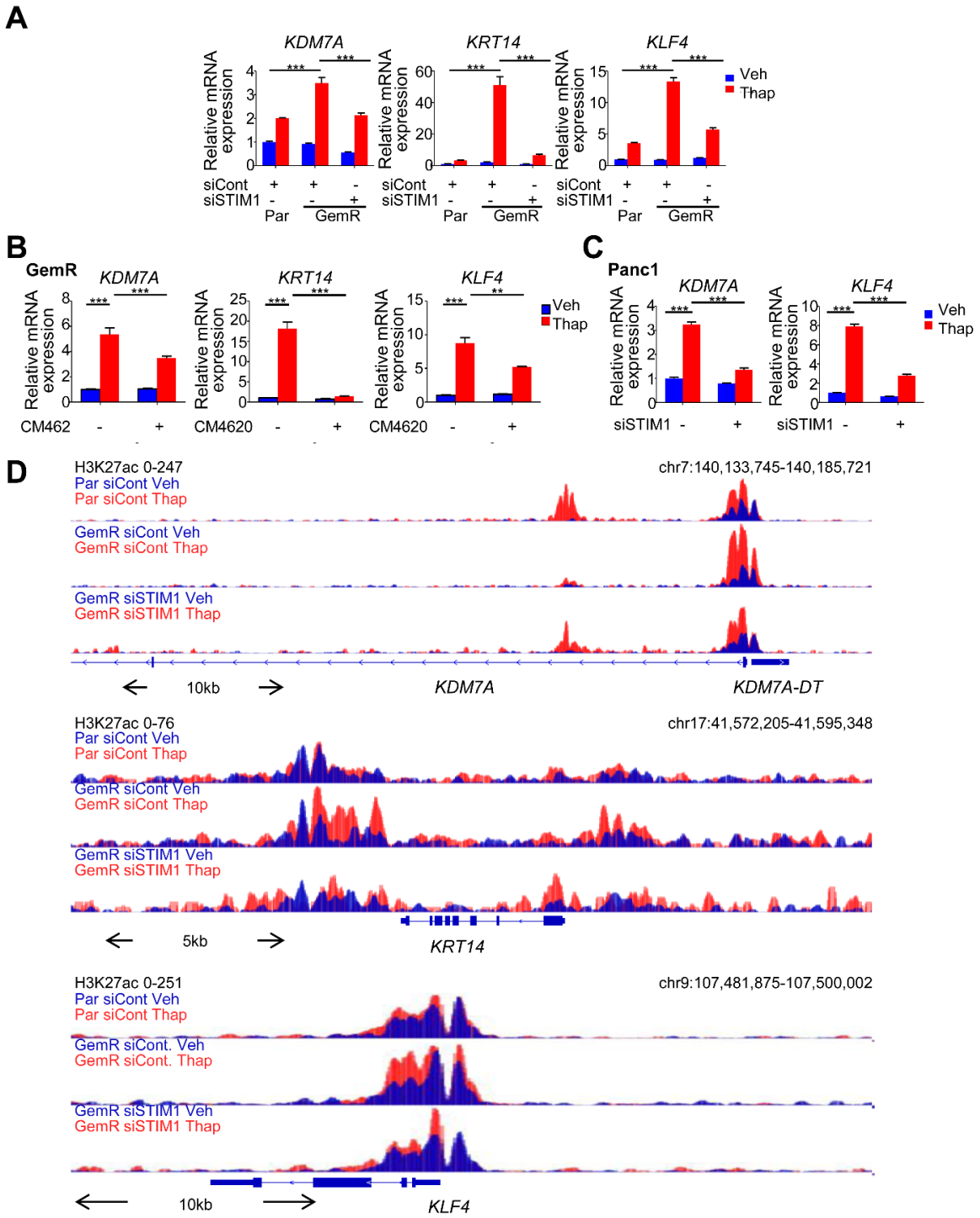

Fig. 27 Upon ER stress, *STIM1*-amplified cells upregulate and gain H3K27ac around the TSS of UP-reversed genes. (A) Gene expression of UP-reversed genes upon thapsigargin (Thap) treatment and STIM1 depletion in Par and GemR. Mean ±SD, n=3. (B) Gene expression of UP-reversed genes upon thapsigargin (Thap) treatment and SOCE inhibition by CM4620 in GemR. Mean ±SD, n=3. (C) Gene expression of UP-reversed genes upon thapsigargin (Thap) treatment and STIM1 depletion in Panc1. Mean ±SD, n=3. (D) H3K27ac profile around the TSS of UP-reversed genes in Par, GemR and STIM1-depleted GemR treated with thapsigargin (Thap). *P≤0.05, **P≤0.01, ***P≤0.001, ns=not significant.

To uncover the underlying mechanisms by which this subset of genes was specifically induced in response to ER stress in GemR cells, we employed EnrichR and GSEA. NFAT-related pathways were identified by EnrichR, while GSEA displayed an enrichment for the “NFAT transcription factor pathway” in thapsigargin-treated GemR cells (siCont vs siSTIM1) (Fig. 28A-B and Table S5). Consistently, NFAT and NFAT-AP1 motifs were enriched in genomic regions displaying increased H3K27ac in the same comparison (Fig. 28C). NFAT activation by calcium signaling promotes its translocation to the nucleus, thereby enabling target gene activation. Consistent with our findings that GemR cells display pronounced SOCE, NFAT nuclear translocation was increased in thapsigargin-treated GemR and decreased by STIM1 depletion (Fig. 28D-E).

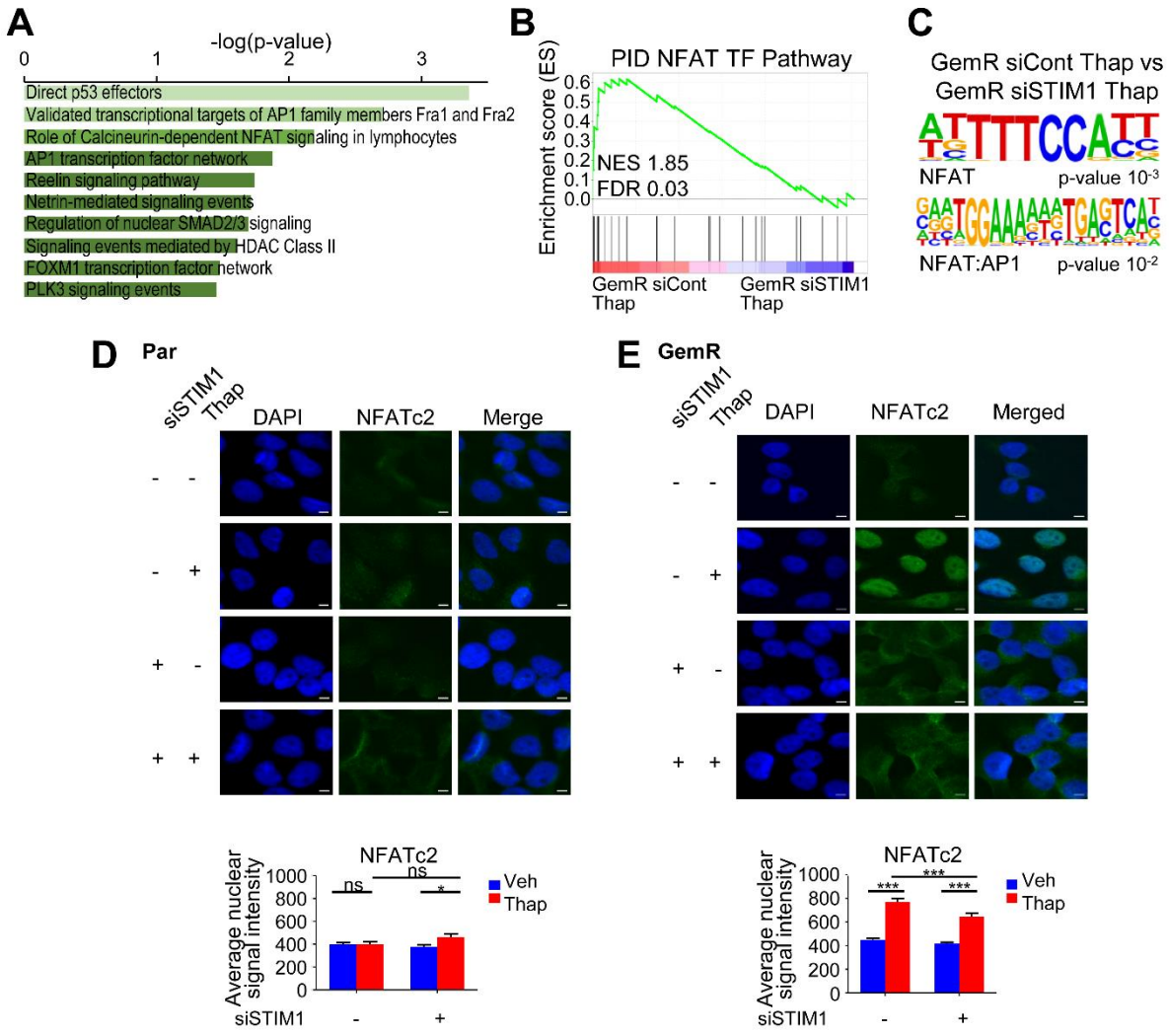

Fig. 28 GemR aberrantly activate NFAT upon ER stress. (A) NCI-2016 signature of UP-reversed genes from EnrichR showing an enrichment for Calcineurin-dependent NFAT signaling. (B) GSEA showing an enrichment for the NFAT TF pathway in GemR compared to STIM1-depleted GemR both treated with thapsigargin (Thap). (C) Motif analysis showing a significant enrichment for NFAT motifs on gained H3K27ac regions in GemR compared to STIM1-depleted GemR both treated with thapsigargin (Thap). (D) NFATc2 immunofluorescence and average nuclear signal intensity in Par. Scale=5µm. Mean ±SEM, *n*=47 (Par siCont Veh), 34 (Par siCont Thap), 34 (Par si*STIM1* Veh), 41 (Par si*STIM1* Thap). (E) NFATc2 immunofluorescence and average nuclear signal intensity in GemR. Scale=5µm. Mean ±SEM, *n*=68 (GemR siCont Veh), 57 (GemR siCont Thap), 30 (GemR siSTIM1 Veh), 82 (GemR siSTIM1 Thap). **P*≤0.05, ***P*≤0.01, ****P*≤0.001, ns=not significant.

To confirm the importance of NFAT in driving the expression of UP-reversed genes, we treated GemR with the calcineurin inhibitor cyclosporine A (CSA) to attenuate NFAT activation. We observed that the induction of UP-reversed genes by thapsigargin was dampened upon CSA treatment (Fig. 29A). Among the various NFAT proteins, NFATc2 is more tightly linked to STIM1 and SOCE (Kar and Parekh, 2015; Kar et al., 2011). *NFATc2* is also the only NFAT family member contained in the UP-reversed gene cluster. Consistent with a critical role in mediating the effects of altered calcium signaling in STIM1-amplified cells, NFATc2 depletion significantly dampened the induction of UP-reversed genes in thapsigargin-treated GemR (Fig. 29B-C). Overexpression of STIM1 in Par, BxPC-3 and CFPAC-1 further confirmed that the upregulation of these genes by thapsigargin was due to increased SOCE elicited by higher STIM1 (Fig. 29D-F). Notably, the overexpression of NFATc2 in Par did not affect ATF4 levels and the ER stress response (Fig. 29G). This suggests that heightened SOCE independently leads to a dampened ER stress response and an aberrant NFATc2 activation. In conclusion, *STIM1* amplification facilitates and increased SOCE, thereby promoting the upregulation of *NFATc2* and calcium-mediated activation of NFATc2-dependent gene expression.

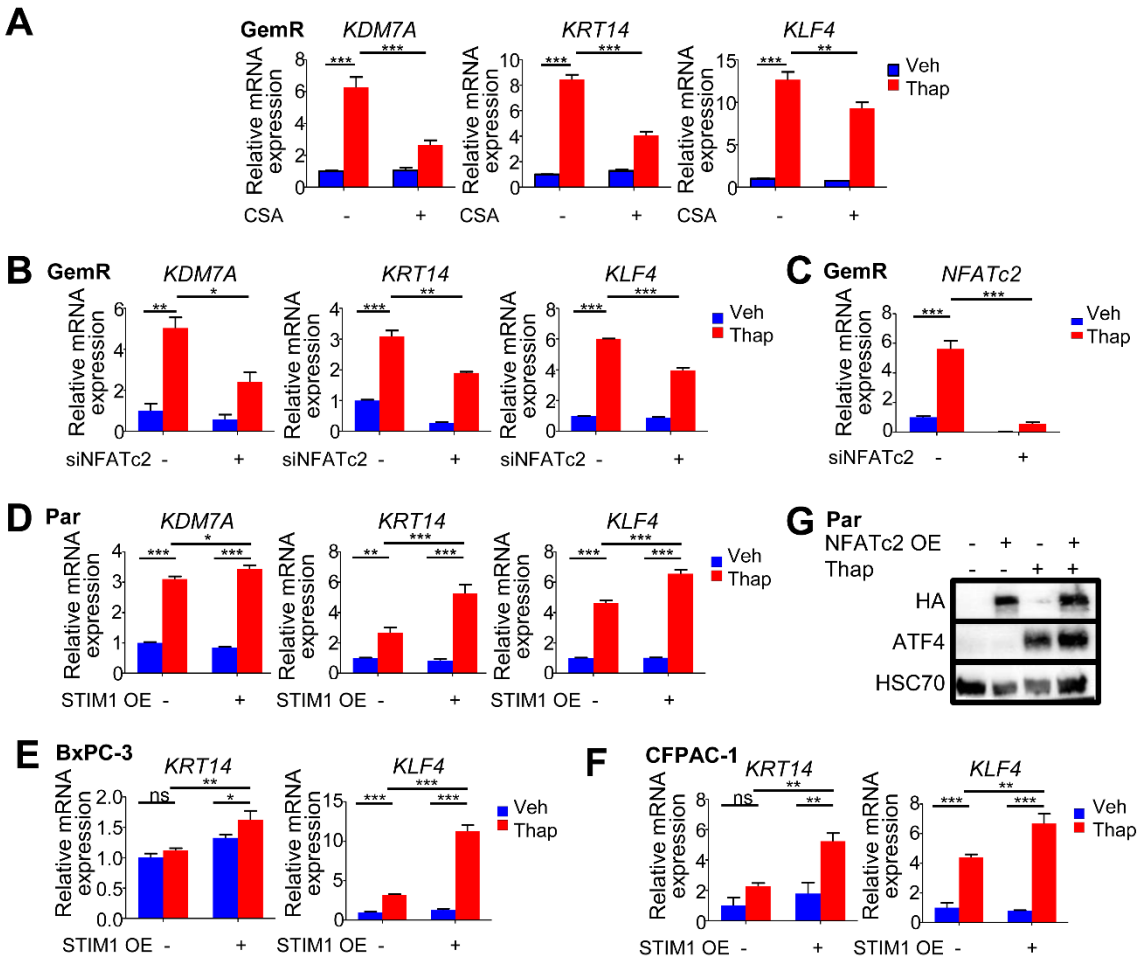

Fig. 29 NFATs drive the expression of UP-reversed genes in a STIM1-dependent manner. (A) Expression of UP-reversed genes upon cyclosporine A (CSA) and thapsigargin (Thap) treatments in GemR. Mean ±SD, n=3. (B) Expression of UP-reversed genes upon NFATc2 knockdown and thapsigargin (Thap) treatment in GemR. Mean ±SD, n=2. (C) NFATc2 knockdown validation. Mean ±SD, n=2. (D) Expression of UP-reversed genes upon STIM1 overexpression and thapsigargin (Thap) treatment in Par. Mean ±SD, n=3. (E) Expression of UP-reversed genes upon STIM1 overexpression and thapsigargin (Thap) treatment in BxPC-3. Mean ±SD, n=3. (F) Expression of UP-reversed genes upon STIM1 overexpression and thapsigargin (Thap) treatment in CFPAC-1. Mean ±SD, n=3. (G) Western blot of HA and ATF4 levels upon NFATc2 overexpression and thapsigargin (Thap) treatment in Par. *P≤0.05, **P≤0.01, ***P≤0.001, ns=not significant.

2.4.6 STIM1 levels correlate with ATF4 and NFAT activity in primary PDAC and patient-derived xenografts

To examine the *in vivo* relevance of our findings, we performed immunohistochemistry for STIM1, KRT14, and ATF4 in naïve primary tumor tissue derived from resected PDAC patients and in corresponding PDX-models derived from these specimens (Fig. 30A). Remarkably, in one patient tumor (GöPat15: Fig. 30B and D) and its corresponding PDX (GöPDX15; Fig. 30C-E), where STIM1

expression was low, we observed readily detectable nuclear ATF4, but only low levels of KRT14 expression. In contrast, another patient tumor (GöPat4; Fig. 30B and D) and its corresponding PDX sample (GöPDX4; Fig. 30C-D) displayed higher STIM1 and correspondingly high KRT14 levels, but only cytoplasmic ATF4 expression.

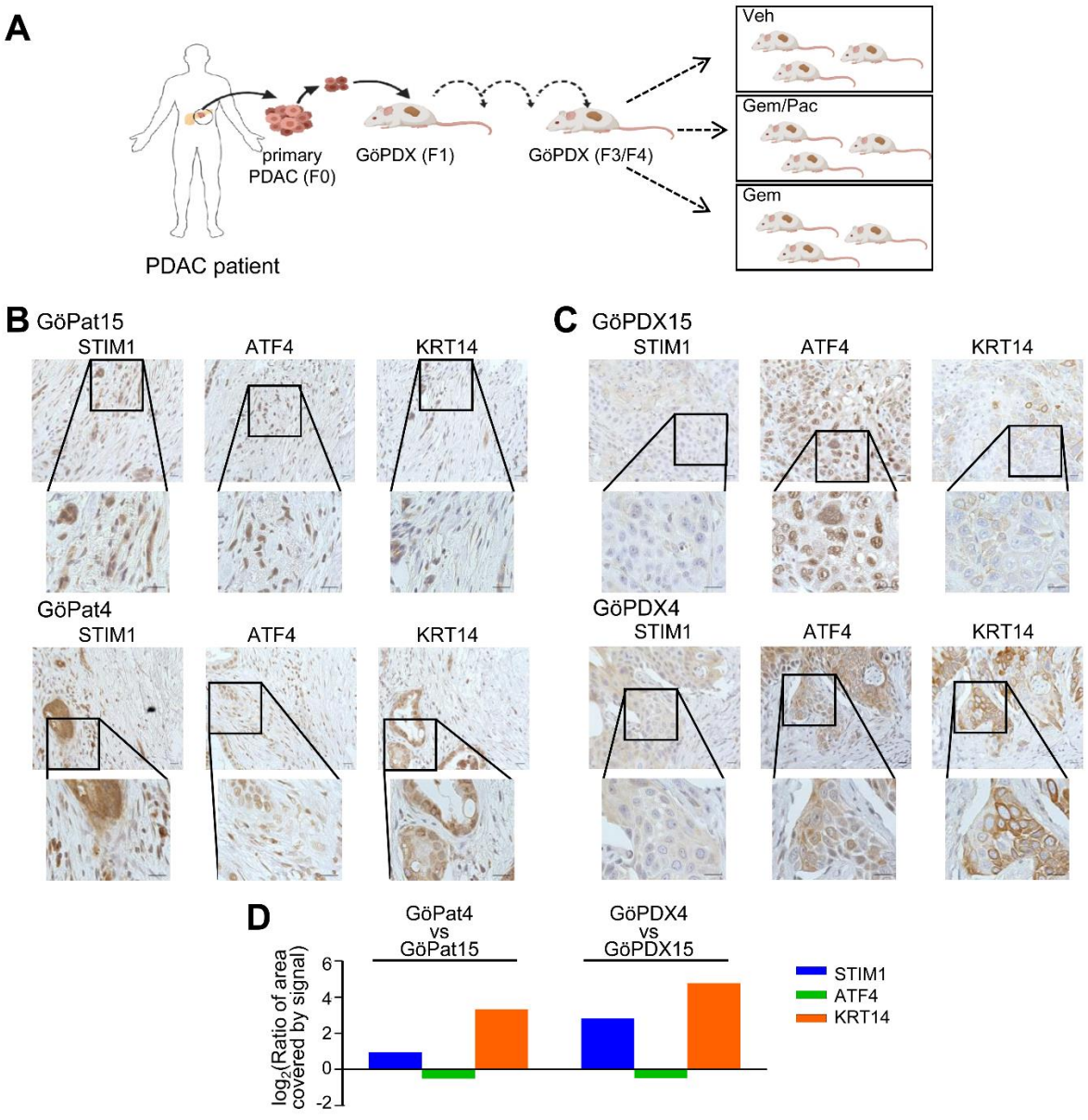

Fig. 30 ATF4 and KRT14 expression correlate with STIM1 levels in treatment-naïve PDAC patients and PDXs. (A) Scheme depicting the generation of PDXs and the treatment schedule of mice with vehicle (Veh), gemcitabine (Gem) or a combination of gemcitabine and nab-paclitaxel (Gem/Pac). (B & C) Immunohistochemistry for STIM1, ATF4 and KRT14 in naïve patient tumor material (Pat) (C) and in the respective naïve PDX. (D) Quantification of STIM1, ATF4 and KRT14 staining in naïve patient samples and PDXs. For all immunohistochemistry images: scale=20 µm (zoomed out) and 50 µm (zoomed in).

Next, we tested the effects of chemotherapy by treating PDXs with gemcitabine alone or in combination with nab-paclitaxel (Fig. 30A) and subsequently explored the expression of the aforementioned proteins. Notably, treatment of GöPDX13 with gemcitabine alone, or co-treatment with gemcitabine and nab-paclitaxel, resulted in increased STIM1 and KRT14 expression and lower nuclear ATF4 levels compared to the vehicle-treated GöPDX13 (Fig. 31A-C). Furthermore, mRNA-seq and GSEA analysis revealed an enrichment for UP-reversed genes in GöPDX13 co-treated with gemcitabine and nab-paclitaxel compared to untreated (Fig. 31D). Taken together, STIM1 is not only positively and negatively correlated with KRT14 expression and ATF4 nuclear localization, respectively, in naïve patient tumors, but is also altered in response to treatment both *in vitro* and *in vivo*. Thus, STIM1 levels could be exploited as a potential biomarker and/or therapeutic target for naïve and treated patients presenting *a priori* and acquired ER stress, and possibly gemcitabine resistance.

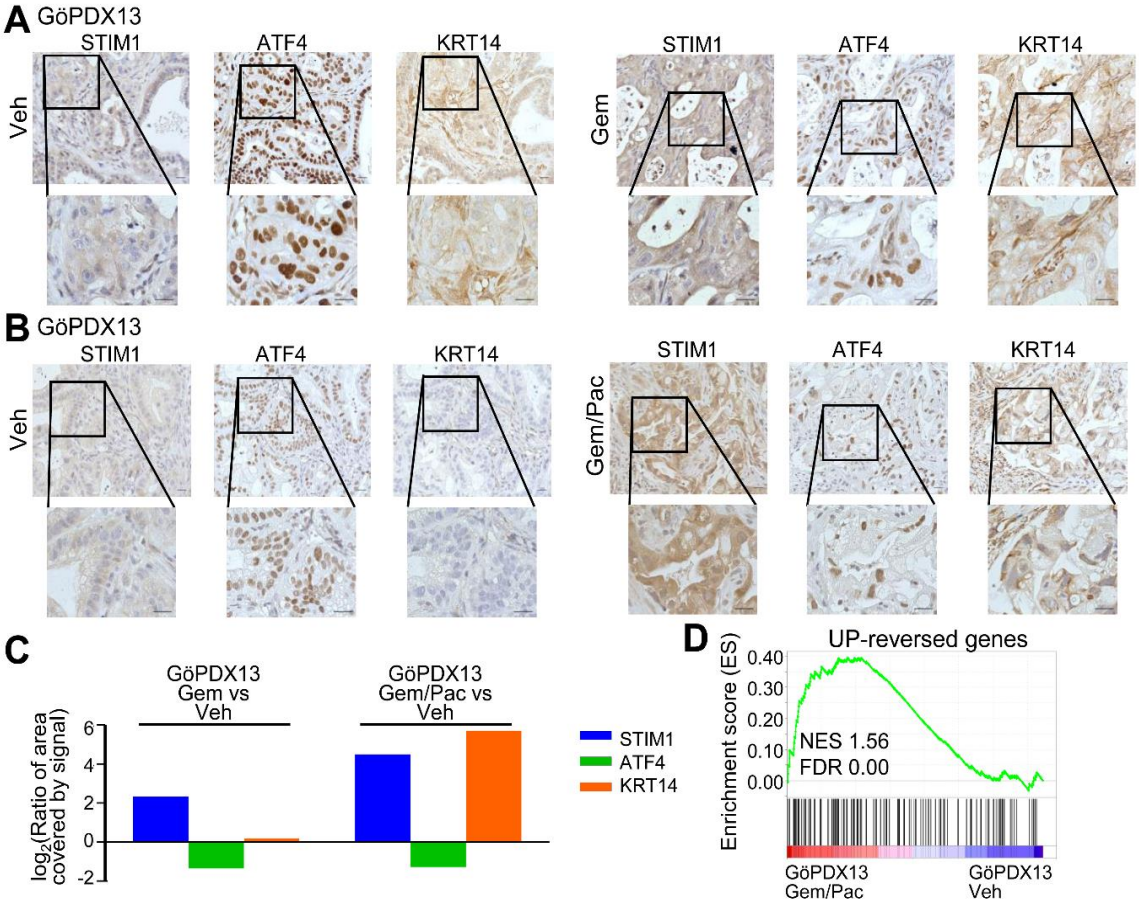

Fig. 31 STIM1 levels increase upon chemotherapy treatment in PDXs. (A) STIM1, ATF4 and KRT14 staining in vehicle (Veh) as well as in gemcitabine (Gem) treated PDXs. (B) Immunohistochemistry for STIM1, ATF4 and KRT14 in vehicle (Veh) and gemcitabine and nab-paclitaxel (Gem/Pac) co-treated PDXs. (C) Quantification of STIM1, ATF4 and KRT14 staining in gemcitabine and gemcitabine and nab-paclitaxel co-treated PDXs. (D) GSEA showing an enrichment for the UP-reversed genes in GöPDX13 co-treated with gemcitabine and nab-paclitaxel (Gem/Pac) compared to vehicle-treated GöPDX13. For all immunohistochemistry images: scale=20 µm (zoomed out) and 50 µm (zoomed in).

2.5 Discussion

In this study, we examined molecular alterations resulting from prolonged gemcitabine treatment of PDAC and identified the co-amplification of *RRM1* and *STIM1* as responsible for gemcitabine resistance and for altered calcium signaling, downstream transcriptomic and epigenomic alterations, respectively. While *STIM1* amplification does not augment RRM1-driven gemcitabine resistance, it shifts calcium signaling via increased SOCE, thereby reciprocally dampening the ER stress response and increasing NFAT activity (Fig. 32A).

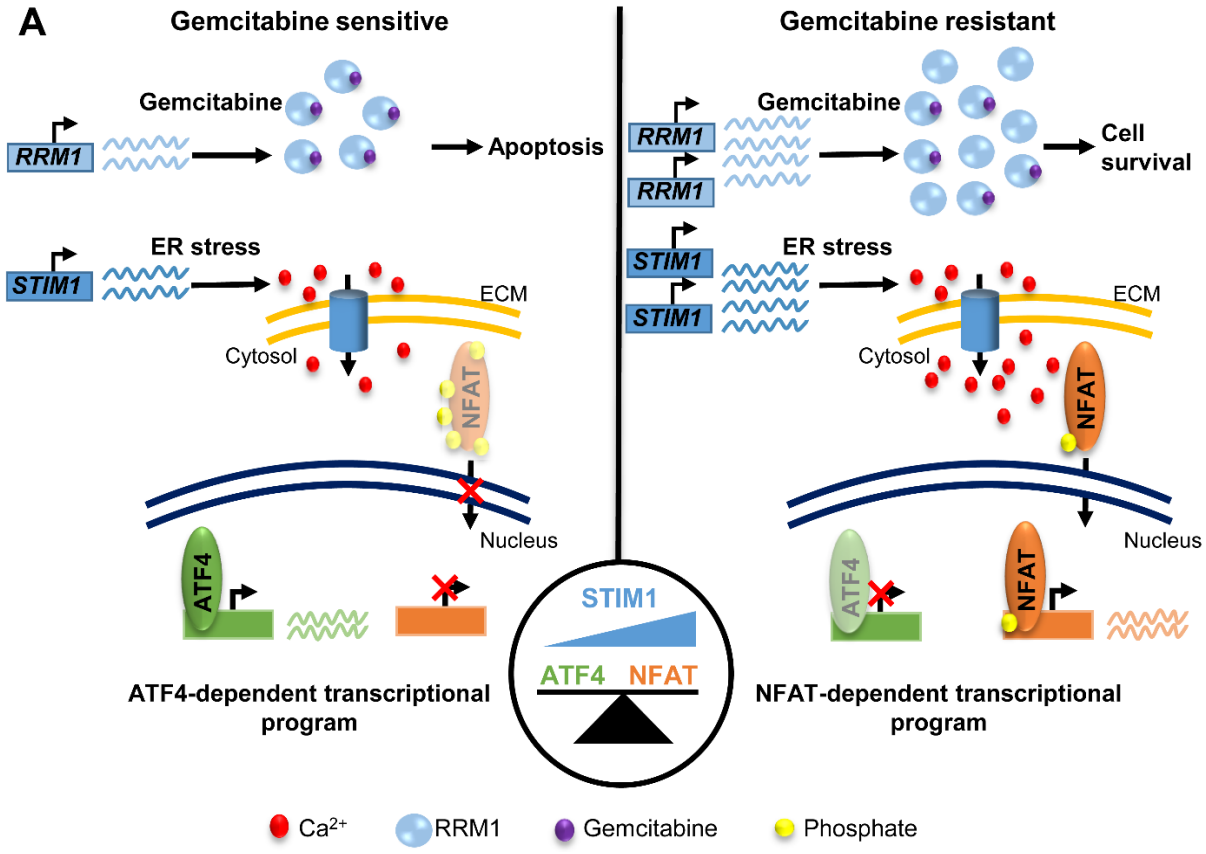

Fig. 32 STIM1 acts as rheostat balancing between ATF4 and NFAT-dependent transcriptional programs. (A) Scheme depicting the amplification of RRM1 and STIM1 upon gemcitabine resistance. While the upregulation of RRM1 drives gemcitabine resistance, increased STIM1 levels elicit a calcium signaling shift, leading to a dampened ER stress response and an aberrant NFAT activation.

RRM1, one of the main targets of gemcitabine, was found to be amplified in GemR and to drive gemcitabine resistance. To date, studies have failed to show that RRM1 levels are prognostic since its expression in naïve patients did not correlate with therapeutic response to gemcitabine (Ashida et al., 2009; Maréchal et al., 2012). We postulate that RRM1 levels and copy number might correlate with gemcitabine

response only in patient tumors after selective pressure caused by treatment. Thus, examining patient samples after treatment would help address this.

Gene amplifications are common in tumors, and their overexpression is known to drive cancer progression. Recently, studies have revealed the importance of co-amplified neighboring genes in tumorigenesis. For example, in HER2-positive breast cancer, the amplified region encompasses not only the oncogenic driver *ERBB2*, but also *GRB7*, *MIEN1, PNMT, PGAP3,* and *TCAP* (Ferrari et al., 2016). While HER2 overexpression drives HER2-positive breast cancer, GRB7 and MIEN1 affect tumorigenesis downstream and independent of HER-2, respectively (Chu et al., 2010; Janes et al., 1997; Katz et al., 2010). Similarly, the co-amplification of *RRM1* and *STIM1* elicits independent effects, where RRM1 does not affect ER stress resistance and NFAT activation, while STIM1 does not influence gemcitabine resistance. This suggests that the co-amplification of these genes endows tumor cells with distinct molecular properties, thereby potentially providing multiple survival advantages. Moreover, it is plausible that persistent ER stress or perturbed SOCE stimulation may elicit a selective pressure to amplify *STIM1*, which could result in the co-amplification of *RRM1* and elicit gemcitabine resistance. This is supported by our finding that many treatment-naïve tumors display a co-amplification of *STIM1* and *RRM1*. It is also possible that the upregulation of *STIM1* may help promote or facilitate the emergence gemcitabine resistance by promoting cell survival upon gemcitabine treatment during resistance acquisition. In support of this, STIM1 depletion was shown to promote the pro-apoptotic effects of gemcitabine in pancreatic cancer cells (Kondratska et al., 2014). Furthermore, STIM1, and thereby SOCE, are known to regulate various metabolic processes (Maus et al., 2017; Vaeth et al., 2017), and could thereby help tumor cells adapt to metabolic changes which could arise as a consequence of *RRM1* upregulation during the acquisition of resistance.

ER stress activates ATF4 and elicits an initial pro-survival and secondary pro-apoptotic response, where the former is suggested to be hijacked by many tumors (Urra et al., 2016). One such example is the hijacking of the pro-survival pathway upon hypoxia, where ATF4 promotes the transcription of VEGF, while activating antioxidant genes (Bi et al., 2005; Rouschop et al., 2013; Urra et al., 2016). Thus, the prevailing view is that rather than leading to apoptosis, ER stress is used by

tumors to adapt to stressful environments. Still, some PDAC tumors have been characterized to express higher levels of factors controlling ER homeostasis and conferring ER stress resistance (Milan et al., 2020). Our data supports this alternative mechanism whereby increased SOCE in *STIM1*-amplified tumors leads to ER stress resistance and NFAT activation. Interestingly, NFAT promotes the transcription of *HIF1A* in a STIM1-dependent manner in T cells (Vaeth et al., 2017), while STIM1 itself has been associated with hypoxic-driven tumorigenesis in hepatocarcinoma (Li et al., 2015). STIM1 and thereby SOCE are important regulators of melanoma aggressive behavior, controlling cellular oxidative stress through redox regulation of NFATc2 (Stanisz et al., 2014; Zhang et al., 2019a). Moreover, STIM and ORAI are important regulators of the pathobiology of several cancers (Prevarskaya et al., 2011). In PDAC, NFATs have been extensively characterized and shown to drive pancreatic cancer development and growth. NFATs are central in inflammation-driven pancreatic cancer development (Baumgart et al., 2014, 2016) and promote the silencing of *CDKN2B* in late-stage pancreatic intraepithelial neoplasia lesions (Baumgart et al., 2012). Furthermore, NFATs have been described to promote cell proliferation and tumor growth by fostering *MYC* expression in pancreatic cancer (Buchholz et al., 2006; König et al., 2010c; Singh et al., 2010). Taken together, we suggest that rather than hijacking the pro-survival pathway of the ER stress response, *STIM1*-overexpressing tumors profit from an alternative STIM1-dependent/ATF4-independent pro-survival mechanism. In this case, STIM1 may act as a rheostat balancing between ER stress and NFAT activation, making STIM1 an attractive potential therapeutic target. Thus, STIM1 may also serve as a potential indicator of NFAT activation and ER stress resistance.

While very little is known about calcium homeostasis in PDAC, calcium signaling is key in the development of acute pancreatitis (Raraty et al., 2000) where its therapeutic utility has been recently studied. In fact, the ORAI1 inhibitor CM4620 is currently being tested in a phase II clinical trial in acute pancreatitis patients (NCT04195347) (NCT03401190, 2018; NCT03709342, 2018; NCT04195347, 2019). Notably, chronic pancreatitis is a known risk factor for the development of pancreatic cancer and is characterized by increased inflammation (Saluja et al., 2019). While the role of ORAI and SOCE has been described specifically in acute

pancreatitis, it is worth noting that heightened NFAT activity promotes acinar to ductal metaplasia and fosters the progression of chronic pancreatitis to pancreatic cancer in mouse models (Chen et al., 2015, 2017). Consequently, SOCE inhibitors may prevent progression from chronic pancreatitis to PDAC. Hence, it is possible that some PDACs display aberrant calcium signaling obtained during previous chronic pancreatitis or due to other selective pressures. Therefore, analyzing STIM1 levels in PDAC could potentially predict tumor sensitivity to stress, while tumors with high STIM1 expression might benefit from STIM and ORAI inhibitors.

In conclusion, this study unravels novel independent molecular properties of gemcitabine-resistant tumors in PDAC. Through the amplification of *RRM1,* tumors become resistant to gemcitabine, while STIM1 acts as a rheostat balancing ER stress and NFAT activity in a SOCE-dependent manner. Furthermore, the co-amplification can occur spontaneously in treatment-naïve cancer cells, making STIM1 a potential mediator of aberrant NFAT activation and SOCE inhibitors potential novel therapeutic agents for PDAC patients.

2.6 Materials and Methods

2.6.1 Cell culture

L3.6pl (Par) (RRID:CVCL_0384) and GemR were cultured in Minimum Essential Medium Eagle (Gibco, life technologies); Panc1 (RRID:CVCL_0480), CFPAC-1 (RRID:CVCL_1119), SJSA (RRID:CVCL_1697), MG63 (RRID:CVCL_0426) in Dulbecco's Modified Eagle's Medium (Gibco, life technologies); BxPC-3 (RRID:CVCL_0186) and DLD-1 (RRID:CVCL_0248) in Roswell Park Memorial Institute Medium (Gibco, life technologies); and HCT116 (RRID:CVCL_0291) in McCoy's 5A Medium (Gibco, life technologies). All media were supplemented with 10% FBS (Sigma-Aldrich) and 1% penicillin and streptomycin (Sigma-Aldrich); Minimum Essential Medium Eagle was supplemented with 1% L-glutamine (Sigma-Aldrich). All cells were obtained after 2014 at which time numerous parental cell stocks were cryopreserved. Cells were maintained in culture for a maximum of 2-3 months on average before thawing new stocks. All cells tested negative for Mycoplasma using the MycoAlert Mycoplasma Detection Kit (Lonza #LT07-318).

2.6.2 Establishment of gemcitabine-resistant cells

GemR were established by treating L3.6pl with increasing concentrations of gemcitabine (Sigma-Aldrich #G6432), starting at 4 nM and doubling the concentration once cells started to thrive again. This process was continued for 14 weeks until reaching 64 nM, when cells were considered resistant and maintained at this concentration.

2.6.3 Establishment of stable STIM1 overexpressing cell lines

HEK293T (RRID:CVCL_0063) cells were transfected with pMD2.G (Addgene #12259), psPAX2 (Addgene #12260) and p2K7bsdUBI-mCherry-STIM1 (Addgene #114178) or p2K7-bsd-UBI-tagRFP-KDEL (Addgene #114179) using Lipofectamine 3000 (Invitrogen) following manufacturer's instructions. The virus was isolated and pooled by collecting the media at 24, 48, and 72 hours post-transfection and centrifuged at 500x g for 10 min to remove any cellular material. 500,000 L3.6pl, BxPC-3 and CFPAC-1 cells were reverse transfected and spin-occulated at 1000x g for 2 h at 30 °C using 8 ug/mL polybrene in a dilution of viral supernatant and

normal culture media. After 48 h, the cells were resuspended in appropriate culture medium supplemented with 10 ug/mL Blasticidin S Hydrochloride (Millipore #203350). Selection was maintained throughout all experiments.

2.6.4 Transient NFATc2 overexpression

L3.6pl cells were forward transfected with either a constitutively active NFATc2 pcDNA3.1 plasmid or an empty pcDNA3.1 vector (both provided by Dr. Singh, UMG, Göttingen) using Lipofectamine 3000 (Invitrogen) and following manufacturer's instructions. Protein was harvested 48 h after transfection.

2.6.5 siRNA transfections

L3.6pl, GemR and Panc1 cells were reverse transfected with SmartPool siGENOME siRNA (Dharmacon) (Table S6) using Lipofectamine RNAiMax (Invitrogen) according to manufacturer's instructions. All experiments were conducted after a 48 h knockdown.

2.6.6 Inhibitor treatments

L3.6pl, GemR and Panc1 cells or transfected cells were treated with 500 nM thapsigargin (Focus Biomolecules #10-2105) for 3 h and/or 1 µM CM4620 (Hycultec # HY-101942), 1.5 mM EGTA (Sigma-Aldrich), 500 nM Cyclosporine A (Targetmol #59865-13-3) for 3.5 h prior to protein and/or RNA harvesting. For immunofluorescence, siRNA reverse transfected cells were treated with 500 nM thapsigargin (Focus Biomolecules #10-2105) for 40 min.

2.6.7 Proliferation assay

L3.6pl, GemR, DLD1 and HCT116 cells in a 96-well plate were seeded, alternatively, siRNA reverse transfected cells were used. One day after seeding, cells were treated with gemcitabine (Sigma-Aldrich #G6432), thapsigargin (Focus Biomolecules #10-2105) or 1 µM CM4620 (Hycultec # HY-101942). After 7 days of treatment, cells were fixed with methanol for 15 min, stained with 1% crystal violet in 20% ethanol for 15 min and scanned. Cell viability was assessed using cell titer blue (Promega #G8080) following manufacturer's instructions and measuring the

absorbance at 590 nm after 7 days. Alternatively, crystal violet was solubilized in 40% acetic acid and the absorbance measured at 590 nm. IC_{50} values were calculated by assessing the normalized absorbance at 590 nm.

2.6.8 Protein harvesting and western blot

Protein was harvested and western blot performed as described (Hamdan and Johnsen, 2018; Nagarajan et al., 2014). Briefly, cells were washed with PBS and resuspended in RIPA buffer (1X PBS, 1% NP-40, 0.5% Na-deoxycholate and 0.1% SDS) with 100 µM β-glycerophosphate, 100 µM N-Ethylmaleimeide, 100 µM Pefabloc, 1 µM Aprotinin and 1 µM Leupeptin. Protein extracts were sonicated for 10 cycles (30 s on/off) using the Bioruptor Pico (Diagenode). Proteins were denatured for 10 min at 95 °C in lämmli buffer (375 mM Tris-HCl, 10% SDS, 30% glycerol, 0.02% bromophenol blue and 9.3% DTT). Polyacrylamide gels were used to separate the proteins, which were then transferred onto nitrocellulose membranes and incubated with primary antibodies overnight and secondary antibodies for 1 h. The Bio-Rad ChemiDoc imager was used to develop the membranes. The following antibodies were used: RRM1 (Cell Signaling #8637, RRID:AB_11217623), STIM1 (Sigma-Aldrich S6197, RRID:AB_1079007), ATF4 (Cell Signaling #11815, RRID:AB_2616025), HA (Roche #3F10, RRID:AB_2314622), GAPDH (Origene #TA802519, RRID:AB_2626378), HSC70 (Santa Cruz #sc-7298, RRID:AB_627761), anti-rabbit IgG (Jackson ImmunoResearch Labs #211-032-171, RRID:AB_2339149) and anti-mouse IgG (Jackson ImmunoResearch Labs #115-035-174, RRID:AB_2338512).

2.6.9 RNA extraction and quantitative PCR

RNA was extracted and qPCR run as described earlier (Hamdan and Johnsen, 2018; Mishra et al., 2017). Briefly, tissues were homogenized in QIAzol and submitted to the same procedure as cells. RNA was harvested using QIAzol (Qiagen) and following manufacturer's instructions. 1 µg of RNA was reverse transcribed using M-MuLV reverse transcriptase (NEB) and random nonamer primers according to manufacturer's instructions. The CFX Connect Real Time System (Biorad) was used to perform qPCR with an initial denaturation step of 2 min at 95 °C followed by 40 cycles of 10 s at 95 °C and 30 s at 60 °C. Gene expression

levels were normalized to the housekeeping gene *GAPDH* (primer sequences in Table S7).

2.6.10 Chromatin immunoprecipitation

ChIP was performed as previously described (Hamdan and Johnsen, 2018; Najafova et al., 2017). Briefly, cells were fixed for 20 min with 1% formaldehyde in PBS and quenched for 5 min with 1.25 mM Glycine. Cells were scraped, mildly lysed and washed once with Nelson Buffer (150 mM NaCl, 20 mM EDTA (pH 8.0), 50 mM Tris-HCl (pH 7.5), 0.5% NP-40, 1% Triton X-100 and 20 mM NaF) with 100 µM β-glycerophosphate, 100 µM N-Ethylmaleimeide, 100 µM Pefabloc, 10 µM Iodoacetamide, 1 µM Aprotinin and 1 µM Leupeptin. A stronger lysis was achieved with Gomes Lysis Buffer (150 mM NaCl, 1% NP-40, 0.5% Sodium-deoxycholate, 50 mM Tris-HCl (pH 8.0), 20 mM EDTA (pH 8.0), 20 mM NaF and 0.1% SDS) with 100 µM β-glycerophosphate, 100 µM N-Ethylmaleimeide, 100 µM Pefabloc, 10 µM iodoacetamide, 1 µM Aprotinin and 1 µM Leupeptin. The chromatin was sonicated for 30 cycles (30 s on/off) using the Bioruptor Pico (Diagenode) and precleared with 100 µl Sepharose 4B (GE Healthcare). 1 µg or 10 µl of antibody were added to the pre-cleared chromatin extract and incubated overnight. Following, 30 µl of a BSA-blocked 50% Protein-A Sepharose (GE Healthcare) slurry were incubated with the chromatin extracts for 2 h at 4 °C. The complexes were washed once with Gomes Lysis Buffer, twice with Gomes Wash Buffer (100 mM Tris-HCl (pH 8.5), 500 mM LiCl, 1% NP-40, 1% Sodium deoxycholate, 20 mM EDTA (pH 8.0) and 20 mM NaF), twice with Gomes Lysis Buffer and finally twice with TE Buffer (10 mM Tris-HCl (pH 8.0) and 1 mM EDTA (pH 8.0)). 10 µg of RNAse A in 10 mM Tris-HCl (pH 8.0) were incubated with the washed complexes for 30 min at 37 °C. Following, proteins were digested overnight at 65 °C by diluting the immunoprecipitated complexes to a final 10 mM EDTA (pH 8.0), 50 mM Tris-HCl (pH 8.0), 1% SDS and incubating them with 20 µg Proteinase K. ChIP DNA was eluted from the beads with 10 mM Tris-HCl (pH 8.0), precipitated with 0.4 M LiCl and linear acrylamide and isolated using phenol/chloroform/isomaylic alcohol extraction. ATF4 ChIP was only performed in Par treated with 500 nM thapsigargin for 3 h.
The following antibodies were used: H3K27ac (Diagenode #C15410196, RRID:AB_2637079) and ATF4 (Cell Signaling #11815, RRID:AB_2616025). qPCR

was used to probe IP and the enrichment at each site was calculated by normalizing the IP values to their respective inputs. Primer sequences used to probe IP enrichment at each site can be found in Table S8.

2.6.11 Publicly available data

The H3K27ac ChIP-seq and respective inputs in L3.6pl can be found in ArrayExpress (RRID:SCR_002964) (E-MTAB-7034). Thapsigargin and Gemcitabine sensitivity information from pancreatic cancer cell lines (Sanger GDSC1 data set (Iorio et al., 2016)) and *STIM1* and *RRM1* copy number variation information from cancer cell lines (DepMap Public 19Q4 data set (DepMap, 2020)) were downloaded from the Dependency Map portal (RRID:SCR_017655) from the Broad Institute (Ghandi et al., 2019) and plotted using the LSD package in R. Oncoprints with the expression gain rates of *STIM1* and *RRM1* in pancreatic cancer patients were generated by cBioportal for Cancer Genomics (RRID:SCR_014555)(Cerami et al., 2012; Gao et al., 2013) using the TCGA PanCancer Atlas Studies data set (Press).

2.6.12 Next generation sequencing

Sequencing libraries for ChIP-seq and RNA-seq were prepared using the KAPA HyperPrep (Roche) or the Microplex Library Preparation V2 (Diagenode) and the TruSeq RNA Library Prep V2 (Illumina) kits, respectively. Library quality was assessed using a Bioanalyzer 2100 (Agilent). The samples were sequenced on a HiSeq4000 (Illumina) at the NGS Integrative Genomics Core Unit (NIG) at the UMG or at the Genome Analysis Core at the Mayo Clinic. CASAVA 1.8.2 was used to demultiplex the bcl files to fastq files.

2.6.13 Transcript Profiling

The high throughput sequencing data in this publication has been deposited in NCBI's Gene Expression Omnibus (Edgar et al., 2002) and are accessible through GEO Series accession number GSE152124 (https://www.ncbi.nlm.nih.gov/geo/query/acc.cgi?acc=GSE152124).

2.6.14 RNA-seq analysis

Fastq files were mapped to the human genome (hg38) using STAR (Dobin et al., 2013) (version 2.6.0c, RRID:SCR_015899) followed by HTSeq-count (Anders et al., 2015) (version 0.11.1, RRID:SCR_011867), which was used to obtain the read counts. Differential analysis was performed using DESeq2 (RRID:SCR_015687) (Love et al., 2014) and the thresholds were set to 0.8 log2FC, basemean >=25 for control or treatment and padj <=0.05. Gene Set Enrichment Analysis (GSEA, RRID:SCR_003199) (Subramanian et al., 2005) was performed using default settings and a gene set permutation type. Normalized read counts for each condition obtained from DESeq2 were filtered to contain only expressed genes (normalized count value >=30, 10 for PDX data) and used as input files for GSEA. Up and downregulated genes of thapsigargin-treated Par compared to vehicle-treated Par were identified. The corresponding log2 fold change values from these genes from Par, GemR and STIM1-depleted GemR treated with thapsigargin all compared to vehicle-treated Par were extracted and used for hierarchical clustering using the pheatmap package in R (RRID:SCR_016418). A heatmap was generated with the identified 4 gene clusters and the Z scores for all replicates. Pathways associated with each cluster were identified using EnrichR (RRID:SCR_001575) (Chen et al., 2013; Kuleshov et al., 2016).

2.6.15 ChIP-seq and copy number variation analysis

Bowtie2 (Langmead and Salzberg, 2012) (version 2.3.4.1, RRID:SCR_005476) with a very sensitive read alignment setting was used to map fastq files to the human genome (hg38). Bam files for each condition were merged and PCR duplicates removed using Samtools (version 1.9, RRID:SCR_002105). Bamcoverage (Ramírez et al., 2016) from deeptools (version 3.0.1, RRID:SCR_016366) with default settings and RPKM normalization was used to generate initial bigwig files for visualization using the Integrative Genomics Viewer (RRID:SCR_011793) (Robinson et al., 2011; Thorvaldsdóttir et al., 2013). Final bigwig files were scaled, as differences in global background signal intensity were found between conditions. The scaling factor for each condition was individually defined as the ratio of the median signal intensity of control (vehicle-treated Par) across all TSSs +/- 1kb divided by the median signal intensity of each individual condition across all TSSs

+/- 1kb. Untreated Par and GemR bigwig files were not scaled. ComputeMatrix from deeptools with the mode set to reference-point and a window of 1kb up and downstream of the region of interest was used to quantify the signal intensity within a region and to generate heatmaps and aggregate plots. Peaks were called using MACS2 (version 2.1.2, RRID:SCR_013291) with the input file as control, without building the model and with a cutoff of 0.05 for broad peak calling. Broad peaks were called for H3K27ac, while narrow peaks were called for ATF4. The R package Diffbind (RRID:SCR_012918) (Ross-Innes et al., 2012) was used to perform differential binding analysis using edgeR. Thresholds were set for gained regions (log2 >=1, conc. treatment >=4, FDR <=0.05) as well as lost regions (log2 <=-1, conc. control >=4, FDR <=0.05). Enrichment for transcription factor motifs on gained and lost regions was determined using HOMER (RRID:SCR_010881) (Heinz et al., 2010).

Copy number variation analysis was performed using CNVkit (Talevich et al., 2016) for whole genome sequencing and the input files of GemR as treatment and of Par as control. Thresholds for amplified and deleted regions were set to log2 >=1 and log2 <=-1, respectively.

2.6.16 Calcium imaging

Cytosolic calcium levels were assessed using a Zeiss Axiovert S100TV equipped with a pE-340fura (CoolLED) LED lightsource, a sCMOS pco.edge camera and a Fluar 20x/0.75 objective. siRNA reverse transfected cells were loaded with 1 µM Fura-2 AM (Thermo Fisher Scientific #F1221) for 30 min at room temperature in growth medium. The measurements were performed in Ringer's buffer (pH 7.4) containing 145 mM NaCl, 4 mM KCl, 10 mM glucose, 10 mM HEPES (4-(2-hydroxyethyl)-1-piperazineethanesulfonic acid), 2 mM $MgCl_2$ and concentrations of $CaCl_2$ as indicated, or 0 mM $CaCl_2$ with 1 mM EGTA. SOCE was induced by addition of 1 µM thapsigargin. Ratiometric time-lapse imaging was performed using LED excitation at 340 nm (excitation filter: 340/20) and 380 nm (excitation filter: 380/20) together with a T400 LP dichroic mirror and 515/80 excitation filter. Data were analyzed with VisiView® Software (Visitron Systems GmbH). The obtained 340/380 nm fluorescence ratios were converted to calibrated data by using the formula $[Ca^{2+}]$

= K*(R − Rmin)/(Rmax − R), while the values of K, Rmin, and Rmax were determined as described previously (Grynkiewicz et al., 1985).

2.6.17 Immunofluorescence

Cells were washed twice with PBS and fixed using 4% Paraformaldehyde in PBS for 10 min. Three additional PBS washes were performed prior to permeabilization with 0.5% Triton X-100 in PBS for 10 min. Subsequently, cells were washed three times with PBS and blocked for 30 min with 3% BSA in PBS. The samples were incubated in a 1:100 dilution of the NFATc2 antibody (Abcam #ab2722, RRID:AB_303247) in 3% BSA in PBS overnight at 4 °C. After washing with PBS twice, a 1:500 dilution of the secondary antibody Alexa 488 donkey anti-mouse (Invitrogen #A-21202, RRID:AB_141607) was applied for 1 h at room temperature. The samples were washed three times with PBS, incubated with a 1:1000 dilution of DAPI in PBS for 30 min, and mounted in mounting media (9.6% (w/v) Mowiol 4-88, 24% (w/v) Glycerol, 100 mM Tris-HCl (pH 8.5)). Confocal images were acquired using a Zeiss LSM 510 Meta microscope (Carl Zeiss AG) and the NFATc2 nuclear signal intensity was quantified using Fiji (RRID:SCR_002285) (Schindelin et al., 2012; Schneider et al., 2012), where DAPI was used to mark the regions of interest (ROI).

2.6.18 Patient-derived xenografts

For patient-derived xenograft (PDX) model generation, pieces of bulk primary PDAC tissue from patients who underwent tumor resection at the UMG were subcutaneously transplanted in both flanks of NMRI$^{nu/nu}$ mice. Tumors grew until their volume exceeded 1cm³ (F1 generation). Upon harvesting of tumors, one portion of the tissue was embedded in paraffin as described previously (Chen et al., 2017), while the other half was subcutaneously transplanted into both flanks of another NMRI$^{nu/nu}$ mouse for further tumor expansion (F2 generation). For gemcitabine/nab-paclitaxel co-treatment, F3-generation PDX-material from GöPDX13 was transplanted into both flanks of four NMRI$^{nu/nu}$ mice. When tumor volumes reached 200mm³, mice were randomized into vehicle (0.9% saline) and chemotherapy arms. Gemcitabine (Sigma-Aldrich; 100mg/kg) was administered intraperitoneally 2x/week, nab-paclitaxel (Abraxane, Celgene; 30mg/kg) was given weekly by tail vain injection. For gemcitabine treatment alone, F4 generation

GöPDX13 material was transplanted into seven NMRI$^{nu/nu}$ mice, which were randomized into vehicle and gemcitabine (100mg/kg) arms. Here, gemcitabine was administered 3x/week. Mice were sacrificed when endpoint criteria (e.g. weight loss ≥ 20%) were reached (evident upon 3x nab-paclitaxel injections for the gemcitabine/nab-paclitaxel study and upon 6 injections in the gemcitabine solo arm) and PDX tumors were paraffin-embedded for histological assessment. Animal procedures were conducted in accordance with the protocols approved by the Institutional Animal Care and Use Committee (33.9-42502-04-17/2407). The generation and utilization of PDX models have been approved by the ethical review board of the UMG (70112108).

2.6.19 Immunohistochemistry

Immunohistochemical analyses of paraffin-embedded primary PDAC patient tissue or PDX tumors were performed as described previously (Chen et al., 2017) utilizing the Peroxidase Rabbit IgG Vectastain ABC kits (Biozol). The following primary antibodies were used: STIM1 (Sigma-Aldrich #S6197, RRID:AB_1079007; 1:900), KRT14 (Sigma-Aldrich #HPA023040, RRID:AB_1852201; 1:500) and ATF4 (Novus #NBP2-67766, RRID:AB_2877169; 1:100). Representative images were acquired using a Zeiss Axio Scope A1 (Carl Zeiss AG) microscope. The area covered by signal was measured using Fiji (RRID:SCR_002285) (Schindelin et al., 2012; Schneider et al., 2012), where the images were deconvoluted using HDAB Colour Deconvolution (Ruifrok and Johnston, 2001) and the signal area in the DAB channel measured after setting the threshold.

2.6.20 Statistics

GraphPad Prism v5.04 (RRID:SCR_002798) was used for statistical analyses. One-way ANOVA followed by Newman-Keuls multiple comparison test was used for comparisons of more than two conditions. A non-linear regression with a variable slope and a bottom constrain between 0 and 2 was used to determine IC_{50} values, which were analyzed using unpaired two-tailed student's t-test. Linear regressions were analyzed using Spearman's correlation. $P<=0.05$ were considered statistically significant. *$P\leq0.05$, **$P\leq0.01$, ***$P\leq0.001$, ns=not significant.

3. Discussion

In this project we investigated the driver and consequences of gemcitabine resistance in pancreatic cancer. We identified the amplification of *RRM1* as the main driver of gemcitabine resistance, and as being accompanied by the amplification of its neighboring gene, *STIM1*. The overexpression of the ER calcium sensor and vital SOCE component, STIM1, has proven to elicit ER stress resistance, protecting tumor cells from apoptosis. Furthermore, an increase in cytosolic calcium levels provoked the activation and translocation of NFATs, a family of transcription factors tightly associated with pancreatic cancer development and tumorigenesis. Finally, the overexpression of RRM1 did not influence the ER stress response, while higher levels of STIM1 did not affect gemcitabine resistance.

3.1. Overexpression of gemcitabine targets and metabolic enzymes as prognostic markers

In this study (Section 2.4.1), we identify the amplification and overexpression of *RRM1* as being the main mechanism driving gemcitabine resistance. This is not surprising, as several other studies have pointed at the fact that gemcitabine resistance can arise due to the regulation of gemcitabine metabolizing enzymes and/or targets. In fact, the prognostic value of the expression level of gemcitabine metabolizing enzymes has proven to be very promising. *In vitro* studies as well as patient biopsies have shown that the levels of the transporting enzymes hENTs and hCNTs and of the kinase dCK correlate with the tumor's response to chemotherapy (Bhutia et al., 2011; Farrell et al., 2009; Giovannetti et al., 2006; Maréchal et al., 2010, 2012; Mori et al., 2007; Spratlin et al., 2004). Furthermore, gemcitabine catabolic enzymes, such as CDA and NT5Cs, have been implicated in gemcitabine resistance (Patzak et al., 2019; Weizman et al., 2014). In our hands no great difference was seen in the expression levels of these and other gemcitabine metabolizing enzymes in parental compared to gemcitabine resistant cells (data not shown). Thus, it is possible that the levels of these proteins correspond to the initial responsiveness of patients to gemcitabine, but are not the drivers of acquired gemcitabine resistance. In order to validate this hypothesis, a wider panel of parental and gemcitabine resistant cells lines would have to be established and tested. Ideally these cells would also be characterized at various stages during their

resistance acquisition. Lastly, the levels of these enzymes would be compared in *in vivo* studies as well as biopsies of naïve and treated patients.

A similar phenomenon is seen regarding the overexpression of *RRM1* as a driver of gemcitabine resistance. While we and several other groups have reported the upregulation of *RRM1* upon gemcitabine resistance in *in vitro* and *in vivo* studies (Bergman et al., 2005; Nakahira et al., 2007; Nakano et al., 2007; Wang et al., 2015; Zhou et al., 2019), its prognostic value in patient material remains under debate (Akita et al., 2009; Aoyama et al., 2017; Maréchal et al., 2012). This may be attributed to the fact that the upregulation of RRM1 may be a gradual process during gemcitabine treatment. Consequently, its protein levels in naïve patient biopsies may not be indicative of the patient's likelihood to develop chemotherapy resistance. This ability of cancer cells to substantially upregulate genes and adapt to external stresses is further supported by the fact that alterations in the tumor's genomic copy number, subtype and chemotherapy response have been observed when monitoring PDAC progression (Tiriac et al., 2018). Thus, to draw any conclusions on the development of gemcitabine resistance and the response of individual patients to treatment, it would be of greatest importance to compare naïve as well as treated patient biopsies.

Moreover, as we also show, it is possible that several PDAC tumors presenting an acquired gemcitabine resistance upregulate *RRM1* by amplifying it. Even though, none of the aforementioned studies has ever identified an amplification of *RRM1*, one study has shown that, in their gemcitabine resistant cell lines, *STIM1* and *TRIM21* were also upregulated (Zhou et al., 2019). Interestingly, these two genes fall within our identified amplification region, suggesting that pancreatic cancer cell lines from other studies may also amplify a portion of chromosome 11 containing *RRM1.* Remarkably, the amplification of the segment of chromosome 11 has been reported in a gemcitabine resistant non-small lung cancer cell line (Tooker et al., 2007). This further suggests that some genomic amplifications are selected for and provide an advantage to the tumor and that our model most likely represents a much wider array of gemcitabine resistant tumors.

Taken together, assessing the levels of gemcitabine transporting and metabolizing enzymes may aid in gauging the initial response of tumors to the chemotherapeutic

agent. Still, as the disease progresses, a closer monitoring of RRM1 protein levels, as well as, copy numbers may be more indicative of acquired resistance, serving as a better prognostic marker.

3.2. The advantage of (co-)amplifications

It is common that tumor cells present genomic aberrations, many times amplifying or deleting entire segments of their genomes. Such genomic rearrangements are mainly due to failures to conventionally resolve double stranded breaks, while also being a consequence of major catastrophic events (Korbel and Campbell, 2013; Li et al., 2020; Willis et al., 2015). Thus, copy number variations take place rather randomly and may be selected for in tumors as they provide the cell with additional characteristics. In fact, mutant *K-RAS* was found to be amplified in many pancreatic tumors, while *SMAD4* and *CDKN2A* were frequently deleted. As mentioned previously, mutations in *K-RAS* and silencing of *CDKN2A* and *SMAD4* are key events in the development of PanIN lesions to pancreatic cancer (Notta et al., 2016; Singhi et al., 2017). Moreover, other genes such as c-*MYC, CDK6, NOV, MET, SOX9, BRAF, PREX2, ERBB2* and *PIK3CA* are commonly amplified in pancreatic cancer patients (Singhi et al., 2019; Waddell et al., 2015). While, the transcription factors *GATA6* and *FOXA2* are known to be amplified in the classical subtype (Chan-Seng-Yue et al., 2020). This suggests that many early pro-tumorigenic events take place in the form of genomic aberrations. They shape the cellular transcriptome, while also affecting several processes such as DNA damage response and cell cycle arrest.

Not only crucial in the development of cancer, genomic amplifications may affect the tumor's response to chemotherapy and may take place after chemotherapeutic treatment. This may be due to the high chromotrypsis and plasticity associated with cancer cells. Several studies have described a correlation between the tumor's genetic background and its responsiveness to chemotherapy. For example, PDAC's response to platinum-based agents has been associated with the tumor's genomic stability and mutation frequency on DNA damage responsive genes, such as *BRCA1* and *BRCA2* (Singhi et al., 2019; Waddell et al., 2015). Furthermore, major *K-RAS* genomic imbalances have been correlated with higher chemotherapy resistance, with worse prognosis and with the more aggressive metastatic basal-like

subtype (Chan-Seng-Yue et al., 2020). In the rare absence of a *K-RAS* mutation, some PDAC tumors have displayed an amplification of *EGFR, ERBB2* and *AKT* instead. Tumors with such atypical genomic background presented higher sensitivity to tyrosine receptor kinase inhibitors, such as afatinib (Singhi et al., 2019; Tiriac et al., 2018). This suggests that the genetic background of cells may highly influence their sensitivity to chemotherapy. It further implies that tumors are extremely plastic, favoring certain genetic mutations and/or undergoing major genomic rearrangements upon a selective pressure.

Thus, the amplification of chromosome 11 upon gemcitabine acquired resistance, as identified in section 2.4.1, serves as another example for such occurrences. It may also be a, so far unreported, feature of several studied PDAC tumors and should be included in the future characterization of naïve and treated patient biopsies. The fact that some naïve cancer cell lines already display the amplification of *STIM1* and/or *RRM1*, exemplifies the randomness of such events. The maintenance of the amplification, on the other hand, suggests it confers survival advantages even to naïve cells. Thus, the reported amplification of *RRM1* and *STIM1* (Section 2.4.3) may serve to gauge how well tumors will respond to treatment, as well as how fast they may become resistant to a specific chemotherapeutic agent.

Even though many times the focus lies on the amplification of one specific gene, genomic aberrations imply that an entire chromosomal segment is amplified. Thus, several other genes, whose functions may have been less studied, are also overexpressed. One such examples is the amplification of *ERBB2* in breast cancer, which extends from chr17:37,818,020 to chr17:37,924,454 and encompasses not only *ERBB2*, but also *TCAP, PNMT, PGAP3, MIEN1* and *GRB7* (Ferrari et al., 2016; Staaf et al., 2010). Later studies revealed that the co-amplification of *GRB7* further augments the effects of HER2 overexpression. GRB7 interacts with HER2 directly via its SH2-domain, and activates Ras triggering the initiation of the MAPK signaling cascade upon EGF signaling (Chu et al., 2010; Janes et al., 1997). On the other hand, the overexpression of *MIEN1* has been associated with increased migratory potential in breast cancer in a HER2-independent manner. In this case, MIEN1 was shown to promote migration by triggering downstream Syk-dependent signaling and interacting with Annexin A2 (Katz et al., 2010; Kpetemey et al., 2015). Thus, the

overexpression of co-amplified genes may synergistically promote tumorigenesis or endow cells with different oncogenic properties. Our data supports this idea in which the amplification of *RRM1* confers gemcitabine resistance, while the overexpression of *STIM1* leads to ER stress resistance and NFAT signaling activation.

Furthermore, it is possible that other genes co-amplified with *RRM1* and *STIM1* provide the cells with additional oncogenic properties or enhance gemcitabine resistance and/or ER stress resistance and NFAT activation. The co-amplified genes identified on chromosome 11 in section 2.4.1 also encompass *ILK* and *WEE1*, which have been previously linked to oncogenic pathways. ILK has been shown to promote cell proliferation and migration by activating the Akt/mTOR and GSK3β pathways, while also fostering the expression of SNAI1 (Hannigan et al., 2005; Sawai et al., 2006). Furthermore, ILK inhibition in pancreatic cancer has been proven to prevent tumor growth and to synergize with acute gemcitabine treatment (Yau et al., 2005). Thus, it is possible that in our case the amplification of *ILK* enhances gemcitabine resistance, while also potentially increasing cell migration. The overexpression of *WEE1* may also augment gemcitabine resistance in our system, as gemcitabine targets DNA Polymerase triggering replication stress, while WEE1 is known to protect cells from DNA damage by inducing cell cycle arrest (Beck et al., 2012; Sørensen and Syljuåsen, 2012). This way, the upregulation of *WEE1* could play a cytoprotective role upon gemcitabine treatment. In fact, WEE1 inhibition in combination with gemcitabine and radiation therapy has shown promising results in pancreatic cancer patients (Cuneo et al., 2019; Koh et al., 2018). Thus, it would be interesting to test whether gemcitabine resistant cells can be sensitized to gemcitabine with ILK or WEE1 inhibitors. If so, tracing the percentage of gemcitabine resistant tumors that co-amplify *RRM1* and *ILK* or *WEE1* can be of great prognostic value.

In conclusion, characterizing gene amplifications is not only valuable to dissect cancer development, but also to better understand how tumors may adapt to stresses, such as chemotherapeutic agents. Even though specific gene amplifications are regarded as the drivers of a certain cancer type or chemotherapeutic resistance mechanism, their co-amplified genes may also contribute to tumorigenesis. Therefore, considering the genetic background in

studies is crucial, while dissecting the interplay between genomic aberrations may widen our understanding of cancer and chemotherapy resistance.

3.3. Are co-amplifications by chance or selected for?

As described in the previous section, genomic amplifications are a common feature in cancer, which take place randomly and may be associated with metastasis and chemotherapy response. Furthermore, co-amplifications may reinforce each other or confer independent properties to tumors (Section 3.2). Interestingly, some co-amplifications have been reported to present a high co-occurrence rate, while others have been shown to be mutually exclusive, revealing the importance of the selection applied on genomic aberration events. Mutual exclusivity can be a result of genomic aberration redundancy or synthetic lethality, where cells cannot handle both alterations at the same time. On the other hand, co-occurrence of genomic aberrations suggests that the alterations complement each other (Deng et al., 2012; Sanchez-Vega et al., 2018).

In PDAC, mutual exclusivity is often seen in the context of *K-RAS* mutations and amplifications. In the absence of an amplified and mutated *K-RAS,* pancreatic cancer tumors frequently amplify *ERBB2* and present a higher dependency on MAPK and mTOR signaling (Singhi et al., 2019; The Cancer Genome Atlas Research Network et al., 2017; Tiriac et al., 2018). Similarly, while deletions of *SMAD4* are frequent in pancreatic cancer, a tendency has been described for basal pancreatic cancer tumors to present an intact *SMAD4* copy (Chan-Seng-Yue et al., 2020). Interestingly, the co-occurrence of *SMAD4* loss and *GATA6* amplification was observed in the classical subtype of pancreatic cancer (Notta et al., 2016). Furthermore, *FOXA2* has been shown to be amplified in the small fraction of classical tumors harboring an intact *SMAD4*, hinting at a possible mutual exclusivity with *GATA6* amplification and co-occurrence with intact *SMAD4* (Chan-Seng-Yue et al., 2020). An even better example of co-occurring genomic aberration is the mutation and amplification of *K-RAS,* accompanied by the deletion of *CDKN2A* and *SMAD4* driving pancreatic cancer progression (Notta et al., 2016). This exemplifies how different sets of genomic aberrations are selected for during pancreatic cancer development and progression, highlighting the effects of selective pressure on the

cells. Thus, even though genomic aberrations are random in origin, they are selected for by several internal and external cues.

Our findings pose a similar scenario in which several genes are co-amplified upon the selective pressure of gemcitabine treatment. The co-amplification of *RRM1* and *STIM1* confers the cells with different oncogenic properties, these being gemcitabine resistance and ER stress resistance accompanied by NFAT activation, respectively. Still, it is possible that the co-amplification of *STIM1* is selected for and is not just a “passenger” effect arising from the amplification of *RRM1* upon gemcitabine. This could be rationalized through the impact of STIM1 and calcium signaling in NFAT activation and the stress response. It is possible that during an initial response to gemcitabine, cells upregulate *RRM1* and face major changes in their metabolic pathways. RRM1 is responsible for catalyzing the rate limiting step in the *de novo* dNTP synthesis pathway and is thus regarded as a key player in metabolic processes (Aye et al., 2014; Kohnken et al., 2015). The upregulation of *STIM1* in this case could further promote RRM1 activity, by preventing the activation of the integrated stress response and thus evading apoptosis and the shutdown of energy consuming metabolic processes elicited by RRM1. Moreover, upregulating *STIM1* could help the cells cope with metabolic changes by promoting the activation of NFAT and its downstream targets c-*MYC* and *HIF1a* (König et al., 2010b; Singh et al., 2010; Vaeth et al., 2017). These factors have been shown to stimulate the transcription of several metabolic genes (Dejure and Eilers, 2017; Stine et al., 2015), such that STIM1 could aid in the initial metabolic adaptation of the cells. Still, once adapted to high levels of RRM1 and STIM1, cells may employ other mechanisms to maintain their metabolic processes, such that the effects of the co-amplification may become independent. Therefore, it is possible that the co-amplification of *RRM1* and *STIM1* poses another example of genomic aberration co-occurrence in cancer. We can speculate that the co-amplification of *STIM1* and *RRM1* will present a high co-occurrence rate in gemcitabine resistant PDAC and may serve to monitor tumor responsiveness to chemotherapy and stress.

Expanding this hypothesis, stress elicited by the tumor’s microenvironment may promote the amplification of *STIM1.* In this case, the co-amplification of *RRM1* may be regarded as a “passenger” effect or as a co-occurrence depending on the source of stress. In order to evade stress-triggered apoptosis, the cells may upregulate

STIM1, thriving under stress. Still, while doing so, cells would fail to halt energy-consuming processes, possibly being faced with the challenge of rewiring their metabolic dependencies. Thus, during the adaptation period and depending on the source of stress, the cells may profit from the metabolic changes accompanied by the upregulation of *RRM1*. This way, the co-amplification of *RRM1* and *STIM1* would again co-occur and synergize only during the adaptation of the cells to specific sources of stress. The fact that naïve cancer cell lines and tumors present a high co-occurrence rate of the co-amplification of *RRM1* and *STIM1* further supports the idea. In which the tumor microenvironment may impose a selective pressure on tumors thriving under stressful conditions, favoring those with a co-amplification of *RRM1* and *STIM1.* Therefore, it would be of great importance to assess STIM1 and RRM1 levels in cells and tumors upon a wide array of stresses. This would not only prove the hypothesis but also provide evidence as to which stress sources would be responsible for selecting for the co-amplification.

Taken together, even though the properties conferred by the co-amplification of *RRM1* and *STIM1* are independent of each other, they may have both been selected for during the adaptation process to gemcitabine treatment. This way, serving as an example for genomic aberration co-occurrence in gemcitabine-treated tumors. Furthermore, it is highly probable that other sources of stress would also favor the co-amplification of *STIM1* and *RRM1*. Thus, even though random in nature, the co-amplification of *RRM1* and *STIM1* may be selected for by different stimuli.

3.4. ER stress response: essential or dispensable for the tumor?

Here we identify the amplification of *STIM1* and concomitant increased SOCE as responsible for a dampened ER stress response in gemcitabine resistant tumors. We further hypothesize that other stresses may also serve as a selective pressure for the amplification of *STIM1*. Still, several studies have pointed at the fact that tumors may take advantage of their stressful environment by hijacking the pro-survival branch of the ISR. In fact, the pro-survival ATF4-triggered response has been associated with several tumorigenic processes such as angiogenesis, metastasis, genomic instability, and therapeutic resistance (Bi et al., 2005; Dufey et al., 2015; Moore et al., 2019; Terai et al., 2018; Urra et al., 2016).

One of the best characterized examples is that of hypoxia triggered ER stress response and the tumor's consequent adaptation to oxygen-deprived environments. In this case, ATF4 activation by PERK upon ER stress, has been proposed to be crucial for the transcription of angiogenic genes. Both, ATF4 and XBP1 have been reported to bind the promoter region of *VEGFA*, while ATF4 has been shown to be a driver of *VEGFA* expression upon stress (Pereira et al., 2014; Wang et al., 2012). Furthermore, ATF4 has been shown to interact with and to stabilize HIF1a, promoting angiogenesis in bone (Zhu et al., 2013). HIF1a is also a driver of several cancers, promoting invasion and metastasis in PDAC (Zhang et al., 2017; Zhao et al., 2014). Thus, it is possible that highly hypoxic tumors, such as PDAC, rather profit from the activation of the ISR and from ATF4 activity upon hypoxia.

Following this hypothesis, it is possible that PDAC tumors expressing high STIM1 levels, may be more vulnerable to hypoxia, as they present a dampened ER stress response. At the same time that increased STIM1 and SOCE levels may protect pancreatic cancer cells from the pro-apoptotic branch of the ISR, they may impede them from hijacking the pro-survival branch upon hypoxia and other ER stresses. One could speculate that these tumors would fail to activate ATF4, thus failing to upregulate *VEGFA* and to stabilize HIF1a upon hypoxia.

On the other hand, STIM1 and SOCE have been shown to promote HIF1a expression and stabilization during hepatocarcinogenesis. In this case, upon hypoxia, elevated SOCE lead to the activation of CAMKII and consequently of the p300 acetyltransferase (Li et al., 2015). p300, in turn, interacts with the transactivation domain of HIF1a, stabilizing and preventing the degradation of the latter (Yuan et al., 2005). Interestingly, in a feedback mechanism, HIF1a has been shown to bind the promoter region of *STIM1* increasing its expression upon hypoxia. Furthermore, several different tumor types have shown a positive correlation between STIM1 and HIF1a levels (Li et al., 2015; Wang et al., 2019). Thus, it is also plausible that some tumors rely on the activation of SOCE by STIM1 to cope with hypoxia.

For this reason, *STIM1* amplifying cell lines may be able to thrive under hypoxic conditions by activating HIF1a through SOCE, circumventing the dampened ER stress response and ATF4-dependent HIF1a activation. In this case, the benefits of

hijacking the pro-survival pathway of the ER stress response upon hypoxia may become dispensable for the cell. Instead, tumors may employ SOCE-dependent alternative mechanisms and pathways to cope with oxygen-deprivation. Thus, redundant signaling pathways may aid tumors with very different genetic and epigenetic backgrounds to adapt to the same source of stress. This may apply not only to hypoxia-induced stress, but also to other external stimuli.

In order to test the hypotheses above, one would have to first determine whether cells expressing high levels of STIM1 present a greater susceptibility to hypoxia or not. If the cells rely on the ER stress response to cope with hypoxia, it is plausible that STIM1 overexpressing cells display a survival disadvantage under hypoxia. Alternatively, if relying on elevated SOCE to cope with oxygen-deprivation, these cells may present a similar or improved survival advantage compared to cells expressing lower levels of STIM1. Finally, in order to confirm the ER stress or SOCE dependency of these cells in response to hypoxia, cells could be deprived from STIM1, ATF4 and PERK and their response to hypoxia assessed. In conclusion, tumors present different genetic and epigenetic backgrounds, which may affect the pathways activated upon stimuli. Even though many cancers rely on the pro-survival branch of the ER stress response to overcome several stresses, cells may also adapt and employ alternative mechanisms to thrive under the same stimuli and conditions.

3.5. The possible advantages of aberrant NFAT activation

As identified in section 2.4.5, an alternative pathway activated in STIM1 overexpressing cells upon heighted SOCE is the NFAT signaling pathway. The NFAT family of transcription factors is best described in the immunology field, where it regulates T cell activation and differentiation, while also affecting the function of other immune cells (Müller and Rao, 2010). Still, NFATs have been reported to be crucial in other cell systems as well and their dysregulation associated with several diseases, including heart problems and cancer (Dewenter et al., 2017; Mancini and Toker, 2009). In the case of cancer, NFATs have been described to promote angiogenesis, metastasis and tumor progression (Mancini and Toker, 2009). Thus, aberrant NFAT activation in STIM1 overexpressing cells may confer these tumors with novel oncogenic properties.

Angiogenesis is a hallmark of cancer, in which tumors upon different stimuli, including hypoxia, activate HIF1a, upregulating and secreting VEGF, while also reprogramming their metabolism to adapt to oxygen-deprived environments. Endothelial cells surrounding the tumor, in turn, can bind VEGF, which stimulates their proliferation and fosters angiogenesis (Majmundar et al., 2010). In many endothelial cells, the response to VEGF and the subsequent upregulation of angiogenic genes, such as *COX2*, has been proven to be SOCE and NFAT-dependent (Mancini and Toker, 2009; Suehiro et al., 2014). Interestingly, NFATs have also been described to induce *HIF1a* expression to promote a metabolic rewiring in T cells. T cell proliferation has been shown to be dependent on a metabolic reprogramming elicited by SOCE and subsequent NFAT and Akt/mTOR signaling pathway activation. In this case, NFATs promoted the upregulation of the transcription factors *HIF1a* and *IRF4,* while Akt/mTOR signaling lead to c-MYC activation. Together, NFATs, HIF1a, IRF4 and c-MYC induced the expression of various metabolic genes involved in glycolysis, oxidative phosphorylation and nucleotide metabolism (Vaeth et al., 2017). Taken together, there is evidence suggesting that NFATs control several players involved in angiogenesis and the response to hypoxia. Thus, it is possible that in STIM1 overexpressing tumors, NFATs may promote the upregulation of *HIF1a* and the initiation of angiogenesis upon hypoxia and other SOCE-promoting stimuli. Furthermore, it is plausible, that similar to T cells, NFAT activation upon different stimuli, may rewire the metabolic dependencies of STIM1 overexpressing cells.

Even though, the above speculations have to be tested, an NFAT-dependent upregulation of *HIF1a* could confer *STIM1* amplifying cells with an alternative pathway to respond to stress signals, which is independent from the ER stress response pathway. Furthermore, an NFAT-driven metabolic rewiring upon SOCE stimulation, may help the cells cope with several metabolic stresses. Thus, it is possible that potential metabolic changes, elicited by the upregulation of RRM1 during the establishment of gemcitabine resistance, are further accommodated by a metabolic reprogramming elicited by aberrant NFAT activation due to STIM1 upregulation. This would, in turn, favor the co-amplification of *RRM1* and *STIM1* during the establishment of gemcitabine resistance.

Aberrant NFAT activation in STIM1 overexpressing tumors may not only lead to increased angiogenesis and a possible metabolic reprogramming, but also to heightened metastatic rates. In melanoma, increased NFAT signaling in epithelial cells lead to heightened BMP2 secretion, which promoted cancer cell dedifferentiation and metastasis. NFAT activity has also been associated with increased cell migration and invasion in breast cancer, while being characterized as the driver of several metastatic factors in colon cancer (Jauliac et al., 2002; Tripathi et al., 2014; Yiu and Toker, 2006). In PDAC, aberrant NFATc1 activation led to increased expression of several EMT genes (Hendrikx et al., 2019). By dimerizing with SOX2, NFATc1 drove the upregulation of the EMT-promoting transcription factors *ZEB1, TWIST* and *SNAI1* (Singh et al., 2015). Thus, it is highly likely that cells expressing higher STIM1 and therefore SOCE levels, present a more dedifferentiated phenotype and higher metastatic potential.

Interestingly, NFATs have also been extensively characterized as drivers of pancreatic cancer development and growth. Several studies demonstrated that NFAT is key for inflammation-driven pancreatic cancer development (Baumgart et al., 2014, 2016). The promoter of NFAT itself has also been shown to be methylated by EZH2 and consequently silenced in pancreatic acinar cells. This was reversed upon KRAS activation during PDAC development, leading to the de-repression and concomitant activation of *NFATc1* (Chen et al., 2017). Moreover, NFATc2 has been shown to promote the silencing of the tumor suppressor *CDKN2B* further fostering tumorigenesis (Baumgart et al., 2012). NFATs further promote *c-MYC* expression and cell proliferation in pancreatic cancer (Buchholz et al., 2006; König et al., 2010c). For example, TGFβ has been reported to activate NFAT, which in turn displaces SMAD3 allowing TGFβ responsive genes, such as *c-MYC*, to be activated, ultimately promoting tumor growth (Singh et al., 2010). Therefore, it is highly likely that STIM1 overexpressing pancreatic cancer cells display a tumorigenic and proliferative advantage elicited by aberrant NFAT activation compared to STIM1 lowly expressing cells.

In order to validate all aforementioned hypotheses, functional assays comparing low and high STIM1 expressing cells under resting conditions as well as under several stresses would have to be conducted. Xenograft experiments could also be performed, in which STIM1 high and low expressing cells are injected into mice and

tumor progression, volume and metastasis occurrence are monitored. Still, even though the consequences of an aberrant NFAT activation in STIM1 overexpressing cells have to be better characterized, previous studies highly suggest that ectopic NFAT activation may confer these cells with important additional tumorigenic properties.

3.6. The benefits and drawbacks of targeting calcium signaling in pancreatic cancer

As described in the sections above, the amplification of *STIM1* in pancreatic cancer cells upon gemcitabine resistance elicits a shift in calcium signaling and an epigenetic reprogramming. The consequent increased SOCE and NFAT activity may confer the cells with several additional oncogenic properties, while the dampened response to ER stress protects the cells from apoptosis. Therefore, the targeting of NFAT and SOCE may prevent the activation of pro-tumorigenic processes, while also reestablishing the sensitivity to ER stress.

NFAT activation can be targeted by inhibiting calcineurin activity employing cyclosporine A (CSA) and FK506 (tacrolimus). These compounds are routinely used in the clinic as immunosuppressants, preventing organ transplantation rejection, and their potential in cancer treatment is still under investigation (Azzi et al., 2013; Kaufman et al., 2004). Studies have shown the benefits of using these FDA-approved drugs in the treatment of different cancer entities. In bladder cancer, both CSA and tacrolimus lead to decreased migration and invasion *in vitro* as well as decreased tumor volume *in vivo* (Kawahara et al., 2015). In breast cancer, tacrolimus treatment reduced cancer cell proliferation and migration, while inhibiting angiogenesis (Siamakpour-Reihani et al., 2011). Still, the use of these compounds for cancer treatment has to be carefully assessed and treatment schedules wisely planned. Prolonged exposure to CSA or tacrolimus has been associated with increased cancer incidence (Dantal and Soulillou, 2005; Mancini and Toker, 2009), while both compounds are also known to elicit severe side effects (Azzi et al., 2013; Rezzani, 2004). Furthermore, in our case, where pancreatic cancer cells amplify and overexpress STIM1, inhibiting calcineurin with CSA or tacrolimus would solely inhibit potential pro-oncogenic pathways that arise due to aberrant NFAT activation.

Thus, the SOCE-dependent ER stress resistance observed in these cells would most likely perdure.

In order to target the potential pro-oncogenic properties elicited by aberrant NFAT activation, while also sensitizing the cells to ER stress, STIM1 overexpressing pancreatic cancer cells could be treated with SOCE inhibitors. Even though, no SOCE inhibitor has been approved by the FDA yet, several ones have been developed and some are being tested in clinical trials for the treatment of acute pancreatitis. Aberrant calcium signaling is one of the first events leading to the development of acute pancreatitis, where increased SOCE leads to early exocytosis of zymogens and premature activation of proenzymes in the intracellular space and inside acinar cells. Consequently, the pancreas is slowly digested, triggering pancreatitis (Raraty et al., 2000; Ward et al., 1995). During preclinical trial studies, the SOCE inhibitors GSK7975A and CM128 have shown very promising results in treating acute pancreatitis, while also preventing pancreatic acinar cell injury (Gerasimenko et al., 2013; Wen et al., 2015). Among SOCE inhibitors, CM4620 (also known as Auxora) is currently in phase 2 clinical trials for the treatment of acute pancreatitis.

As clinical trials with CM4620 and other SOCE inhibitors evolve, scientists may better gauge the impact of SOCE inhibition in the body. It is highly possible that SOCE inhibitors lead to the immunosuppression of patients, as SOCE is upstream of NFAT activation, and as the immunosuppressants CSA and tacrolimus are known repressors of NFAT activity. Furthermore, several important SOCE-dependent physiological processes, such as the release of insulin in the pancreas, the glomerular hemodynamics in the kidney, the formation of osteoclasts in the bone and the differentiation of myoblasts in skeletal muscle, among others, may be transiently impaired during SOCE inhibitor treatment (Soboloff et al., 2012). Still, the occurrence of these potential side effects will largely depend on the concentration and duration of the inhibitor treatment.

Assuming CM4620 and/or other SOCE inhibitors are approved by the FDA and little to mild side effects are detected, SOCE inhibitors may be a suitable candidate to treat pancreatic tumors, where STIM1 is overexpressed. Thus, assessing the expression of STIM1 in patient biopsies before and after chemotherapy, may help

stratify tumors and gauge their sensitivity to stress as well as their suitability for SOCE inhibitor treatments. Furthermore, by restoring the cellular sensitivity to ER stress, upon SOCE inhibitor treatment, these tumors may be more sensitive to alternative chemotherapies, which trigger apoptosis via ER stress. Taken together, SOCE inhibition may pose an alternative treatment option for pancreatic cancer patients presenting increased STIM1 expression and *a priori* or acquired gemcitabine resistance.

4. Conclusion

Gemcitabine resistance is recurrent in pancreatic cancer and a major factor contributing to the low 5-year survival rate faced by PDAC patients. Even though gemcitabine resistance itself has been studied extensively before, the molecular changes accompanying gemcitabine treatment remained largely unknown. In this study, we identify genomic, epigenomic and transcriptomic changes taking place upon gemcitabine resistance. We further unravel changes in signaling pathway and stress response dependencies upon acquired gemcitabine resistance, and propose their targeting as an alternative treatment to gemcitabine (Fig. 32).

When characterizing gemcitabine resistant cells, two neighboring genes, *RRM1* and *STIM1*, were identified as highly amplified and highly upregulated in gemcitabine resistant cells compared to parental cells. The role of RRM1 in gemcitabine resistance had been characterized previously, and was further validated in our experiments as driving resistance in GemR. Still, the amplification of *RRM1* has never been reported in gemcitabine resistant PDAC tumors and its monitoring during treatment may serve to gauge gemcitabine response in patients and to assess the need to switch to alternative treatment options.

The overexpression of *STIM1,* on the other hand, had not been implicated in gemcitabine resistance before and the high co-occurrence rate of its co-amplification with *RRM1* not reported previously. High levels of STIM1 did not contribute to gemcitabine resistance in GemR, but elicited an increase in SOCE, which triggered an epigenetic and transcriptomic reprogramming. Heightened SOCE elicited a dampened ER stress response in GemR compared to parental cells, as observed in proliferation assays, transcriptomic studies and by comparing the histone mark for active transcription, H3K27ac. The role of SOCE in preventing the activation of the ER stress response in cancer is described for the first time in this study. Even though a few recent publications have hinted at the interplay between SOCE and the ER stress response in diabetes, the exact mechanism by which SOCE prevents the activation of the ER stress response remains elusive. Thus, our findings open a new field for investigation, where the role of cytosolic calcium influx in the ER stress response has to be better characterized.

Increased SOCE not only led to an ER stress resistance and failure to activate the stress responsive ATF4, but also triggered NFAT activation. Further characterization of the consequences of aberrant NFAT activation in STIM1 overexpressing cells is needed, but, based on previous studies, it is highly plausible that NFATs drive oncogenic programs in these cells. This way, possibly providing gemcitabine resistant or STIM1 overexpressing tumors with additional advantages to thrive in hostile microenvironments. Furthermore, SOCE is known to also stimulate CAMKII leading to the activation of a vast array of transcription factors. Thus, it is of great importance to elucidate what other transcription factors are activated upon heightened SOCE and what transcriptomic and phenotypic changes they elicit in STIM1 overexpressing and gemcitabine resistant tumors.

Moreover, further investigation revealed that there is a propensity of cancer cells to overexpress RRM1 and STIM1 even without treatment. Similarly, different STIM1 expression levels were observed in treatment naïve pancreatic cancer patient specimens and patient-derived xenografts. In this case, STIM1 levels also correlated with NFAT activity and ATF4 nuclear localization, further validating our findings *in vivo*. Gemcitabine treatment of patient-derived xenografts further promoted the overexpression of STIM1, increased NFAT activity and decreased ATF4 nuclear localization. This proves that even though STIM1 may be highly expressed in some treatment naïve tumors, an increase in STIM1 levels is selected for upon gemcitabine treatment. It further highlights the potential benefits of SOCE inhibitors in the treatment of STIM1-overexpressing gemcitabine resistant as well as treatment naïve pancreatic tumors.

Thus, SOCE and NFAT inhibition pose novel treatment options for pancreatic cancer patients that present *a priori* or acquired gemcitabine resistance. Cyclosporine A or tacrolimus could be employed to prevent NFAT activation and thus impair any pro-oncogenic program elicited by increased SOCE. Alternatively, SOCE inhibition could not only impair the effects of NFAT activation, but also restore ER stress sensitivity in STIM1 overexpressing tumors. This could make gemcitabine resistant and STIM1 overexpressing tumors more susceptible to alternative therapeutic agents, which elicit ER stress.

Taken together, our study unravels molecular changes elicited upon acquired gemcitabine resistance. While the amplification of *RRM1* drives gemcitabine resistance, the amplification of *STIM1* leads to a shift in SOCE and calcium signaling. Increased SOCE dampens ER stress activation, thus preventing the accumulation of the transcription factor ATF4, while promoting the activation of NFATs. Therefore, we can conclude that STIM1 acts as a rheostat, fine tuning SOCE and consequently balancing between an ATF4-driven ER stress-responsive and an NFAT-driven transcriptional program.

5. References

Akita, H., Zheng, Z., Takeda, Y., Kim, C., Kittaka, N., Kobayashi, S., Marubashi, S., Takemasa, I., Nagano, H., Dono, K., et al. (2009). Significance of RRM1 and ERCC1 expression in resectable pancreatic adenocarcinoma. Oncogene *28*, 2903–2909.

Ali, M.M.U., Bagratuni, T., Davenport, E.L., Nowak, P.R., Silva-Santisteban, M.C., Hardcastle, A., McAndrews, C., Rowlands, M.G., Morgan, G.J., Aherne, W., et al. (2011). Structure of the Ire1 autophosphorylation complex and implications for the unfolded protein response. EMBO J. *30*, 894–905.

Allis, C.D., and Jenuwein, T. (2016). The molecular hallmarks of epigenetic control. Nat. Rev. Genet. *17*, 487–500.

American Cancer Society (2020). Cancer Facts & Figures 2020.

Amrutkar, M., and Gladhaug, I.P. (2017). Pancreatic cancer chemoresistance to gemcitabine. Cancers (Basel). *9*, 1–23.

Anders, S., Pyl, P.T., and Huber, W. (2015). HTSeq-A Python framework to work with high-throughput sequencing data. Bioinformatics *31*, 166–169.

Aoyama, T., Miyagi, Y., Murakawa, M., Yamaoku, K., Atsumi, Y., Shiozawa, M., Ueno, M., Morimoto, M., Oshima, T., Yukawa, N., et al. (2017). Clinical implications of ribonucleotide reductase subunit M1 in patients with pancreatic cancer who undergo curative resection followed by adjuvant chemotherapy with gemcitabine. Oncol. Lett. *13*, 3423–3430.

Ashida, R., Nakata, B., Shigekawa, M., Mizuno, N., Sawaki, A., Hirakawa, K., Arakawa, T., and Yamao, K. (2009). Gemcitabine sensitivity-related mRNA expression in endoscopic ultrasound-guided fine-needle aspiration biopsy of unresectable pancreatic cancer. J. Exp. Clin. Cancer Res. *28*, 1–7.

Aung, K.L., Fischer, S.E., Denroche, R.E., Jang, G.H., Dodd, A., Creighton, S., Southwood, B., Liang, S. Ben, Chadwick, D., Zhang, A., et al. (2018). Genomics-driven precision medicine for advanced pancreatic cancer: Early results from the COMPASS trial. Clin. Cancer Res. *24*, 1344–1354.

Avril, T., Vauléon, E., and Chevet, E. (2017). Endoplasmic reticulum stress signaling and chemotherapy resistance in solid cancers. Oncogenesis *6*, e373.

Aye, Y., Li, M., Long, M.J.C., and Weiss, R.S. (2014). Ribonucleotide reductase and

cancer: Biological mechanisms and targeted therapies. Oncogene *34*, 2011–2021.

Azzi, J.R., Sayegh, M.H., and Mallat, S.G. (2013). Calcineurin Inhibitors: 40 Years Later, Can't Live Without …. J. Immunol. *191*, 5785–5791.

B'Chir, W., Maurin, A.C., Carraro, V., Averous, J., Jousse, C., Muranishi, Y., Parry, L., Stepien, G., Fafournoux, P., and Bruhat, A. (2013). The eIF2α/ATF4 pathway is essential for stress-induced autophagy gene expression. Nucleic Acids Res. *41*, 7683–7699.

Backs, J., Song, K., Bezprozvannaya, S., Chang, S., and Olson, E.N. (2006). CaM kinase II selectively signals to histone deacetylase 4 during cardiomyocyte hypertrophy. J. Clin. Invest. *116*, 1853–1864.

Backs, J., Worst, B.C., Lehmann, L.H., Patrick, D.M., Jebessa, Z., Kreusser, M.M., Sun, Q., Chen, L., Heft, C., Katus, H.A., et al. (2011). Selective repression of MEF2 activity by PKA-dependent proteolysis of HDAC4. J. Cell Biol. *195*, 403–415.

Bailey, P., Chang, D.K., Nones, K., Johns, A.L., Patch, A.M., Gingras, M.C., Miller, D.K., Christ, A.N., Bruxner, T.J.C., Quinn, M.C., et al. (2016). Genomic analyses identify molecular subtypes of pancreatic cancer. Nature *531*, 47–52.

Balachandran, S., Roberts, P.C., Brown, L.E., Truong, H., Pattnaik, A.K., Archer, D.R., and Barber, G.N. (2000). Essential role for the dsRNA-dependent protein kinase PKR in innate immunity to viral infection. Immunity *13*, 129–141.

Bardeesy, N., Cheng, K.H., Berger, J.H., Chu, G.C., Pahler, J., Olson, P., Hezel, A.F., Horner, J., Lauwers, G.Y., Hanahan, D., et al. (2006). Smad4 is dispensable for normal pancreas development yet critical in progression and tumor biology of pancreas cancer. Genes Dev. *20*, 3130–3146.

Baumgart, S., Glesel, E., Singh, G., Chen, N., Reutlinger, K., Zhang, J., Billadeau, D.D., Fernandezzapico, M.E., Gress, T.M., Singh, S.K., et al. (2012). Restricted heterochromatin formation links NFATc2 repressor activity with growth promotion in pancreatic cancer. Gastroenterology *142*, 1–21.

Baumgart, S., Ellenrieder, V., and Fernandez-Zapico, M.E. (2013). Oncogenic transcription factors: Cornerstones of inflammation-linked pancreatic carcinogenesis. Gut *62*, 310–316.

Baumgart, S., Chen, N.M., Siveke, J.T., König, A., Zhang, J.S., Singh, S.K., Wolf,

E., Bartkuhn, M., Esposito, I., Heßmann, E., et al. (2014). Inflammation-Induced NFATc1-STAT3 transcription complex promotes pancreatic cancer initiation by KrasG12D. Cancer Discov. *4*, 688–701.

Baumgart, S., Chen, N.M., Zhang, J.S., Billadeau, D.D., Gaisina, I.N., Kozikowski, A.P., Singh, S.K., Fink, D., Ströbel, P., Klindt, C., et al. (2016). GSK-3β governs inflammation-induced NFATc2 signaling hubs to promote pancreatic cancer progression. Mol. Cancer Ther. *15*, 491–502.

Beck, H., Nahse-Kumpf, V., Larsen, M.S.Y., O'Hanlon, K.A., Patzke, S., Holmberg, C., Mejlvang, J., Groth, A., Nielsen, O., Syljuasen, R.G., et al. (2012). Cyclin-Dependent Kinase Suppression by WEE1 Kinase Protects the Genome through Control of Replication Initiation and Nucleotide Consumption. Mol. Cell. Biol. *32*, 4226–4236.

Becker, J.S., Nicetto, D., and Zaret, K.S. (2016). H3K9me3-Dependent Heterochromatin: Barrier to Cell Fate Changes. Trends Genet. *32*, 29–41.

Bergman, A.M., Giaccone, G., Van Moorsel, C.J.A., Mauritz, R., Noordhuis, P., Pinedo, H.M., and Peters, G.J. (2000). Cross-resistance in the 2',2'-difluorodeoxycytidine (gemcitabine)- resistant human ovarian cancer cell line AG6000 to standard and investigational drugs. Eur. J. Cancer *36*, 1974–1983.

Bergman, A.M., Eijk, P.P., Ruiz Van Haperen, V.W.T., Smid, K., Veerman, G., Hubeek, I., Van Den Ijssel, P., Ylstra, B., and Peters, G.J. (2005). In vivo induction of resistance to gemcitabine results in increased expression of ribonucleotide reductase subunit M1 as the major determinant. Cancer Res. *65*, 9510–9516.

Berridge, M.J., Lipp, P., and Bootman, M.D. (2000). The versatility and universality of calcium signalling. Nat. Rev. Mol. Cell Biol. *1*, 11–21.

Berridge, M.J., Bootman, M.D., and Roderick, H.L. (2003). Calcium signalling: Dynamics, homeostasis and remodelling. Nat. Rev. Mol. Cell Biol. *4*, 517–529.

Bertolotti, A., Zhang, Y., Hendershot, L.M., Harding, H.P., and Ron, D. (2000). Dynamic interaction of BiP and ER stress transducers in the unfolded- protein response. Nat. Cell Biol. *2*, 1–7.

Bhutia, Y.D., Hung, S.W., Patel, B., Lovin, D., and Govindarajan, R. (2011). CNT1 expression influences proliferation and chemosensitivity in drug-resistant pancreatic

cancer cells. Cancer Res. *71*, 1825–1835.

Bi, M., Naczki, C., Koritzinsky, M., Fels, D., Blais, J., Hu, N., Harding, H., Novoa, I., Varia, M., Raleigh, J., et al. (2005). ER stress-regulated translation increases tolerance to extreme hypoxia and promotes tumor growth. EMBO J. *24*, 3470–3481.

Blais, J.D., Filipenko, V., Bi, M., Harding, H.P., Ron, D., Koumenis, C., Wouters, B.G., and Bell, J.C. (2004). Activating Transcription Factor 4 Is Translationally Regulated by Hypoxic Stress. Mol. Cell. Biol. *24*, 7469–7482.

Blaustein, M.P., Lederer, W.J., and Annunziato, L. (2008). Sodium / Calcium Exchange : Its Physiological Implications. Society *79*, 763–854.

Bogeski, I., Kummerow, C., Al-Ansary, D., Schwarz, E.C., Koehler, R., Kozai, D., Takahashi, N., Peinelt, C., Griesemer, D., Bozem, M., et al. (2010). Differential redox regulation of ORAI ion channels: A mechanism to tune cellular Calcium signaling. Sci. Signal. *3*, 1–10.

Bouffard, D.Y., Laliberté, J., and Momparler, R.L. (1993). Kinetic studies on 2',2'-difluorodeoxycytidine (gemcitabine) with purified human deoxycytidine kinase and cytidine deaminase. Biochem. Pharmacol. *45*, 1857–1861.

Brandman, O., Liou, J., Park, W.S., and Meyer, T. (2007). STIM2 Is a Feedback Regulator that Stabilizes Basal Cytosolic and Endoplasmic Reticulum Ca2+ Levels. Cell *131*, 1327–1339.

Breiling, A., Turner, B.M., Bianchi, M.E., and Orlando, V. (2001). General transcription factors bind promoters repressed by Polycomb group proteins. Nature *412*, 651–655.

Buchholz, M., Schatz, A., Wagner, M., Michl, P., Linhart, T., Adler, G., Gress, T.M., and Ellenrieder, V. (2006). Overexpression of c-myc in pancreatic cancer caused by ectopic activation of NFATc1 and the Ca2+/calcineurin signaling pathway. EMBO J. *25*, 3714–3724.

Burris, H.A., Moore, M.J., Andersen, J., Green, M.R., Rothenberg, M.L., Modiano, M.R., Cripps, M.C., Portenoy, R.K., Storniolo, A.M., Tarassoff, P., et al. (1997). Improvements in survival and clinical benefit with gemcitabine as first- line therapy for patients with advanced pancreas cancer: A randomized trial. J. Clin. Oncol. *15*, 2403–2413.

Buscail, L., Bournet, B., and Cordelier, P. (2020). Role of oncogenic KRAS in the diagnosis, prognosis and treatment of pancreatic cancer. Nat. Rev. Gastroenterol. Hepatol. *17*, 153–168.

Carrara, M., Prischi, F., Nowak, P.R., and Ali, M.M. (2015). Crystal structures reveal transient PERK luminal domain tetramerization in endoplasmic reticulum stress signaling . EMBO J. *34*, 1589–1600.

Carreras-Sureda, A., Pihán, P., and Hetz, C. (2018). Calcium signaling at the endoplasmic reticulum: fine-tuning stress responses. Cell Calcium *70*, 24–31.

Casper, E.S., Green, M.R., Kelsen, D.P., Heelan, R.T., Brown, T.D., Flombaum, C.D., Trochanowski, B., and Tarassoff, P.G. (1994). Phase II trial of gemcitabine (2,2′-difiuorodeoxycytidine) in patients with adenocarcinoma of the pancreas. Invest. New Drugs *12*, 29–34.

Catterall, W.A. (2011). Voltage-gated calcium channels. Cold Spring Harb. Perspect. Biol. *3*, 1–23.

Cerami, E., Gao, J., Dogrusoz, U., Gross, B.E., Sumer, S.O., Aksoy, B.A., Jacobsen, A., Byrne, C.J., Heuer, M.L., Larsson, E., et al. (2012). The cBio Cancer Genomics Portal: An open platform for exploring multidimensional cancer genomics data. Cancer Discov. *2*, 401–404.

Chan-Seng-Yue, M., Kim, J.C., Wilson, G.W., Ng, K., Figueroa, E.F., O'Kane, G.M., Connor, A.A., Denroche, R.E., Grant, R.C., McLeod, J., et al. (2020). Transcription phenotypes of pancreatic cancer are driven by genomic events during tumor evolution. Nat. Genet.

Chan, H.M., and La Thangue, N.B. (2001). p300/CBP proteins: HATs for transcriptional bridges and scaffolds. J. Cell Sci. *114*, 2363–2373.

Chauhan, V.P., Martin, J.D., Liu, H., Lacorre, D.A., Jain, S.R., Kozin, S. V., Stylianopoulos, T., Mousa, A.S., Han, X., Adstamongkonkul, P., et al. (2013). Angiotensin inhibition enhances drug delivery and potentiates chemotherapy by decompressing tumour blood vessels. Nat. Commun. *4*.

Chen, E.Y., Tan, C.M., Kou, Y., Duan, Q., Wang, Z., Meirelles, G. V., Clark, N.R., and Ma'ayan, A. (2013). Enrichr: Interactive and collaborative HTML5 gene list enrichment analysis tool. BMC Bioinformatics *14*.

Chen, J., Zhang, Z., Li, L., Chen, B.C., Revyakin, A., Hajj, B., Legant, W., Dahan, M., Lionnet, T., Betzig, E., et al. (2014). Single-molecule dynamics of enhanceosome assembly in embryonic stem cells. Cell *156*, 1274–1285.

Chen, N.M., Singh, G., Koenig, A., Liou, G.Y., Storz, P., Zhang, J.S., Regul, L., Nagarajan, S., Kühnemuth, B., Johnsen, S.A., et al. (2015). NFATc1 links EGFR signaling to induction of sox9 transcription and acinar-ductal transdifferentiation in the pancreas. Gastroenterology *148*, 1024-1034.e9.

Chen, N.M., Neesse, A., Dyck, M.L., Steuber, B., Koenig, A.O., Lubeseder-Martellato, C., Winter, T., Forster, T., Bohnenberger, H., Kitz, J., et al. (2017). Context-Dependent Epigenetic Regulation of Nuclear Factor of Activated T Cells 1 in Pancreatic Plasticity. Gastroenterology *152*, 1507-1520.e15.

Chevray, P.M., and Nathans, D. (1992). Protein interaction cloning in yeast: Identification of mammalian proteins that react with the leucine zipper of Jun. Proc. Natl. Acad. Sci. U. S. A. *89*, 5789–5793.

Chu, P.Y., Li, T.K., Ding, S.T., Lai, I.R., and Shen, T.L. (2010). EGF-induced Grb7 recruits and promotes ras activity essential for the tumorigenicity of Sk-Br3 breast cancer cells. J. Biol. Chem. *285*, 29279–29285.

Collisson, E.A., Sadanandam, A., Olson, P., Gibb, W.J., Truitt, M., Gu, S., Cooc, J., Weinkle, J., Kim, G.E., Jakkula, L., et al. (2011). Subtypes of pancreatic ductal adenocarcinoma and their differing responses to therapy. Nat. Med. *17*, 500–503.

Conceicao, V.N. Da, Sun, Y., Zboril, E.K., De la Chapa, J.J., and Singh, B.B. (2020). Loss of Ca2+ entry via Orai-TRPC1 induces ER stress, initiating immune activation in macrophages. J. Cell Sci. *133*, jcs237610.

Conroy, T., Desseigne, F., Ychou, M., Bouché, O., Guimbaud, R., Bécouarn, Z., Adenis, A., Raoul, J.-L., Gourgou-Bourgade, S., Fouchardière, C. de la, et al. (2011). FOLFIRINOX versus gemcitabine for metastatic pancreatic cancer. N. Engl. J. Med. *364*, 1817–1825.

Cowley, D.O., and Graves, B.J. (2000). Phosphorylation represses Ets-1 DNA binding by reinforcing autoinhibition. Genes Dev. *14*, 366–376.

Cruzalegui, F.H., and Means, A.R. (1993). Biochemical characterization of the multifunctional Ca2+/calmodulin- dependent protein kinase type IV expressed in

insect cells. J. Biol. Chem. *268*, 26171–26178.

Cullinan, S.B., Zhang, D., Hannink, M., Arvisais, E., Kaufman, R.J., and Diehl, J.A. (2003). Nrf2 Is a Direct PERK Substrate and Effector of PERK-Dependent Cell Survival. Mol. Cell. Biol. *23*, 7198–7209.

Cuneo, K.C., Morgan, M.A., Sahai, V., Schipper, M.J., Parsels, L.A., Parsels, J.D., Devasia, T., Al-Hawaray, M., Cho, C.S., Nathan, H., et al. (2019). Dose escalation trial of the WEE1 inhibitor adavosertib (AZD1775) in combination with gemcitabine and radiation for patients with locally advanced pancreatic cancer. J. Clin. Oncol. *37*, 2643–2650.

Cunningham, D., Chau, I., Stocken, D.D., Valle, J.W., Smith, D., Steward, W., Harper, P.G., Dunn, J., Tudur-Smith, C., West, J., et al. (2009). Phase III randomized comparison of gemcitabine versus gemcitabine plus capecitabine in patients with advanced pancreatic cancer. J. Clin. Oncol. *27*, 5513–5518.

Dantal, J., and Soulillou, J.P. (2005). Immunosuppressive drugs and the risk of cancer after organ transplantation. N. Engl. J. Med. *352*, 1371–1373.

Davis, F.J., Gupta, M., Camoretti-Mercado, B., Schwartz, R.J., and Gupta, M.P. (2003). Calcium/calmodulin-dependent protein kinase activates serum response factor transcription activity by its dissociation from histone deacetylase, HDAC4. Implications in cardiac muscle gene regulation during hypertrophy. J. Biol. Chem. *278*, 20047–20058.

Dejure, F.R., and Eilers, M. (2017). MYC and tumor metabolism: chicken and egg. EMBO J. *36*, 3409–3420.

den Dekker, E., Hoenderop, J.G.J., Nilius, B., and Bindels, R.J.M. (2003). The epithelial calcium channels, TRPV5 & TRPV6: From identification towards regulation. Cell Calcium *33*, 497–507.

Dellino, G.I., Schwartz, Y.B., Farkas, G., McCabe, D., Elgin, S.C.R., and Pirrotta, V. (2004). Polycomb silencing blocks transcription initiation. Mol. Cell *13*, 887–893.

Deng, N., Goh, L.K., Wang, H., Das, K., Tao, J., Tan, I.B., Zhang, S., Lee, M., Wu, J., Lim, K.H., et al. (2012). A comprehensive survey of genomic alterations in gastric cancer reveals systematic patterns of molecular exclusivity and co-occurrence among distinct therapeutic targets. Gut *61*, 673–684.

DepMap, B. (2020). DepMap 19Q4 Public.

Dewenter, M., Von Der Lieth, A., Katus, H.A., and Backs, J. (2017). Calcium signaling and transcriptional regulation in cardiomyocytes. Circ. Res. *121*, 1000–1020.

Distler, M., Aust, D., Weitz, J., Pilarsky, C., and Grützmann, R. (2014). Precursor lesions for sporadic pancreatic cancer: PanIN, IPMN, and MCN. Biomed Res. Int. *2014*.

Dixon, J.R., Selvaraj, S., Yue, F., Kim, A., Li, Y., Shen, Y., Hu, M., Liu, J.S., and Ren, B. (2012). Topological domains in mammalian genomes identified by analysis of chromatin interactions. Nature *485*, 376–380.

Dobin, A., Davis, C.A., Schlesinger, F., Drenkow, J., Zaleski, C., Jha, S., Batut, P., Chaisson, M., and Gingeras, T.R. (2013). STAR: Ultrafast universal RNA-seq aligner. Bioinformatics *29*, 15–21.

Dufey, E., Urra, H., and Hetz, C. (2015). ER proteostasis addiction in cancer biology: Novel concepts. Semin. Cancer Biol. *33*, 40–47.

Edgar, R., Domrachev, M., and Lash, A.E. (2002). Gene Expression Omnibus: NCBI gene expression and hybridization array data repository. Nucleic Acids Res. *30*, 207–210.

Eletto, D., Eletto, D., Dersh, D., Gidalevitz, T., and Argon, Y. (2014). Protein Disulfide Isomerase A6 Controls the Decay of IRE1α Signaling via Disulfide-Dependent Association. Mol. Cell *53*, 562–576.

Faeron, E.R., and Vogelstein, B. (1990). A genetic model for colorectal tumorigenesis. Cell *61*, 758–767.

Farrell, J.J., Elsaleh, H., Garcia, M., Lai, R., Ammar, A., Regine, W.F., Abrams, R., Benson, A.B., Macdonald, J., Cass, C.E., et al. (2009). Human Equilibrative Nucleoside Transporter 1 Levels Predict Response to Gemcitabine in Patients With Pancreatic Cancer. Gastroenterology *136*, 187–195.

Ferrandina, G., Mey, V., Nannizzi, S., Ricciardi, S., Petrillo, M., Ferlini, C., Danesi, R., Scambia, G., and Del Tacca, M. (2010). Expression of nucleoside transporters, deoxycitidine kinase, ribonucleotide reductase regulatory subunits, and gemcitabine catabolic enzymes in primary ovarian cancer. Cancer Chemother. Pharmacol. *65*,

679–686.

Ferrari, A., Vincent-Salomon, A., Pivot, X., Sertier, A.S., Thomas, E., Tonon, L., Boyault, S., Mulugeta, E., Treilleux, I., MacGrogan, G., et al. (2016). A whole-genome sequence and transcriptome perspective on HER2-positive breast cancers. Nat. Commun. *7*.

Feske, S. (2007). Calcium signalling in lymphocyte activation and disease. Nat. Rev. Immunol. *7*, 690–702.

Filippakopoulos, P., Picaud, S., Mangos, M., Keates, T., Lambert, J.P., Barsyte-Lovejoy, D., Felletar, I., Volkmer, R., Müller, S., Pawson, T., et al. (2012). Histone recognition and large-scale structural analysis of the human bromodomain family. Cell *149*, 214–231.

Flück, M., Booth, F.W., and Waxham, M.N. (2000). Skeletal muscle CaMKII enriches in nuclei and phosphorylates myogenic factor SRF at multiple sites. Biochem. Biophys. Res. Commun. *270*, 488–494.

Galehdar, Z., Swan, P., Fuerth, B., Callaghan, S.M., Park, D.S., and Cregan, S.P. (2010). Neuronal apoptosis induced by endoplasmic reticulum stress is regulated by ATF4-CHOP-mediated induction of the Bcl-2 homology 3-only member PUMA. J. Neurosci. *30*, 16938–16948.

Gao, J., Aksoy, B.A., Dogrusoz, U., Dresdner, G., Gross, B., Sumer, S.O., Sun, Y., Jacobsen, A., Sinha, R., Larsson, E., et al. (2013). Integrative analysis of complex cancer genomics and clinical profiles using the cBioPortal. Sci. Signal. *6*.

García-Manteiga, J., Molina-Arcas, M., Casado, F.J., Mazo, A., and Pastor-Anglada, M. (2003). Nucleoside Transporter Profiles in Human Pancreatic Cancer Cells: Role of hCNT1 in 2′,2′-Difluorodeoxycytidine-Induced Cytotoxicity. Clin. Cancer Res. *9*, 5000–5008.

Gebhardt, J.C.M., Suter, D.M., Roy, R., Zhao, Z.W., Chapman, A.R., Basu, S., Maniatis, T., and Xie, X.S. (2013). Single-molecule imaging of transcription factor binding to DNA in live mammalian cells. Nat. Methods *10*, 421–426.

Gerasimenko, J. V., Gryshchenko, O., Ferdek, P.E., Stapleton, E., Hébert, T.O.G., Bychkova, S., Peng, S., Begg, M., Gerasimenko, O. V., and Petersen, O.H. (2013). Ca2+ release-activated Ca2+ channel blockade as a potential tool in antipancreatitis

therapy. Proc. Natl. Acad. Sci. U. S. A. *110*, 13186–13191.

Ghandi, M., Huang, F.W., Jané-Valbuena, J., Kryukov, G. V., Lo, C.C., McDonald, E.R., Barretina, J., Gelfand, E.T., Bielski, C.M., Li, H., et al. (2019). Next-generation characterization of the Cancer Cell Line Encyclopedia. Nature *569*, 503–508.

Gilon, P., Roe, M.W., Evans-Molina, C., Kono, T., Tong, X., Taleb, S., Bone, R.N., Iida, H., Lee, C.C., and Sohn, P. (2018). Impaired store-operated calcium entry and STIM1 loss lead to reduced insulin secretion and increased endoplasmic reticulum stress in the diabetic B-cell. Diabetes *67*, 2293–2304.

Giorgi, C., Marchi, S., and Pinton, P. (2018). The machineries, regulation and cellular functions of mitochondrial calcium. Nat. Rev. Mol. Cell Biol. *19*, 713–730.

Giovannetti, E., Del Tacca, M., Mey, V., Funel, N., Nannizzi, S., Ricci, S., Orlandini, C., Boggi, U., Campani, D., Del Chiaro, M., et al. (2006). Transcription analysis of human equilibrative nucleoside transporter-1 predicts survival in pancreas cancer patients treated with gemcitabine. Cancer Res. *66*, 3928–3935.

Giraldo, A.M.V., Medus, M.L., Lebrero, M.G., Pagano, R.S., Labriola, C.A., Landolfo, L., Delfino, J.M., Parodi, A.J., and Caramelo, J.J. (2010). The structure of calreticulin C-terminal domain is modulated by physiological variations of calcium concentration. J. Biol. Chem. *285*, 4544–4553.

Gray, C.B.B., Suetomi, T., Xiang, S., Blackwood, E.A., Glembotski, C.C., Miyamoto, S., Westenbrink, B.D., and Brown, J.H. (2017). CaMKIIδ subtypes differentially regulate infarct formation following ex vivo myocardial ischemia/reperfusion through NF-κB and TNF-α. J. Mol. Cell. Cardiol. *103*, 48–55.

Grynkiewicz, G., Poenie, M., and Tsien, R.Y. (1985). A new generation of Ca2+ indicators with greatly improved fluorescence properties. J. Biol. Chem. *260*, 3440–3450.

Guan, B.J., van Hoef, V., Jobava, R., Elroy-Stein, O., Valasek, L.S., Cargnello, M., Gao, X.H., Krokowski, D., Merrick, W.C., Kimball, S.R., et al. (2017). A Unique ISR Program Determines Cellular Responses to Chronic Stress. Mol. Cell *68*, 885-900.e6.

Gukovskaya, A.S., Gorelick, F.S., Groblewski, G.E., Mareninova, O.A., Lugea, A., Antonucci, L., Waldron, R.T., Habtezion, A., Karin, M., Pandol, S.J., et al. (2019).

Recent Insights into the Pathogenic Mechanism of Pancreatitis: Role of Acinar Cell Organelle Disorders. Pancreas *48*, 459–470.

Gutiérrez, T., and Simmen, T. (2018). Endoplasmic reticulum chaperones tweak the mitochondrial calcium rheostat to control metabolism and cell death. Cell Calcium *70*, 64–75.

Habtezion, A. (2015). Inflammation in acute and chronic pancreatitis. Curr. Opin. Gastroenterol. *31*, 395–399.

Hai, T., and Curran, T. (1991). Cross-family dimerization of transcription factors Fos/Jun and ATF/CREB alters DNA binding specificity. Proc. Natl. Acad. Sci. U. S. A. *88*, 3720–3724.

Hamada, C., Okusaka, T., Ikari, T., Isayama, H., Furuse, J., Ishii, H., Nakai, Y., Imai, S., and Okamura, S. (2017). Efficacy and safety of gemcitabine plus S-1 in pancreatic cancer: A pooled analysis of individual patient data. Br. J. Cancer *116*, 1544–1550.

Hamanaka, R.B., Bobrovnikova-Marjon, E., Ji, X., Liebhaber, S.A., and Diehl, J.A. (2009). PERK-dependent regulation of IAP translation during ER stress. Oncogene *28*, 910–920.

Hamdan, F.H., and Johnsen, S.A. (2018). DeltaNp63-dependent super enhancers define molecular identity in pancreatic cancer by an interconnected transcription factor network. Proc. Natl. Acad. Sci. 201812915.

Han, A.P., Yu, C., Lu, L., Fujiwara, Y., Browne, C., Chin, G., Fleming, M., Leboulch, P., Orkin, S.H., and Chen, J.J. (2001). Heme-regulated eIF2α kinase (HRI) is required for translational regulation and survival of erythroid precursors in iron deficiency. EMBO J. *20*, 6909–6918.

Hanlon, C.D., and Andrew, D.J. (2015). Outside-in signaling - A brief review of GPCR signaling with a focus on the Drosophila GPCR family. J. Cell Sci. *128*, 3533–3542.

Hannigan, G., Troussard, A.A., and Dedhar, S. (2005). Integrin-linked kinase: A cancer therapeutic target unique among its ILK. Nat. Rev. Cancer *5*, 51–63.

Hansen, K.H., Bracken, A.P., Pasini, D., Dietrich, N., Gehani, S.S., Monrad, A., Rappsilber, J., Lerdrup, M., and Helin, K. (2008). A model for transmission of the

H3K27me3 epigenetic mark. Nat. Cell Biol. *10*, 1291–1300.

Harding, H.P., Novoa, I., Zhang, Y., Zeng, H., Wek, R., Schapira, M., and Ron, D. (2000). Regulated translation initiation controls stress-induced gene expression in mammalian cells. Mol. Cell *6*, 1099–1108.

Harding, H.P., Zeng, H., Zhang, Y., Jungries, R., Chung, P., Plesken, H., Sabatini, D.D., and Ron, D. (2001). Diabetes mellitus and exocrine pancreatic dysfunction in Perk-/- mice reveals a role for translational control in secretory cell survival. Mol. Cell *7*, 1153–1163.

Harding, H.P., Zhang, Y., Scheuner, D., Chen, J.J., Kaufman, R.J., and Ron, D. (2009). Ppp1r15 gene knockout reveals an essential role for translation initiation factor 2 alpha (eIF2α) dephosphorylation in mammalian development. Proc. Natl. Acad. Sci. U. S. A. *106*, 1832–1837.

Hatzis, P., Al-Madhoon, A.S., Jüllig, M., Petrakis, T.G., Eriksson, S., and Talianidis, I. (1998). The intracellular localization of deoxycytidine kinase. J. Biol. Chem. *273*, 30239–30243.

Hayes, J.D., and Dinkova-Kostova, A.T. (2014). The Nrf2 regulatory network provides an interface between redox and intermediary metabolism. Trends Biochem. Sci. *39*, 199–218.

Haze, K., Yoshida, H., Yanagi, H., Yura, T., and Mori, K. (1999). Mammalian transcription factor ATF6 is synthesized as a transmembrane protein and activated by proteolysis in response to endoplasmic reticulum stress. Mol. Biol. Cell *10*, 3787–3799.

Hegyi, E., and Sahin-Tóth, M. (2019). Human CPA1 mutation causes digestive enzyme misfolding and chronic pancreatitis in mice. Gut *68*, 301–312.

Heinemann, V., Hertel, L.W., Grindey, G.B., and Plunkett, W. (1988). Comparison of the Cellular Pharmacoldnetics and Toxicity of 2',2'-Difluorodeoxycytidine and 1-β-D-Arabinofuranosylcytosine. Cancer Res. *48*, 4024–4031.

Heinemann, V., Xu, Y.Z., Chubb, S., Sen, A., Hertel, L.W., Grindey, G.B., and Plunkett, W. (1990). Inhibition of ribonucleotide reduction in CCRF-CEM cells by 2',2'-difluorodeoxycytidine. Mol. Pharmacol. *38*, 567–572.

Heinemann, V., Xu, Y.Z., Chubb, S., Sen, A., Plunkett, W., Hertel, L.W., Grindey,

G.B., and Heinemann, V. (1992). Cellular Elimination of 2′,2′-Difluorodeoxycytidine 5′-Triphosphate: A Mechanism of Self-Potentiation. Cancer Res. *52*, 533–539.

Heinz, S., Benner, C., Spann, N., Bertolino, E., Lin, Y.C., Laslo, P., Cheng, J.X., Murre, C., Singh, H., and Glass, C.K. (2010). Simple Combinations of Lineage-Determining Transcription Factors Prime cis-Regulatory Elements Required for Macrophage and B Cell Identities. Mol. Cell *38*, 576–589.

Hendrikx, S., Coso, S., Prat-Luri, B., Wetterwald, L., Sabine, A., Franco, C.A., Nassiri, S., Zangger, N., Gerhardt, H., Delorenzi, M., et al. (2019). Endothelial Calcineurin Signaling Restrains Metastatic Outgrowth by Regulating Bmp2. Cell Rep. *26*, 1227-1241.e6.

Herrmann, R., Bodoky, G., Ruhstaller, T., Glimelius, B., Bajetta, E., Schüller, J., Saletti, P., Bauer, J., Figer, A., Pestalozzi, B., et al. (2007). Gemcitabine plus capecitabine compared with gemcitabine alone in advanced pancreatic cancer: A randomized, multicenter, phase III trial of the Swiss Group for Clinical Cancer Research and the Central European Cooperative Oncology Group. J. Clin. Oncol. *25*, 2212–2217.

Hessmann, E., Patzak, M.S., Klein, L., Chen, N., Kari, V., Ramu, I., Bapiro, T.E., Frese, K.K., Gopinathan, A., Richards, F.M., et al. (2018). Fibroblast drug scavenging increases intratumoural gemcitabine accumulation in murine pancreas cancer. Gut *67*, 497–507.

Hetz, C. (2012). The unfolded protein response: Controlling cell fate decisions under ER stress and beyond. Nat. Rev. Mol. Cell Biol. *13*, 89–102.

Hezel, A.F., Kimmelman, A.C., Stanger, B.Z., N., B., and DePinho, R.A. (2006). Genetics and biology of pancreatic ductal adenocarcinoma. Genes Dev. *20*, 1218–1249.

Hidalgo, M., Plaza, C., Musteanu, M., Illei, P., Brachmann, C.B., Heise, C., Pierce, D., Lopez-Casas, P.P., Menendez, C., Tabernero, J., et al. (2015). SPARC expression did not predict efficacy of nab-paclitaxel plus gemcitabine or gemcitabine alone for metastatic pancreatic cancer in an exploratory analysis of the phase III MPACT trial. Clin. Cancer Res. *21*, 4811–4818.

Higa, A., Taouji, S., Lhomond, S., Jensen, D., Fernandez-Zapico, M.E., Simpson, J.C., Pasquet, J.-M., Schekman, R., and Chevet, E. (2014). Endoplasmic Reticulum

Stress-Activated Transcription Factor ATF6 Requires the Disulfide Isomerase PDIA5 To Modulate Chemoresistance. Mol. Cell. Biol. *34*, 1839–1849.

Higo, T., Hamada, K., Hisatsune, C., Nukina, N., Hashikawa, T., Hattori, M., Nakamura, T., and Mikoshiba, K. (2010). Mechanism of ER Stress-Induced Brain Damage by IP3 Receptor. Neuron *68*, 865–878.

Hillary, R.F., and Fitzgerald, U. (2018). A lifetime of stress: ATF6 in development and homeostasis. J. Biomed. Sci. *25*, 1–10.

Holmberg, C.I., Hietakangas, V., Mikhailov, A., Rantanen, J.O., Kallio, M., Meinander, A., Hellman, J., Morrice, N., MacKintosh, C., Morimoto, R.I., et al. (2001). Phosphorylation of serine 230 promotes inducible transcriptional activity of heat shock factor 1. EMBO J. *20*, 3800–3810.

Holt, M.T., David, Y., Pollock, S., Tang, Z., Jeon, J., Kim, J., Roeder, R.G., and Muir, T.W. (2015). Identification of a functional hotspot on ubiquitin required for stimulation of methyltransferase activity on chromatin. Proc. Natl. Acad. Sci. U. S. A. *112*, 10365–10370.

Hoover, P.J., and Lewis, R.S. (2011). Stoichiometric requirements for trapping and gating of Ca 2+ release-activated Ca 2+ (CRAC) channels by stromal interaction molecule 1 (STIM1). Proc. Natl. Acad. Sci. U. S. A. *108*, 13299–13304.

Hruban, R.H., Goggins, M., Parsons, J., and Kern, S.E. (2000). Progression model for pancreatic cancer. Clin. Cancer Res. *6*, 2969–2972.

Hu, J., Dang, N., Menu, E., De Bryune, E., Xu, D., Van Camp, B., Van Valckenborgh, E., and Vanderkerken, K. (2012). Activation of ATF4 mediates unwanted Mcl-1 accumulation by proteasome inhibition. Blood *119*, 826–837.

Hu, P., Han, Z., Couvillon, A.D., and Exton, J.H. (2004). Critical role of endogenous Akt/IAPs and MEK1/ERK pathways in counteracting endoplasmic reticulum stress-induced cell death. J. Biol. Chem. *279*, 49420–49429.

Huang, P., Chubb, S., Hertel, L.W., Grindey, G.B., and Plunkett, W. (1991). Action of 2',2'-Difluorodeoxycytidine on DNA Synthesis. Cancer Res. *51*, 6110–6117.

Hunsucker, S.A., Spychala, J., and Mitchell, B.S. (2001). Human cytosolic 5′-nucleotidase I: Characterization and role in nucleoside analog resistance. J. Biol. Chem. *276*, 10498–10504.

Hunsucker, S.A., Mitchell, B.S., and Spychala, J. (2005). The 5′-nucleotidases as regulators of nucleotide and drug metabolism. Pharmacol. Ther. *107*, 1–30.

Iorio, F., Knijnenburg, T.A., Vis, D.J., Bignell, G.R., Menden, M.P., Schubert, M., Aben, N., Gonçalves, E., Barthorpe, S., Lightfoot, H., et al. (2016). A Landscape of Pharmacogenomic Interactions in Cancer. Cell *166*, 740–754.

Ivessa, N.E., De Lemos-Chiarandini, C., Gravotta, D., Sabatini, D.D., and Kreibich, G. (1995). The brefeldin A-induced retrograde transport from the Golgi apparatus to the endoplasmic reticulum depends on calcium sequestered to intracellular stores. J. Biol. Chem. *270*, 25960–25967.

Jacobetz, M.A., Chan, D.S., Neesse, A., Bapiro, T.E., Cook, N., Frese, K.K., Feig, C., Nakagawa, T., Caldwell, M.E., Zecchini, H.I., et al. (2013). Hyaluronan impairs vascular function and drug delivery in a mouse model of pancreatic cancer. Gut *62*, 112–120.

Janes, P.W., Lackmann, M., Church, W.B., Sanderson, G.M., Sutherland, R.L., and Daly, R.J. (1997). Structural determinants of the interaction between the erbB2 receptor and the Src homology 2 domain of Grb7. J. Biol. Chem. *272*, 8490–8497.

Jauliac, S., López-Rodriguez, C., Shaw, L.M., Brown, L.F., Rao, A., and Toker, A. (2002). The role of NFAT transcription factors in integrin-mediated carcinoma invasion. Nat. Cell Biol. *4*, 540–544.

Jha, A., Ahuja, M., Maléth, J., Moreno Claudia, C., Yuan Joseph, J., Kim, M.S., and Muallem, S. (2013). The STIM1 CTID domain determines access of SARAF to SOAR to regulate Orai1 channel function. J. Cell Biol. *202*, 71–78.

Jing, J., Wei, M., Tan, P., Zhang, S.L., Ma, G., Senes, A., Wang, Y., He, L., Zhou, W., Li, M., et al. (2015). Inside-out Ca2+ signalling prompted by STIM1 conformational switch. Nat. Commun. *6*.

Jolma, A., Yan, J., Whitington, T., Toivonen, J., Nitta, K.R., Rastas, P., Morgunova, E., Enge, M., Taipale, M., Wei, G., et al. (2013). DNA-binding specificities of human transcription factors. Cell *152*, 327–339.

Jolma, A., Yin, Y., Nitta, K.R., Dave, K., Popov, A., Taipale, M., Enge, M., Kivioja, T., Morgunova, E., and Taipale, J. (2015). DNA-dependent formation of transcription factor pairs alters their binding specificity. Nature *527*, 384–388.

Jousse, C., Deval, C., Maurin, A.C., Parry, L., Chérasse, Y., Chaveroux, C., Lefloch, R., Lenormand, P., Bruhat, A., and Fafournoux, P. (2007). TRB3 inhibits the transcriptional activation of stress-regulated genes by a negative feedback on the ATF4 pathway. J. Biol. Chem. *282*, 15851–15861.

Kagey, M.H., Newman, J.J., Bilodeau, S., Zhan, Y., Orlando, D.A., Van Berkum, N.L., Ebmeier, C.C., Goossens, J., Rahl, P.B., Levine, S.S., et al. (2010). Mediator and cohesin connect gene expression and chromatin architecture. Nature *467*, 430–435.

Kar, P., and Parekh, A.B. (2015). Distinct Spatial Ca2+ Signatures Selectively Activate Different NFAT Transcription Factor Isoforms. Mol. Cell *58*, 232–243.

Kar, P., Nelson, C., and Parekh, A.B. (2011). Selective activation of the transcription factor NFAT1 by calcium microdomains near Ca2+ release-activated Ca2+ (CRAC) channels. J. Biol. Chem. *286*, 14795–14803.

Kashiwase, K., Higuchi, Y., Hirotani, S., Yamaguchi, O., Hikoso, S., Takeda, T., Watanabe, T., Taniike, M., Nakai, A., Tsujimoto, I., et al. (2005). CaMKII activates ASK1 and NF-κB to induce cardiomyocyte hypertrophy. Biochem. Biophys. Res. Commun. *327*, 136–142.

Katz, E., Dubois-Marshall, S., Sims, A.H., Faratian, D., Li, J., Smith, E.S., Quinn, J.A., Edward, M., Meehan, R.R., Evans, E.E., et al. (2010). A gene on the HER2 amplicon, C35, is an oncogene in breast cancer whose actions are prevented by inhibition of Syk. Br. J. Cancer *103*, 401–410.

Kaufman, D.B., Shapiro, R., Lucey, M.R., Cherikh, W.S., Bustami, R.T., and Dyke, D.B. (2004). Immunosuppression: Practice and trends. Am. J. Transplant. *4*, 38–53.

Kawahara, T., Kashiwagi, E., Ide, H., Li, Y., Zheng, Y., Miyamoto, Y., Netto, G.J., Ishiguro, H., and Miyamoto, H. (2015). Cyclosporine A and tacrolimus inhibit bladder cancer growth through down-regulation of NFATc1. Oncotarget *6*, 1582–1593.

Kilberg, M.S., Shan, J., and Su, N. (2009). ATF4-dependent transcription mediates signaling of amino acid limitation. Trends Endocrinol. Metab. *20*, 436–443.

Kirkegård, J., Cronin-Fenton, D., Heide-Jørgensen, U., and Mortensen, F.V. (2018). Acute Pancreatitis and Pancreatic Cancer Risk: A Nationwide Matched-Cohort Study in Denmark. Gastroenterology *154*, 1729–1736.

Kloesch, B., Hruschka, N., Ionasz, V., Oellinger, R., Mueller, S., de Villareal, J.M., Dienes, H.-P., Schindl, M., Gruber, E., Stift, J., et al. (2020). A GATA6-centered gene regulatory network involving HNFs and ΔNp63 controls plasticity and immune escape in pancreatic cancer. 1–38.

Koay, E.J., Baio, F.E., Ondari, A., Truty, M.J., Cristini, V., Thomas, R.M., Chen, R., Chatterjee, D., Kang, Y., Zhang, J., et al. (2014a). Intra-tumoral heterogeneity of gemcitabine delivery and mass transport in human pancreatic cancer. Phys. Biol. *11*.

Koay, E.J., Truty, M.J., Cristini, V., Thomas, R.M., Chen, R., Chatterjee, D., Kang, Y., Bhosale, P.R., Tamm, E.P., Crane, C.H., et al. (2014b). Transport properties of pancreatic cancer describe gemcitabine delivery and response. J. Clin. Invest. *124*, 1525–1536.

Koh, S.B., Wallez, Y., Dunlop, C.R., De Quiros Fernandez, S.B., Bapiro, T.E., Richards, F.M., and Jodrell, D.I. (2018). Mechanistic distinctions between CHK1 and WEE1 inhibition guide the scheduling of triple therapy with gemcitabine. Cancer Res. *78*, 3054–3066.

Kohnken, R., Kodigepalli, K.M., and Wu, L. (2015). Regulation of deoxynucleotide metabolism in cancer: Novel mechanisms and therapeutic implications. Mol. Cancer *14*, 1–11.

Kojima, K., Vickers, S.M., Adsay, N.V., Jhala, N.C., Kim, H.G., Schoeb, T.R., Grizzle, W.E., and Klug, C.A. (2007). Inactivation of Smad4 accelerates KrasG12D-mediated pancreatic neoplasia. Cancer Res. *67*, 8121–8130.

Kondratska, K., Kondratskyi, A., Yassine, M., Lemonnier, L., Lepage, G., Morabito, A., Skryma, R., and Prevarskaya, N. (2014). Orai1 and STIM1 mediate SOCE and contribute to apoptotic resistance of pancreatic adenocarcinoma. Biochim. Biophys. Acta - Mol. Cell Res. *1843*, 2263–2269.

König, A., Fernandez-Zapico, M.E., and Ellenrieder, V. (2010a). Primers on molecular pathways - The NFAT transcription pathway in pancreatic cancer. Pancreatology *10*, 416–422.

König, A., Linhart, T., Schlengemann, K., Reutlinger, K., Wegele, J., Adler, G., Singh, G., Hofmann, L., Kunsch, S., Büch, T., et al. (2010b). NFAT-Induced Histone Acetylation Relay Switch Promotes c-Myc-Dependent Growth in Pancreatic Cancer

Cells. Gastroenterology *138*, 1189-1199.e2.

König, A., Linhart, T., Schlengemann, K., Reutlinger, K., Wegele, J., Adler, G., Singh, G., Hofmann, L., Kunsch, S., Büch, T., et al. (2010c). NFAT-Induced Histone Acetylation Relay Switch Promotes c-Myc-Dependent Growth in Pancreatic Cancer Cells. Gastroenterology *138*, 1–18.

Kopp, M.C., Larburu, N., Durairaj, V., Adams, C.J., and Ali, M.M.U. (2019). UPR proteins IRE1 and PERK switch BiP from chaperone to ER stress sensor. Nat. Struct. Mol. Biol. *26*, 1053–1062.

Korbel, J.O., and Campbell, P.J. (2013). Criteria for inference of chromothripsis in cancer genomes. Cell *152*, 1226–1236.

Koritzinsky, M., Magagnin, M.G., Van Den Beucken, T., Seigneuric, R., Savelkouls, K., Dostie, J., Pyronnet, S., Kaufman, R.J., Weppler, S.A., Voncken, J.W., et al. (2006). Gene expression during acute and prolonged hypoxia is regulated by distinct mechanisms of translational control. EMBO J. *25*, 1114–1125.

Kpetemey, M., Dasgupta, S., Rajendiran, S., Das, S., Gibbs, L.D., Shetty, P., Gryczynski, Z., and Vishwanatha, J.K. (2015). MIEN1, a novel interactor of Annexin A2, promotes tumor cell migration by enhancing AnxA2 cell surface expression. Mol. Cancer *14*, 1–13.

Kreusser, M.M., Lehmann, L.H., Keranov, S., Hoting, M.O., Oehl, U., Kohlhaas, M., Reil, J.C., Neumann, K., Schneider, M.D., Hill, J.A., et al. (2014). Cardiac CaM kinase II genes δ and γ contribute to adverse remodeling but redundantly inhibit calcineurin-induced myocardial hypertrophy. Circulation *130*, 1262–1273.

Kroemer, G., Mariño, G., and Levine, B. (2010). Autophagy and the Integrated Stress Response. Mol. Cell *40*, 280–293.

Kroep, J.R., Loves, W.J.P., Van Der Wilt, C.L., Alvarez, E., Talianidis, I., Boven, E., Braakhuis, B.J.M., Van Groeningen, C.J., Pinedo, H.M., and Peters, G.J. (2002). Pretreatment deoxycytidine kinase levels predict in vivo gemcitabine sensitivity. Mol. Cancer Ther. *1*, 371–376.

Kubisch, C.H., Sans, M.D., Arumugam, T., Ernst, S.A., Williams, J.A., and Logsdon, C.D. (2006). Early activation of endoplasmic reticulum stress is associated with arginine-induced acute pancreatitis. Am. J. Physiol. - Gastrointest. Liver Physiol.

291, 238–245.

Kuleshov, M. V., Jones, M.R., Rouillard, A.D., Fernandez, N.F., Duan, Q., Wang, Z., Koplev, S., Jenkins, S.L., Jagodnik, K.M., Lachmann, A., et al. (2016). Enrichr: a comprehensive gene set enrichment analysis web server 2016 update. Nucleic Acids Res. *44*, W90–W97.

Lachner, M., O'Carroll, D., Rea, S., Mechtler, K., and Jenuwein, T. (2001). Methylation of histone H3 lysine 9 creates a binding site for HP1 proteins. Nature *410*, 116–120.

Ladiges, W.C., Knoblaugh, S.E., Morton, J.F., Korth, M.J., Sopher, B.L., Baskin, C.R., MacAuley, A., Goodman, A.G., LeBoeuf, R.C., and Katze, M.G. (2005). Pancreatic β-cell failure and diabetes in mice with a deletion mutation of the endoplasmic reticulum molecular chaperone gene P58IPK. Diabetes *54*, 1074–1081.

Langmead, B., and Salzberg, S.L. (2012). Fast gapped-read alignment with Bowtie 2. Nat. Methods *9*, 357–359.

Laugesen, A., Westergaard Hojfeldt, J., and Helin, K. (2016). Role of the Polycomb Repressive Complex 2 (PRC2) in Transcriptional Regulation and Cancer. Cold Spring Harb. Perspect. Med. *6*, 1–20.

Lee, A.-H., Iwakoshi, N.N., and Glimcher, L.H. (2003). XBP-1 Regulates a Subset of Endoplasmic Reticulum Resident Chaperone Genes in the Unfolded Protein Response. Mol. Cell. Biol. *23*, 7448–7459.

Lemmon, M.A., and Schlessinger, J. (2010). Cell signaling by receptor tyrosine kinases. Cell *141*, 1117–1134.

Li, Q.L., Wang, D.Y., Ju, L.G., Yao, J., Gao, C., Lei, P.J., Li, L.Y., Zhao, X.L., and Wu, M. (2019). The hyper-activation of transcriptional enhancers in breast cancer. Clin. Epigenetics *11*, 1–17.

Li, Y., Guo, B., Xie, Q., Ye, D., Zhang, D., Zhu, Y., Chen, H., and Zhu, B. (2015). STIM1 Mediates Hypoxia-Driven Hepatocarcinogenesis via Interaction with HIF-1. Cell Rep. *12*, 388–395.

Li, Y., Roberts, N.D., Wala, J.A., Shapira, O., Schumacher, S.E., Kumar, K., Khurana, E., Waszak, S., Korbel, J.O., Haber, J.E., et al. (2020). Patterns of somatic

structural variation in human cancer genomes. Nature *578*, 112–121.

Li, Z., Liu, L., Deng, Y., Ji, W., Du, W., Xu, P., Chen, L., and Xu, T. (2011). Graded activation of CRAC channel by binding of different numbers of STIM1 to Orai1 subunits. Cell Res. *21*, 305–315.

Lièvremont, J.P., Rizzuto, R., Hendershot, L., and Meldolesi, J. (1997). BiP, a major chaperone protein of the endoplasmic reticulum lumen, plays a direct and important role in the storage of the rapidly exchanging pool of Ca2+. J. Biol. Chem. *272*, 30873–30879.

Liew, C.W., Bochenski, J., Kawamori, D., Hu, J., Leech, C.A., Wanic, K., Malecki, M., Warram, J.H., Qi, L., Krolewski, A.S., et al. (2010). The pseudokinase tribbles homolog 3 interacts with ATF4 to negatively regulate insulin exocytosis in human and mouse β cells. J. Clin. Invest. *120*, 2876–2888.

Ligorio, M., Sil, S., Malagon-Lopez, J., Nieman, L.T., Misale, S., Di Pilato, M., Ebright, R.Y., Karabacak, M.N., Kulkarni, A.S., Liu, A., et al. (2019). Stromal Microenvironment Shapes the Intratumoral Architecture of Pancreatic Cancer. Cell *178*, 160-175.e27.

Ling, H., Gray, C.B.B., Zambon, A.C., Grimm, M., Gu, Y., Dalton, N., Purcell, N.H., Peterson, K., and Brown, J.H. (2013). Ca2+/calmodulin-dependent protein kinase ii δ mediates myocardial ischemia/reperfusion injury through nuclear factor-κb. Circ. Res. *112*, 935–944.

Lipp, P., and Reither, G. (2011). Protein kinase C: The “Masters” of calcium and lipid. Cold Spring Harb. Perspect. Biol. *3*, 1–17.

Liu, C.Y., Xu, Z., and Kaufman, R.J. (2003). Structure and intermolecular interactions of the luminal dimerization domain of human IRE1α. J. Biol. Chem. *278*, 17680–17687.

Logsdon, C.D., and Ji, B. (2013). The role of protein synthesis and digestive enzymes in acinar cell injury. Nat. Rev. Gastroenterol. Hepatol. *10*, 362–370.

Lomax, R.B., Camello, C., Van Coppenolle, F., Petersen, O.H., and Tepikin, A. V. (2002). Basal and physiological Ca2+ leak from the endoplasmic reticulum of pancreatic acinar cells. Second messenger-activated channels and translocons. J. Biol. Chem. *277*, 26479–26485.

Lopez, E., Jardin, I., Berna-Erro, A., Bermejo, N., Salido, G.M., Sage, S.O., Rosado, J.A., and Redondo, P.C. (2012). STIM1 tyrosine-phosphorylation is required for STIM1-Orai1 association in human platelets. Cell. Signal. *24*, 1315–1322.

Love, M.I., Huber, W., and Anders, S. (2014). Moderated estimation of fold change and dispersion for RNA-seq data with DESeq2. Genome Biol. *15*, 1–21.

Lovén, J., Hoke, H.A., Lin, C.Y., Lau, A., Orlando, D.A., Vakoc, C.R., Bradner, J.E., Lee, T.I., and Young, R.A. (2013). Selective inhibition of tumor oncogenes by disruption of super-enhancers. Cell *153*, 320–334.

Lu, P.D., Harding, H.P., and Ron, D. (2004). Translation reinitiation at alternative open reading frames regulates gene expression in an integrated stress response. J. Cell Biol. *167*, 27–33.

Lugea, A., Tischler, D., Nguyen, J., Gong, J., Gukovsky, I., Samuel, W., Gorelick, F.S., and Pandol, S.J. (2012). Adaptive Unfolded Protein Response Attenuates Alcohol- induced Pancreatic Damage. Gastroenterology *140*, 987–997.

Luik, R.M., Wang, B., Prakriya, M., Wu, M.M., and Lewis, R.S. (2008). Oligomerization of STIM1 couples ER calcium depletion to CRAC channel activation. Nature *454*, 538–542.

Lupiáñez, D.G., Kraft, K., Heinrich, V., Krawitz, P., Brancati, F., Klopocki, E., Horn, D., Kayserili, H., Opitz, J.M., Laxova, R., et al. (2015). Disruptions of topological chromatin domains cause pathogenic rewiring of gene-enhancer interactions. Cell *161*, 1012–1025.

Ma, Y., and Hendershot, L.M. (2003). Delineation of a negative feedback regulatory loop that controls protein translation during endoplasmic reticulum stress. J. Biol. Chem. *278*, 34864–34873.

Ma, Y., and Hendershot, L.M. (2004). The role of the unfolded protein response in tumour development: Friend or foe? Nat. Rev. Cancer *4*, 966–977.

Ma, H., Groth, R.D., Cohen, S.M., Emery, J.F., Li, B., Hoedt, E., Zhang, G., Neubert, T.A., and Tsien, R.W. (2014). γcaMKII shuttles Ca2+/CaM to the nucleus to trigger CREB phosphorylation and gene expression. Cell *159*, 281–294.

Maas, N.L., and Diehl, J.A. (2015). Molecular pathways: The perks and pitfalls of targeting the unfolded protein response in cancer. Clin. Cancer Res. *21*, 675–679.

MacDonnell, S.M., Weisser-Thomas, J., Kubo, H., Hanscome, M., Liu, Q., Jaleel, N., Berretta, R., Chen, X., Brown, J.H., Sabri, A.K., et al. (2009). CaMKII negatively regulates calcineurin-NFAT signaling in cardiac myocytes. Circ. Res. *105*, 316–325.

Macian, F. (2005). NFAT proteins: Key regulators of T-cell development and function. Nat. Rev. Immunol. *5*, 472–484.

Mackey, J.R., Baldwin, S.A., Young, J.D., and Cass, C.E. (1998a). Nucleoside transport and its significance for anticancer drug resistance. Drug Resist. Updat. *1*, 310–324.

Mackey, J.R., Mani, R.S., Selner, M., Mowles, D., Young, J.D., Belt, J.A., Crawford, C.R., and Cass, C.E. (1998b). Functional nucleoside transporters are required for gemcitabine influx and manifestation of toxicity in cancer cell lines. Cancer Res. *58*, 4349–4357.

Mackey, J.R., Yao, S.Y.M., Smith, K.M., Karpinski, E., Baldwin, S.A., Cass, C.E., and Young, J.D. (1999). Gemcitabine transport in Xenopus oocytes expressing recombinant plasma membrane mammalian nucleoside transporters. J. Natl. Cancer Inst. *91*, 1876–1881.

Di Magliano, M.P., and Logsdon, C.D. (2013). Roles for KRAS in pancreatic tumor development and progression. Gastroenterology *144*, 1220–1229.

Majmundar, A.J., Wong, W.J., and Simon, M.C. (2010). Hypoxia-Inducible Factors and the Response to Hypoxic Stress. Mol. Cell *40*, 294–309.

Makohon-Moore, A.P., Zhang, M., Reiter, J.G., Bozic, I., Allen, B., Kundu, D., Chatterjee, K., Wong, F., Jiao, Y., Kohutek, Z.A., et al. (2017). Limited heterogeneity of known driver gene mutations among the metastases of individual patients with pancreatic cancer. Nat. Genet. *49*, 358–366.

Malka, D., Hammel, P., Maire, F., Rufat, P., Madeira, I., Pessione, F., Lévy, P., and Rusyniewski, P. (2002). Risk of pancreatic ductal adenocarcinoma in chronic pancreatitis. Gut *51*, 765–766.

Mancini, M., and Toker, A. (2009). NFAT proteins: Emerging roles in cancer progression. Nat. Rev. Cancer *9*, 810–820.

Marciniak, S.J., Yun, C.Y., Oyadomari, S., Novoa, I., Zhang, Y., Jungreis, R., Nagata, K., Harding, H.P., and Ron, D. (2004). CHOP induces death by promoting

protein synthesis and oxidation in the stressed endoplasmic reticulum. Genes Dev. *18*, 3066–3077.

Maréchal, R., MacKey, J.R., Lai, R., Demetter, P., Peeters, M., Polus, M., Cass, C.E., Salmon, I., Devière, J., and Van Laethem, J.L. (2010). Deoxycitidine kinase is associated with prolonged survival after adjuvant gemcitabine for resected pancreatic adenocarcinoma. Cancer *116*, 5200–5206.

Maréchal, R., Bachet, J.B., MacKey, J.R., Dalban, C., Demetter, P., Graham, K., Couvelard, A., Svrcek, M., Bardier-Dupas, A., Hammel, P., et al. (2012). Levels of gemcitabine transport and metabolism proteins predict survival times of patients treated with gemcitabine for pancreatic adenocarcinoma. Gastroenterology *143*, 664-674.e6.

Margueron, R., Justin, N., Ohno, K., Sharpe, M.L., Son, J., Drury, W.J., Voigt, P., Martin, S.R., Taylor, W.R., De Marco, V., et al. (2009). Role of the polycomb protein EED in the propagation of repressive histone marks. Nature *461*, 762–767.

Maus, M., Cuk, M., Patel, B., Lian, J., Ouimet, M., Kaufmann, U., Yang, J., Horvath, R., Hornig-Do, H.T., Chrzanowska-Lightowlers, Z.M., et al. (2017). Store-Operated Ca2+ Entry Controls Induction of Lipolysis and the Transcriptional Reprogramming to Lipid Metabolism. Cell Metab. *25*, 698–712.

Milan, M., Balestrieri, C., Alfarano, G., Polletti, S., Prosperini, E., Nicoli, P., Spaggiari, P., Zerbi, A., Cirulli, V., Diaferia, G.R., et al. (2020). Pancreatic Cancer Cells Require the Transcription Factor MYRF to Maintain ER Homeostasis. Dev. Cell *55*, 398-412.e7.

Miranti, C.M., Ginty, D.D., Huang, G., Chatila, T., and Greenberg, M.E. (1995). Calcium Activates Serum Response Factor-Dependent Transcription by a Ras- and Elk-1-Independent Mechanism That Involves a Ca2+/Calmoculin-Dependent Kinase. Mol. Cell. Biol. *15*, 3672–3684.

Mishra, V.K., Wegwitz, F., Kosinsky, R.L., Sen, M., Baumgartner, R., Wulff, T., Siveke, J.T., Schildhaus, H.U., Najafova, Z., Kari, V., et al. (2017). Histone deacetylase class-I inhibition promotes epithelial gene expression in pancreatic cancer cells in a BRD4-and MYC-dependent manner. Nucleic Acids Res. *45*, 6334–6349.

Moffitt, R.A., Marayati, R., Flate, E.L., Volmar, K.E., Loeza, S.G.H., Hoadley, K.A.,

Rashid, N.U., Williams, L.A., Eaton, S.C., Chung, A.H., et al. (2015). Virtual microdissection identifies distinct tumor- and stroma-specific subtypes of pancreatic ductal adenocarcinoma. Nat. Genet. *47*, 1168–1178.

Mogami, H., Tepikin, A. V., and Petersen, O.H. (1998). Termination of cytosolic Ca2+ signals: Ca2+ reuptake into intracellular stores is regulated by the free Ca2+ concentration in the store lumen. EMBO J. *17*, 435–442.

Monteith, G.R., Prevarskaya, N., and Roberts-Thomson, S.J. (2017). The calcium-cancer signalling nexus. Nat. Rev. Cancer *17*, 367–380.

Moon, K.J., Mochizuki, K., Zhou, M., Jeong, H.S., Brady, J.N., and Ozato, K. (2005). The bromodomain protein Brd4 is a positive regulatory component of P-TEFb and stimulates RNA polymerase II-dependent transcription. Mol. Cell *19*, 523–534.

Moore, P.C., Qi, J.Y., Thamsen, M., Ghosh, R., Peng, J., Gliedt, M.J., Meza-Acevedo, R., Warren, R.E., Hiniker, A., Kim, G.E., et al. (2019). Parallel signaling through IRE1a and PERK regulates pancreatic neuroendocrine tumor growth and survival. Cancer Res. *79*, 6190–6203.

Mori, R., Ishikawa, T., Ichikawa, Y., Taniguchi, K., Matsuyama, R., Ueda, M., Fujii, Y., Endo, I., Togo, S., Danenberg, P. V., et al. (2007). Human equilibrative nucleoside transporter 1 is associated with the chemosensitivity of gemcitabine in human pancreatic adenocarcinoma and biliary tract carcinoma cells. Oncol. Rep. *17*, 1201–1205.

Mujcic, H., Nagelkerke, A., Rouschop, K.M.A., Chung, S., Chaudary, N., Span, P.N., Clarke, B., Milosevic, M., Sykes, J., Hill, R.P., et al. (2013). Hypoxic activation of the PERK/eIF2α arm of the unfolded protein response promotes metastasis through induction of LAMP3. Clin. Cancer Res. *19*, 6126–6137.

Mukaigasa, K., Tsujita, T., Nguyen, V.T., Li, L., Yagi, H., Fuse, Y., Nakajima-Takagi, Y., Kato, K., Yamamoto, M., and Kobayashi, M. (2018). Nrf2 activation attenuates genetic endoplasmic reticulum stress induced by a mutation in the phosphomannomutase 2 gene in zebrafish. Proc. Natl. Acad. Sci. U. S. A. *115*, 2758–2763.

Müller, M.R., and Rao, A. (2010). NFAT, immunity and cancer: A transcription factor comes of age. Nat. Rev. Immunol. *10*, 645–656.

Nadanaka, S., Okada, T., Yoshida, H., and Mori, K. (2007). Role of Disulfide Bridges Formed in the Luminal Domain of ATF6 in Sensing Endoplasmic Reticulum Stress. Mol. Cell. Biol. *27*, 1027–1043.

Nagarajan, S., Hossan, T., Alawi, M., Najafova, Z., Indenbirken, D., Bedi, U., Taipaleenmäki, H., Ben-Batalla, I., Scheller, M., Loges, S., et al. (2014). Bromodomain Protein BRD4 Is Required for Estrogen Receptor-Dependent Enhancer Activation and Gene Transcription. Cell Rep. *8*, 460–469.

Nagarajan, S., Benito, E., Fischer, A., and Johnsen, S.A. (2015). H4K12ac is regulated by estrogen receptor-alpha and is associated with BRD4 function and inducible transcription. Oncotarget *6*, 7305–7317.

Najafova, Z., Tirado-Magallanes, R., Subramaniam, M., Hossan, T., Schmidt, G., Nagarajan, S., Baumgart, S.J., Mishra, V.K., Bedi, U., Hesse, E., et al. (2017). BRD4 localization to lineage-specific enhancers is associated with a distinct transcription factor repertoire. Nucleic Acids Res. *45*, 127–141.

Nakahira, S., Nakamori, S., Tsujie, M., Takahashi, Y., Okami, J., Yoshioka, S., Yamasaki, M., Marubashi, S., Takemasa, I., Miyamoto, A., et al. (2007). Involvement of ribonucleotide reductase M1 subunit overexpression in gemcitabine resistance of human pancreatic cancer. Int. J. Cancer *120*, 1355–1363.

Nakai, Y., Isayama, H., Sasaki, T., Sasahira, N., Tsujino, T., Toda, N., Kogure, H., Matsubara, S., Ito, Y., Togawa, O., et al. (2012). A multicentre randomised phase II trial of gemcitabine alone vs gemcitabine and S-1 combination therapy in advanced pancreatic cancer: GEMSAP study. Br. J. Cancer *106*, 1934–1939.

Nakano, Y., Tanno, S., Koizumi, K., Nishikawa, T., Nakamura, K., Minoguchi, M., Izawa, T., Mizukami, Y., Okumura, T., and Kohgo, Y. (2007). Gemcitabine chemoresistance and molecular markers associated with gemcitabine transport and metabolism in human pancreatic cancer cells. Br. J. Cancer *96*, 457–463.

NCT03401190 (2018). CM4620 Injectable Emulsion Versus Supportive Care in Patients With Acute Pancreatitis and SIRS.

NCT03709342 (2018). A PK/PD Study of CM4620-IE in Patients With Acute Pancreatitis.

NCT04195347 (2019). Study of CM4620 to Reduce the Severity of Pancreatitis Due

to Asparaginase.

Neesse, A., Michl, P., Frese, K.K., Feig, C., Cook, N., Jacobetz, M.A., Lolkema, M.P., Buchholz, M., Olive, K.P., Gress, T.M., et al. (2011). Stromal biology and therapy in pancreatic cancer. Gut *60*, 861–868.

Nicholson, T.B., Veland, N., and Chen, T. (2015). Writers, Readers, and Erasers of Epigenetic Marks (Elsevier Inc.).

Nolan-Stevaux, O., Lau, J., Truitt, M.L., Chu, G.C., Hebrok, M., Fernández-Zapico, M.E., and Hanahan, D. (2009). GLI1 is regulated through Smoothened-independent mechanisms in neoplastic pancreatic ducts and mediates PDAC cell survival and transformation. Genes Dev. *23*, 24–36.

Notta, F., Chan-Seng-Yue, M., Lemire, M., Li, Y., Wilson, G.W., Connor, A.A., Denroche, R.E., Liang, S. Ben, Brown, A.M.K., Kim, J.C., et al. (2016). A renewed model of pancreatic cancer evolution based on genomic rearrangement patterns. Nature *538*, 378–382.

Novoa, I., Zeng, H., Harding, H.P., and Ron, D. (2001). Feedback inhibition of the unfolded protein response by GADD34-mediated dephosphorylation of eIF2α. J. Cell Biol. *153*, 1011–1021.

Oettle, H., Neuhaus, P., Hochhaus, A., Hartmann, J.T., Gellert, K., Ridwelski, K., Niedergethmann, M., Zülke, C., Fahlke, J., Arning, M.B., et al. (2013). Adjuvant chemotherapy with gemcitabine and long-term outcomes among patients with resected pancreatic cancer: The CONKO-001 randomized trial. JAMA - J. Am. Med. Assoc. *310*, 1473–1481.

Ogawa, M., Hori, H., Ohta, T., Onozato, K., Miyahara, M., and Komada, Y. (2005). Sensitivity to gemcitabine and its metabolizing enzymes in neuroblastoma. Clin. Cancer Res. *11*, 3485–3493.

Ohoka, N., Yoshii, S., Hattori, T., Onozaki, K., and Hayashi, H. (2005). TRB3, a novel ER stress-inducible gene, is induced via ATF4-CHOP pathway and is involved in cell death. EMBO J. *24*, 1243–1255.

Olive, K.P., Jacobetz, M.A., Davidson, C.J., Gopinathan, A., McIntyre, D., Honess, D., Madhu, B., Goldgraben, M.A., Caldwell, M.E., Allard, D., et al. (2009). Inhibition of Hedgehog signaling enhances delivery of chemotherapy in a mouse model of

pancreatic cancer. Science (80-.). *324*, 1457–1461.

Van Oort, R.J., Van Rooij, E., Bourajjaj, M., Schimmel, J., Jansen, M.A., Van Der Nagel, R., Doevendans, P.A., Schneider, M.D., Van Echteld, C.J.A., and De Windt, L.J. (2006). MEF2 activates a genetic program promoting chamber dilation and contractile dysfunction in calcineurin-induced heart failure. Circulation *114*, 298–308.

Pakos-Zebrucka, K., Koryga, I., Mnich, K., Ljujic, M., Samali, A., and Gorman, A.M. (2016). The integrated stress response. EMBO Rep. *17*, 1374–1395.

Palam, L.R., Gore, J., Craven, K.E., Wilson, J.L., and Korc, M. (2015). Integrated stress response is critical for gemcitabine resistance in pancreatic ductal adenocarcinoma. Cell Death Dis.

Palty, R., Silverman, W.F., Hershfinkel, M., Caporale, T., Sensi, S.L., Parnis, J., Nolte, C., Fishman, D., Shoshan-Barmatz, V., Herrmann, S., et al. (2010). NCLX is an essential component of mitochondrial Na+/Ca 2+ exchange. Proc. Natl. Acad. Sci. U. S. A. *107*, 436–441.

Palty, R., Raveh, A., Kaminsky, I., Meller, R., and Reuveny, E. (2012). SARAF inactivates the store operated calcium entry machinery to prevent excess calcium refilling. Cell *149*, 425–438.

Pandol, S.J., Saluja, A.K., Imrie, C.W., and Banks, P.A. (2007). Acute Pancreatitis: Bench to the Bedside. Gastroenterology *132*, 1127–1151.

Parekh, A.B. (2011). Decoding cytosolic Ca2+ oscillations. Trends Biochem. Sci. *36*, 78–87.

Patzak, M.S., Kari, V., Patil, S., Hamdan, F.H., Goetze, R.G., Brunner, M., Gaedcke, J., Kitz, J., Jodrell, D.I., Richards, F.M., et al. (2019). Cytosolic 5′-nucleotidase 1A is overexpressed in pancreatic cancer and mediates gemcitabine resistance by reducing intracellular gemcitabine metabolites. EBioMedicine *40*, 394–405.

Peng, W., Zhang, Y., Zheng, M., Cheng, H., Zhu, W., Cao, C.-M., and Xiao, R.-P. (2010). Cardioprotection by CaMKII-δB Is Mediated by Phosphorylation of HSF1 and Subsequent Expression of Inducible HSP70. Circ. Res. *106*, 1–20.

Pereira, E.R., Frudd, K., Awad, W., and Hendershot, L.M. (2014). Endoplasmic Reticulum (ER) stress and Hypoxia response pathways interact to Potentiate

Hypoxia-inducible Factor 1 (HIF-1) Transcriptional activity on targets like Vascular Endothelial Growth Factor (VEGF). J. Biol. Chem. *289*, 3352–3364.

Perocchi, F., Gohil, V.M., Girgis, H.S., Bao, X.R., McCombs, J.E., Palmer, A.E., and Mootha, V.K. (2010). MICU1 encodes a mitochondrial EF hand protein required for Ca2+ uptake. Nature *467*, 291–296.

Plank, J.L., and Dean, A. (2014). Enhancer function: Mechanistic and genome-wide insights come together. Mol. Cell *55*, 5–14.

Pognonec, P., Boulukos, K.E., Gesquière, J.C., Stéhelin, D., and Ghysdael, J. (1988). Mitogenic stimulation of thymocytes results in the calcium-dependent phosphorylation of c-ets-1 proteins. EMBO J. *7*, 977–983.

Pombo, A., and Dillon, N. (2015). Three-dimensional genome architecture: Players and mechanisms. Nat. Rev. Mol. Cell Biol. *16*, 245–257.

Pommier, A., Anaparthy, N., Memos, N., Larkin Kelley, Z., Gouronnec, A., Yan, R., Auffray, C., Albrengues, J., Egeblad, M., Iacobuzio-Donahue, C.A., et al. (2018). Unresolved endoplasmic reticulum stress engenders immune-resistant, latent pancreatic cancer metastases. Science (80-.). *360*.

Prakriya, M., and Lewis, R.S. (2015a). Store-operated calcium channels. Physiol. Rev. *95*, 1383–1436.

Prakriya, M., and Lewis, R.S. (2015b). Store-operated calcium channels. Physiol. Rev. *95*, 1383–1436.

Press, C. Pan-Cancer Atlas.

Prevarskaya, N., Skryma, R., and Shuba, Y. (2011). Calcium in tumour metastasis: New roles for known actors. Nat. Rev. Cancer *11*, 609–618.

Prins, D., and Michalak, M. (2011). Organellar calcium buffers. Cold Spring Harb. Perspect. Biol. *3*, 1–16.

Provenzano, P.P., Cuevas, C., Chang, A.E., Goel, V.K., Von Hoff, D.D., and Hingorani, S.R. (2012). Enzymatic Targeting of the Stroma Ablates Physical Barriers to Treatment of Pancreatic Ductal Adenocarcinoma. Cancer Cell *21*, 418–429.

Puthalakath, H., O'Reilly, L.A., Gunn, P., Lee, L., Kelly, P.N., Huntington, N.D., Hughes, P.D., Michalak, E.M., McKimm-Breschkin, J., Motoyama, N., et al. (2007). ER Stress Triggers Apoptosis by Activating BH3-Only Protein Bim. Cell *129*, 1337–

1349.

Qiu, Y., Mao, T., Zhang, Y., Shao, M., You, J., Ding, Q., Chen, Y., Wu, D., Xie, D., Lin, X., et al. (2010). A crucial role for RACK1 in the regulation of glucose-stimulated IRE1α activation in pancreatic β cells. Sci. Signal. *3*, 1–11.

Rajurkar, M., De Jesus-Monge, W.E., Driscoll, D.R., Appleman, V.A., Huang, H., Cotton, J.L., Klimstra, D.S., Zhu, L.J., Simin, K., Xu, L., et al. (2012). The activity of Gli transcription factors is essential for Kras-induced pancreatic tumorigenesis. Proc. Natl. Acad. Sci. U. S. A. *109*.

Ramírez, F., Ryan, D.P., Grüning, B., Bhardwaj, V., Kilpert, F., Richter, A.S., Heyne, S., Dündar, F., and Manke, T. (2016). deepTools2: a next generation web server for deep-sequencing data analysis. Nucleic Acids Res. *44*, W160–W165.

Raraty, M., Ward, J., Erdemli, G., Vaillant, C., Neoptolemos, J.P., Sutton, R., and Petersen, O.H. (2000). Calcium-dependent enzyme activation and vacuole formation in the apical granular region of pancreatic acinar cells. Proc. Natl. Acad. Sci. U. S. A. *97*, 13126–13131.

Reichard, P. (1997). The evolution of ribonucleotide reduction. Trends Biochem. Sci. *22*, 81–85.

Reichert, M., Takano, S., Von Burstin, J., Kim, S.B., Lee, J.S., Ihida-Stansbury, K., Hahn, C., Heeg, S., Schneider, G., Rhim, A.D., et al. (2013). The Prrx1 homeodomain transcription factor plays a central role in pancreatic regeneration and carcinogenesis. Genes Dev. *27*, 288–300.

Reiter, F., Wienerroither, S., and Stark, A. (2017). Combinatorial function of transcription factors and cofactors. Curr. Opin. Genet. Dev. *43*, 73–81.

Rezzani, R. (2004). Cyclosporine A and adverse effects on organs: Histochemical studies. Prog. Histochem. Cytochem. *39*, 85–128.

Ringer, S. (1883). A further Contribution regarding the influence of the different Constituents of the Blood on the Contraction of the Heart. J. Physiol. *4*, 29–42.

Ritzel, M.W., Ng, A.M., Yao, S.Y., Graham, K., Loewen, S.K., Smith, K.M., Hyde, R.J., Karpinski, E., Cass, C.E., Baldwin, S.A., et al. (2001). Recent molecular advances in studies of the concentrative Na+-dependent nucleoside transporter (CNT) family: identification and characterization of novel human and mouse proteins

(hCNT3 and mCNT3) broadly selective for purine and pyrimidine nucleosides (s. Mol. Membr. Biol. *18*, 65–72.

Robinson, J.T., Thorvaldsdóttir, H., Winckler, W., Guttman, M., Lander, E.S., Getz, G., and Mesirov, J.P. (2011). Integrative Genome Viewer. Nat. Biotechnol. *29*, 24–26.

Van Rompay, A.R., Johansson, M., and Karlsson, A. (1999). Phosphorylation of deoxycytidine analog monophosphates by UMP-CMP kinase: Molecular characterization of the human enzyme. Mol. Pharmacol. *56*, 562–569.

Ron, D. (2002). Translational control in the endoplasmic reticulum stress response. J. Clin. Invest. *110*, 1383–1388.

Ross-Innes, C.S., Stark, R., Teschendorff, A.E., Holmes, K.A., Ali, H.R., Dunning, M.J., Brown, G.D., Gojis, O., Ellis, I.O., Green, A.R., et al. (2012). Differential oestrogen receptor binding is associated with clinical outcome in breast cancer. Nature *481*, 389–393.

Rothenberg, M.L., Moore, M.J., Cripps, M.C., Andersen, J.S., Portenoy, R.K., Burris, H.A., Green, M.R., Tarassoff, P.G., Brown, T.D., Casper, E.S., et al. (1996). A phase II trial of gemcitabine in patients with 5-FU-refractory pancreas cancer. Ann. Oncol. *7*, 347–353.

Rouschop, K.M., Dubois, L.J., Keulers, T.G., Van Den Beucken, T., Lambin, P., Bussink, J., Van Der Kogel, A.J., Koritzinsky, M., and Wouters, B.G. (2013). PERK/eIF2α signaling protects therapy resistant hypoxic cells through induction of glutathione synthesis and protection against ROS. Proc. Natl. Acad. Sci. U. S. A. *110*, 4622–4627.

Rouschop, K.M.A., Van Den Beucken, T., Dubois, L., Niessen, H., Bussink, J., Savelkouls, K., Keulers, T., Mujcic, H., Landuyt, W., Voncken, J.W., et al. (2010). The unfolded protein response protects human tumor cells during hypoxia through regulation of the autophagy genes MAP1LC3B and ATG5. J. Clin. Invest. *120*, 127–141.

Rozenblum, E., Schutte, M., Goggins, M., Hahn, S.A., Panzer, S., Zahurak, M., Goodman, S.N., Sohn, T.A., Hruban, R.H., Yeo, C.J., et al. (1997). Tumor-suppressive pathways in pancreatic carcinoma. Cancer Res. *57*, 1731–1734.

Ruifrok, A.C., and Johnston, D.A. (2001). Quantification of histochemical staining by color deconvolution. Anal. Quant. Cytol. Histol. *23*, 291–299.

Rutkowski, D.T., and Hegde, R.S. (2010). Regulation of basal cellular physiology by the homeostatic unfolded protein response. J. Cell Biol. *189*, 783–794.

Ryan, D.P. (2020a). Initial systemic chemotherapy for metastatic exocrine pancreatic cancer. In UpToDate, R.M. Goldberg, and D.M.F. Savarese, eds. (UpToDate in Waltham, MA), p.

Ryan, D.P. (2020b). Chemotherapy for advanced exocrine pancreatic cancer. In UpToDate, R.M. Goldberg, and D.M.F. Savarese, eds. (UpToDate in Waltham, MA), p.

Ryan, D.P., and Mamon, H. (2020a). Initial chemotherapy and radiation for nonmetastatic, locally advanced, unresectable and borderline resectable, exocrine pancreatic cancer. In UpToDate, R.M. Goldberg, S.W. Ashley, C.G. Willett, and D.M.F. Savarese, eds. (UpToDate in Waltham, MA), p.

Ryan, D.P., and Mamon, H. (2020b). Treatment for potentially resectable exocrine pancreatic cancer. In UpToDate, R.M. Goldberg, C.G. Willett, and D.M.F. Savarese, eds. (UpToDate in Waltham, MA), p.

Sabari, B.R., Dall'Agnese, A., Boija, A., Klein, I.A., Coffey, E., Shrinivas, K., Abraham, B.J., Hannett, N.M., Zamudio, A. V, Manteiga, J.C., et al. (2018). Coactivator condensation at super - enhancers links phase separation and gene control - Science resubmission. Science (80-.). *361*, eaar3958.

Sah, R.P., Garg, S.K., Dixit, A.K., Dudeja, V., Dawra, R.K., and Saluja, A.K. (2014). Endoplasmic reticulum stress is chronically activated in chronic pancreatitis. J. Biol. Chem. *289*, 27551–27561.

Salazar, M., Lorente, M., García-Taboada, E., Pérez Gómez, E., Dávila, D., Zúñiga-García, P., María Flores, J., Rodríguez, A., Hegedus, Z., Mosén-Ansorena, D., et al. (2015). Loss of Tribbles pseudokinase-3 promotes Akt-driven tumorigenesis via FOXO inactivation. Cell Death Differ. *22*, 131–144.

Saluja, A., Dudeja, V., Dawra, R., and Sah, R.P. (2019). Early Intra-Acinar Events in Pathogenesis of Pancreatitis. Gastroenterology *156*, 1979–1993.

Sanchez-Vega, F., Mina, M., Armenia, J., Chatila, W.K., Luna, A., La, K.C.,

Dimitriadoy, S., Liu, D.L., Kantheti, H.S., Saghafinia, S., et al. (2018). Oncogenic Signaling Pathways in The Cancer Genome Atlas. Cell *173*, 321-337.e10.

Saul, S., Gibhardt, C.S., Schmidt, B., Lis, A., Pasieka, B., Conrad, D., Jung, P., Gaupp, R., Wonnenberg, B., Diler, E., et al. (2016). A calcium-redox feedback loop controls human monocyte immune responses: The role of ORAI Ca2+ channels. Sci. Signal. *9*, 1–14.

Sawai, H., Okada, Y., Funahashi, H., Matsuo, Y., Takahashi, H., Takeyama, H., and Manabe, T. (2006). Integrin-linked kinase activity is associated with interleukin-1α-induced progressive behavior of pancreatic cancer and poor patient survival. Oncogene *25*, 3237–3246.

Scheithauer, W., Schüll, B., Ulrich-Pur, H., Schmid, K., Raderer, M., Haider, K., Kwasny, W., Depisch, D., Schneeweiss, B., Lang, F., et al. (2003). Biweekly high-dose gemcitabine alone or in combination with capecitabine in patients with metastatic pancreatic adenocarcinoma: A randomized phase II trial. Ann. Oncol. *14*, 97–104.

Schindelin, J., Arganda-Carreras, I., Frise, E., Kaynig, V., Longair, M., Pietzsch, T., Preibisch, S., Rueden, C., Saalfeld, S., Schmid, B., et al. (2012). Fiji: An open-source platform for biological-image analysis. Nat. Methods *9*, 676–682.

Schindler, A.J., and Schekman, R. (2009). In vitro reconstitution of ER-stress induced ATF6 transport in COPII vesicles. Proc. Natl. Acad. Sci. U. S. A. *106*, 17775–17780.

Schneider, C.A., Rasband, W.S., and Eliceiri, K.W. (2012). NIH Image to ImageJ: 25 years of image analysis. Nat. Methods *9*, 671–675.

Schotta, G., Ebert, A., Krauss, V., Fischer, A., Hoffmann, J., Rea, S., Jenuwein, T., Dorn, R., and Reuter, G. (2002). Central role of Drosophila SU(VAR)3-9 in histone H3-K9 methylation and heterochromatic gene silencing. EMBO J. *21*, 1121–1131.

Sebastiani, V., Ricci, F., Rubio-Viquiera, B., Kulesza, P., Yeo, C.J., Hidalgo, M., Klein, A., Laheru, D., and Iacobuzio-Donahue, C.A. (2006). Immunohistochemical and genetic evaluation of deoxycytidine kinase in pancreatic cancer: Relationship to molecular mechanisms of gemcitabine resistance and survival. Clin. Cancer Res. *12*, 2492–2497.

Shamu, C.E., and Walter, P. (1996). Oligomerization and phosphorylation of the Ire1p kinase during intracellular signaling from the endoplasmic reticulum to the nucleus. EMBO J. *15*, 3028–3039.

Shan, J., Fu, L., Balasubramanian, M.N., Anthony, T., and Kilberg, M.S. (2012). ATF4-dependent regulation of the JMJD3 gene during amino acid deprivation can be rescued in Atf4-deficient cells by inhibition of deacetylation. J. Biol. Chem. *287*, 36393–36403.

Sherman, M.H., Yu, R.T., Engle, D.D., Ding, N., Atkins, A.R., Tiriac, H., Collisson, E.A., Connor, F., Van Dyke, T., Kozlov, S., et al. (2014). Vitamin D receptor-mediated stromal reprogramming suppresses pancreatitis and enhances pancreatic cancer therapy. Cell *159*, 80–93.

Shigeto, M., Ramracheya, R., Tarasov, A.I., Cha, C.Y., Chibalina, M. V., Hastoy, B., Philippaert, K., Reinbothe, T., Rorsman, N., Salehi, A., et al. (2015). GLP-1 stimulates insulin secretion by PKC-dependent TRPM4 and TRPM5 activation. J. Clin. Invest. *125*, 4714–4728.

Siamakpour-Reihani, S., Caster, J., Nepal, D.B., Courtwright, A., Hilliard, E., Usary, J., Ketelsen, D., Darr, D., Shen, X.J., Patterson, C., et al. (2011). The Role of calcineurin/NFAT in SFRP2 induced angiogenesis-A rationale for breast cancer treatment with the calcineurin inhibitor Tacrolimus. PLoS One *6*, 1–9.

Singh, G., Singh, S.K., König, A., Reutlinger, K., Nye, M.D., Adhikary, T., Eilers, M., Gress, T.M., Fernandez-Zapico, M.E., and Ellenrieder, V. (2010). Sequential activation of NFAT and c-Myc transcription factors mediates the TGF-β switch from a suppressor to a promoter of cancer cell proliferation. J. Biol. Chem. *285*, 27241–27250.

Singh, S.K., Chen, N., Hessmann, E., Siveke, J., Lahmann, M., Singh, G., Voelker, N., Vogt, S., Esposito, I., Schmidt, A., et al. (2015). Antithetical NFAT c1–Sox2 and p53–miR200 signaling networks govern pancreatic cancer cell plasticity . EMBO J. *34*, 517–530.

Singhi, A.D., McGrath, K., Brand, R.E., Khalid, A., Zeh, H.J., Chennat, J.S., Fasanella, K.E., Papachristou, G.I., Slivka, A., Bartlett, D.L., et al. (2017). Preoperative next-generation sequencing of pancreatic cyst fluid is highly accurate in cyst classification and detection of advanced neoplasia. Gut 2131–2141.

Singhi, A.D., George, B., Greenbowe, J.R., Chung, J., Suh, J., Maitra, A., Klempner, S.J., Hendifar, A., Milind, J.M., Golan, T., et al. (2019). Real-Time Targeted Genome Profile Analysis of Pancreatic Ductal Adenocarcinomas Identifies Genetic Alterations That Might Be Targeted With Existing Drugs or Used as Biomarkers. Gastroenterology *156*, 2242-2253.e4.

Slattery, M., Riley, T., Liu, P., Abe, N., Gomez-Alcala, P., Dror, I., Zhou, T., Rohs, R., Honig, B., Bussemaker, H.J., et al. (2011). Cofactor binding evokes latent differences in DNA binding specificity between hox proteins. Cell *147*, 1270–1282.

Smith, G.L., and Eisner, D.A. (2019). Calcium Buffering in the Heart in Health and Disease. Circulation *139*, 2358–2371.

Soboloff, J., Rothberg, B.S., Madesh, M., and Gill, D.L. (2012). STIM proteins: Dynamic calcium signal transducers. Nat. Rev. Mol. Cell Biol. *13*, 549–565.

Sohal, D.P.S., Kennedy, E.B., Khorana, A., Copur, M.S., Crane, C.H., Garrido-Laguna, I., Krishnamurthi, S., Moravek, C., O'Reilly, E.M., Philip, P.A., et al. (2018). Metastatic pancreatic cancer: ASCO clinical practice guideline update. J. Clin. Oncol. *36*, 2545–2556.

Sørensen, C.S., and Syljuåsen, R.G. (2012). Safeguarding genome integrity: The checkpoint kinases ATR, CHK1 and WEE1 restrain CDK activity during normal DNA replication. Nucleic Acids Res. *40*, 477–486.

Soufi, A., Donahue, G., and Zaret, K.S. (2012). Facilitators and impediments of the pluripotency reprogramming factors' initial engagement with the genome. Cell *151*, 994–1004.

De Sousa Cavalcante, L., and Monteiro, G. (2014). Gemcitabine: Metabolism and molecular mechanisms of action, sensitivity and chemoresistance in pancreatic cancer. Eur. J. Pharmacol. *741*, 8–16.

Soutourina, J. (2018). Transcription regulation by the Mediator complex. Nat. Rev. Mol. Cell Biol. *19*, 262–274.

Spratlin, J., Sangha, R., Glubrecht, D., Dabbagh, L., Young, J.D., Dumontet, C., Cass, C., Lai, R., and Mackey, J.R. (2004). The absence of human equilibrative nucleoside transporter 1 is associated with reduced survival in patients with gemcitabine-treated pancreas adenocarcinoma. Clin. Cancer Res. *10*, 6956–6961.

Staaf, J., Jönsson, G., Ringnér, M., Vallon-Christersson, J., Grabau, D., Arason, A., Gunnarsson, H., Agnarsson, B.A., Malmström, P.O., Johannsson, O.T., et al. (2010). High-resolution genomic and expression analyses of copy number alterations in HER2-amplified breast cancer. Breast Cancer Res. *12*.

Stanisz, H., Saul, S., Müller, C.S.L., Kappl, R., Niemeyer, B.A., Vogt, T., Hoth, M., Roesch, A., and Bogeski, I. (2014). Inverse regulation of melanoma growth and migration by Orai1/STIM2-dependent calcium entry. Pigment Cell Melanoma Res. *27*, 442–453.

De Stefani, D., Rizzuto, R., and Pozzan, T. (2016). Enjoy the Trip: Calcium in Mitochondria Back and Forth. Annu. Rev. Biochem. *85*, 161–192.

Stine, Z.E., Walton, Z.E., Altman, B.J., Hsieh, A.L., and Dang, C. V. (2015). MYC, metabolism, and cancer. Cancer Discov. *5*, 1024–1039.

Strehler, E.E., and Zacharias, D.A. (2001). Role of alternative splicing in generating isoform diversity among plasma membrane calcium pumps. Physiol. Rev. *81*, 21–50.

Stubbe, J.A. (2003). Di-iron-tyrosyl radical ribonucleotide reductases. Curr. Opin. Chem. Biol. *7*, 183–188.

Subramanian, A., Tamayo, P., Mootha, V.K., Mukherjee, S., Ebert, B.L., Gillette, M.A., Paulovich, A., Pomeroy, S.L., Golub, T.R., Lander, E.S., et al. (2005). Gene set enrichment analysis: A knowledge-based approach for interpreting genome-wide expression profiles. Proc. Natl. Acad. Sci. U. S. A. *102*, 15545–15550.

Suehiro, J.I., Kanki, Y., Makihara, C., Schadler, K., Miura, M., Manabe, Y., Aburatani, H., Kodama, T., and Minami, T. (2014). Genome-wide approaches reveal functional vascular endothelial growth factor (VEGF)-inducible nuclear factor of activated T cells (NFAT) c1 binding to angiogenesis-related genes in the endothelium. J. Biol. Chem. *289*, 29044–29059.

Sun, Z.W., and Allis, C.D. (2002). Ubiquitination of histone H2B regulates H3 methylation and gene silencing in yeast. Nature *418*, 104–108.

Sun, L., Song, L., Wan, Q., Wu, G., Li, X., Wang, Y., Wang, J., Liu, Z., Zhong, X., He, X., et al. (2015). cMyc-mediated activation of serine biosynthesis pathway is critical for cancer progression under nutrient deprivation conditions. Cell Res. *25*,

429–444.

Sun, P., Enslen, H., Myung, P.S., and Maurer, R.A. (1994). Differential activation of CREB by Ca2+/calmodulin-dependent protein kinases type II and type IV involves phosphorylation of a site that negatively regulates activity. Genes Dev. *8*, 2527–2539.

Suraweera, A., Münch, C., Hanssum, A., and Bertolotti, A. (2012). Failure of amino acid homeostasis causes cell death following proteasome inhibition. Mol. Cell *48*, 242–253.

Tabas, I., and Ron, D. (2011). Integrating the mechanisms of apoptosis induced by endoplasmic reticulum stress. Nat. Cell Biol. *13*, 184–190.

Tadros, S., Shukla, S.K., King, R.J., Gunda, V., Vernucci, E., Abrego, J., Chaika, N. V., Yu, F., Lazenby, A.J., Berim, L., et al. (2017). De Novo lipid synthesis facilitates gemcitabine resistance through endoplasmic reticulum stress in pancreatic cancer. Cancer Res. *77*, 5503–5517.

Takano, S., Reichert, M., Bakir, B., Das, K.K., Nishida, T., Miyazaki, M., Heeg, S., Collins, M.A., Marchand, B., Hicks, P.D., et al. (2016). Prrx1 isoform switching regulates pancreatic cancer invasion and metastatic colonization. Genes Dev. *30*, 233–247.

Talevich, E., Shain, A.H., Botton, T., and Bastian, B.C. (2016). CNVkit: Genome-Wide Copy Number Detection and Visualization from Targeted DNA Sequencing. PLoS Comput. Biol. *12*, 1–18.

Taylor, G.C.A., Eskeland, R., Hekimoglu-Balkan, B., Pradeepa, M.M., and Bickmore, W.A. (2013). H4K16 acetylation marks active genes and enhancers of embryonic stem cells, but does not alter chromatin compaction. Genome Res. *23*, 2053–2065.

Teich, N., Rosendahl, J., Tóth, M., Mössner, J., and Sahin-Tóth, M. (2006). Mutations of human cationic trypsinogen (PRSS1) and chronic pancreatitis. Hum. Mutat. *27*, 721–730.

Terai, H., Kitajima, S., Potter, D.S., Matsui, Y., Quiceno, L.G., Chen, T., Kim, T.J., Rusan, M., Thai, T.C., Piccioni, F., et al. (2018). ER stress signaling promotes the survival of cancer “Persister Cells” tolerant to EGFR tyrosine Kinase inhibitors.

Cancer Res. *78*, 1044–1057.

The Cancer Genome Atlas Research Network, Raphael, B.J., Hruban, R.H., Aguirre, A.J., Moffitt, R.A., Yeh, J.J., Stewart, C., Robertson, A.G., Cherniack, A.D., Gupta, M., et al. (2017). Integrated Genomic Characterization of Pancreatic Ductal Adenocarcinoma. Cancer Cell *32*, 185-203.e13.

Thorvaldsdóttir, H., Robinson, J.T., and Mesirov, J.P. (2013). Integrative Genomics Viewer (IGV): High-performance genomics data visualization and exploration. Brief. Bioinform. *14*, 178–192.

Tiriac, H., Belleau, P., Engle, D.D., Plenker, D., Deschênes, A., Somerville, T.D.D., Froeling, F.E.M., Burkhart, R.A., Denroche, R.E., Jang, G.H., et al. (2018). Organoid profiling identifies common responders to chemotherapy in pancreatic cancer. Cancer Discov. *8*, 1112–1129.

Tooker, P., Yen, W.C., Ng, S.C., Negro-Vilar, A., and Hermann, T.W. (2007). Bexarotene (LGD1069, Targretin), a selective retinoid X receptor agonist, prevents and reverses gemcitabine resistance in NSCLC cells by modulating gene amplification. Cancer Res. *67*, 4425–4433.

Tripathi, M.K., Deane, N.G., Zhu, J., An, H., Mima, S., Wang, X., Padmanabhan, S., Shi, Z., Prodduturi, N., Ciombor, K.K., et al. (2014). Nuclear factor of activated T-cell activity is associated with metastatic capacity in colon cancer. Cancer Res. *74*, 6947–6957.

Tsuru, A., Imai, Y., Saito, M., and Kohno, K. (2016). Novel mechanism of enhancing IRE1α-XBP1 signalling via the PERK-ATF4 pathway. Sci. Rep. *6*, 1–8.

Tu, Q., Hao, J., Zhou, X., Yan, L., Dai, H., Sun, B., Yang, D., An, S., Lv, L., Jiao, B., et al. (2018). CDKN2B deletion is essential for pancreatic cancer development instead of unmeaningful co-deletion due to juxtaposition to CDKN2A. Oncogene *37*, 128–138.

Uchida, K., Dezaki, K., Damdindorj, B., Inada, H., Shiuchi, T., Mori, Y., Yada, T., Minokoshi, Y., and Tominaga, M. (2011). Lack of TRPM2 impaired insulin secretion and glucose metabolisms in mice. Diabetes *60*, 119–126.

Ueno, H., Ioka, T., Ikeda, M., Ohkawa, S., Yanagimoto, H., Boku, N., Fukutomi, A., Sugimori, K., Baba, H., Yamao, K., et al. (2013). Randomized phase iii study of

gemcitabine plus S-1, S-1 alone, or gemcitabine alone in patients with locally advanced and metastatic pancreatic cancer in Japan and Taiwan: Gest study. J. Clin. Oncol. *31*, 1640–1648.

Uhlin, U., and Eklund, H. (1994). Structure of ribonucleotide reductase protein R1. Nature *370*, 533–539.

Urano, F., Wang, X.Z., Bertolotti, A., Zhang, Y., Chung, P., Harding, H.P., and Ron, D. (2000). Coupling of stress in the ER to activation of JNK protein kinases by transmembrane protein kinase IRE1. Science (80-.). *287*, 664–666.

Urra, H., Dufey, E., Avril, T., Chevet, E., and Hetz, C. (2016). Endoplasmic Reticulum Stress and the Hallmarks of Cancer. Trends in Cancer *2*, 252–262.

Ushioda, R., Miyamoto, A., Inoue, M., Watanabe, S., Okumura, M., Maegawa, K.I., Uegaki, K., Fujii, S., Fukuda, Y., Umitsu, M., et al. (2016). Redox-assisted regulation of Ca2+ homeostasis in the endoplasmic reticulum by disulfide reductase ERdj5. Proc. Natl. Acad. Sci. U. S. A. *113*, E6055–E6063.

Vaeth, M., Maus, M., Klein-Hessling, S., Freinkman, E., Yang, J., Eckstein, M., Cameron, S., Turvey, S.E., Serfling, E., Berberich-Siebelt, F., et al. (2017). Store-Operated Ca2+ Entry Controls Clonal Expansion of T Cells through Metabolic Reprogramming. Immunity *47*, 664-679.e6.

Vallejo, M., Ron, D., Miller, C.P., and Habener, J.F. (1993). C/ATF, a member of the activating transcription factor family of DNA- binding proteins, dimerizes with CAAT/enhancer-binding proteins and directs their binding to cAMP response elements. Proc. Natl. Acad. Sci. U. S. A. *90*, 4679–4683.

Vandecaetsbeek, I., Vangheluwe, P., Raeymaekers, L., Wuytack, F., and Vanoevelen, J. (2011). The Ca2+ Pumps of the Endoplasmic Reticulum and Golgi Apparatus. Cold Spring Harb. Perspect. Biol. *3*, 1–24.

VanRenterghem, B., Browning, M.D., and Maller, J.L. (1994). Regulation of mitogen-activated protein kinase activation by protein kinases A and C in a cell-free system. J. Biol. Chem. *269*, 24666–24672.

Vassilakos, A., Michalak, M., Lehrman, M.A., and Williams, D.B. (1998). Oligosaccharide binding characteristics of the molecular chaperones calnexin and calreticulin. Biochemistry *37*, 3480–3490.

Vazquez de Aldana, C.R., Wek, R.C., Segundo, P.S., Truesdell, A.G., and Hinnebusch, A.G. (1994). Multicopy tRNA genes functionally suppress mutations in yeast eIF-2 alpha kinase GCN2: evidence for separate pathways coupling GCN4 expression to unchanged tRNA. Mol. Cell. Biol. *14*, 7920–7932.

Vekich, J.A., Belmont, P.J., Thuerauf, D.J., and Glembotski, C.C. (2012). Protein Disulfide Isomerase-associated 6 is an ATF6-inducible ER Stress Response Protein that Protects Cardiac Myocytes from Ischemia/Reperfusion-mediated Cell Death. J. Mol. Cell. Cardiol. *53*, 259–267.

Waddell, N., Pajic, M., Patch, A.M., Chang, D.K., Kassahn, K.S., Bailey, P., Johns, A.L., Miller, D., Nones, K., Quek, K., et al. (2015). Whole genomes redefine the mutational landscape of pancreatic cancer. Nature *518*, 495–501.

Waldron, R.T., Su, H.Y., Piplani, H., Capri, J., Cohn, W., Whitelegge, J.P., Faull, K.F., Sakkiah, S., Abrol, R., Yang, W., et al. (2018). Ethanol Induced Disordering of Pancreatic Acinar Cell Endoplasmic Reticulum: An ER Stress/Defective Unfolded Protein Response Model. Cmgh *5*, 479–497.

Walter, P., and Ron, D. (2011). The unfolded protein response: From stress pathway to homeostatic regulation. Science (80-.). *334*, 1081–1086.

Wang, C., Zhang, W., Juan Fu, M., Yang, A., Huang, H., and Xie, J. (2015). Establishment of human pancreatic cancer gemcitabine-resistant cell line with ribonucleotide reductase overexpression. Oncol. Rep. *33*, 383–390.

Wang, J., Takeuchi, T., Tanaka, S., Kubo, S.-K., Kayo, T., Lu, D., Takata, K., Koizumi, A., and Izumi, T. (1999). A mutation in the insulin 2 gene induces diabetes with severe pancreatic. J. Clin. Invest. *103*, 27–37.

Wang, J., Shen, J., Zhao, K., Hu, J., Dong, J., and Sun, J. (2019). STIM1 overexpression in hypoxia microenvironment contributes to pancreatic carcinoma progression. Cancer Biol. Med. *16*, 100–108.

Wang, P., Li, J., Tao, J., and Sha, B. (2018). The luminal domain of the ER stress sensor protein PERK binds misfolded proteins and thereby triggers PERK oligomerization. J. Biol. Chem. *293*, 4110–4121.

Wang, Q.C., Zheng, Q., Tan, H., Zhang, B., Li, X., Yang, Y., Yu, J., Liu, Y., Chai, H., Wang, X., et al. (2016). TMCO1 is an ER Ca2+ load-activated Ca2+ channel. Cell

165, 1454–1466.

Wang, S.P., Tang, Z., Chen, C.W., Shimada, M., Koche, R.P., Wang, L.H., Nakadai, T., Chramiec, A., Krivtsov, A. V., Armstrong, S.A., et al. (2017). A UTX-MLL4-p300 Transcriptional Regulatory Network Coordinately Shapes Active Enhancer Landscapes for Eliciting Transcription. Mol. Cell *67*, 308-321.e6.

Wang, Y., Alam, G.N., Ning, Y., Visioli, F., Dong, Z., Nör, J.E., and Polverini, P.J. (2012). The unfolded protein response induces the angiogenic switch in human tumor cells through the PERK/ATF4 pathway. Cancer Res. *72*, 5396–5406.

Ward, J.B., Jenkins, S.A., Sutton, R., and Petersen, O.H. (1995). Is an elevated concentration of acinar cytosolic free ionised calcium the trigger for acute pancreatitis? Lancet *346*, 1016–1019.

Weake, V.M., and Workman, J.L. (2008). Histone Ubiquitination: Triggering Gene Activity. Mol. Cell *29*, 653–663.

Wei, D., Wang, L., Yan, Y., Jia, Z., Gagea, M., Li, Z., Zuo, X., Kong, X., Huang, S., and Xie, K. (2016). KLF4 Is Essential for Induction of Cellular Identity Change and Acinar-to-Ductal Reprogramming during Early Pancreatic Carcinogenesis. Cancer Cell *29*, 324–338.

Weizman, N., Krelin, Y., Shabtay-Orbach, A., Amit, M., Binenbaum, Y., Wong, R.J., and Gil, Z. (2014). Macrophages mediate gemcitabine resistance of pancreatic adenocarcinoma by upregulating cytidine deaminase. Oncogene *33*, 3812–3819.

Wen, L., Voronina, S., Javed, M.A., Awais, M., Szatmary, P., Latawiec, D., Chvanov, M., Collier, D., Huang, W., Barrett, J., et al. (2015). Inhibitors of ORAI1 prevent cytosolic calcium-associated injury of human pancreatic acinar cells and acute pancreatitis in 3 mouse models. Gastroenterology *149*, 481-492.e7.

Whyte, W.A., Orlando, D.A., Hnisz, D., Abraham, B.J., Lin, C.Y., Kagey, M.H., Rahl, P.B., Lee, T.I., and Young, R.A. (2013). Master transcription factors and mediator establish super-enhancers at key cell identity genes. Cell *153*, 307–319.

Willis, N.A., Rass, E., and Scully, R. (2015). Deciphering the Code of the Cancer Genome: Mechanisms of Chromosome Rearrangement. Trends in Cancer *1*, 217–230.

Wong, A., Soo, R.A., Yong, W.P., and Innocenti, F. (2009). Clinical pharmacology

and pharmacogenetics of gemcitabine. Drug Metab. Rev. *41*, 77–88.

Wortel, I.M.N., van der Meer, L.T., Kilberg, M.S., and van Leeuwen, F.N. (2017). Surviving Stress: Modulation of ATF4-Mediated Stress Responses in Normal and Malignant Cells. Trends Endocrinol. Metab. *28*, 794–806.

Wunderlich, Z., and Mirny, L.A. (2009). Different gene regulation strategies revealed by analysis of binding motifs. Trends Genet. *25*, 434–440.

Xu, Y.-Z., and Plunkett, W. (1992). Modulation of deoxycytidylate deaminase in intact human leukemia cells. Action of 2',2'-difluorodeoxycytidine. Biochem. Pharmacol. *44*, 1819–1827.

Xu, C., Bailly-Maitre, B., and Reed, J.C. (2005). Review series Endoplasmic reticulum stress: cell life and death decisions. J Clin Invest *115*, 2656–2664.

Yan, W., Frank, C.L., Korth, M.J., Sopher, B.L., Novoa, I., Ron, D., and Katze, M.G. (2002). Control of PERK eIF2α kinase activity by the endoplasmic reticulum stress-induced molecular chaperone P58IPK. Proc. Natl. Acad. Sci. U. S. A. *99*, 15920–15925.

Yau, C.Y.F., Wheeler, J.J., Sutton, K.L., and Hedley, D.W. (2005). Inhibition of integrin-linked kinase by QLT0254 inhibits Akt-dependent pathways and is growth inhibitory in orthotopic primary pancreatic cancer xenografts. Cancer Res. *65*, 1497–1504.

Ye, J., Rawson, R.B., Komuro, R., Chen, X., Davé, U.P., Prywes, R., Brown, M.S., and Goldstein, J.L. (2000). ER stress induces cleavage of membrane-bound ATF6 by the same proteases that process SREBPs. Mol. Cell *6*, 1355–1364.

Ye, J., Kumanova, M., Hart, L.S., Sloane, K., Zhang, H., De Panis, D.N., Bobrovnikova-Marjon, E., Diehl, J.A., Ron, D., and Koumenis, C. (2010). The GCN2-ATF4 pathway is critical for tumour cell survival and proliferation in response to nutrient deprivation. EMBO J. *29*, 2082–2096.

Yiu, G.K., and Toker, A. (2006). NFAT induces breast cancer cell invasion by promoting the induction of cyclooxygenase-2. J. Biol. Chem. *281*, 12210–12217.

Yoshida, H., Matsui, T., Yamamoto, A., Okada, T., and Mori, K. (2001). XBP1 mRNA is induced by ATF6 and spliced by IRE1 in response to ER stress to produce a highly active transcription factor. Cell *107*, 881–891.

Yuan, G., Nanduri, J., Bhasker, C.R., Semenza, G.L., and Prabhakar, N.R. (2005). Ca2+/calmodulin kinase-dependent activation of hypoxia inducible factor 1 transcriptional activity in cells subjected to intermittent hypoxia. J. Biol. Chem. *280*, 4321–4328.

Zhang, Q., Lou, Y., Zhang, J., Fu, Q., Wei, T., Sun, X., Chen, Q., Yang, J., Bai, X., and Liang, T. (2017). Hypoxia-inducible factor-2α promotes tumor progression and has crosstalk with Wnt/β-catenin signaling in pancreatic cancer. Mol. Cancer *16*, 1–14.

Zhang, X., Gibhardt, C.S., Will, T., Stanisz, H., Körbel, C., Mitkovski, M., Stejerean, I., Cappello, S., Pacheu-Grau, D., Dudek, J., et al. (2019a). Redox signals at the ER –mitochondria interface control melanoma progression . EMBO J. *38*, 1–22.

Zhang, Z., Zhang, L., Zhou, L., Lei, Y., Zhang, Y., and Huang, C. (2019b). Redox signaling and unfolded protein response coordinate cell fate decisions under ER stress. Redox Biol. *25*, 101047.

Zhao, Y., and Garcia, B.A. (2015). Comprehensive catalog of currently documented histone modifications. Cold Spring Harb. Perspect. Biol. *7*, 1–21.

Zhao, E., Ding, J., Xia, Y., Liu, M., Ye, B., Choi, J.H., Yan, C., Dong, Z., Huang, S., Zha, Y., et al. (2016). KDM4C and ATF4 Cooperate in Transcriptional Control of Amino Acid Metabolism. Cell Rep. *14*, 506–519.

Zhao, X., Gao, S., Sun, W., Zhang, H., Sun, J., Yang, S., and Hao, J. (2014). Hypoxia-Inducible factor-1 promotes pancreatic ductal adenocarcinoma invasion and metastasis by activating transcription of the actin-Bundling protein fascin. Cancer Res. *74*, 2455–2464.

Zhou, J., Zhang, L., Zheng, H., Ge, W., Huang, Y., Yan, Y., Zhou, X., Zhu, W., Kong, Y., Ding, Y., et al. (2019). Identification of chemoresistance-related mRNAs based on gemcitabine-resistant pancreatic cancer cell lines. Cancer Med. 1–16.

Zhou, W., Zhu, P., Wang, J., Pascual, G., Ohgi, K.A., Lozach, J., Glass, C.K., and Rosenfeld, M.G. (2008). Histone H2A Monoubiquitination Represses Transcription by Inhibiting RNA Polymerase II Transcriptional Elongation. Mol. Cell *29*, 69–80.

Zhu, K., Jaio, H., Li, S., Cao, H., Galson, D.L., Zhao, Z., Zhao, X., Lai, Y., Fan, J., Im, H.-J., et al. (2013). ATF4 promotes bone angiogenesis by increasing VEGF

expression and release in the bone environment. J. Bone Miner. Res. *28*, 1870–1884.

Supplemental Material

Table S1 GSEA of curated gene sets (C2) identified in GemR compared to Par.

Ranking	NAME	NES	FDR
1	BROWNE_INTERFERON_RESPONSIVE_GENES	2.11	0.02
2	SMID_BREAST_CANCER_LUMINAL_A_UP	2.10	0.01
3	REACTOME_INTERFERON_GAMMA_SIGNALING	2.07	0.01
4	SANA_RESPONSE_TO_IFNG_UP	2.03	0.02
5	BOWIE_RESPONSE_TO_EXTRACELLULAR_MATRIX	2.01	0.02
6	REACTOME_COMPLEX_I_BIOGENESIS	2.00	0.03
7	REACTOME_INTERFERON_ALPHA_BETA_SIGNALING	1.94	0.06
8	EINAV_INTERFERON_SIGNATURE_IN_CANCER	1.93	0.06
9	REACTOME_MITOCHONDRIAL_TRANSLATION	1.93	0.06
10	STAMBOLSKY_TARGETS_OF_MUTATED_TP53_DN	1.92	0.06
11	SATO_SILENCED_BY_METHYLATION_IN_PANCREATIC_CANCER_2	1.91	0.06
12	CAVARD_LIVER_CANCER_MALIGNANT_VS_BENIGN	1.91	0.05
13	MOSERLE_IFNA_RESPONSE	1.89	0.06
14	NATSUME_RESPONSE_TO_INTERFERON_BETA_DN	1.88	0.06
15	DER_IFN_ALPHA_RESPONSE_UP	1.88	0.06
16	REACTOME_RESPIRATORY_ELECTRON_TRANSPORT_ATP_SYNTHESIS_BY_CHEMIOSMOTIC_COUPLING_AND_HEAT_PRODUCTION_BY_UNCOUPLING_PROTEINS	1.86	0.07
17	REACTOME_RESPIRATORY_ELECTRON_TRANSPORT	1.86	0.07
18	REACTOME_INTERFERON_SIGNALING	1.81	0.11
19	TOOKER_GEMCITABINE_RESISTANCE_UP	1.81	0.11
20	BOYLAN_MULTIPLE_MYELOMA_PCA3_DN	1.81	0.11
21	DER_IFN_BETA_RESPONSE_UP	1.80	0.11
22	KEGG_HISTIDINE_METABOLISM	1.78	0.14
23	LEE_LIVER_CANCER_DENA_DN	1.77	0.15
24	KEGG_DRUG_METABOLISM_CYTOCHROME_P450	1.76	0.16
25	BOYLAN_MULTIPLE_MYELOMA_D_CLUSTER_DN	1.75	0.16
26	KEGG_METABOLISM_OF_XENOBIOTICS_BY_CYTOCHROME_P450	1.75	0.17
27	HELLER_SILENCED_BY_METHYLATION_UP	1.74	0.17
28	MUELLER_METHYLATED_IN_GLIOBLASTOMA	1.73	0.18
29	HUANG_FOXA2_TARGETS_DN	1.73	0.18
30	LANDIS_ERBB2_BREAST_TUMORS_65_DN	1.73	0.18
31	REACTOME_METABOLISM_OF_FAT_SOLUBLE_VITAMINS	1.71	0.20
32	GUTIERREZ_CHRONIC_LYMPHOCYTIC_LEUKEMIA_DN	1.69	0.24

Table S2 Amplified and deleted regions and genes in GemR compared to Par.

Chromosome	Start	End	Gene	log2	Depth	Probes	Weight
chr11	3810838	4210927	PGAP2 RHOG STIM1 MIR4687 RRM1 LOC100506082	3.22983	3.85219	8	6.72007
chr11	4210927	5161140	OR52B4 TRIM21 OR52K2 OR52K1 OR52M1 C11orf40 OR52I2 OR52I1 TRIM68 OR51D1 OR51E1 OR51E2 OR51F1 OR52R1 OR51F2 OR51S1 OR51T1 OR51A7 OR51G2 OR51G1 OR51A4 OR51A2 MMP26 OR51L1 OR52J3 OR52E2 OR52A5 OR52A1	1.97323	0.983756	19	14.5736
chr11	5161140	9312068	OR51V1 HBB HBD HBBP1 BGLT3 HBG1 HBG2 HBE1 OR51B4	1.54782	1.03833	83	66.5243

			OR51B2 OR51B5 OR51B6 OR51M1 OR51Q1 OR51I1 OR51I2 OR52D1 UBQLN3 UBQLNL OR52H1 OR52B6 TRIM6 TRIM6-TRIM34 TRIM34 TRIM5 TRIM22 OR56B1 OR52N4 OR52N5 OR52N1 OR52N2 OR52E6 OR52E8 OR52E4 OR56A3 OR56A5 OR52L1 OR56A4 OR56A1 OR56B4 OR52B2 OR52W1 C11orf42 FAM160A2 CNGA4 CCKBR PRKCDBP SMPD1 APBB1 HPX TRIM3 ARFIP2 TIMM10B DNHD1 RRP8				

			ILK TAF10 TPP1 DCHS1 MRPL17 GVINP1 OR2AG2 OR2AG1 OR6A2 OR10A5 OR10A2 OR10A4 OR2D2 OR2D3 ZNF215 ZNF214 NLRP14 RBMXL2 MIR302E SYT9 LOC100506258 OLFML1 PPFIBP2 CYB5R2 OVCH2 OR5P2 OR5P3 OR5E1P LOC283299 OR10A6 OR10A3 NLRP10 EIF3F CASC23 TUB TUB-AS1 RIC3 LMO1 STK33 TRIM66 RPL27A SNORA45A SNORA45B ST5 LOC102724784 AKIP1				

			C11orf16 ASCL3 TMEM9B TMEM9B-AS1 NRIP3 SCUBE2 MIR5691 KRT8P41 DENND5A TMEM41B				
chr11	9312068	10012224	TMEM41B IPO7 SNORA23 LOC644656 ZNF143 WEE1 SWAP70 LOC440028 SBF2-AS1 SBF2 LOC101928008	1.25557	0.965728	14	11.3253
chr14	84228005	85128232	-	-1.04811	0.081776	17	10.7958
chrX	29445701	56760650	IL1RAPL1 MAGEB2 MAGEB3 MAGEB4 MAGEB1 NR0B1 CXorf21 GK TAB3 FTHL17 DMD MIR3915 MIR548F5 FAM47A TMEM47 FAM47B MAGEB16 CFAP47 RP11-87M18.2 FAM47C FTH1P18 PRRG1 LANCL3 XK	-1.0741	0.151218	534	408.442

			CYBB DYNLT3 HYPM SYTL5 MIR548AJ2 SRPX RPGR OTC TSPAN7 MID1IP1-AS1 MID1IP1 LINC01281 LINC01282 MIR3937 MIR1587 BCOR LOC101927476 ATP6AP2 MPC1L CXorf38 MED14 MED14OS LOC100132831 USP9X MIR7641-2 DDX3X NYX CASK GPR34 GPR82 PPP1R2P9 LOC101927501 MAOA MAOB NDP EFHC2 FUNDC1 DUSP21 KDM6A CXorf36 LINC01204 LOC392452 MIR221 MIR222 LOC401585 LINC01186				

			KRBOX4 ZNF674 ZNF674-AS1 CHST7 SLC9A7 RP2 LINC01545 JADE3 RGN NDUFB11 RBM10 UBA1 INE1 CDK16 USP11 ZNF157 SNORA11C ZNF41 LINC01560 ARAF SYN1 TIMP1 MIR4769 CFP ELK1 UXT UXT-AS1 CXXC1P1 ZNF81 ZNF182 SPACA5 SPACA5B ZNF630-AS1 ZNF630 SSX6 SSX5 SSX1 SSX9 SSX3 SSX4B SSX4 SLC38A5 FTSJ1 PORCN EBP TBC1D25				

			RBM3 WDR13 WAS SUV39H1 GLOD5 GATA1 HDAC6 ERAS PCSK1N TIMM17B PQBP1 SLC35A2 PIM2 OTUD5 KCND1 GRIPAP1 TFE3 CCDC120 PRAF2 WDR45 GPKOW MAGIX PLP2 PRICKLE3 SYP SYP-AS1 CACNA1F CCDC22 FOXP3 PPP1R3F GAGE10 GAGE12D GAGE12J GAGE2D GAGE13 GAGE2E GAGE8 GAGE12F GAGE12G GAGE4 GAGE6 GAGE5 GAGE12I GAGE7 GAGE12C GAGE12H				

			GAGE12E GAGE12B GAGE2A GAGE2B GAGE2C GAGE1 PAGE1 PAGE4 USP27X-AS1 USP27X CLCN5 MIR532 MIR188 MIR500A MIR362 MIR501 MIR500B MIR660 MIR502 AKAP4 CCNB3 DGKK SHROOM4 BMP15 LINC01284 NUDT10 CXorf67 NUDT11 LINC01496 CENPVP2 CENPVP1 GSPT2 MAGED1 MAGED4 MAGED4B SNORA11D SNORA11E MIR8088 XAGE2 XAGE1E XAGE1B SSX8 SSX7 SSX2B SSX2 SPANXN5				

			XAGE5 XAGE3 FAM156A FAM156B GPR173 TSPYL2 KANTR KDM5C MIR6895 MIR6894 IQSEC2 SMC1A MIR6857 RIBC1 HSD17B10 HUWE1 MIR98 MIRLET7F2 PHF8 FAM120C WNK3 TSR2 FGD1 GNL3L ITIH6 MAGED2 SNORA11 TRO PFKFB1 APEX2 ALAS2 PAGE2B PAGE2 FAM104B MTRNR2L10 PAGE5 PAGE3 LOC100421746 MIR4536-2 MIR4536-1 MAGEH1 USP51 FOXR2 RRAGB KLF8 UBQLN2				

			LINC01420 UQCRBP1				
chrX	58056987	62412542	-	-1.23988	0.118965	86	55.0013

Table S3 GSEA of curated gene sets (C2) identified in Par compared to GemR, both treated with thapsigargin.

Ranking	NAME	NES	FDR
1	KRIGE_AMINO_ACID_DEPRIVATION	2.37	0.00
2	HELLER_SILENCED_BY_METHYLATION_DN	2.35	0.00
3	TIEN_INTESTINE_PROBIOTICS_24HR_DN	2.24	0.00
4	CHEN_HOXA5_TARGETS_9HR_UP	2.22	0.00
5	BLUM_RESPONSE_TO_SALIRASIB_UP	2.20	0.00
6	MCMURRAY_TP53_HRAS_COOPERATION_RESPONSE_UP	2.18	0.00
7	HUANG_FOXA2_TARGETS_UP	2.17	0.00
8	PACHER_TARGETS_OF_IGF1_AND_IGF2_UP	2.12	0.00
9	RICKMAN_HEAD_AND_NECK_CANCER_A	2.12	0.00
10	MADAN_DPPA4_TARGETS	2.11	0.00
11	NAKAMURA_CANCER_MICROENVIRONMENT_DN	2.05	0.01
12	VALK_AML_CLUSTER_2	2.04	0.01
13	CUI_GLUCOSE_DEPRIVATION	2.04	0.01
14	REACTOME_UNFOLDED_PROTEIN_RESPONSE_UPR	2.03	0.01
15	ZHAN_MULTIPLE_MYELOMA_CD1_VS_CD2_UP	2.02	0.01
16	TAKEDA_TARGETS_OF_NUP98_HOXA9_FUSION_16D_DN	2.00	0.01
17	HELLER_HDAC_TARGETS_DN	2.00	0.01
18	HOLLERN_EMT_BREAST_TUMOR_DN	1.99	0.01
19	DELPUECH_FOXO3_TARGETS_DN	1.98	0.01
20	BHATI_G2M_ARREST_BY_2METHOXYESTRADIOL_DN	1.97	0.01
21	LIN_NPAS4_TARGETS_DN	1.96	0.01
22	ZHAN_MULTIPLE_MYELOMA_CD1_UP	1.94	0.02
23	HUNSBERGER_EXERCISE_REGULATED_GENES	1.93	0.02
24	LIANG_SILENCED_BY_METHYLATION_UP	1.92	0.02
25	REACTOME_CELL_CELL_JUNCTION_ORGANIZATION	1.91	0.02
26	POOLA_INVASIVE_BREAST_CANCER_UP	1.90	0.03
27	REACTOME_TIGHT_JUNCTION_INTERACTIONS	1.90	0.03
28	REACTOME_PERK_REGULATES_GENE_EXPRESSION	1.89	0.03
29	MORI_PLASMA_CELL_UP	1.88	0.03
30	AIGNER_ZEB1_TARGETS	1.88	0.03
31	REACTOME_CYTOSOLIC_TRNA_AMINOACYLATION	1.86	0.04
32	NIKOLSKY_BREAST_CANCER_15Q26_AMPLICON	1.85	0.05
33	REACTOME_INTRA_GOLGI_TRAFFIC	1.84	0.05
34	CEBALLOS_TARGETS_OF_TP53_AND_MYC_DN	1.83	0.06
35	VALK_AML_CLUSTER_13	1.81	0.07
36	WAMUNYOKOLI_OVARIAN_CANCER_GRADES_1_2_UP	1.81	0.07
37	KEGG_TIGHT_JUNCTION	1.80	0.07
38	CHIANG_LIVER_CANCER_SUBCLASS_CTNNB1_DN	1.79	0.08
39	REACTOME_ATF4_ACTIVATES_GENES_IN_RESPONSE_TO_ENDOPLASMIC_RETICULUM_STRESS	1.79	0.08
40	BORCZUK_MALIGNANT_MESOTHELIOMA_DN	1.79	0.08

41	PLASARI_NFIC_TARGETS_BASAL_UP	1.78	0.08
42	GARGALOVIC_RESPONSE_TO_OXIDIZED_PHOSPHOLIPIDS_RED_UP	1.78	0.08
43	PASQUALUCCI_LYMPHOMA_BY_GC_STAGE_UP	1.78	0.08
44	CORRE_MULTIPLE_MYELOMA_UP	1.78	0.08
45	LIU_PROSTATE_CANCER_UP	1.78	0.08
46	KANG_FLUOROURACIL_RESISTANCE_DN	1.78	0.08
47	MIKKELSEN_ES_ICP_WITH_H3K4ME3_AND_H3K27ME3	1.77	0.08
48	TARTE_PLASMA_CELL_VS_B_LYMPHOCYTE_UP	1.77	0.08
49	HELLER_HDAC_TARGETS_SILENCED_BY_METHYLATION_DN	1.76	0.09
50	LIN_SILENCED_BY_TUMOR_MICROENVIRONMENT	1.76	0.09
51	CHUANG_OXIDATIVE_STRESS_RESPONSE_UP	1.76	0.08
52	ANDERSEN_CHOLANGIOCARCINOMA_CLASS2	1.76	0.08
53	YAO_TEMPORAL_RESPONSE_TO_PROGESTERONE_CLUSTER_11	1.76	0.09
54	REACTOME_IRE1ALPHA_ACTIVATES_CHAPERONES	1.76	0.09
55	FURUKAWA_DUSP6_TARGETS_PCI35_DN	1.76	0.08
56	KEGG_TYPE_I_DIABETES_MELLITUS	1.75	0.09
57	HUANG_GATA2_TARGETS_DN	1.74	0.10
58	PID_SHP2_PATHWAY	1.73	0.11
59	WESTON_VEGFA_TARGETS	1.73	0.11
60	REACTOME_SIGNALING_BY_NTRK2_TRKB	1.72	0.12
61	HANN_RESISTANCE_TO_BCL2_INHIBITOR_DN	1.72	0.12
62	COLIN_PILOCYTIC_ASTROCYTOMA_VS_GLIOBLASTOMA_UP	1.72	0.12
63	YANG_BREAST_CANCER_ESR1_BULK_DN	1.71	0.12
64	FISCHER_G2_M_CELL_CYCLE	1.71	0.12
65	REACTOME_COLLAGEN_CHAIN_TRIMERIZATION	1.71	0.12
66	KRASNOSELSKAYA_ILF3_TARGETS_DN	1.71	0.12
67	ZWANG_EGF_INTERVAL_UP	1.70	0.13
68	HOFMANN_MYELODYSPLASTIC_SYNDROM_RISK_UP	1.70	0.13
69	NABA_COLLAGENS	1.70	0.13
70	KIM_LIVER_CANCER_POOR_SURVIVAL_DN	1.69	0.13
71	NADERI_BREAST_CANCER_PROGNOSIS_UP	1.69	0.14
72	URS_ADIPOCYTE_DIFFERENTIATION_DN	1.68	0.14
73	FARMER_BREAST_CANCER_CLUSTER_2	1.68	0.14
74	KEGG_PRION_DISEASES	1.68	0.14
75	MURAKAMI_UV_RESPONSE_6HR_UP	1.68	0.14
76	PID_CMYB_PATHWAY	1.68	0.14
77	FARMER_BREAST_CANCER_BASAL_VS_LULMINAL	1.68	0.14
78	BOYAULT_LIVER_CANCER_SUBCLASS_G6_DN	1.67	0.14
79	SMITH_TERT_TARGETS_UP	1.67	0.14
80	SU_PLACENTA	1.67	0.15
81	ROZANOV_MMP14_TARGETS_UP	1.66	0.15
82	BENPORATH_ES_1	1.66	0.16

83	HOWLIN_CITED1_TARGETS_1_DN	1.66	0.16
84	LIM_MAMMARY_LUMINAL_PROGENITOR_UP	1.65	0.16
85	ROSS_AML_WITH_AML1_ETO_FUSION	1.65	0.16
86	CHARAFE_BREAST_CANCER_LUMINAL_VS_MESENCHYMAL_UP	1.65	0.17
87	WANG_SMARCE1_TARGETS_UP	1.65	0.17
88	AZARE_NEOPLASTIC_TRANSFORMATION_BY_STAT3_UP	1.65	0.17
89	MAYBURD_RESPONSE_TO_L663536_UP	1.64	0.17
90	SMID_BREAST_CANCER_NORMAL_LIKE_UP	1.64	0.17
91	PANGAS_TUMOR_SUPPRESSION_BY_SMAD1_AND_SMAD5_DN	1.64	0.17
92	NIKOLSKY_BREAST_CANCER_8P12_P11_AMPLICON	1.64	0.16
93	WALLACE_PROSTATE_CANCER_RACE_UP	1.64	0.16
94	JIANG_TIP30_TARGETS_DN	1.64	0.16
95	WESTON_VEGFA_TARGETS_6HR	1.64	0.16
96	CHIBA_RESPONSE_TO_TSA_DN	1.64	0.16
97	NIKOLSKY_BREAST_CANCER_8Q23_Q24_AMPLICON	1.64	0.16
98	REACTOME_NCAM_SIGNALING_FOR_NEURITE_OUT_GROWTH	1.64	0.16
99	MARKEY_RB1_CHRONIC_LOF_DN	1.64	0.16
100	ZHAN_MULTIPLE_MYELOMA_PR_UP	1.64	0.16
101	HOFFMANN_SMALL_PRE_BII_TO_IMMATURE_B_LYMPHOCYTE_DN	1.63	0.16
102	ZWANG_DOWN_BY_2ND_EGF_PULSE	1.63	0.17
103	REACTOME_TRANSPORT_OF_MATURE_TRANSCRIPT_TO_CYTOPLASM	1.63	0.17
104	KEGG_O_GLYCAN_BIOSYNTHESIS	1.63	0.16
105	REACTOME_NOTCH3_INTRACELLULAR_DOMAIN_REGULATES_TRANSCRIPTION	1.63	0.16
106	PID_ECADHERIN_KERATINOCYTE_PATHWAY	1.63	0.17
107	REACTOME_PEPTIDE_LIGAND_BINDING_RECEPTORS	1.63	0.17
108	GROSS_HYPOXIA_VIA_ELK3_DN	1.62	0.17
109	REACTOME_DEGRADATION_OF_THE_EXTRACELLULAR_MATRIX	1.62	0.18
110	TANG_SENESCENCE_TP53_TARGETS_DN	1.62	0.18
111	KORKOLA_EMBRYONIC_CARCINOMA_VS_SEMINOMA_UP	1.62	0.18
112	COLDREN_GEFITINIB_RESISTANCE_UP	1.61	0.18
113	SENGUPTA_NASOPHARYNGEAL_CARCINOMA_WITH_LMP1_DN	1.61	0.18
114	REACTOME_COPI_DEPENDENT_GOLGI_TO_ER_RETROGRADE_TRAFFIC	1.61	0.18
115	WANG_METHYLATED_IN_BREAST_CANCER	1.61	0.18
116	SENESE_HDAC1_AND_HDAC2_TARGETS_UP	1.61	0.18
117	WESTON_VEGFA_TARGETS_3HR	1.61	0.18
118	REACTOME_SYNDECAN_INTERACTIONS	1.61	0.18
119	PODAR_RESPONSE_TO_ADAPHOSTIN_UP	1.60	0.19
120	REACTOME_DOWNSTREAM_SIGNALING_OF_ACTIVATED_FGFR1	1.60	0.19

121	XU_HGF_SIGNALING_NOT_VIA_AKT1_48HR_UP	1.60	0.19
122	MCCLUNG_CREB1_TARGETS_DN	1.60	0.19
123	HOELZEL_NF1_TARGETS_UP	1.60	0.19
124	REACTOME_ECM_PROTEOGLYCANS	1.59	0.19
125	REACTOME_EGFR_DOWNREGULATION	1.59	0.19
126	REACTOME_COLLAGEN_DEGRADATION	1.59	0.19
127	ROVERSI_GLIOMA_COPY_NUMBER_UP	1.59	0.19
128	MIKKELSEN_MEF_HCP_WITH_H3K27ME3	1.59	0.19
129	WOOD_EBV_EBNA1_TARGETS_DN	1.59	0.19
130	TSENG_ADIPOGENIC_POTENTIAL_UP	1.59	0.19
131	PID_FRA_PATHWAY	1.59	0.19
132	MOLENAAR_TARGETS_OF_CCND1_AND_CDK4_DN	1.59	0.19
133	KANG_DOXORUBICIN_RESISTANCE_DN	1.59	0.19
134	CHARAFE_BREAST_CANCER_LUMINAL_VS_BASAL_UP	1.59	0.19
135	REACTOME_NUCLEAR_PORE_COMPLEX_NPC_DISASSEMBLY	1.58	0.19
136	REACTOME_COLLAGEN_FORMATION	1.58	0.20
137	ONDER_CDH1_TARGETS_3_UP	1.58	0.20
138	LIU_SMARCA4_TARGETS	1.58	0.20
139	VALK_AML_WITH_FLT3_ITD	1.58	0.20
140	GRUETZMANN_PANCREATIC_CANCER_DN	1.57	0.21
141	SHAFFER_IRF4_TARGETS_IN_PLASMA_CELL_VS_MATURE_B_LYMPHOCYTE	1.57	0.21
142	REACTOME_CELL_JUNCTION_ORGANIZATION	1.57	0.21
143	ONDER_CDH1_TARGETS_2_DN	1.57	0.21
144	LANDEMAINE_LUNG_METASTASIS	1.57	0.21
145	WILLIAMS_ESR1_TARGETS_UP	1.57	0.21
146	REACTOME_COLLAGEN_BIOSYNTHESIS_AND_MODIFYING_ENZYMES	1.56	0.21
147	BILANGES_SERUM_SENSITIVE_VIA_TSC2	1.56	0.22
148	IIZUKA_LIVER_CANCER_PROGRESSION_G1_G2_DN	1.56	0.22
149	ANDERSEN_CHOLANGIOCARCINOMA_CLASS1	1.56	0.22
150	MARCHINI_TRABECTEDIN_RESISTANCE_DN	1.56	0.22
151	LEE_LIVER_CANCER_MYC_UP	1.56	0.21
152	REACTOME_MET_ACTIVATES_PTK2_SIGNALING	1.56	0.22
153	CHARAFE_BREAST_CANCER_BASAL_VS_MESENCHYMAL_UP	1.55	0.22
154	FLORIO_NEOCORTEX_BASAL_RADIAL_GLIA_DN	1.55	0.22
155	BIOCARTA_ARAP_PATHWAY	1.55	0.22
156	REACTOME_FORMATION_OF_THE_CORNIFIED_ENVELOPE	1.55	0.22
157	ADDYA_ERYTHROID_DIFFERENTIATION_BY_HEMIN	1.55	0.22
158	GARGALOVIC_RESPONSE_TO_OXIDIZED_PHOSPHOLIPIDS_BLACK_UP	1.55	0.22
159	BOSCO_EPITHELIAL_DIFFERENTIATION_MODULE	1.55	0.22
160	REACTOME_TRANSPORT_OF_MATURE_MRNAS_DERIVED_FROM_INTRONLESS_TRANSCRIPTS	1.55	0.22

161	DACOSTA_ERCC3_ALLELE_XPCS_VS_TTD_DN	1.55	0.22
162	KEGG_ALANINE_ASPARTATE_AND_GLUTAMATE_METABOLISM	1.55	0.22
163	KATSANOU_ELAVL1_TARGETS_UP	1.54	0.23
164	GAUSSMANN_MLL_AF4_FUSION_TARGETS_F_DN	1.54	0.23
165	WANG_RESPONSE_TO_BEXAROTENE_UP	1.54	0.23
166	GHANDHI_BYSTANDER_IRRADIATION_UP	1.54	0.24
167	NOJIMA_SFRP2_TARGETS_UP	1.53	0.23
168	REACTOME_SIGNALING_BY_WNT_IN_CANCER	1.53	0.23
169	BURTON_ADIPOGENESIS_12	1.53	0.23
170	CHIARADONNA_NEOPLASTIC_TRANSFORMATION_CDC25_UP	1.53	0.23
171	REACTOME_SIGNALING_BY_FGFR1	1.53	0.23
172	KANG_IMMORTALIZED_BY_TERT_UP	1.53	0.24
173	SMID_BREAST_CANCER_RELAPSE_IN_BONE_DN	1.53	0.23
174	NABA_CORE_MATRISOME	1.53	0.24
175	BERNARD_PPAPDC1B_TARGETS_DN	1.53	0.24
176	MORI_EMU_MYC_LYMPHOMA_BY_ONSET_TIME_DN	1.53	0.24
177	REACTOME_ION_TRANSPORT_BY_P_TYPE_ATPASES	1.53	0.24
178	NAGASHIMA_NRG1_SIGNALING_UP	1.52	0.24
179	BILD_HRAS_ONCOGENIC_SIGNATURE	1.52	0.24
180	FINETTI_BREAST_CANCER_KINOME_RED	1.52	0.24
181	SESTO_RESPONSE_TO_UV_C2	1.52	0.24
182	TERAMOTO_OPN_TARGETS_CLUSTER_7	1.52	0.24
183	CHO_NR4A1_TARGETS	1.52	0.24
184	REACTOME_PLASMA_LIPOPROTEIN_ASSEMBLY_REMODELING_AND_CLEARANCE	1.52	0.24
185	HOLLERN_MICROACINAR_BREAST_TUMOR_UP	1.52	0.24
186	REACTOME_SYNTHESIS_OF_VERY_LONG_CHAIN_FATTY_ACYL_COAS	1.52	0.24
187	WENG_POR_TARGETS_GLOBAL_DN	1.52	0.24
188	NABA_MATRISOME	1.52	0.24
189	REACTOME_CELL_CELL_COMMUNICATION	1.52	0.24
190	SHI_SPARC_TARGETS_UP	1.52	0.24
191	SWEET_KRAS_ONCOGENIC_SIGNATURE	1.52	0.24
192	GAUSSMANN_MLL_AF4_FUSION_TARGETS_A_DN	1.52	0.24
193	WANG_CISPLATIN_RESPONSE_AND_XPC_UP	1.52	0.24
194	REICHERT_MITOSIS_LIN9_TARGETS	1.51	0.24
195	TURASHVILI_BREAST_LOBULAR_CARCINOMA_VS_DUCTAL_NORMAL_UP	1.51	0.24
196	PID_GLYPICAN_1PATHWAY	1.51	0.24
197	MARCINIAK_ER_STRESS_RESPONSE_VIA_CHOP	1.51	0.24
198	ONDER_CDH1_TARGETS_1_DN	1.51	0.24
199	PID_SYNDECAN_1_PATHWAY	1.51	0.24
200	REACTOME_BINDING_AND_UPTAKE_OF_LIGANDS_BY_SCAVENGER_RECEPTORS	1.51	0.25

201	TURASHVILI_BREAST_DUCTAL_CARCINOMA_VS_DUCTAL_NORMAL_UP	1.51	0.25
202	YAMAZAKI_TCEB3_TARGETS_UP	1.51	0.25
203	REACTOME_KERATINIZATION	1.51	0.25
204	REACTOME_EXTRACELLULAR_MATRIX_ORGANIZATION	1.50	0.25

Table S4 Genes comprised in DN-reversed and UP-reversed clusters.

DN-reversed genes	UP-reversed genes
CHAC1	KRT14
AAK1	EGR3
DDIT3	NOV
C8orf4	NR4A3
SESN2	NFATC2
HERPUD1	FOSB
ZSCAN12P1	MMP10
ADM2	KLF4
TNFRSF9	KDM7A
ADAMTSL4	ADGRF4
ZNF165	VGLL3
TSC22D3	SOCS1
ADPRM	MAP3K8
STC2	NR4A1
SLC7A11-AS1	PELI1
DDIT4	TRIM36
AIM1	RFX2
TRIB3	CLDN4
BHLHA15	ABTB2
ULBP1	SECTM1
CDH15	ANKRD37
LINC00365	TPPP
ANG	GAREM
SLC38A2	TCTEX1D4
ANKRD11	WNT9A
ISL2	UNC5B
CEBPB	BTBD19
FICD	DENND2C
HSPA5	MAP1B
ARHGAP29	SOWAHC
CBX4	NKX6-1
FLJ46906	LIF
RNF144B	PLK3
ARMCX5	LOC101928841
SDF2L1	PAG1
MSTO2P	ARID5B
ZNF222	HDAC5
SLFN5	INSIG1
SEC24D	ELF3
AVIL	ZBTB43
ZFP69B	JUND
HBEGF	KLF7
VEGFA	SGMS2

CTH	DCLK1
RWDD2A	FOXO6
NCOA7	DYRK3
CCNG2	GPR87
SLC6A9	MAST4
ZNF555	MIR100HG
GADD45B	EPPK1
PNPLA8	STK17B
FRAT1	SYBU
SLFN11	TRPS1
PLEKHA6	FAM83B
C9orf84	IL16
C9orf91	BCL6
C14orf28	IRX4
TMEM154	UGDH
APTR	CA13
ATF7IP2	EFNB2
ERN1	SPATA7
PRKG2	PDLIM3
CARS	TTLL7
RNASE4	MAK
CCDC171	AGPAT4
CCDC173	MFSD2A
LOC100272217	SLC4A7
CHD2	CASP9
CCDC71L	ANXA1
DUSP16	PRDM1
FAM214A	ZSWIM6
TSPYL2	DGKD
ERO1B	AKR7A2P1
MIS12	FAM46C
NBEAL1	SERPINE1
DNAJC6	FHL2
TES	ANKRD42
CDH1	LINC00473
FAM84B	AATK
HSPA13	RAPH1
CCDC149	SERPINB5
CDKN2B	LINC00707
GDF15	PPP1R15B
MTMR4	JARID2
PRRC1	MVD
MANF	IGF2BP2
TMEM50B	MAPK8IP1
FBXO16	LINC00880
RAB33B	C11orf98

ZNF217	CMTM3
SNX22	DLX1
NBR2	FGF18
AREG	FOXD2
SLC7A1	GBX2
CNOT3	GINS2
SEL1L	IL22RA1
XDH	KCTD2
BTG1	LFNG
CPEB3	LRRC3
THAP5	LSM11
SYVN1	MGC57346
ATF4	FOXF2
CTAGE5	TIGD5
CTGF	ACTR5
TMEM47	THAP11
CYB561	MFSD5
XRRA1	NRARP
PPM1E	LMNB1
PRICKLE1	SALL2
C4orf32	KLHL42
DDN	RHOV
STX5	HSPA8
MZF1	GINS1
CEP120	ABHD17C
HYOU1	SOX4
CCDC186	MAP6D1
TULP3	CALML4
MSTO1	NR2F6
DLC1	TSKU
PDCD4	SKP2
DMTF1	XYLT2
GTPBP2	TFAP2E
DNAAF3	SOX7
MOSPD2	PRAME
BRD2	MEX3A
ZMYM5	PPARGC1B
IFRD1	KANK2
SOS2	SMAD6
OSBP	TNFAIP8L1
ELL2	GEMIN4
GOLPH3L	TPRG1
EAF2	LOC441666
ECM2	UBL4A
EDEM1	BCL7A
PLIN5	DUSP2

MAP1LC3B	TRIM7
EGFR	CDCA4
EID3	IER5L
TMEM263	SOX2
TUBB3	GAS1
BIRC2	XKR8
PDIA4	ZC3HAV1L
ANKRD12	ZNF775
DERL2	
EIF1B	
AKAP13	
PJA2	
EML2-AS1	
EPB41L4A-AS1	
EPC2	
HOXB9	
GARS	
ESRP1	
GOLGA5	
NIT1	
GZF1	
FNDC3B	
SNX9	
FAM129A	
NFKB2	
PHYKPL	
FAM86B3P	
FAM86HP	
WDR25	
DNAJB11	
PPAPDC1B	
HSP90B2P	
INTS6	
FBXO32	
RIOK3	
CRELD2	
ATP2A2	
FLRT1	
FN3K	
SLCO1A2	
HSP90B1	
FREM2	
NUDT4	
FSIP1	
MC1R	
ETV5	

AARS	
THAP9-AS1	
KDM6A	
C17orf100	
TRIM39	
TVP23C	
CEBPG	
GOT1	
LMO4	
MIA3	
DDX59	
GPRASP1	
GRB10	
KDM4A	
SH2B3	
UFL1	
FAM53C	
UBA6-AS1	
HEATR5A	
WARS	
RNF41	
HID1	
OSMR	
SLC38A1	
SH3BP2	
CDC6	
ARFGAP3	
UBE2J1	
C1orf226	
SEC16A	
CCDC174	
IL13RA2	
BACH1	
ZCCHC8	
IL1A	
IL7R	
INO80	
INSIG2	
CHMP4C	
RNF113A	
PABPC1L	
CALCOCO2	
IFI16	
TUBE1	
GPT2	
EGR1	

ARMCX3	
MAGT1	
TARS	
KLF15	
TUFT1	
BET1	
SHCBP1	
SLC35B1	
JMY	
LARP6	
TMEM39A	
LINC00176	
LINC00662	
C6orf48	
DUSP5	
SLC7A11	
LINC01348	
C17orf51	
LOC100499484	
LOC344887	
LOC729218	
SUCO	
LPXN	
LRIF1	
SLC39A14	
EPRS	
TRIM38	
SERP1	
SEC23B	
NFE2L2	
MCFD2	
MOCOS	
MTHFD2	
TXNRD1	
MZF1-AS1	
NEBL	
NFXL1	
NLRP1	
NOS1AP	
NUCB2	
OSBPL6	
PAQR6	
ELMSAN1	
PRKCZ	
PSPH	
PTPN14	

PTPRH	
PXDN	
PYROXD1	
RHOQ	
RP1L1	
RPE65	
RASSF6	
S100A1	
SELPLG	
SERPINB8	
SGPP2	
SLC1A4	
SLC22A15	
SMG1P3	
SNHG8	
ZNF773	
SP1	
SPEF2	
SPTBN5	
ZNF568	
STK40	
STPG1	
SYT5	
TFAP2A	
INHBE	
TJP1	
TMED7	
TMEM214	
TMEM40	
TNFSF18	
LAMP3	
KCNG1	
TTC25	
U2AF1L4	
UBE2Q2P2	
UHRF1BP1	
IL1B	
USP6NL	
VLDLR	
VLDLR-AS1	
AHRR	
ZBED3	
ZBED6	
ZDHHC11	
HMOX1	
ZKSCAN1	

ZNF184	
ZNF280C	
ZNF432	
ARHGAP25	
EPGN	
ZNF529	
FKBP9P1	
ZNF614	
ZNF630	
ZNF674	
ZNF697	
ZNF814	
OLR1	
ZNF841	
ZXDA	
GATA4	
ERCC6L	
PPIF	
AMD1	
RPP25	
MCM10	
LRP3	
LMTK3	
ALX1	
CHST10	
PRKCQ-AS1	
PLCL2	
JPH1	
ESRP2	
WNT7A	
ZNF850	
TNS4	
PSRC1	
E2F8	
AMIGO1	
PRDM13	
PLD6	
MANEAL	
FAM155B	
KIF18B	
RGS3	
CCNF	
MARVELD3	
AXIN2	
HES1	
NTF3	

E2F2 LOC101927318 MTCL1 COL26A1	

Table S5 GSEA of curated gene sets (C2) identified in GemR compared to STIM1-depleted GemR, both treated with thapsigargin.

Ranking	NAME	NES	FDR
1	AMIT_SERUM_RESPONSE_40_MCF10A	2.43	0.00
2	SMIRNOV_RESPONSE_TO_IR_2HR_UP	2.35	0.00
3	HORTON_SREBF_TARGETS	2.35	0.00
4	QI_HYPOXIA	2.32	0.00
5	DAZARD_RESPONSE_TO_UV_NHEK_UP	2.31	0.00
6	PICCALUGA_ANGIOIMMUNOBLASTIC_LYMPHOMA_DN	2.27	0.00
7	SCHMIDT_POR_TARGETS_IN_LIMB_BUD_UP	2.27	0.00
8	JAEGER_METASTASIS_DN	2.24	0.00
9	DAZARD_UV_RESPONSE_CLUSTER_G2	2.22	0.00
10	REACTOME_KERATINIZATION	2.21	0.00
11	REACTOME_FORMATION_OF_THE_CORNIFIED_ENVELOPE	2.20	0.00
12	NAGASHIMA_NRG1_SIGNALING_UP	2.19	0.00
13	SMIRNOV_RESPONSE_TO_IR_6HR_DN	2.18	0.00
14	REACTOME_CHOLESTEROL_BIOSYNTHESIS	2.17	0.00
15	UZONYI_RESPONSE_TO_LEUKOTRIENE_AND_THROMBIN	2.15	0.00
16	RASHI_RESPONSE_TO_IONIZING_RADIATION_1	2.15	0.00
17	NAGASHIMA_EGF_SIGNALING_UP	2.14	0.00
18	ZWANG_CLASS_3_TRANSIENTLY_INDUCED_BY_EGF	2.14	0.00
19	AMIT_EGF_RESPONSE_40_HELA	2.13	0.00
20	OSWALD_HEMATOPOIETIC_STEM_CELL_IN_COLLAGEN_GEL_UP	2.12	0.00
21	CHEN_LVAD_SUPPORT_OF_FAILING_HEART_UP	2.10	0.00
22	WANG_BARRETTS_ESOPHAGUS_AND_ESOPHAGUS_CANCER_DN	2.06	0.00
23	CROMER_METASTASIS_DN	2.05	0.00
24	BERENJENO_TRANSFORMED_BY_RHOA_REVERSIBLY_DN	2.04	0.01
25	SEMENZA_HIF1_TARGETS	2.04	0.01
26	DELLA_RESPONSE_TO_TSA_AND_BUTYRATE	2.04	0.01
27	RODRIGUES_NTN1_AND_DCC_TARGETS	2.03	0.01
28	KEGG_CYTOKINE_CYTOKINE_RECEPTOR_INTERACTION	2.03	0.01
29	BURTON_ADIPOGENESIS_PEAK_AT_2HR	2.03	0.01
30	FARDIN_HYPOXIA_11	2.03	0.01
31	HAHTOLA_MYCOSIS_FUNGOIDES_CD4_UP	2.03	0.01
32	PEREZ_TP53_AND_TP63_TARGETS	2.02	0.01
33	INGA_TP53_TARGETS	2.02	0.01
34	PLASARI_TGFB1_TARGETS_10HR_UP	2.02	0.01
35	SANSOM_APC_TARGETS_UP	2.00	0.01
36	HUPER_BREAST_BASAL_VS_LUMINAL_UP	2.00	0.01
37	WARTERS_IR_RESPONSE_5GY	1.99	0.01
38	KIM_WT1_TARGETS_UP	1.99	0.01

39	REACTOME_REGULATION_OF_CHOLESTEROL_BIOSYNTHESIS_BY_SREBP_SREBF	1.98	0.01
40	SASSON_RESPONSE_TO_GONADOTROPHINS_DN	1.98	0.01
41	AMIT_SERUM_RESPONSE_60_MCF10A	1.98	0.01
42	GENTILE_UV_RESPONSE_CLUSTER_D8	1.98	0.01
43	DAZARD_UV_RESPONSE_CLUSTER_G4	1.98	0.01
44	LE_EGR2_TARGETS_DN	1.97	0.01
45	REACTOME_ACTIVATION_OF_GENE_EXPRESSION_BY_SREBF_SREBP	1.97	0.01
46	PID_DELTA_NP63_PATHWAY	1.96	0.01
47	PHONG_TNF_TARGETS_UP	1.96	0.01
48	ZHOU_INFLAMMATORY_RESPONSE_LIVE_UP	1.96	0.01
49	BILD_HRAS_ONCOGENIC_SIGNATURE	1.95	0.01
50	PODAR_RESPONSE_TO_ADAPHOSTIN_DN	1.95	0.01
51	PEREZ_TP63_TARGETS	1.95	0.01
52	HOLLERN_SQUAMOUS_BREAST_TUMOR	1.94	0.01
53	DAUER_STAT3_TARGETS_UP	1.94	0.01
54	TAKEDA_TARGETS_OF_NUP98_HOXA9_FUSION_6HR_DN	1.94	0.01
55	PROVENZANI_METASTASIS_DN	1.94	0.01
56	WILLERT_WNT_SIGNALING	1.94	0.01
57	SARRIO_EPITHELIAL_MESENCHYMAL_TRANSITION_DN	1.93	0.01
58	RICKMAN_METASTASIS_DN	1.93	0.01
59	SCHAEFFER_PROSTATE_DEVELOPMENT_48HR_DN	1.92	0.01
60	CHOW_RASSF1_TARGETS_DN	1.92	0.02
61	TURASHVILI_BREAST_DUCTAL_CARCINOMA_VS_LOBULAR_NORMAL_DN	1.92	0.01
62	WARTERS_RESPONSE_TO_IR_SKIN	1.92	0.02
63	REACTOME_PI3K_AKT_SIGNALING_IN_CANCER	1.91	0.02
64	BENPORATH_PRC2_TARGETS	1.91	0.02
65	BROCKE_APOPTOSIS_REVERSED_BY_IL6	1.90	0.02
66	DORN_ADENOVIRUS_INFECTION_48HR_DN	1.90	0.02
67	QUINTENS_EMBRYONIC_BRAIN_RESPONSE_TO_IR	1.90	0.02
68	PHONG_TNF_RESPONSE_VIA_P38_PARTIAL	1.90	0.02
69	PEART_HDAC_PROLIFERATION_CLUSTER_UP	1.89	0.02
70	REACTOME_IRS_MEDIATED_SIGNALLING	1.89	0.02
71	DIRMEIER_LMP1_RESPONSE_EARLY	1.88	0.02
72	NAKAMURA_METASTASIS	1.88	0.02
73	DORN_ADENOVIRUS_INFECTION_32HR_DN	1.88	0.02
74	GESERICK_TERT_TARGETS_DN	1.88	0.02
75	KEGG_P53_SIGNALING_PATHWAY	1.88	0.02
76	AMIT_EGF_RESPONSE_60_HELA	1.87	0.02
77	RICKMAN_TUMOR_DIFFERENTIATED_WELL_VS_POORLY_DN	1.87	0.02
78	FARMER_BREAST_CANCER_CLUSTER_7	1.87	0.02
79	KOBAYASHI_EGFR_SIGNALING_6HR_DN	1.87	0.02
80	TIAN_TNF_SIGNALING_NOT_VIA_NFKB	1.87	0.02

81	REACTOME_DOWNSTREAM_SIGNALING_OF_ACTIVATED_FGFR4	1.87	0.02
82	PODAR_RESPONSE_TO_ADAPHOSTIN_UP	1.87	0.02
83	ZHANG_ANTIVIRAL_RESPONSE_TO_RIBAVIRIN_DN	1.86	0.02
84	PID_TCR_CALCIUM_PATHWAY	1.86	0.02
85	BOYLAN_MULTIPLE_MYELOMA_PCA3_UP	1.86	0.02
86	DAZARD_UV_RESPONSE_CLUSTER_G1	1.86	0.02
87	PECE_MAMMARY_STEM_CELL_UP	1.86	0.02
88	REACTOME_SIGNALING_BY_TYPE_1_INSULIN_LIKE_GROWTH_FACTOR_1_RECEPTOR_IGF1R	1.86	0.02
89	PID_REG_GR_PATHWAY	1.85	0.02
90	KEGG_STEROID_BIOSYNTHESIS	1.85	0.02
91	REACTOME_GAP_JUNCTION_ASSEMBLY	1.85	0.03
92	PID_NFAT_TFPATHWAY	1.85	0.03
93	TENEDINI_MEGAKARYOCYTE_MARKERS	1.84	0.03
94	BROWNE_HCMV_INFECTION_2HR_UP	1.84	0.03
95	SESTO_RESPONSE_TO_UV_C7	1.84	0.03
96	MIKKELSEN_NPC_HCP_WITH_H3K4ME3_AND_H3K27ME3	1.84	0.03
97	BIOCARTA_FCER1_PATHWAY	1.84	0.03
98	SASSON_RESPONSE_TO_FORSKOLIN_DN	1.83	0.03
99	MENSE_HYPOXIA_UP	1.82	0.03
100	GHANDHI_DIRECT_IRRADIATION_UP	1.82	0.03
101	GU_PDEF_TARGETS_DN	1.82	0.03
102	JECHLINGER_EPITHELIAL_TO_MESENCHYMAL_TRANSITION_DN	1.82	0.03
103	REACTOME_ATTENUATION_PHASE	1.82	0.03
104	HOFFMANN_PRE_BI_TO_LARGE_PRE_BII_LYMPHOCYTE_UP	1.82	0.03
105	PID_HIF1_TFPATHWAY	1.82	0.03
106	BENPORATH_EED_TARGETS	1.82	0.03
107	SABATES_COLORECTAL_ADENOMA_UP	1.82	0.03
108	REACTOME_GAP_JUNCTION_TRAFFICKING_AND_REGULATION	1.81	0.03
109	BASSO_CD40_SIGNALING_DN	1.81	0.03
110	YAMASHITA_LIVER_CANCER_STEM_CELL_UP	1.81	0.03
111	BRACHAT_RESPONSE_TO_METHOTREXATE_UP	1.81	0.03
112	KOBAYASHI_RESPONSE_TO_ROMIDEPSIN	1.81	0.04
113	MARTORIATI_MDM4_TARGETS_FETAL_LIVER_UP	1.80	0.04
114	ENK_UV_RESPONSE_EPIDERMIS_DN	1.80	0.04
115	WONG_ADULT_TISSUE_STEM_MODULE	1.80	0.04
116	REACTOME_DOWNSTREAM_SIGNALING_OF_ACTIVATED_FGFR3	1.80	0.04
117	HOWLIN_PUBERTAL_MAMMARY_GLAND	1.80	0.04
118	GROSS_HYPOXIA_VIA_HIF1A_DN	1.80	0.04
119	WANG_RESPONSE_TO_FORSKOLIN_UP	1.80	0.04
120	PID_MYC_ACTIV_PATHWAY	1.80	0.04
121	AMIT_SERUM_RESPONSE_240_MCF10A	1.79	0.04

122	ONDER_CDH1_TARGETS_3_DN	1.79	0.04
123	DAZARD_UV_RESPONSE_CLUSTER_G28	1.79	0.04
124	BRACHAT_RESPONSE_TO_CISPLATIN	1.79	0.04
125	FRIDMAN_SENESCENCE_UP	1.79	0.04
126	REACTOME_HSF1_DEPENDENT_TRANSACTIVATION	1.79	0.04
127	MARTORIATI_MDM4_TARGETS_NEUROEPITHELIUM_UP	1.79	0.04
128	NABA_SECRETED_FACTORS	1.79	0.04
129	AMIT_EGF_RESPONSE_120_HELA	1.79	0.04
130	TONKS_TARGETS_OF_RUNX1_RUNX1T1_FUSION_GRANULOCYTE_UP	1.78	0.04
131	PID_FGF_PATHWAY	1.78	0.04
132	MA_MYELOID_DIFFERENTIATION_UP	1.78	0.04
133	KAMIKUBO_MYELOID_MN1_NETWORK	1.78	0.04
134	REACTOME_TRANSPORT_OF_VITAMINS_NUCLEOSIDES_AND_RELATED_MOLECULES	1.78	0.04
135	KYNG_ENVIRONMENTAL_STRESS_RESPONSE_DN	1.77	0.04
136	JECHLINGER_EPITHELIAL_TO_MESENCHYMAL_TRANSITION_UP	1.77	0.04
137	FAELT_B_CLL_WITH_VH_REARRANGEMENTS_UP	1.77	0.04
138	BORLAK_LIVER_CANCER_EGF_UP	1.77	0.04
139	ZWANG_CLASS_2_TRANSIENTLY_INDUCED_BY_EGF	1.77	0.04
140	SARTIPY_BLUNTED_BY_INSULIN_RESISTANCE_UP	1.77	0.04
141	ONDER_CDH1_TARGETS_2_DN	1.77	0.04
142	SEITZ_NEOPLASTIC_TRANSFORMATION_BY_8P_DELETION_DN	1.77	0.04
143	ELVIDGE_HYPOXIA_BY_DMOG_UP	1.77	0.04
144	SCHRAETS_MLL_TARGETS_UP	1.77	0.04
145	PLASARI_TGFB1_SIGNALING_VIA_NFIC_1HR_DN	1.77	0.04
146	WANG_METHYLATED_IN_BREAST_CANCER	1.77	0.04
147	GALINDO_IMMUNE_RESPONSE_TO_ENTEROTOXIN	1.77	0.04
148	STREICHER_LSM1_TARGETS_DN	1.77	0.04
149	MEISSNER_BRAIN_HCP_WITH_H3K4ME2_AND_H3K27ME3	1.76	0.04
150	WINZEN_DEGRADED_VIA_KHSRP	1.76	0.04
151	BOYLAN_MULTIPLE_MYELOMA_C_DN	1.76	0.04
152	LEE_TARGETS_OF_PTCH1_AND_SUFU_UP	1.76	0.04
153	REACTOME_METABOLISM_OF_STEROIDS	1.76	0.04
154	CHANG_IMMORTALIZED_BY_HPV31_DN	1.76	0.04
155	REACTOME_INTERLEUKIN_6_FAMILY_SIGNALING	1.76	0.04
156	GROSS_HYPOXIA_VIA_ELK3_AND_HIF1A_UP	1.76	0.04
157	WELCSH_BRCA1_TARGETS_DN	1.76	0.04
158	PID_CD8_TCR_DOWNSTREAM_PATHWAY	1.76	0.04
159	WINTER_HYPOXIA_UP	1.76	0.04
160	CONRAD_STEM_CELL	1.75	0.04
161	LEONARD_HYPOXIA	1.75	0.04
162	AIYAR_COBRA1_TARGETS_DN	1.75	0.05

163	TONKS_TARGETS_OF_RUNX1_RUNX1T1_FUSION_HSC_DN	1.75	0.05
164	SHIN_B_CELL_LYMPHOMA_CLUSTER_8	1.75	0.05
165	REACTOME_DOWNSTREAM_SIGNALING_OF_ACTIVATED_FGFR2	1.74	0.05
166	PID_MAPK_TRK_PATHWAY	1.74	0.05
167	SHAFFER_IRF4_TARGETS_IN_ACTIVATED_B_LYMPHOCYTE	1.74	0.05
168	AMIT_EGF_RESPONSE_40_MCF10A	1.74	0.05
169	RICKMAN_TUMOR_DIFFERENTIATED_WELL_VS_MODERATELY_DN	1.74	0.05
170	REACTOME_INSULIN_RECEPTOR_SIGNALLING_CASCADE	1.74	0.05
171	PID_WNT_SIGNALING_PATHWAY	1.74	0.05
172	SCHUHMACHER_MYC_TARGETS_UP	1.74	0.05
173	GARGALOVIC_RESPONSE_TO_OXIDIZED_PHOSPHOLIPIDS_BLUE_UP	1.74	0.05
174	KERLEY_RESPONSE_TO_CISPLATIN_UP	1.73	0.05
175	MULLIGHAN_NPM1_MUTATED_SIGNATURE_1_DN	1.73	0.05
176	ENGELMANN_CANCER_PROGENITORS_UP	1.73	0.05
177	CHEN_PDGF_TARGETS	1.73	0.05
178	PID_P53_DOWNSTREAM_PATHWAY	1.73	0.05
179	BROWNE_HCMV_INFECTION_30MIN_UP	1.73	0.05
180	PASINI_SUZ12_TARGETS_DN	1.73	0.05
181	NEMETH_INFLAMMATORY_RESPONSE_LPS_UP	1.72	0.05
182	BENPORATH_SUZ12_TARGETS	1.72	0.05
183	REACTOME_NEGATIVE_REGULATION_OF_MAPK_PATHWAY	1.72	0.05
184	SATO_SILENCED_BY_DEACETYLATION_IN_PANCREATIC_CANCER	1.72	0.05
185	GENTILE_UV_RESPONSE_CLUSTER_D9	1.72	0.05
186	GENTILE_UV_LOW_DOSE_UP	1.72	0.05
187	MULLIGHAN_NPM1_SIGNATURE_3_DN	1.72	0.05
188	REACTOME_CONSTITUTIVE_SIGNALING_BY_ABERRANT_PI3K_IN_CANCER	1.72	0.05
189	KEGG_MELANOMA	1.72	0.05
190	WINTER_HYPOXIA_METAGENE	1.71	0.05
191	PLASARI_TGFB1_TARGETS_1HR_UP	1.71	0.05
192	CAFFAREL_RESPONSE_TO_THC_DN	1.71	0.05
193	ADDYA_ERYTHROID_DIFFERENTIATION_BY_HEMIN	1.71	0.05
194	KEGG_FRUCTOSE_AND_MANNOSE_METABOLISM	1.71	0.05
195	BIOCARTA_ETS_PATHWAY	1.71	0.05
196	GRAESSMANN_RESPONSE_TO_MC_AND_SERUM_DEPRIVATION_DN	1.71	0.05
197	KIM_WT1_TARGETS_8HR_UP	1.71	0.06
198	BILD_E2F3_ONCOGENIC_SIGNATURE	1.71	0.06
199	SMID_BREAST_CANCER_RELAPSE_IN_BONE_DN	1.71	0.06
200	HARRIS_HYPOXIA	1.70	0.06

201	BALDWIN_PRKCI_TARGETS_UP	1.70	0.06
202	BENPORATH_ES_WITH_H3K27ME3	1.70	0.06
203	KYNG_ENVIRONMENTAL_STRESS_RESPONSE_NOT_BY_4NQO_IN_WS	1.70	0.06
204	FIGUEROA_AML_METHYLATION_CLUSTER_5_DN	1.70	0.06
205	NAKAMURA_ADIPOGENESIS_EARLY_UP	1.70	0.06
206	JAATINEN_HEMATOPOIETIC_STEM_CELL_DN	1.70	0.06
207	AUNG_GASTRIC_CANCER	1.70	0.06
208	BROWNE_HCMV_INFECTION_8HR_UP	1.70	0.06
209	CAIRO_PML_TARGETS_BOUND_BY_MYC_UP	1.70	0.06
210	SCIBETTA_KDM5B_TARGETS_DN	1.70	0.06
211	KEGG_ACUTE_MYELOID_LEUKEMIA	1.70	0.06
212	KEGG_PATHOGENIC_ESCHERICHIA_COLI_INFECTION	1.69	0.06
213	BOQUEST_STEM_CELL_CULTURED_VS_FRESH_UP	1.69	0.06
214	DASU_IL6_SIGNALING_SCAR_UP	1.69	0.06
215	PID_SHP2_PATHWAY	1.69	0.06
216	LIM_MAMMARY_STEM_CELL_UP	1.69	0.06
217	TONKS_TARGETS_OF_RUNX1_RUNX1T1_FUSION_MONOCYTE_DN	1.69	0.06
218	ALTEMEIER_RESPONSE_TO_LPS_WITH_MECHANICAL_VENTILATION	1.69	0.06
219	KASLER_HDAC7_TARGETS_1_UP	1.69	0.06
220	DALESSIO_TSA_RESPONSE	1.69	0.06
221	NELSON_RESPONSE_TO_ANDROGEN_UP	1.68	0.07
222	RIZKI_TUMOR_INVASIVENESS_3D_UP	1.68	0.07
223	SHETH_LIVER_CANCER_VS_TXNIP_LOSS_PAM6	1.68	0.07
224	KIM_WT1_TARGETS_12HR_UP	1.68	0.07
225	CEBALLOS_TARGETS_OF_TP53_AND_MYC_UP	1.68	0.07
226	PID_AP1_PATHWAY	1.68	0.07
227	WU_CELL_MIGRATION	1.68	0.07
228	YAMASHITA_LIVER_CANCER_WITH_EPCAM_UP	1.68	0.07
229	MATTIOLI_MULTIPLE_MYELOMA_WITH_14Q32_TRANSLOCATIONS	1.67	0.07
230	REACTOME_HSF1_ACTIVATION	1.67	0.07
231	GROSS_HYPOXIA_VIA_ELK3_ONLY_DN	1.67	0.07
232	MATTIOLI_MGUS_VS_PCL	1.67	0.07
233	REACTOME_SIGNALING_BY_FGFR4	1.67	0.07
234	WANG_ESOPHAGUS_CANCER_VS_NORMAL_DN	1.67	0.07
235	SMID_BREAST_CANCER_LUMINAL_B_DN	1.67	0.07
236	ELVIDGE_HIF1A_TARGETS_DN	1.67	0.07
237	MCMURRAY_TP53_HRAS_COOPERATION_RESPONSE_DN	1.67	0.07
238	NAKAYAMA_FRA2_TARGETS	1.67	0.07
239	LIN_NPAS4_TARGETS_DN	1.67	0.07
240	REACTOME_SIGNALING_BY_FGFR_IN_DISEASE	1.67	0.07
241	KEGG_ARGININE_AND_PROLINE_METABOLISM	1.67	0.07

242	SMIRNOV_RESPONSE_TO_IR_6HR_UP	1.66	0.07
243	TURASHVILI_BREAST_DUCTAL_CARCINOMA_VS_DUCTAL_NORMAL_DN	1.66	0.07
244	AMIT_SERUM_RESPONSE_120_MCF10A	1.66	0.07
245	REACTOME_ASSEMBLY_AND_CELL_SURFACE_PRESENTATION_OF_NMDA_RECEPTORS	1.66	0.07
246	REACTOME_SIGNALING_BY_INSULIN_RECEPTOR	1.66	0.07
247	REACTOME_RAB_GERANYLGERANYLATION	1.66	0.07
248	TING_SILENCED_BY_DICER	1.66	0.07
249	DIAZ_CHRONIC_MEYLOGENOUS_LEUKEMIA_DN	1.66	0.07
250	DOANE_RESPONSE_TO_ANDROGEN_DN	1.66	0.07
251	BURTON_ADIPOGENESIS_10	1.65	0.07
252	SAFFORD_T_LYMPHOCYTE_ANERGY	1.65	0.07
253	DOANE_BREAST_CANCER_ESR1_DN	1.65	0.07
254	DASU_IL6_SIGNALING_UP	1.65	0.08
255	LOPEZ_TRANSLATION_VIA_FN1_SIGNALING	1.65	0.08
256	VALK_AML_CLUSTER_1	1.65	0.08
257	YANG_BREAST_CANCER_ESR1_LASER_DN	1.65	0.08
258	CHIARADONNA_NEOPLASTIC_TRANSFORMATION_KRAS_CDC25_UP	1.65	0.08
259	TIAN_TNF_SIGNALING_VIA_NFKB	1.65	0.08
260	MEISSNER_NPC_HCP_WITH_H3K4ME2_AND_H3K27ME3	1.65	0.08
261	FOSTER_TOLERANT_MACROPHAGE_DN	1.65	0.08
262	HELLER_HDAC_TARGETS_SILENCED_BY_METHYLATION_UP	1.65	0.08
263	HILLION_HMGA1_TARGETS	1.64	0.08
264	BIOCARTA_BCR_PATHWAY	1.64	0.08
265	REACTOME_CONSTITUTIVE_SIGNALING_BY_AKT1_E17K_IN_CANCER	1.64	0.08
266	WIKMAN_ASBESTOS_LUNG_CANCER_DN	1.64	0.08
267	KYNG_ENVIRONMENTAL_STRESS_RESPONSE_NOT_BY_GAMMA_IN_WS	1.64	0.08
268	NIKOLSKY_BREAST_CANCER_11Q12_Q14_AMPLICON	1.64	0.08
269	CHENG_IMPRINTED_BY_ESTRADIOL	1.64	0.08
270	ZWANG_CLASS_1_TRANSIENTLY_INDUCED_BY_EGF	1.64	0.08
271	DURAND_STROMA_NS_UP	1.64	0.08
272	BROWNE_HCMV_INFECTION_12HR_UP	1.64	0.08
273	NAGASHIMA_NRG1_SIGNALING_DN	1.64	0.08
274	REACTOME_CELL_CELL_COMMUNICATION	1.64	0.08
275	PID_P73PATHWAY	1.64	0.08
276	TURASHVILI_BREAST_LOBULAR_CARCINOMA_VS_DUCTAL_NORMAL_DN	1.64	0.08
277	RAMASWAMY_METASTASIS_DN	1.64	0.08
278	DOANE_BREAST_CANCER_CLASSES_DN	1.63	0.08
279	KAN_RESPONSE_TO_ARSENIC_TRIOXIDE	1.63	0.08
280	GARGALOVIC_RESPONSE_TO_OXIDIZED_PHOSPHOLIPIDS_YELLOW_UP	1.63	0.08

281	DAZARD_RESPONSE_TO_UV_SCC_UP	1.63	0.08
282	REACTOME_NEGATIVE_REGULATION_OF_FGFR4_SIGNALING	1.63	0.08
283	DACOSTA_UV_RESPONSE_VIA_ERCC3_COMMON_UP	1.63	0.08
284	RASHI_RESPONSE_TO_IONIZING_RADIATION_2	1.63	0.08
285	GARGALOVIC_RESPONSE_TO_OXIDIZED_PHOSPHOLIPIDS_MAGENTA_UP	1.63	0.08
286	REACTOME_FATTY_ACYL_COA_BIOSYNTHESIS	1.63	0.08
287	REACTOME_METABOLISM_OF_FAT_SOLUBLE_VITAMINS	1.63	0.08
288	KEGG_LEUKOCYTE_TRANSENDOTHELIAL_MIGRATION	1.62	0.08
289	REACTOME_SIGNALING_BY_FGFR2_IN_DISEASE	1.62	0.08
290	WANG_RESPONSE_TO_GSK3_INHIBITOR_SB216763_DN	1.62	0.08
291	PID_NEPHRIN_NEPH1_PATHWAY	1.62	0.08
292	MULLIGHAN_NPM1_MUTATED_SIGNATURE_2_DN	1.62	0.09
293	WEST_ADRENOCORTICAL_TUMOR_UP	1.62	0.09
294	ROVERSI_GLIOMA_LOH_REGIONS	1.62	0.09
295	KANG_IMMORTALIZED_BY_TERT_DN	1.62	0.09
296	BIOCARTA_IL2RB_PATHWAY	1.62	0.09
297	REACTOME_NEURODEGENERATIVE_DISEASES	1.62	0.09
298	CHANDRAN_METASTASIS_DN	1.62	0.09
299	LEE_LIVER_CANCER_SURVIVAL_UP	1.62	0.09
300	TERAO_AOX4_TARGETS_HG_UP	1.62	0.09
301	SCHLESINGER_METHYLATED_DE_NOVO_IN_CANCER	1.61	0.09
302	TRAYNOR_RETT_SYNDROM_UP	1.61	0.09
303	DACOSTA_UV_RESPONSE_VIA_ERCC3_TTD_UP	1.61	0.09
304	PID_HDAC_CLASSII_PATHWAY	1.61	0.09
305	REACTOME_RAF_INDEPENDENT_MAPK1_3_ACTIVATION	1.61	0.09
306	KEGG_BIOSYNTHESIS_OF_UNSATURATED_FATTY_ACIDS	1.61	0.09
307	REACTOME_DOWNSTREAM_SIGNAL_TRANSDUCTION	1.61	0.09
308	WANG_ESOPHAGUS_CANCER_VS_NORMAL_UP	1.61	0.09
309	CHIANG_LIVER_CANCER_SUBCLASS_CTNNB1_UP	1.61	0.09
310	LI_INDUCED_T_TO_NATURAL_KILLER_UP	1.61	0.09
311	ONO_FOXP3_TARGETS_DN	1.61	0.09
312	BECKER_TAMOXIFEN_RESISTANCE_DN	1.61	0.09
313	BROWNE_HCMV_INFECTION_10HR_UP	1.61	0.09
314	VALK_AML_CLUSTER_6	1.60	0.09
315	MACAEVA_PBMC_RESPONSE_TO_IR	1.60	0.09
316	GAL_LEUKEMIC_STEM_CELL_DN	1.60	0.09
317	CAMPS_COLON_CANCER_COPY_NUMBER_UP	1.60	0.09
318	REACTOME_GPCR_LIGAND_BINDING	1.60	0.09
319	PID_HNF3B_PATHWAY	1.60	0.09
320	ELVIDGE_HIF1A_AND_HIF2A_TARGETS_DN	1.60	0.09
321	BIOCARTA_NGF_PATHWAY	1.60	0.09
322	REACTOME_DEACTIVATION_OF_THE_BETA_CATENIN_TRANSACTIVATING_COMPLEX	1.60	0.09

323	TAKEDA_TARGETS_OF_NUP98_HOXA9_FUSION_10D_DN	1.60	0.09
324	PRAMOONJAGO_SOX4_TARGETS_DN	1.60	0.09
325	HUMMEL_BURKITTS_LYMPHOMA_UP	1.60	0.09
326	DACOSTA_UV_RESPONSE_VIA_ERCC3_UP	1.60	0.09
327	ELVIDGE_HYPOXIA_UP	1.60	0.09
328	SMID_BREAST_CANCER_BASAL_UP	1.60	0.09
329	MCDOWELL_ACUTE_LUNG_INJURY_UP	1.60	0.09
330	REACTOME_TRANSCRIPTIONAL_REGULATION_OF_PLURIPOTENT_STEM_CELLS	1.60	0.09
331	BIOCARTA_GPCR_PATHWAY	1.60	0.09
332	POMEROY_MEDULLOBLASTOMA_PROGNOSIS_DN	1.60	0.09
333	BRACHAT_RESPONSE_TO_CAMPTOTHECIN_UP	1.60	0.09
334	SCHAEFFER_PROSTATE_DEVELOPMENT_12HR_UP	1.60	0.09
335	NAKAMURA_METASTASIS_MODEL_UP	1.59	0.09
336	BILANGES_RAPAMYCIN_SENSITIVE_GENES	1.59	0.09
337	DITTMER_PTHLH_TARGETS_DN	1.59	0.09
338	FISCHER_DIRECT_P53_TARGETS_META_ANALYSIS	1.59	0.09
339	REACTOME_NEGATIVE_REGULATION_OF_FGFR3_SIGNALING	1.59	0.09
340	TAKEDA_TARGETS_OF_NUP98_HOXA9_FUSION_16D_UP	1.59	0.09
341	KANG_CISPLATIN_RESISTANCE_UP	1.59	0.09
342	BRUINS_UVC_RESPONSE_VIA_TP53_GROUP_C	1.59	0.10
343	MUELLER_METHYLATED_IN_GLIOBLASTOMA	1.59	0.09
344	GARGALOVIC_RESPONSE_TO_OXIDIZED_PHOSPHOLIPIDS_TURQUOISE_UP	1.59	0.10
345	REACTOME_TOLL_LIKE_RECEPTOR_TLR1:TLR2_CASCADE	1.59	0.10
346	MASSARWEH_RESPONSE_TO_ESTRADIOL	1.59	0.10
347	SMIRNOV_CIRCULATING_ENDOTHELIOCYTES_IN_CANCER_UP	1.59	0.10
348	SHIN_B_CELL_LYMPHOMA_CLUSTER_7	1.59	0.10
349	LEI_MYB_TARGETS	1.59	0.10
350	GRAESSMANN_APOPTOSIS_BY_SERUM_DEPRIVATION_DN	1.59	0.10
351	REACTOME_NONSENSE_MEDIATED_DECAY_NMD_INDEPENDENT_OF_THE_EXON_JUNCTION_COMPLEX_EJC	1.59	0.10
352	XU_GH1_EXOGENOUS_TARGETS_DN	1.59	0.10
353	MAHAJAN_RESPONSE_TO_IL1A_DN	1.59	0.10
354	CHAUHAN_RESPONSE_TO_METHOXYESTRADIOL_UP	1.59	0.10
355	HONRADO_BREAST_CANCER_BRCA1_VS_BRCA2	1.58	0.10
356	CASORELLI_ACUTE_PROMYELOCYTIC_LEUKEMIA_UP	1.58	0.10
357	NOJIMA_SFRP2_TARGETS_DN	1.58	0.10
358	CHUANG_OXIDATIVE_STRESS_RESPONSE_UP	1.58	0.10
359	REACTOME_SIGNALING_BY_FGFR3	1.58	0.10
360	YAO_TEMPORAL_RESPONSE_TO_PROGESTERONE_CLUSTER_8	1.58	0.10
361	PID_IL23_PATHWAY	1.58	0.10

362	TAVOR_CEBPA_TARGETS_UP	1.58	0.10
363	PAPASPYRIDONOS_UNSTABLE_ATEROSCLEROTIC_PLAQUE_DN	1.58	0.10
364	SCHLINGEMANN_SKIN_CARCINOGENESIS_TPA_UP	1.58	0.10
365	CROONQUIST_NRAS_SIGNALING_UP	1.58	0.10
366	KOKKINAKIS_METHIONINE_DEPRIVATION_96HR_UP	1.58	0.10
367	PID_TAP63_PATHWAY	1.57	0.10
368	REACTOME_RAF_ACTIVATION	1.57	0.10
369	JIANG_HYPOXIA_NORMAL	1.57	0.10
370	SARTIPY_NORMAL_AT_INSULIN_RESISTANCE_UP	1.57	0.10
371	REACTOME_SIGNALING_BY_INTERLEUKINS	1.57	0.10
372	REACTOME_CELL_JUNCTION_ORGANIZATION	1.57	0.10
373	OLSSON_E2F3_TARGETS_UP	1.57	0.10
374	SASSON_RESPONSE_TO_FORSKOLIN_UP	1.57	0.10
375	REACTOME_INTERLEUKIN_1_SIGNALING	1.57	0.10
376	PID_GMCSF_PATHWAY	1.57	0.11
377	REACTOME_HSP90_CHAPERONE_CYCLE_FOR_STEROID_HORMONE_RECEPTORS_SHR	1.57	0.11
378	WANG_LSD1_TARGETS_UP	1.57	0.11
379	BENPORATH_MYC_TARGETS_WITH_EBOX	1.56	0.11
380	IVANOVSKA_MIR106B_TARGETS	1.56	0.11
381	BURTON_ADIPOGENESIS_9	1.56	0.11
382	IIZUKA_LIVER_CANCER_PROGRESSION_G2_G3_UP	1.56	0.11
383	ISSAEVA_MLL2_TARGETS	1.56	0.11
384	WILCOX_RESPONSE_TO_PROGESTERONE_UP	1.56	0.11
385	REACTOME_MAPK_FAMILY_SIGNALING_CASCADES	1.56	0.11
386	BRUNO_HEMATOPOIESIS	1.56	0.11
387	CHARAFE_BREAST_CANCER_BASAL_VS_MESENCHYMAL_UP	1.56	0.11
388	MARTINEZ_RESPONSE_TO_TRABECTEDIN_UP	1.56	0.11
389	REACTOME_POST_CHAPERONIN_TUBULIN_FOLDING_PATHWAY	1.56	0.11
390	BIOCARTA_TCR_PATHWAY	1.56	0.11
391	COULOUARN_TEMPORAL_TGFB1_SIGNATURE_UP	1.56	0.11
392	GUO_TARGETS_OF_IRS1_AND_IRS2	1.56	0.11
393	SHAFFER_IRF4_TARGETS_IN_MYELOMA_VS_MATURE_B_LYMPHOCYTE	1.56	0.11
394	KEGG_INSULIN_SIGNALING_PATHWAY	1.56	0.11
395	MOREAUX_B_LYMPHOCYTE_MATURATION_BY_TACI_UP	1.55	0.11
396	SHEPARD_CRUSH_AND_BURN_MUTANT_UP	1.55	0.11
397	SIMBULAN_UV_RESPONSE_NORMAL_DN	1.55	0.11
398	ABE_VEGFA_TARGETS_30MIN	1.55	0.11
399	YAGI_AML_WITH_INV_16_TRANSLOCATION	1.55	0.11
400	BIOCARTA_FMLP_PATHWAY	1.55	0.12
401	LEE_NEURAL_CREST_STEM_CELL_DN	1.55	0.12
402	WENG_POR_TARGETS_LIVER_UP	1.55	0.12

403	DELYS_THYROID_CANCER_DN	1.55	0.12
404	PID_IL12_STAT4_PATHWAY	1.55	0.12
405	BAE_BRCA1_TARGETS_DN	1.55	0.12
406	KEGG_MELANOGENESIS	1.55	0.12
407	EPPERT_HSC_R	1.55	0.12
408	SHIPP_DLBCL_VS_FOLLICULAR_LYMPHOMA_UP	1.55	0.12
409	MARZEC_IL2_SIGNALING_UP	1.55	0.12
410	SMID_BREAST_CANCER_RELAPSE_IN_BRAIN_UP	1.54	0.12
411	MCCABE_HOXC6_TARGETS_CANCER_UP	1.54	0.12
412	DOUGLAS_BMI1_TARGETS_UP	1.54	0.12
413	DELPUECH_FOXO3_TARGETS_UP	1.54	0.12
414	TAVAZOIE_METASTASIS	1.54	0.12
415	AMIT_EGF_RESPONSE_240_HELA	1.54	0.12
416	HOLLEMAN_VINCRISTINE_RESISTANCE_B_ALL_UP	1.54	0.12
417	TAKAO_RESPONSE_TO_UVB_RADIATION_UP	1.54	0.12
418	IZADPANAH_STEM_CELL_ADIPOSE_VS_BONE_UP	1.54	0.12
419	MARTENS_BOUND_BY_PML_RARA_FUSION	1.54	0.12
420	GRESHOCK_CANCER_COPY_NUMBER_UP	1.54	0.12
421	ZHAN_MULTIPLE_MYELOMA_MF_UP	1.54	0.12
422	ZHAN_LATE_DIFFERENTIATION_GENES_UP	1.53	0.12
423	PAPASPYRIDONOS_UNSTABLE_ATEROSCLEROTIC_PLAQUE_UP	1.53	0.13
424	MCCLUNG_COCAIN_REWARD_4WK	1.53	0.13
425	BIOCARTA_VIP_PATHWAY	1.53	0.13
426	PHONG_TNF_RESPONSE_NOT_VIA_P38	1.53	0.13
427	MCLACHLAN_DENTAL_CARIES_UP	1.53	0.13
428	HOFMANN_CELL_LYMPHOMA_UP	1.53	0.13
429	MORI_EMU_MYC_LYMPHOMA_BY_ONSET_TIME_UP	1.53	0.13
430	BONCI_TARGETS_OF_MIR15A_AND_MIR16_1	1.53	0.13
431	REACTOME_NEGATIVE_REGULATION_OF_FGFR2_SIGNALING	1.53	0.13
432	WEST_ADRENOCORTICAL_TUMOR_MARKERS_UP	1.53	0.13
433	AMIT_EGF_RESPONSE_240_MCF10A	1.53	0.13
434	HSIAO_HOUSEKEEPING_GENES	1.53	0.13
435	REACTOME_INTERFERON_GAMMA_SIGNALING	1.52	0.13
436	GEISS_RESPONSE_TO_DSRNA_UP	1.52	0.13
437	MATSUDA_NATURAL_KILLER_DIFFERENTIATION	1.52	0.13
438	WIERENGA_STAT5A_TARGETS_DN	1.52	0.13
439	SESTO_RESPONSE_TO_UV_C8	1.52	0.13
440	STREICHER_LSM1_TARGETS_UP	1.52	0.13
441	TOMIDA_METASTASIS_DN	1.52	0.13
442	RIZ_ERYTHROID_DIFFERENTIATION_HBZ	1.52	0.13
443	BIOCARTA_IGF1_PATHWAY	1.52	0.13
444	REACTOME_MISCELLANEOUS_TRANSPORT_AND_BINDING_EVENTS	1.52	0.13

445	REACTOME_GROWTH_HORMONE_RECEPTOR_SIGNALING	1.52	0.13
446	REACTOME_TRANSLOCATION_OF_SLC2A4_GLUT4_TO_THE_PLASMA_MEMBRANE	1.52	0.13
447	STOSSI_RESPONSE_TO_ESTRADIOL	1.52	0.13
448	HOLLMANN_APOPTOSIS_VIA_CD40_UP	1.52	0.13
449	YU_BAP1_TARGETS	1.52	0.13
450	ZHOU_INFLAMMATORY_RESPONSE_FIMA_UP	1.52	0.13
451	PARK_TRETINOIN_RESPONSE_AND_PML_RARA_FUSION	1.52	0.13
452	REACTOME_REGULATION_OF_TP53_EXPRESSION_AND_DEGRADATION	1.52	0.13
453	FULCHER_INFLAMMATORY_RESPONSE_LECTIN_VS_LPS_UP	1.51	0.13
454	FRASOR_RESPONSE_TO_ESTRADIOL_UP	1.51	0.13
455	VALK_AML_CLUSTER_4	1.51	0.13
456	HOEBEKE_LYMPHOID_STEM_CELL_DN	1.51	0.13
457	SWEET_LUNG_CANCER_KRAS_DN	1.51	0.13
458	PID_IL12_2PATHWAY	1.51	0.13
459	REACTOME_REGULATION_OF_HSF1_MEDIATED_HEAT_SHOCK_RESPONSE	1.51	0.13
460	PID_HIF2PATHWAY	1.51	0.13
461	AFFAR_YY1_TARGETS_DN	1.51	0.13
462	KEGG_MAPK_SIGNALING_PATHWAY	1.51	0.13
463	BIOCARTA_HDAC_PATHWAY	1.51	0.14
464	LEE_LIVER_CANCER_MYC_E2F1_DN	1.51	0.14
465	CUI_TCF21_TARGETS_DN	1.51	0.14
466	CHOW_RASSF1_TARGETS_UP	1.51	0.14
467	PID_ALK1_PATHWAY	1.51	0.14
468	COULOUARN_TEMPORAL_TGFB1_SIGNATURE_DN	1.51	0.14
469	REACTOME_PREFOLDIN_MEDIATED_TRANSFER_OF_SUBSTRATE_TO_CCT_TRIC	1.51	0.14
470	LUI_THYROID_CANCER_CLUSTER_1	1.51	0.14
471	REACTOME_CARDIAC_CONDUCTION	1.51	0.14
472	HOOI_ST7_TARGETS_DN	1.51	0.14
473	TONKS_TARGETS_OF_RUNX1_RUNX1T1_FUSION_SUSTAINED_IN_MONOCYTE_UP	1.51	0.14
474	BIOCARTA_GLEEVEC_PATHWAY	1.51	0.14
475	UEDA_PERIFERAL_CLOCK	1.51	0.14
476	PACHER_TARGETS_OF_IGF1_AND_IGF2_UP	1.51	0.14
477	YAO_TEMPORAL_RESPONSE_TO_PROGESTERONE_CLUSTER_1	1.51	0.14
478	SHAFFER_IRF4_MULTIPLE_MYELOMA_PROGRAM	1.50	0.14
479	SMID_BREAST_CANCER_LUMINAL_A_UP	1.50	0.14
480	CONCANNON_APOPTOSIS_BY_EPOXOMICIN_UP	1.50	0.14
481	REACTOME_PLATELET_SENSITIZATION_BY_LDL	1.50	0.14
482	LINSLEY_MIR16_TARGETS	1.50	0.14
483	ENK_UV_RESPONSE_KERATINOCYTE_UP	1.50	0.14

484	SHIPP_DLBCL_CURED_VS_FATAL_UP	1.50	0.14
485	KIM_LIVER_CANCER_POOR_SURVIVAL_UP	1.50	0.14
486	ELVIDGE_HYPOXIA_DN	1.50	0.14
487	MOREIRA_RESPONSE_TO_TSA_UP	1.50	0.14
488	LINDSTEDT_DENDRITIC_CELL_MATURATION_A	1.50	0.14
489	PID_SMAD2_3NUCLEAR_PATHWAY	1.50	0.14
490	WANG_RESPONSE_TO_ANDROGEN_UP	1.50	0.14
491	TONKS_TARGETS_OF_RUNX1_RUNX1T1_FUSION_SUSTAINED_IN_ERYTHROCYTE_UP	1.50	0.14
492	GENTILE_UV_HIGH_DOSE_UP	1.50	0.14
493	GUO_HEX_TARGETS_DN	1.50	0.14
494	PID_IL2_1PATHWAY	1.50	0.14
495	WIERENGA_STAT5A_TARGETS_GROUP1	1.50	0.14
496	KEGG_TYPE_II_DIABETES_MELLITUS	1.50	0.14
497	GARGALOVIC_RESPONSE_TO_OXIDIZED_PHOSPHOLIPIDS_GREEN_UP	1.50	0.14
498	GHANDHI_BYSTANDER_IRRADIATION_UP	1.49	0.14
499	REACTOME_ACTIVATION_OF_BH3_ONLY_PROTEINS	1.49	0.14
500	SCHAEFFER_PROSTATE_DEVELOPMENT_48HR_UP	1.49	0.14
501	HORIUCHI_WTAP_TARGETS_DN	1.49	0.14
502	KEGG_JAK_STAT_SIGNALING_PATHWAY	1.49	0.14
503	CROMER_TUMORIGENESIS_UP	1.49	0.14
504	MARZEC_IL2_SIGNALING_DN	1.49	0.14
505	REACTOME_SLC_MEDIATED_TRANSMEMBRANE_TRANSPORT	1.49	0.14
506	VART_KSHV_INFECTION_ANGIOGENIC_MARKERS_DN	1.49	0.14
507	TAKEDA_TARGETS_OF_NUP98_HOXA9_FUSION_8D_DN	1.49	0.14
508	BOYLAN_MULTIPLE_MYELOMA_C_UP	1.49	0.14
509	HILLION_HMGA1B_TARGETS	1.49	0.14
510	KAYO_AGING_MUSCLE_UP	1.49	0.14
511	HUMMERICH_SKIN_CANCER_PROGRESSION_UP	1.49	0.14
512	LIU_CMYB_TARGETS_UP	1.49	0.14
513	REACTOME_CLASS_B_2_SECRETIN_FAMILY_RECEPTORS	1.49	0.14
514	HALMOS_CEBPA_TARGETS_DN	1.49	0.15
515	TONKS_TARGETS_OF_RUNX1_RUNX1T1_FUSION_MONOCYTE_UP	1.49	0.15
516	AMIT_SERUM_RESPONSE_480_MCF10A	1.49	0.15
517	CHARAFE_BREAST_CANCER_LUMINAL_VS_BASAL_DN	1.49	0.15
518	DAVICIONI_MOLECULAR_ARMS_VS_ERMS_DN	1.48	0.15
519	CONCANNON_APOPTOSIS_BY_EPOXOMICIN_DN	1.48	0.15
520	REACTOME_CELLULAR_RESPONSE_TO_HEAT_STRESS	1.48	0.15
521	DELYS_THYROID_CANCER_UP	1.48	0.15
522	BIOCARTA_IL6_PATHWAY	1.48	0.15
523	CORRE_MULTIPLE_MYELOMA_DN	1.48	0.15
524	HELLER_HDAC_TARGETS_UP	1.48	0.15

525	CROONQUIST_STROMAL_STIMULATION_UP	1.48	0.15
526	BURTON_ADIPOGENESIS_8	1.48	0.15
527	REACTOME_FORMATION_OF_TUBULIN_FOLDING_INTERMEDIATES_BY_CCT_TRIC	1.48	0.15
528	FLORIO_NEOCORTEX_BASAL_RADIAL_GLIA_UP	1.48	0.15
529	ZHONG_RESPONSE_TO_AZACITIDINE_AND_TSA_UP	1.48	0.15
530	IGARASHI_ATF4_TARGETS_DN	1.48	0.15
531	REACTOME_ION_HOMEOSTASIS	1.48	0.15
532	ONO_AML1_TARGETS_DN	1.48	0.15
533	KEGG_ENDOCYTOSIS	1.48	0.15
534	ONDER_CDH1_TARGETS_1_UP	1.48	0.15
535	KORKOLA_YOLK_SAC_TUMOR	1.48	0.15
536	PID_AR_NONGENOMIC_PATHWAY	1.48	0.15
537	FEVR_CTNNB1_TARGETS_UP	1.48	0.15
538	PEDERSEN_TARGETS_OF_611CTF_ISOFORM_OF_ERBB2	1.48	0.15
539	KEGG_RIBOSOME	1.48	0.15
540	KEGG_BASAL_CELL_CARCINOMA	1.47	0.15
541	TARTE_PLASMA_CELL_VS_PLASMABLAST_DN	1.47	0.15
542	YAO_HOXA10_TARGETS_VIA_PROGESTERONE_UP	1.47	0.15
543	REACTOME_SIGNALING_BY_FGFR	1.47	0.15
544	REACTOME_TOLL_LIKE_RECEPTOR_9_TLR9_CASCADE	1.47	0.15
545	REACTOME_DISEASES_OF_SIGNAL_TRANSDUCTION	1.47	0.15
546	SAKAI_CHRONIC_HEPATITIS_VS_LIVER_CANCER_DN	1.47	0.15
547	GOTZMANN_EPITHELIAL_TO_MESENCHYMAL_TRANSITION_DN	1.47	0.15
548	BILBAN_B_CLL_LPL_DN	1.47	0.15
549	MARSON_FOXP3_TARGETS_DN	1.47	0.15
550	ACOSTA_PROLIFERATION_INDEPENDENT_MYC_TARGETS_UP	1.47	0.15
551	MONNIER_POSTRADIATION_TUMOR_ESCAPE_DN	1.47	0.15
552	BEIER_GLIOMA_STEM_CELL_UP	1.47	0.15
553	BIOCARTA_MEF2D_PATHWAY	1.47	0.16
554	SMID_BREAST_CANCER_RELAPSE_IN_LUNG_UP	1.47	0.16
555	KEGG_HEMATOPOIETIC_CELL_LINEAGE	1.47	0.16
556	DAVICIONI_RHABDOMYOSARCOMA_PAX_FOXO1_FUSION_UP	1.47	0.16
557	PID_EPHRINB_REV_PATHWAY	1.47	0.16
558	NABA_MATRISOME_ASSOCIATED	1.47	0.16
559	BIOCARTA_P53_PATHWAY	1.47	0.16
560	OHGUCHI_LIVER_HNF4A_TARGETS_UP	1.46	0.16
561	REACTOME_PYRUVATE_METABOLISM	1.46	0.16
562	HU_ANGIOGENESIS_UP	1.46	0.16
563	MARSHALL_VIRAL_INFECTION_RESPONSE_DN	1.46	0.16
564	BIOCARTA_CALCINEURIN_PATHWAY	1.46	0.16
565	COATES_MACROPHAGE_M1_VS_M2_UP	1.46	0.16
566	CAIRO_HEPATOBLASTOMA_UP	1.46	0.16

567	FARMER_BREAST_CANCER_APOCRINE_VS_BASAL	1.46	0.16
568	REACTOME_GLYCOLYSIS	1.46	0.16
569	LI_PROSTATE_CANCER_EPIGENETIC	1.46	0.16
570	CHANG_IMMORTALIZED_BY_HPV31_UP	1.46	0.16
571	REACTOME_FGFR2_MUTANT_RECEPTOR_ACTIVATION	1.46	0.16
572	REACTOME_CYCLIN_A_B1_B2_ASSOCIATED_EVENTS_DURING_G2_M_TRANSITION	1.46	0.16
573	PID_ERBB2_ERBB3_PATHWAY	1.46	0.16
574	ELVIDGE_HYPOXIA_BY_DMOG_DN	1.46	0.16
575	REACTOME_NEGATIVE_REGULATION_OF_THE_PI3K_AKT_NETWORK	1.46	0.16
576	GAVIN_FOXP3_TARGETS_CLUSTER_P7	1.46	0.16
577	WNT_SIGNALING	1.46	0.16
578	KEGG_GLIOMA	1.46	0.16
579	RHEIN_ALL_GLUCOCORTICOID_THERAPY_DN	1.46	0.16
580	YAO_TEMPORAL_RESPONSE_TO_PROGESTERONE_CLUSTER_5	1.46	0.16
581	ABBUD_LIF_SIGNALING_1_DN	1.46	0.16
582	LANDIS_ERBB2_BREAST_TUMORS_65_UP	1.46	0.16
583	MARTINEZ_RB1_AND_TP53_TARGETS_UP	1.46	0.16
584	BEGUM_TARGETS_OF_PAX3_FOXO1_FUSION_DN	1.45	0.16
585	ZHENG_FOXP3_TARGETS_IN_THYMUS_UP	1.45	0.16
586	SASSON_RESPONSE_TO_GONADOTROPHINS_UP	1.45	0.16
587	MOREAUX_MULTIPLE_MYELOMA_BY_TACI_UP	1.45	0.16
588	REACTOME_DISASSEMBLY_OF_THE_DESTRUCTION_COMPLEX_AND_RECRUITMENT_OF_AXIN_TO_THE_MEMBRANE	1.45	0.16
589	GAUSSMANN_MLL_AF4_FUSION_TARGETS_E_UP	1.45	0.16
590	REACTOME_SIGNALING_BY_WNT_IN_CANCER	1.45	0.16
591	AMIT_EGF_RESPONSE_480_HELA	1.45	0.16
592	CREIGHTON_ENDOCRINE_THERAPY_RESISTANCE_5	1.45	0.16
593	ZHENG_BOUND_BY_FOXP3	1.45	0.16
594	KOHOUTEK_CCNT1_TARGETS	1.45	0.16
595	MCBRYAN_PUBERTAL_BREAST_4_5WK_UP	1.45	0.16
596	FUJII_YBX1_TARGETS_UP	1.45	0.16
597	FARMER_BREAST_CANCER_BASAL_VS_LULMINAL	1.45	0.16
598	YAO_TEMPORAL_RESPONSE_TO_PROGESTERONE_CLUSTER_17	1.45	0.17
599	SHAFFER_IRF4_TARGETS_IN_PLASMA_CELL_VS_MATURE_B_LYMPHOCYTE	1.45	0.17
600	RIZ_ERYTHROID_DIFFERENTIATION_12HR	1.45	0.17
601	DAZARD_RESPONSE_TO_UV_SCC_DN	1.45	0.17
602	RIGGINS_TAMOXIFEN_RESISTANCE_DN	1.45	0.17
603	YAMAZAKI_TCEB3_TARGETS_DN	1.45	0.17
604	BIOCARTA_EPO_PATHWAY	1.45	0.17
605	PID_PDGFRA_PATHWAY	1.45	0.17
606	HESS_TARGETS_OF_HOXA9_AND_MEIS1_DN	1.45	0.17

607	IKEDA_MIR30_TARGETS_UP	1.45	0.17
608	REACTOME_MYD88_CASCADE_INITIATED_ON_PLASMA_MEMBRANE	1.45	0.17
609	PID_PI3KCI_PATHWAY	1.45	0.17
610	BIOCARTA_NO1_PATHWAY	1.45	0.17
611	HINATA_NFKB_TARGETS_KERATINOCYTE_UP	1.44	0.17
612	SESTO_RESPONSE_TO_UV_C3	1.44	0.17
613	OZEN_MIR125B1_TARGETS	1.44	0.17
614	BROWNE_HCMV_INFECTION_1HR_UP	1.44	0.17
615	REACTOME_COPI_INDEPENDENT_GOLGI_TO_ER_RETROGRADE_TRAFFIC	1.44	0.17
616	SMITH_TERT_TARGETS_DN	1.44	0.17
617	PETROVA_PROX1_TARGETS_UP	1.44	0.17
618	FERRARI_RESPONSE_TO_FENRETINIDE_UP	1.44	0.17
619	BILBAN_B_CLL_LPL_UP	1.44	0.17
620	REACTOME_CELL_CELL_JUNCTION_ORGANIZATION	1.44	0.17
621	ZHANG_RESPONSE_TO_IKK_INHIBITOR_AND_TNF_UP	1.44	0.17
622	ZHOU_INFLAMMATORY_RESPONSE_LPS_UP	1.44	0.17
623	REACTOME_BASIGIN_INTERACTIONS	1.44	0.17
624	BROWNE_HCMV_INFECTION_20HR_UP	1.44	0.17
625	MARTINEZ_TP53_TARGETS_UP	1.44	0.17
626	KEGG_WNT_SIGNALING_PATHWAY	1.44	0.17
627	SAMOLS_TARGETS_OF_KHSV_MIRNAS_DN	1.44	0.17
628	RIGGI_EWING_SARCOMA_PROGENITOR_UP	1.44	0.17
629	REACTOME_WNT_LIGAND_BIOGENESIS_AND_TRAFFICKING	1.44	0.17
630	REACTOME_ROS_AND_RNS_PRODUCTION_IN_PHAGOCYTES	1.44	0.17
631	SUBTIL_PROGESTIN_TARGETS	1.44	0.17
632	PID_FRA_PATHWAY	1.44	0.17
633	RUTELLA_RESPONSE_TO_HGF_UP	1.44	0.17
634	NAKAYAMA_SOFT_TISSUE_TUMORS_PCA2_UP	1.44	0.17
635	REACTOME_INTERLEUKIN_4_AND_INTERLEUKIN_13_SIGNALING	1.43	0.17
636	REACTOME_CLASS_A_1_RHODOPSIN_LIKE_RECEPTORS	1.43	0.17
637	PID_PDGFRB_PATHWAY	1.43	0.17
638	MIYAGAWA_TARGETS_OF_EWSR1_ETS_FUSIONS_DN	1.43	0.17
639	CHIARADONNA_NEOPLASTIC_TRANSFORMATION_KRAS_DN	1.43	0.17
640	BIOCARTA_INSULIN_PATHWAY	1.43	0.17
641	GOLDRATH_IMMUNE_MEMORY	1.43	0.17
642	HUNSBERGER_EXERCISE_REGULATED_GENES	1.43	0.17
643	REACTOME_COOPERATION_OF_PREFOLDIN_AND_TRIC_CCT_IN_ACTIN_AND_TUBULIN_FOLDING	1.43	0.17
644	NUTT_GBM_VS_AO_GLIOMA_UP	1.43	0.17
645	REACTOME_ACTIVATION_OF_AMPK_DOWNSTREAM_OF_NMDARS	1.43	0.18

646	VERRECCHIA_RESPONSE_TO_TGFB1_C1	1.43	0.18
647	REACTOME_DETOXIFICATION_OF_REACTIVE_OXYGEN_SPECIES	1.43	0.18
648	SENESE_HDAC3_TARGETS_UP	1.43	0.18
649	GERY_CEBP_TARGETS	1.42	0.18
650	FRASOR_RESPONSE_TO_SERM_OR_FULVESTRANT_UP	1.42	0.18
651	REACTOME_TP53_REGULATES_TRANSCRIPTION_OF_CELL_DEATH_GENES	1.42	0.18
652	REACTOME_ACTIVATION_OF_NMDA_RECEPTORS_AND_POSTSYNAPTIC_EVENTS	1.42	0.18
653	REACTOME_DOWNSTREAM_SIGNALING_EVENTS_OF_B_CELL_RECEPTOR_BCR	1.42	0.18
654	REACTOME_FOXO_MEDIATED_TRANSCRIPTION_OF_CELL_CYCLE_GENES	1.42	0.18
655	RUTELLA_RESPONSE_TO_HGF_VS_CSF2RB_AND_IL4_DN	1.42	0.18
656	PID_IL6_7_PATHWAY	1.42	0.18
657	KEGG_ALDOSTERONE_REGULATED_SODIUM_REABSORPTION	1.42	0.18
658	BHAT_ESR1_TARGETS_VIA_AKT1_DN	1.42	0.18
659	ACEVEDO_LIVER_CANCER_DN	1.42	0.18
660	ALFANO_MYC_TARGETS	1.42	0.18
661	ZHENG_FOXP3_TARGETS_UP	1.42	0.18
662	RHEIN_ALL_GLUCOCORTICOID_THERAPY_UP	1.42	0.18
663	COATES_MACROPHAGE_M1_VS_M2_DN	1.42	0.19
664	UEDA_CENTRAL_CLOCK	1.42	0.19
665	FLECHNER_BIOPSY_KIDNEY_TRANSPLANT_REJECTED_VS_OK_DN	1.42	0.19
666	REACTOME_INTERLEUKIN_10_SIGNALING	1.42	0.19
667	DANG_REGULATED_BY_MYC_DN	1.42	0.19
668	JIANG_VHL_TARGETS	1.42	0.19
669	CUI_GLUCOSE_DEPRIVATION	1.41	0.19
670	ACEVEDO_LIVER_CANCER_WITH_H3K27ME3_UP	1.41	0.19
671	MIYAGAWA_TARGETS_OF_EWSR1_ETS_FUSIONS_UP	1.41	0.19
672	VERHAAK_AML_WITH_NPM1_MUTATED_DN	1.41	0.19
673	SATO_SILENCED_BY_METHYLATION_IN_PANCREATIC_CANCER_2	1.41	0.19
674	PLASARI_TGFB1_SIGNALING_VIA_NFIC_1HR_UP	1.41	0.19
675	MITSIADES_RESPONSE_TO_APLIDIN_UP	1.41	0.19
676	MCBRYAN_PUBERTAL_BREAST_5_6WK_UP	1.41	0.19
677	MMS_MOUSE_LYMPH_HIGH_4HRS_UP	1.41	0.19
678	DANG_REGULATED_BY_MYC_UP	1.41	0.19
679	LI_LUNG_CANCER	1.41	0.19
680	KEGG_PATHWAYS_IN_CANCER	1.41	0.19
681	SESTO_RESPONSE_TO_UV_C0	1.41	0.19
682	BIOCARTA_P53HYPOXIA_PATHWAY	1.41	0.19
683	SCHUETZ_BREAST_CANCER_DUCTAL_INVASIVE_DN	1.41	0.19
684	YU_MYC_TARGETS_UP	1.41	0.19

685	REACTOME_TRANSFERRIN_ENDOCYTOSIS_AND_RECYCLING	1.41	0.20
686	REACTOME_ACTIVATION_OF_BAD_AND_TRANSLOCATION_TO_MITOCHONDRIA	1.40	0.20
687	MOOTHA_GLUCONEOGENESIS	1.40	0.20
688	UDAYAKUMAR_MED1_TARGETS_DN	1.40	0.20
689	NIKOLSKY_OVERCONNECTED_IN_BREAST_CANCER	1.40	0.20
690	VERHAAK_AML_WITH_NPM1_MUTATED_UP	1.40	0.20
691	BHAT_ESR1_TARGETS_NOT_VIA_AKT1_DN	1.40	0.20
692	REACTOME_SIGNALING_BY_THE_B_CELL_RECEPTOR_BCR	1.40	0.20
693	BURTON_ADIPOGENESIS_1	1.40	0.20
694	REACTOME_MAP3K8_TPL2_DEPENDENT_MAPK1_3_ACTIVATION	1.40	0.20
695	PID_S1P_S1P2_PATHWAY	1.40	0.20
696	SHEDDEN_LUNG_CANCER_POOR_SURVIVAL_A6	1.40	0.20
697	REACTOME_INTERLEUKIN_1_FAMILY_SIGNALING	1.40	0.20
698	SANSOM_APC_TARGETS_REQUIRE_MYC	1.40	0.20
699	WIEDERSCHAIN_TARGETS_OF_BMI1_AND_PCGF2	1.40	0.20
700	REACTOME_NEPHRIN_FAMILY_INTERACTIONS	1.40	0.20
701	HAN_JNK_SINGALING_UP	1.40	0.20
702	KEGG_CELL_ADHESION_MOLECULES_CAMS	1.40	0.20
703	PID_P38_MK2_PATHWAY	1.40	0.20
704	CHESLER_BRAIN_HIGHEST_EXPRESSION	1.40	0.20
705	MILI_PSEUDOPODIA_CHEMOTAXIS_DN	1.40	0.20
706	CHIANG_LIVER_CANCER_SUBCLASS_UNANNOTATED_DN	1.40	0.20
707	FRIDMAN_IMMORTALIZATION_DN	1.40	0.20
708	CHIANG_LIVER_CANCER_SUBCLASS_INTERFERON_DN	1.40	0.20
709	BIOCARTA_IL2_PATHWAY	1.40	0.20
710	OKUMURA_INFLAMMATORY_RESPONSE_LPS	1.40	0.20
711	GROSS_HYPOXIA_VIA_ELK3_DN	1.39	0.20
712	PID_S1P_S1P3_PATHWAY	1.39	0.20
713	LENAOUR_DENDRITIC_CELL_MATURATION_DN	1.39	0.20
714	STANELLE_E2F1_TARGETS	1.39	0.20
715	KEGG_GLYCEROPHOSPHOLIPID_METABOLISM	1.39	0.20
716	XU_HGF_SIGNALING_NOT_VIA_AKT1_48HR_UP	1.39	0.20
717	PID_ATF2_PATHWAY	1.39	0.20
718	SMITH_LIVER_CANCER	1.39	0.20
719	GYORFFY_DOXORUBICIN_RESISTANCE	1.39	0.20
720	KEGG_BLADDER_CANCER	1.39	0.20
721	HOFMANN_MYELODYSPLASTIC_SYNDROM_RISK_UP	1.39	0.20
722	GENTILE_UV_HIGH_DOSE_DN	1.39	0.20
723	CHIBA_RESPONSE_TO_TSA_UP	1.39	0.21
724	POOLA_INVASIVE_BREAST_CANCER_DN	1.39	0.21
725	LINDVALL_IMMORTALIZED_BY_TERT_UP	1.39	0.21

726	REACTOME_SIGNALING_BY_FGFR2	1.39	0.21
727	VALK_AML_CLUSTER_11	1.39	0.20
728	TONKS_TARGETS_OF_RUNX1_RUNX1T1_FUSION_ERYTHROCYTE_UP	1.39	0.21
729	HADDAD_T_LYMPHOCYTE_AND_NK_PROGENITOR_DN	1.39	0.21
730	PURBEY_TARGETS_OF_CTBP1_AND_SATB1_UP	1.39	0.21
731	LEE_LIVER_CANCER_MYC_TGFA_UP	1.39	0.21
732	REACTOME_METABOLISM_OF_CARBOHYDRATES	1.39	0.21
733	RICKMAN_HEAD_AND_NECK_CANCER_C	1.39	0.21
734	LEE_LIVER_CANCER_CIPROFIBRATE_DN	1.39	0.21
735	BROWNE_HCMV_INFECTION_18HR_UP	1.39	0.21
736	REACTOME_SEMA4D_IN_SEMAPHORIN_SIGNALING	1.38	0.21
737	LOPES_METHYLATED_IN_COLON_CANCER_DN	1.38	0.21
738	KIM_HYPOXIA	1.38	0.21
739	LIN_SILENCED_BY_TUMOR_MICROENVIRONMENT	1.38	0.21
740	PEDRIOLI_MIR31_TARGETS_UP	1.38	0.21
741	REACTOME_TOLL_LIKE_RECEPTOR_4_TLR4_CASCADE	1.38	0.21
742	PETROVA_ENDOTHELIUM_LYMPHATIC_VS_BLOOD_UP	1.38	0.21
743	KIM_RESPONSE_TO_TSA_AND_DECITABINE_UP	1.38	0.21
744	MACLACHLAN_BRCA1_TARGETS_UP	1.38	0.21
745	BIOCARTA_TNFR1_PATHWAY	1.38	0.21
746	PID_S1P_S1P1_PATHWAY	1.38	0.21
747	REACTOME_GLUCOSE_METABOLISM	1.38	0.21
748	MANALO_HYPOXIA_UP	1.38	0.21
749	AFFAR_YY1_TARGETS_UP	1.38	0.21
750	RUTELLA_RESPONSE_TO_CSF2RB_AND_IL4_UP	1.38	0.21
751	LEE_AGING_MUSCLE_DN	1.38	0.21
752	DAVICIONI_PAX_FOXO1_SIGNATURE_IN_ARMS_UP	1.38	0.21
753	HOEBEKE_LYMPHOID_STEM_CELL_UP	1.38	0.21
754	HOWLIN_CITED1_TARGETS_1_UP	1.38	0.21
755	ZHANG_GATA6_TARGETS_DN	1.38	0.21
756	PID_NFAT_3PATHWAY	1.38	0.21
757	REACTOME_INTERLEUKIN_17_SIGNALING	1.38	0.21
758	SWEET_KRAS_TARGETS_UP	1.38	0.21
759	LIAN_LIPA_TARGETS_6M	1.38	0.21
760	ACEVEDO_NORMAL_TISSUE_ADJACENT_TO_LIVER_TUMOR_DN	1.38	0.21
761	CROMER_TUMORIGENESIS_DN	1.38	0.21
762	PID_IL1_PATHWAY	1.38	0.21
763	LUI_TARGETS_OF_PAX8_PPARG_FUSION	1.38	0.21
764	GRAESSMANN_RESPONSE_TO_MC_AND_DOXORUBICIN_UP	1.37	0.22
765	HUANG_GATA2_TARGETS_DN	1.37	0.22
766	LI_CISPLATIN_RESISTANCE_DN	1.37	0.22
767	REACTOME_TRANSCRIPTIONAL_REGULATION_BY_TP53	1.37	0.22
768	REACTOME_HS_GAG_BIOSYNTHESIS	1.37	0.22

769	REACTOME_SIGNALING_BY_NTRK1_TRKA	1.37	0.22
770	BROWNE_HCMV_INFECTION_48HR_UP	1.37	0.22
771	WU_HBX_TARGETS_3_UP	1.37	0.22
772	MEISSNER_BRAIN_HCP_WITH_H3K27ME3	1.37	0.22
773	DEBIASI_APOPTOSIS_BY_REOVIRUS_INFECTION_UP	1.37	0.22
774	RORIE_TARGETS_OF_EWSR1_FLI1_FUSION_UP	1.37	0.22
775	MOOTHA_PGC	1.37	0.22
776	MEISSNER_NPC_HCP_WITH_H3K4ME3_AND_H3K27ME3	1.37	0.22
777	MARTINEZ_RB1_TARGETS_UP	1.37	0.22
778	RUTELLA_RESPONSE_TO_CSF2RB_AND_IL4_DN	1.37	0.22
779	LEE_EARLY_T_LYMPHOCYTE_DN	1.37	0.22
780	NOUZOVA_METHYLATED_IN_APL	1.37	0.22
781	WONG_EMBRYONIC_STEM_CELL_CORE	1.37	0.22
782	TORCHIA_TARGETS_OF_EWSR1_FLI1_FUSION_DN	1.37	0.22
783	YOKOE_CANCER_TESTIS_ANTIGENS	1.37	0.22
784	JOHANSSON_GLIOMAGENESIS_BY_PDGFB_DN	1.37	0.22
785	GRAHAM_CML_QUIESCENT_VS_NORMAL_DIVIDING_UP	1.37	0.22
786	PHONG_TNF_RESPONSE_VIA_P38_COMPLETE	1.37	0.22
787	MODY_HIPPOCAMPUS_NEONATAL	1.37	0.22
788	ZHENG_GLIOBLASTOMA_PLASTICITY_DN	1.37	0.22
789	REACTOME_CHONDROITIN_SULFATE_DERMATAN_SULFATE_METABOLISM	1.37	0.22
790	HOSHIDA_LIVER_CANCER_LATE_RECURRENCE_DN	1.37	0.22
791	VANTVEER_BREAST_CANCER_METASTASIS_DN	1.37	0.22
792	TANAKA_METHYLATED_IN_ESOPHAGEAL_CARCINOMA	1.37	0.22
793	WANG_SMARCE1_TARGETS_DN	1.37	0.22
794	CHAUHAN_RESPONSE_TO_METHOXYESTRADIOL_DN	1.37	0.22
795	BAE_BRCA1_TARGETS_UP	1.36	0.22
796	FARMER_BREAST_CANCER_APOCRINE_VS_LUMINAL	1.36	0.22
797	BOYAULT_LIVER_CANCER_SUBCLASS_G1_DN	1.36	0.22
798	BROWN_MYELOID_CELL_DEVELOPMENT_DN	1.36	0.22
799	LINDSTEDT_DENDRITIC_CELL_MATURATION_C	1.36	0.22
800	DEBIASI_APOPTOSIS_BY_REOVIRUS_INFECTION_DN	1.36	0.23
801	MARKS_HDAC_TARGETS_UP	1.36	0.23
802	QI_HYPOXIA_TARGETS_OF_HIF1A_AND_FOXA2	1.36	0.23
803	WANG_HCP_PROSTATE_CANCER	1.36	0.23
804	LANDIS_ERBB2_BREAST_TUMORS_324_UP	1.36	0.23
805	VERNELL_RETINOBLASTOMA_PATHWAY_DN	1.36	0.23
806	BONOME_OVARIAN_CANCER_POOR_SURVIVAL_DN	1.36	0.23
807	TAKEDA_TARGETS_OF_NUP98_HOXA9_FUSION_6HR_UP	1.36	0.23
808	MULLIGHAN_MLL_SIGNATURE_2_DN	1.36	0.23
809	REACTOME_SIGNALING_BY_NTRK2_TRKB	1.36	0.23
810	MATZUK_IMPLANTATION_AND_UTERINE	1.36	0.23
811	REACTOME_SEMA4D_INDUCED_CELL_MIGRATION_AND_GROWTH_CONE_COLLAPSE	1.36	0.23

812	GRAHAM_CML_QUIESCENT_VS_NORMAL_QUIESCENT_UP	1.36	0.23
813	LU_IL4_SIGNALING	1.36	0.23
814	SPIRA_SMOKERS_LUNG_CANCER_UP	1.36	0.23
815	YAO_TEMPORAL_RESPONSE_TO_PROGESTERONE_CLUSTER_6	1.36	0.23
816	BERENJENO_TRANSFORMED_BY_RHOA_UP	1.35	0.23
817	MARTENS_TRETINOIN_RESPONSE_UP	1.35	0.23
818	PID_CXCR4_PATHWAY	1.35	0.23
819	VALK_AML_CLUSTER_2	1.35	0.23
820	ZAMORA_NOS2_TARGETS_UP	1.35	0.23
821	WEST_ADRENOCORTICAL_TUMOR_DN	1.35	0.23
822	PID_TRKR_PATHWAY	1.35	0.23
823	BASSO_HAIRY_CELL_LEUKEMIA_UP	1.35	0.23
824	MA_MYELOID_DIFFERENTIATION_DN	1.35	0.23
825	PID_PI3K_PLC_TRK_PATHWAY	1.35	0.23
826	LEE_CALORIE_RESTRICTION_NEOCORTEX_DN	1.35	0.23
827	PASQUALUCCI_LYMPHOMA_BY_GC_STAGE_UP	1.35	0.23
828	HENDRICKS_SMARCA4_TARGETS_UP	1.35	0.23
829	ZHAN_MULTIPLE_MYELOMA_CD1_AND_CD2_DN	1.35	0.23
830	REACTOME_INFLUENZA_INFECTION	1.35	0.23
831	IVANOVA_HEMATOPOIESIS_STEM_CELL_AND_PROGENITOR	1.35	0.23
832	ANDERSEN_LIVER_CANCER_KRT19_UP	1.35	0.23
833	ODONNELL_METASTASIS_DN	1.35	0.23
834	BIOCARTA_NFAT_PATHWAY	1.35	0.23
835	PID_HEDGEHOG_2PATHWAY	1.35	0.23
836	BHAT_ESR1_TARGETS_NOT_VIA_AKT1_UP	1.35	0.23
837	ZHANG_RESPONSE_TO_IKK_INHIBITOR_AND_TNF_DN	1.35	0.23
838	COLLER_MYC_TARGETS_UP	1.35	0.23
839	RUTELLA_RESPONSE_TO_HGF_VS_CSF2RB_AND_IL4_UP	1.35	0.24
840	IWANAGA_CARCINOGENESIS_BY_KRAS_PTEN_DN	1.35	0.24
841	KEGG_VIRAL_MYOCARDITIS	1.35	0.24
842	CHIANG_LIVER_CANCER_SUBCLASS_CTNNB1_DN	1.34	0.24
843	GARGALOVIC_RESPONSE_TO_OXIDIZED_PHOSPHOLIPIDS_CYAN_UP	1.34	0.24
844	GAJATE_RESPONSE_TO_TRABECTEDIN_UP	1.34	0.24
845	WIERENGA_STAT5A_TARGETS_UP	1.34	0.24
846	VANTVEER_BREAST_CANCER_ESR1_DN	1.34	0.24
847	ONGUSAHA_TP53_TARGETS	1.34	0.24
848	KEGG_PROSTATE_CANCER	1.34	0.24
849	PID_WNT_CANONICAL_PATHWAY	1.34	0.24
850	CUI_TCF21_TARGETS_UP	1.34	0.24
851	ACEVEDO_LIVER_TUMOR_VS_NORMAL_ADJACENT_TISSUE_DN	1.34	0.24
852	KOKKINAKIS_METHIONINE_DEPRIVATION_48HR_UP	1.34	0.24

853	LEE_AGING_MUSCLE_UP	1.34	0.24
854	LEE_LIVER_CANCER_SURVIVAL_DN	1.34	0.24
855	SATO_SILENCED_EPIGENETICALLY_IN_PANCREATIC_CANCER	1.34	0.24
856	LEE_LIVER_CANCER_MYC_DN	1.34	0.24
857	RUIZ_TNC_TARGETS_UP	1.34	0.24
858	POOLA_INVASIVE_BREAST_CANCER_UP	1.34	0.24
859	MCBRYAN_PUBERTAL_BREAST_4_5WK_DN	1.34	0.24
860	REACTOME_AMINO_ACID_TRANSPORT_ACROSS_THE_PLASMA_MEMBRANE	1.34	0.24
861	LANDIS_ERBB2_BREAST_TUMORS_65_DN	1.34	0.24
862	ONDER_CDH1_TARGETS_1_DN	1.34	0.24
863	KUMAR_TARGETS_OF_MLL_AF9_FUSION	1.34	0.24
864	BIOCARTA_CELLCYCLE_PATHWAY	1.34	0.24
865	SHEN_SMARCA2_TARGETS_DN	1.34	0.24
866	CERVERA_SDHB_TARGETS_1_UP	1.34	0.24
867	GROSS_HIF1A_TARGETS_DN	1.34	0.24
868	AMIT_EGF_RESPONSE_480_MCF10A	1.34	0.24
869	REACTOME_OTHER_INTERLEUKIN_SIGNALING	1.34	0.24
870	BERTUCCI_INVASIVE_CARCINOMA_DUCTAL_VS_LOBULAR_UP	1.34	0.24
871	REACTOME_HOST_INTERACTIONS_OF_HIV_FACTORS	1.34	0.24
872	TURASHVILI_BREAST_CARCINOMA_DUCTAL_VS_LOBULAR_UP	1.34	0.24
873	SEKI_INFLAMMATORY_RESPONSE_LPS_UP	1.34	0.24
874	TONKS_TARGETS_OF_RUNX1_RUNX1T1_FUSION_HSC_UP	1.33	0.24
875	GEORGES_CELL_CYCLE_MIR192_TARGETS	1.33	0.24
876	REACTOME_TRANSCRIPTIONAL_REGULATION_BY_MECP2	1.33	0.24
877	REACTOME_FOXO_MEDIATED_TRANSCRIPTION	1.33	0.24
878	GRAHAM_CML_QUIESCENT_VS_NORMAL_QUIESCENT_DN	1.33	0.24
879	KEGG_B_CELL_RECEPTOR_SIGNALING_PATHWAY	1.33	0.24
880	ABE_VEGFA_TARGETS_2HR	1.33	0.24
881	KAYO_CALORIE_RESTRICTION_MUSCLE_UP	1.33	0.24
882	GAUSSMANN_MLL_AF4_FUSION_TARGETS_G_UP	1.33	0.24
883	REACTOME_SIGNALING_BY_GPCR	1.33	0.24
884	SARTIPY_BLUNTED_BY_INSULIN_RESISTANCE_DN	1.33	0.24
885	FOURNIER_ACINAR_DEVELOPMENT_LATE_2	1.33	0.24
886	OUILLETTE_CLL_13Q14_DELETION_DN	1.33	0.24
887	LIANG_HEMATOPOIESIS_STEM_CELL_NUMBER_LARGE_VS_TINY_UP	1.33	0.24
888	CREIGHTON_ENDOCRINE_THERAPY_RESISTANCE_4	1.33	0.24
889	SCIAN_CELL_CYCLE_TARGETS_OF_TP53_AND_TP73_DN	1.33	0.24
890	SHAFFER_IRF4_TARGETS_IN_ACTIVATED_DENDRITIC_CELL	1.33	0.25
891	ENGELMANN_CANCER_PROGENITORS_DN	1.33	0.25

892	WANG_TARGETS_OF_MLL_CBP_FUSION_DN	1.33	0.25
893	REACTOME_RHO_GTPASES_ACTIVATE_IQGAPS	1.33	0.25
894	REACTOME_TRANSPORT_OF_SMALL_MOLECULES	1.33	0.25
895	KEGG_COLORECTAL_CANCER	1.33	0.25
896	WOOD_EBV_EBNA1_TARGETS_UP	1.33	0.25
897	BAELDE_DIABETIC_NEPHROPATHY_DN	1.33	0.25
898	REACTOME_SIGNALING_BY_FGFR2_IIIA_TM	1.33	0.25
899	SERVITJA_LIVER_HNF1A_TARGETS_UP	1.33	0.25

Table S6 Sequences of siControl and siRNAs used in this study.

Target	Sequences
Non-targeting 5	D-001210-05: UGGUUUACAUGUCGACUAA
RRM1	D-004270-01: GCACAGAAAUAGUGGAGUA D-004270-02: GAACACACAUACGACUUUA D-004270-03: GGACUGGUCUUUGAUGUGU D-004270-04: UGAAACGAGUGGAGACUAA
STIM1	D-011785-01: CAUCAGAAGUAUACAAUUG D-011785-02: AGAAGGAGCUAGAAUCUCA D-011785-03: AGGUGGAGGUGCAAUAUUA D-011785-04: GGUGGUGUCUAUCGUUAUU
NFATc2	D-003606-01: CCAAUAAUGUCACCUCGAA D-003606-04: GCAGAAUCGUCUCUUUACA D-003606-05: GCGGGGAUCUUGAAGCUUA D-003606-06: UCAUGUACUGCGAGAAUUU

Table S7 Gene expression primer sequences.

Gene	Forward primer	Reverse primer
GAPDH	ATGGGGAAGGTGAAGGTCG	GGGGTCATTGATGGCAACAATA
RRM1	ACTACTATCCTGTACCAGAGGCAT	CTGGGCTTCTGCACTCTCAA
STIM1	CCTCCTCTCTTGACTCGCCA	TATAGGCAAACCAGCAGCCG
NFATC2	AAGACCACAGATGGACAGCAAA	CATGTTGGGCTGGCTCTTGT
TRIB3	GCCTTTTTCACTCGGACCCA	CTTCTTCCTCTCACGGTCAGC
ERN1	GGCCTCGGGATTTTTGGAAGTA	ATTGAGCCTGTCCTCTTGCTG
DDIT3	GACCTGCAAGAGGTCCTGTC	CCAGAGAAGCAGGGTCAAGA
KDM7A	CCTTCACCCCACCAAGAGAC	GGACGTTTACCTTTTGTTGCCTG
KRT14	CAGAGATGTGACCTCCTCCA	CTCAGTTCTTGGTGCGAAGG
KLF4	ATCTTTCTCCACGTTCGCGT	CTCCCGCCAGCGGTTATTC

Table S8 Primer sequences used to validate Chromatin Immunoprecipitation

Site	Forward primer	Reverse primer
TRIB3_H3K27ac_pos	GCACGCACGCCCCTTA	CCGGATCAAAAGGGATCTGACC
TRIB3_ATF4_pos	GCACTGACCAGACGCCC	GATCGCACCATCCCCCG
TRIB3_neg	GGAGCTGTGACGGTGATGAG	AACCCACAAAGCAGGAGGAA
ERN1_H3K27ac_pos	CGCGAGCTGTCCTCCAC	TGCTGCTGACGCTGCTG
ERN1_ATF4_pos	CCCAGGCACACCTACCTACT	TCTGATTTGTGGTTGGCAGAAGA
ERN1_neg	GTCCACATGCTTCATGCACTTC	TGCCACCATAAATAAAACCAGTGC
DDIT3_H3K27ac_pos	ATTTCCCAAGGGCAACCGA	CCTATTGCTTCGGACGACGG
DDIT3_ATF4_pos	CGCTAGGGGGTCGACGTA	CCTCCGTGAAGCCTCGTG
DDIT3_neg	ACAGGTCAGTCCCTTGTTCC	GAGGGCACAGCCTTTAGCTT

List of Figures

List of Tables

List of Abbreviations

°C
: Degree celsius.

µ
: Micro (10^{-6}).

5-FU
: 5-Fluorouracil.

ac
: Acetylation.

ADEX
: Aberrantly differentiated exocrine and endocrine.

Akt
: AKT serine/threonine kinase 1.

AP1
: Activator protein 1.

ATF3
: Activating transcription factor 3.

ATF4
: Activating transcription factor 4.

ATF6
: Activating transcription factor 6.

ATG5
: Autophagy related 5.

ATP
: Adenosine triphosphate.

BCL2
: BCL2 apoptosis regulator.

BET
: Bromo- and extraterminal domain protein.

BIM
: BCL2 like 11.

bp
: Base pair.

BRAF
B-Raf proto-oncogene. ,
BRCA1
BRCA1 DNA repair associated.
BRCA2
BRCA2 DNA repair associated.
BRD4
Bromodomain containing 4.
BSA
Bovine serum albumin.
b-ZIP
Basic leucine zipper domain.
C/EBP
CAAT box/enhancer-binding protein.
CAF
Cancer associated fibroblast.
CAMKII
Calcium/calmodulin-dependent protein kinase II.
CAMKIV
cium/calmodulin-dependent protein kinase IV.
CaN
Calcineurin.
CAPN
Calpain.
CARE
CCAAT-enhancer binding protein-activating transcription factor (C/EBP-ATF) response element.
CDA
Cytidine deaminase.
CDK6
Cyclin dependent kinase 6.
CDK9
Cyclin-dependent kinase 9.
CDKN2A

Cyclin dependent kinase inhibitor 2A.

CDKN2B

Cyclin dependent kinase inhibitor 2B.

ChIP

Chromatin immunoprecipitation.

CHOP

DNA damage inducible transcript 3 - protein.

cIAP1

Baculoviral IAP repeat containing 2.

cIAP2

Baculoviral IAP repeat containing 3.

CMPK

UMP-CMP kinase, pyrimidine nuceloside monophosphate kinase.

CNT

Concentrative nucleoside transporter.

CNX

Calnexin.

COF

Co-factor.

COPII

Coat protein complex II.

COX2

Cyclooxygenase 2.

CREB

cAMP response element binding protein.

CRT

Calreticulin.

CSA

Cyclosporine A.

CTCF

CCCTC-binding factor.

CTD

C-terminal domain.

DAG

Diacylglyrcerol.

DBAJC3

DnaJ homolog subfamily C member 3.

dCK

deoxycytidine kinase.

DCTD

Deoxycytidylate deaminase.

DDIT3

DNA damage inducible transcript 3 - gene.

dFdC

2’,2’-difluorodeoxycytidine, Gemcitabine.

dFdCDP

2’,2’-difluorodeoxycytidine diphosphate.

dFdCMP

2’,2’-difluorodeoxycytidine monophosphate.

dFdCTP

2’,2’-difluorodeoxycytidine triphosphate.

dFdU

2’,2’-difluorodeoxyuridine.

dFdUMP

2’,2’-difluorodeoxyuridine monophosphate.

DNA

Deoxyribonucleic acid.

dNDP

Deoxynucleotide diphosphate.

dNTP

Deoxynucleotide triphosphate.

DUB

Deubiquitinase.

ECOG

Eastern Cooperative Oncology Group.

EGFR

Epidermal growth factor receptor.

EGTA

Ethylene glycol tetraacetic acid.

eIF2α

Eukaryotic translation initiation factor 2A, 2

ELK1

ETS transcription factor ELK1.

EMT

Epithelial-to-mesenchymal transition.

ENT

Equilibrative nucleoside transporter.

ER

Endoplasmic reticulum.

ERAD

ER-associated protein degradation.

ERBB2

Erb-b2 receptor tyrosine kinase 2.

ERN1

Endoplasmic reticulum to nucleus signaling 1.

ERO1α

Endoplasmic reticulum oxidoreductase 1 alpha.

ETS1

Protein C-ets-1.

EZH2

Enhancer of zeste 2 polycomb repressive complex 2 subunit.

FBS

Fetal bovine serum.

FDR

False discovery rate.

FOLFIRINOX

5-FU, leucovin, irinotecan and oxaliplatin.

FOLFOX

5-FU, leucovin and oxaliplatin.

FOS

Fos proto-oncogene, AP1 trtanscription factor subunit.

FOXA2

Forkhead box A2.

g

gravity - unit of relative centrifugal force.

GADD34

Protein phosphatase 1 regulatory subunit 15A.

GATA6

GATA binding protein 6.

Gem

Gemcitabine.

GemR

Gemcitabine resistant cell line derived from L3.6pl.

Gene set enrichment analysis.

GLI1

GLI family zinc finger 1.

GLP-1

Glucagon-like peptide 1.

GPCR

G-protein coupled receptor.

GRB7

Growth factor receptor bound protein 7.

GRP78

Heat shock protein family A (Hsp70) member 5.

GSK-3β

Glycogen synthase kinase 3β.

h

Hour.

H2A

Histone 2A.

H2AK119

Lysine 119 on histone 2A.

H2AK119ub

Monoubiquitinated lysine 119 on histone 2A.

H2B

Histone 2B.

H2BK120

Lysine 120 in histone H2B.

H2BK120ub

Monoubiquitinated lysine 120 in histone H2B.

H3

Histone 3.

H3K27

Lysine 27 on histone 3.

H3K27ac

Acetylated lysine 27 on histone 3, 7

H3K27me3

Trimethylated lysine 27 on histone 3, 6

H3K4

Lysine 4 on histone 3.

H3K4me1

Monomethylated lysine 4 on histone 3.

H3K4me3

Trimethylated lysine 4 on histone 3.

H3K9

Lysine 9 on histone 3.

H3K9me

Monomethylated lysine 9 on histone 3.

H3K9me2

Dimethylated lysine 9 on histone 3.

H3K9me3

Trimethylated lysine 9 on histone 3.

H4

Histone 4.

H4K12

Lysine 12 on histone 4.

H4K12ac
: Acetylated lysine 12 on histone 4.

H4K16
: Lysine 16 on histone 4.

H4K16ac
: Acetylated lysine 16 on histone 4.

H4K5
: Lysine 5 on histone 4.

H4K5ac
: Acetylated lysine 5 on histone 4.

H4K8
: Lysine 8 on histone 4.

H4K8ac
: Acetylated lysine 8 on histone 4.

HAT
: Histone acetyltransferase.

hCNT1
: Human concentrative nucleoside transporter 1.

hCNT3
: Human concentrative nucleoside transporter 3.

HDAC
: Histone deacetylase.

HDAC4
: Histone deacetylase 4.

hENT1
: Human equilibrative nucleoside transporter 1.

hENT2
: Human equilibrative nucleoside transporter 2.

HER2
: Human epidermal growth factor receptor 2.

HIF1a
: Hypoxia inducible factor 1 subunit alpha.

HP1

Heterochromatin protein 1.

HSF1

Heat shock factor 1.

IgG

Immunoglobulin G.

IGV

Integrative genomics viewer.

IHC

Immunohistochemistry.

IKK2

inhibitor of nuclear factor kappa B kinase subunit.

ILK

Integrin linked kinase.

IP_3

inositol 1,4,5-triphosphate.

IP3R

Inositol 1,4,5-triphosphate receptor.

IRE1

Inositol requiring enzyme 1.

IRF4

Interferon regulatory factor 4.

ISR

Integrated stress response.

JNK

c-Jun N-terminal kinase.

JUN

Jun proto-oncogene, AP1 trtanscription factor subunit.

KAT

Lysine acetyltransferase.

kb

Kilo base pair.

kDa

Kilodalton.

KDM
Lysine demethylase.
KDM4C
Lysine demethylase 4C.

KEAP1
Kelch-like ECH-associated protein 1.
KLF4
Krüppel like factor 4.
KMT
Lysine methyltransferase.
K-RAS
KRAS proto-oncogene.
L
Liter.
Lys
Lysine.
m
Milli (10^{-3}).
M
Molar.
MAP1LC3
Microtubule associated protein 1 light chain 3 alpha.
MAPK
Mitogen-activated protein kinase.
MCL-1
MCL1 apoptosis regulator, BCL2 family member.
MCU
Mitochondrial calcium uniporter.
me
Methylation.
MEF2
Myocyte enhancer factor 2.
MET

MET proto-oncogene.

MIEN1
Migration and invasion enhancer 1.

min
Minute.

MLL
Mixed lineage leukemia complex.

MLL3
Mixed lineage leukemia complex 3.

MLL4
Mixed lineage leukemia complex 4.

M-MuLV
Moloney-Murine leukemia virus.

mRNA
Messenger RNA.

mTOR
Mechanistic target of rapamycin kinase.

MYC
MYC proto-oncogene.

n
Nano (10^{-9}).

NCLX
Na+/Ca2+ Li+-permeable exchanger.

NCX
plasmalemmal sodium Na+/Ca2+ exchangers.

NDP
Nucleotide diphosphate.

NDPK
Nucleoside diphosphate kinase.

NFAT
Nuclear factor of activated T cells.

NFAT5

Nuclear factor of activated T cells 5.

NFATc1

Nuclear factor of activated T cells 1.

NFATc2

Nuclear factor of activated T cells.

NFATc3

Nuclear factor of activated T cells 3.

NFATc4

Nuclear factor of activated T cells 4.

NF-κB

Nuclear factor kappa B.

NOV

Cellular communication netwrok factor 3.

NRF2

Nuclear factor erythroid 2-related factor 2.

NT

Nucleoside transporter.

NT5C1A

Cytosolic 5'-nucleotidase I A.

NTP

Nucleotide triphosphate.

ORAI

calcium release-activated calcium channel.

ORAI1

ORAI calcium release-activated calcium modulators 1.

ORAI2

ORAI calcium release-activated calcium modulators 2.

ORAI3

ORAI calcium release-activated calcium modulators 3.

P

P-value.

p300/CBP

E1A binding protein p300 and cAMP-response element-binding CREB-binding protein.

p53

Tumor protein p53.

padj

P-value adjusted.

PanIN

Pancreatic intraepithelial neoplasm.

Par

Parental cell line.

PBS

Phosphate buffered saline.

PD-1

Programmed cell death protein 1.

PDAC

Pancreatic ductal adenocarcinoma.

PDIA19

DnaJ heat shock protein family (Hsp40) member C10.

PDIA5

Protein disulfide isomerase family A member 5.

PDIA6

Protein disulfide isomerase family A member 6.

peIF2α

Phosphorylated eukaryotic translation initiation factor 2A.

PERK

PKR-like ER kinase.

PGAP3

Post-GPI attachment to proteins phospholipase 3.

pH

Potentia hydrogenii.

PIK3CA

Phosphatidylinositol-4,5-bisphosphate 3-kinase catalytic subunit alpha.

PIP_2

phosphatidylinositol 4,5-bisphosphate.

PKC
Protein kinase C.
PLC
Phospholipase C.
PMCA
Plasma membrane Ca^{2+}-transporting ATPase.
PNMT
Phenylethanolamine-N-methyltransferase.
pNRF2
Phosphorylated nuclear factor erythroid 2-related factor 2.
PP2A
Protein phosphatase 2A.
PRC1
Polycomb repressor complex 1.
PRC2
Polycomb repressor complex 2.
PREX2
Phosphatidylinositol-3,4,5-triphosphate dependent Rac exchange factor 2.
PRRX1A
Paired related homeobox 1a.
PRRX1B
Paired related homeobox 1b.
PS
Performance Status.

PUMA
BCL2 binding component 3.
QM
Quasimesenchymal.
qPCR
Quantitative polymerase chain reaction.
RACK1
Receptor of activated C kinase 1.
RNA

Ribonucleic acid.

RNA Pol II

RNA Polymerase II.

RNF20

Ring finger protein 20.

RNF40

Ring finger protein 40.

RNR

Ribonucleotide reductase.

ROS

Reactive oxygen species.

RRM1

Ribonucleotide reductase catalytic subunit M1.

RRM2

Ribonucleotide reductase regulatory subunit M2.

RRM2B

Ribonucleotide reductase regulatory TP53 inducible subunit 2B.

RTK

Receptor tyrosine kinase.

S-1

Tegafur, gimeracil and oteracil.

S1P

Site-1 protease.

S2P

Site-2 protease.

SARAF

SOCE-associated regulatory factor.

SD

Standard deviation.

SDS

Sodium dodecyl sulfate.

SE

Super-enhancer.

SEM
Standard error of the mean.
Ser
Serine.
SERCA
sarco/endoplasmic reticulum ATPase.
SETD1A
SET domain containing 1A, histone lysine methyltransferases.
SETD1B
SET domain containing 1B, histone lysine methyltransferases.
SH2-domain
Src homology 2 domain.
siCont
Control non-targeting siRNA.
siRNA
small interfering RNA.
SMAD3
SMAD family member 3.
SMAD4
SMAD family member 4.
SNAI1
Snail family transcriptional repressor 1.
SOCE
Store operated calcium entry.
SOX9
SRY-box transcription factor 9.
SPARC
Secreted protein acidic and cysteine rich.
SQSTM1
Sequestosome 1.
SRF
Serum response factor.
STAT3
Signal transducer and activator of transcription 3.

STIM
Stromal interaction molecules.
STIM1
Stromal interaction molecule 1.
STIM2
Stromal interaction molecule 2.
SUV39H1
Suppressor of variegation 3-9 homolog 1.
SUV39H2
Suppressor of variegation 3-9 homolog 2.
Syk
Tyrosine protein kinase Syk.
TCAP
Titin-cap.
TF
Transcription factor.
TGFβ
Transforming growth factor beta.
Thap
Thapsigargin.
TMCO1
Transmembrane and coiled-coil domains 1.
TRAF2
TNF receptor associated factor 2.
TRIB3
Tribbles pseudokinase 3.
TRIM21
Tripartite motif containing 21.
TRP
Transient receptor potential.
TRPM4
Transient receptor potential cation channel subfamily M member 4.
TRPM5
Transient receptor potential cation channel subfamily M member 5.

TRPV5
Transient receptor potential cation channel subfamily V member 5.
TRPV6
Transient receptor potential cation channel subfamily V member 6.
TS
Thymidylate synthase.
TSS
Transcriptional start site.
TWIST
Twist family bHLH transcription factor 1.
ub
Ubiquitination.
UPR
Unfolded protein response.
VEGF
Vascular endothelial growth factor.
VEGFA
Vascular endothelial growth factor A.
w/v
Weight per volume.
WEE1
WEE1 G2 checkpoint kinase.
XBP1
X-box binding protein 1.
ZEB1
Zinc finger E-box binding homeobox 1.
ΔNp63
Delta N tumor protein p63.

Acknowledgments

This thesis and project would have never come alive without the guidance, help and support of some exceptional people. They created an environment which allowed me to grow scientifically and personally, and I would like to express my sincere gratitude to them.

First, I would like to thank my supervisor Prof. Steven A. Johnsen, who has always encouraged me to think and who has involved me in scientific discussions and meetings starting from my first week of my rotation. I am also very grateful for the time he has invested in me and I will never forget how supportive Steve was when I had to switch projects. We spent an entire day discussing possible new projects and how feasible they were, given the time frame and the fact that Steve was soon moving to the US. I would also like to thank him for listening to my ideas, taking them into account, even when they sounded a bit absurd, developing them further and coming up with experiments to test them. With him I have learned some of the most important skills for a scientist, namely how to “look” at data, how to build a hypothesis based on the data and how to intelligently design experiments to test the hypothesis. Few PhD students are so lucky to have a PI, who they can always reach and with whom they can discuss everything ranging from big ideas and decisions to small experimental details. I will take these experiences with me for the rest of my life and I wish to pass them on, wherever I go.

I would also like to express my gratitude to Prof. Matthias Dobbelstein for his scientific input and, especially, for all of his support. He has taught me a lot about cancer biology, gemcitabine and the integrated stress response, providing me with the basis and helping me further develop the project. I would also like to thank him for all of his support, especially after Steve moved to the US. He took us under his wing, which was very recomforting, inviting us to his lab meetings and providing us with lab and office space. He also ensured a nice environment and it was a pleasure to discuss ideas and to chat with his lab members. Antje was also very supportive and always ready to help! I also learned a lot about p53 and MDM2 from Sabrina and enjoyed our discussions very much! I am very curious to see how her project will develop.

I would like to thank Prof. Johannes Söding for his scientific input, always offering a new perspective on the project. I would also like to thank Prof. Volker Ellenrieder, Dr. Nico Posnien and Dr. Ufuk Günesdogan for agreeing in being in my extended thesis committee. Prof. Volker Ellenrieder was also very supportive, helping to correct the manuscript and pointing out, where major improvements were needed.

Prof. Ivan Bogeski and Dr. Christine S. Gibhardt have also been wonderful collaborators and played a major role in this project. Ivan and Christine have helped us take a simple observation (the amplification of *STIM1*) further, helping us consolidate our findings and guiding us through the calcium field. They have also provided valuable input to the manuscript and shown great support during the revision period. From them, I have also learned a great deal about store-operated calcium entry and life cell imaging.

I would also like to thank the Gastroenterology Department at the UMG, especially Dr. Elisabeth Hessmann and Waltraut Kopp. Lissy has not only helped us with patient material and patient-derived xenografts, greatly contributing to the story, but has also extensively corrected the manuscript and given us very important feedback. Waltraut was also very sweet, cheering on us, being always ready to help and ensuring all experiments were of excellent quality.

I cannot imagine what would have been of my PhD life without Dr. Xin Wang. He is one of the kindest persons I know and has an inspiring way of looking at things. He taught me so much about bioinformatics, from the big concepts behind it to the small technicalities. And I really appreciate that he would let me try using the cluster first, before coming to rescue me, when seeing my countless attempts and desperate face! I would also like to thank him for of the conversations we had, from big hypotheses to Pandas and the way he and his grandparents would make pasta, when he was little. I also appreciate his patience with me and my overthinking abilities, knowing exactly when I was starting to overthink again and listening to me say the same thing over and over again. I am extremely grateful for all the fun moments we had together, including when I tried to make a circus trick to scare Xin, which miserably failed, and he pretended to be scared. I thank him for teaching me a very important skill, namely how to make dumplings, and for the countless, joyful

and memorable hotpot gatherings. Finally, I would like to thank him for his true friendship!

I would also like to thank Dr. Zeynab Najafova for all of her input, support and friendship. I really appreciated the fact that we would show each other even small pieces of data, sometimes discussing something which would not make sense, but other times celebrating experiments that had worked. I am also very grateful for all of what she has done for us, once Steve moved to the US, handling orders, coordinating what had to be moved from the lab and helping us downsize. I also appreciate her friendship and our endless conversations about food. I truly enjoyed sharing different recipes, trying new dishes, ordering 4kg of mangos and having small mango tasting sessions after lunch with her!

I would also like to thank Dr. Florian Wegwitz for all of his scientific input, kindness and support. He always asked very interesting scientific questions, which sparkled very nice discussions. In fact, one of these discussions was the basis for a very important experiment (the rescue experiment with EGTA), which is now in the paper. I am also very thankful for all of his help, especially with microscopy, IHC and technical issues. I will never forget how many times he came to help me with even very simple things. Thank you, Flo!

I am also extremely grateful to Evangelos Prokakis and Garyfallia (Gloria) Prokaki for their input and kindness. Having started working with the integrated stress response around the same time, Evan and I frequently discussed the pathway and its role in our projects, which was always a very enriching experience. I am also very thankful for Evan's and Gloria's friendship and will never forget how Evan picked me up after my teeth implants and how both of them constantly checked on me. With them I got to travel to a small paradisiac island called Paros, met Gloria's sweet family and learned a very important skill, how to bake portokalopita (orange pie).

I first got in contact with Dr. Feda Hamdan, when looking for rotation projects and I am very grateful to have done a rotation with her. She introduced me to the lab and taught me all basic molecular biology experiments, ranging from cell culture to qPCRs. I am also very thankful that, during that time, she ensured I attended meetings with Steve and that I got more involved in the lab. I am also very grateful for all of her support, when I had to switch projects. She too, sat with Steve and I for

an entire day and discussed ideas for new projects, and she was very kind to pass one of her projects on to me, which I am very grateful for. She also later helped with major improvements in the manuscript and with the revision. Having scientific discussions with her has also been and still is a pleasure, where concepts are constantly challenged, revisited and redefined. She has also introduced me to many wonderful restaurants, sharing my love for knaffeh, mochi ice cream and Brazilian barbecue.

I would also like to thank Liezel Tamon for her friendship and for the time spent together in lab. She has shown me what true friendship is and I will never forget the time we were housemates. It was very recomforting to have her around in the lab. I also truly enjoyed chatting with her in the kitchen, cooking and baking. Together we spent many joyful, funny and sometimes also embarrassing moments. I will also never forget our weekend in London together or our spicy ramen challenge, where we started off thinking everything was under control and ended up finishing all dairy products we had at home.

I am also very thankful for Madhobi Sen's and Josephine Choo's friendship and support. I always saw Madhobi as the ChIP expert and every time something would come up, she would come and help me. Jojo was more like the integrated stress response guru, who introduced me to the ISR pathway and who advised me on which stress inducers to use and how to check for ISR induction. Together, we also spent several summer days enjoying the sun by the swimming pool and having little picnics. We also discussed a wide range of topics, from travel destinations to books and little anecdotes. Everything always surrounded by some tea, good food, flowers and grandma prints.

Another friend, who I made in lab is Dr. Iga Mieczkowska. Without knowing, I met her husband Matheusz Mieczkowski, before meeting her, and it has been a pleasure to see them grow as a family ever since. I also enjoyed exercising with Iga very much, and am grateful that she made sure our mind and body remained healthy, during this phase. I would also like to thank all three of them for the spontaneous little gatherings we had and for our unforgettable trip to Vienna together. David and I are also very thankful for the big quarantine entertainment (3 huge puzzles) you provided us with!

I would like to thank the lab members in the US, Dr. Alexander Q. Wixom and Joana Aggrey-Fynn, and the previous lab members Dr. Robyn Kosinski, Dr. Maria Zerche, Dr. Hannah Flebbe, Dr. Vijayalakshmi Kari, Jana Henck and Nicole Molitor for all of their help and support.

I would also like to express my sincere gratitude to the International Max Planck Research School in Molecular Biology program, more specifically to Dr. Steffen Burkhardt and Kerstin Grüniger. They have structured a wonderful program, where I have learned a great deal and have made great friends. I am also very thankful for the opportunity to do rotations and to better know the labs before deciding, in which lab to continue my studies. They were also extremely supportive, when Steve moved to the US, checking on me regularly and providing me with the funds necessary to visit Steve at the Mayo Clinic and attend a conference at Cold Spring Harbor.

I would also like to thank my friends, Ninadini, Roya, Gaurika, Jennifer, Anuruti, Ayesha, Mayumi, Andrea, Beatriz and Lorena for always being there even if miles away! You brighten up my days, always up for a good laugh, some adventure, some baking and eating and some shopping! Thank you for always listening, giving me good advice and for keeping me sane! With you I have collected some of the best and fondest memories!!

I would like to thank, David, my boyfriend, for making every day so light and filled with joy! He has been incredibly patient and loving with me through my ups and downs, making me laugh when I was about to cry and celebrating every little step/experiment. Always saying that if an experiment didn't work it was due to the fact that I "didn't feed my cells well enough, because I should have given them chocolate instead"! I also admire his curiosity and imagination, which led to very interesting scientific discussions, even though he has no scientific background. He also taught me a lot during this time, not only about statistics and coding, but also about airplanes and world of tanks! :-p Together we have traveled to various places, cooked and eaten a whole ton, survived quarantine and enjoyed the little things in life! He, in fact, taught me how to truly appreciate all little moments in life and how to take life so simple and easy. Thank you for all of your love and support during these past years and I can't wait to see what the future holds for us!

I would also like to thank my family for their unbelievable love and support. If it wasn't for my parents, I would not be half of the person I am today! Thank you for teaching me good values, showing me the world, emphasizing on my education and always trying to broaden my opportunities, while also fully respecting and supporting my choices and decisions. I cannot express how grateful I am for having such a loving family, who would fill my days with love and cheer on me, since I was little. I would often get calls after big experiments, asking if it had worked. And going to Stuttgart, Bayreuth or Berlin always felt like going home, where I would forget all the troubles and would be reminded of what really matters: love, family and friends. I would especially like to thank my grandma, whose dream was to visit Göttingen and to attend my defense and who I know will be watching from heaven on that day. I hope I was able and continue to make you proud! You showed me the purest form of love and I will take this with me forever!

Finally, God has guided me through thick and thin, always knowing what is best, as He is never early or late, He is always on time. Thank you for teaching me so much about resilience, faith and trust during these past years. “Entrega o teu caminho ao Senhor; confia Nele, e Ele o fará” Salmos 37:5.